USAAMRDL-TR-77-26

(12) Sc

AD A047872

ADVANCED SCAVENGE SYSTEMS FOR AN INTEGRATED ENGINE INLET PARTICLE SEPARATOR

Avco Lycoming Division
550 South Main Street
Stratford, Connecticut 06497

September 1977

Final Report for Period 21 March 1975 - 21 March 1977

Approved for public release;
distribution unlimited.

Prepared for

EUSTIS DIRECTORATE
U. S. ARMY AIR MOBILITY RESEARCH AND DEVELOPMENT LABORATORY
Fort Eustis, Va. 23604

EUSTIS DIRECTORATE POSITION STATEMENT

The effort reported herein represents a significant advancement in separator scavenge system durability. It is expected that the scanvenge system concept described in this report will be used on future Army gas turbine engines that incorporate integral inlet particle separators.

This Directorate concurs with the conclusions and recommendations contained herein.

Mr. David B. Cale of the Propulsion Technical Area, Technology Applications Division, served as Project Engineer for this effort.

Unclassified
SECURITY CLASSIFICATION OF THIS PAGE (When Data Entered)

REPORT DOCUMENTATION PAGE

READ INSTRUCTIONS BEFORE COMPLETING FORM

1. REPORT NUMBER: USAAMRDL-TR-77-26
2. GOVT ACCESSION NO.
3. RECIPIENT'S CATALOG NUMBER: (rept.)

4. TITLE (and Subtitle): ADVANCED SCAVENGE SYSTEMS FOR AN INTEGRATED ENGINE INLET PARTICLE SEPARATOR,
5. TYPE OF REPORT & PERIOD COVERED: Final / 21 March 1975 to 21 March 1977
6. PERFORMING ORG. REPORT NUMBER: LYC-77-26

7. AUTHOR(s): Michael J. Zoccoli
8. CONTRACT OR GRANT NUMBER(s): DAAJ02-75-C-0026 New

9. PERFORMING ORGANIZATION NAME AND ADDRESS:
Avco Lycoming Division
550 South Main Street
Stratford, Connecticut 06497

10. PROGRAM ELEMENT, PROJECT, TASK AREA & WORK UNIT NUMBERS: 62209A / 1F262209AH76 / 00 049 EK

11. CONTROLLING OFFICE NAME AND ADDRESS:
Eustis Directorate
U. S. Army Air Mobility R & D Laboratory
Fort Eustis, Virginia 23604

12. REPORT DATE: September 1977
13. NUMBER OF PAGES: 200

14. MONITORING AGENCY NAME & ADDRESS (if different from Controlling Office): (12) 292p.

15. SECURITY CLASS. (of this report): Unclassified
15a. DECLASSIFICATION/DOWNGRADING SCHEDULE

16. DISTRIBUTION STATEMENT (of this Report)

Approved for public release; distribution unlimited.

17. DISTRIBUTION STATEMENT (of the abstract entered in Block 20, if different from Report)

18. SUPPLEMENTARY NOTES

19. KEY WORDS (Continue on reverse side if necessary and identify by block number)

Advanced Scavenge System	Reliability
Gas Turbine Engine	Durability
Integral Particle Separator	
Inherent Efficiency	

20. ABSTRACT (Continue on reverse side if necessary and identify by block number)

In designing a device which scavenges the gas turbine engine integral particle separator, the fundamental problem is one of providing primarily a durable design that is practical in other important aspects which include, but is not limited to, power consumption, cost, physical size, and noise.

An advanced scavenge system for an integrated engine inlet protection system was developed to demonstrate a 50-hour operational capability at a specified

DD FORM 1 JAN 73 1473 EDITION OF 1 NOV 65 IS OBSOLETE

Unclassified
SECURITY CLASSIFICATION OF THIS PAGE (When Data Entered)

213150

1B

Block 20.

minimum performance level in the severe erosion environment typical of conditions at the exit from the engine particle separator.

Several alternative configurations were studied; two were selected for detailed design and experimental evaluation.

The first approach, innovative in nature, was a "self-bypassing" scavenge blower which afforded protection to its critical rotating element by means of its own inlet inertial separator. This blower was tested for an initial 50-hour period at a sand ingestion rate of 400 gm/hr, using MIL-E-5007C type sand. Test conditions directly simulated operation in conjunction with a 5.0-lb/sec engine, whose integral separator was 95-percent efficient at 18-percent scavenge rate, and whose inlet sand/air concentration was 1.5 mg/ft^3. At the conclusion of the 50-hour test period, program objectives with respect to durability had been clearly met, with no appreciable change in performance, other than a modest improvement in airflow at design speed. The evaluation program was then extended in order to ascertain the operational life of the blower. After 120 hours, a 4-1/2-percent net loss in airflow had resulted; this was consistent with conventional practice for blower performance margin, and the test was terminated at that point. Relative to the program goals, the durability of the blower exceeded the requirements by 140 percent.

The second approach, also successful in terms of demonstrating a minimum 50-hour scavenge operational capability, was a multiple-tube ejector assembly.

TABLE OF CONTENTS

LIST OF ILLUSTRATIONS

LIST OF TABLES

SUMMARY

The overall objective of this investigation was to evaluate an advanced scavenging unit for an integral engine particle separator in accordance with the following design criteria:

Engine Airflow	5 lb/sec
Scavenge Flow Rate	0.9 lb/sec
Inlet Pressure	20 in. H_2O Below Ambient

The overall program, subdivided according to tasks, is summarized as follows:

1. In Task I, a feasibility study was conducted on several systems including both dynamic and static designs. All designs were competitively evaluated, and at the conclusion of the study, one dynamic design (a "primary" system) and one static design (an "alternate" system) were selected for detailed design, procurement, and evaluation.

2. Task II consisted of detailed aerodynamic and mechanical design of both systems, including their respective test rigs.

3. In Task III, all test item and test rig hardware elements were procured.

4. Task IV, the final phase of the program included assembly, installation, experimental evaluation and data analysis of the primary and alternate systems.

INTRODUCTION

Particle separators currently in use on gas turbine engines typically incorporate a bladed pump to scavenge the contaminant laden air from the separator. This approach is disadvantageous in that the scavenge pump blades are prone to erosion damage in the highly concentrated sand and dust environment.

Consider an engine with 5 lb/sec airflow through the compressor, and 18-percent (0.9 lb/sec) scavenge flow provided by a conventional blower. If the engine separator is assumed to have an 80-percent sand separation efficiency, then the sand concentration (lb sand/lb air) at the scavenge blower will be 22 times higher than the sand concentration at the compressor inlet. With advances in separator technology, the requirements imposed on the conventional blower become even more extreme. At 90-percent engine separator efficiency, the

sand-to-air concentration at the blower is 50 times higher than that at the compressor, for the same engine and scavenge flow rates.

A typical conventional blower design is shown in Figure 1. The 90-degree drive is shown in order to preserve commonality with the type of drive arrangement used on the proposed pump designs described later in this report. The weight of the pump is approximately 6.5 pounds. Total pressure ratio is 1.08, at a speed of 50,000 rpm. Power requirements for the unit at 0.9 lb/sec would be 5.8 horsepower, at a stage adiabatic efficiency of 0.60. Experience with this type of blower design has shown that, although power requirements are low, the unit fails to endure sand ingestion tests using MIL-E-8593B sand, with a rate of performance degradation that is within acceptable limits.

One possible solution to this problem is to provide a means of protecting the bladed pump such that the rotating component is not subject to the erosive environment. One way of accomplishing this is by designing the scavenge unit to be a separator within itself. The degree of protection afforded to the rotor will be a function of the separation efficiency of the scavenge unit, and the quantity of air which bypasses the rotor.

This innovation in scavenge unit design results in an order of magnitude improvement in rotor protection, as is shown by Figure 2. The uppermost curve relates the sand-to-air concentration (C_2) at the inlet of a conventional blower to the sand-to-air concentration (C_1) at the engine compressor. The relative concentration (C_2/C_1) as mentioned earlier is seen to vary from 20 to 100, depending on the efficiency of the engine separator.

If the design is now modified such that approximately 16 percent of the total flow into the scavenge system is diverted past the rotor (i.e., β_2 = bypass ratio = 20%) along with 90 percent of the sand (i.e., η_2 = blower inlet separation efficiency = .90), then the relative concentration C_2/C_1 is reduced from 52:1 to 6.2:1 , assuming η_1 = 90%

By further improving the design so as to obtain 99-percent blower inlet separation efficiency at 100-percent bypass ratio, the concentration factor approaches 1.0, again assuming η_1 = 90%.

However, in each of these two protected pump designs, many other considerations are present, via trade-offs, and these are discussed later.

A second fundamental design approach is to eliminate the rotating pump completely and utilize a static system to pump the required scavenge flow, thus minimizing erosion.

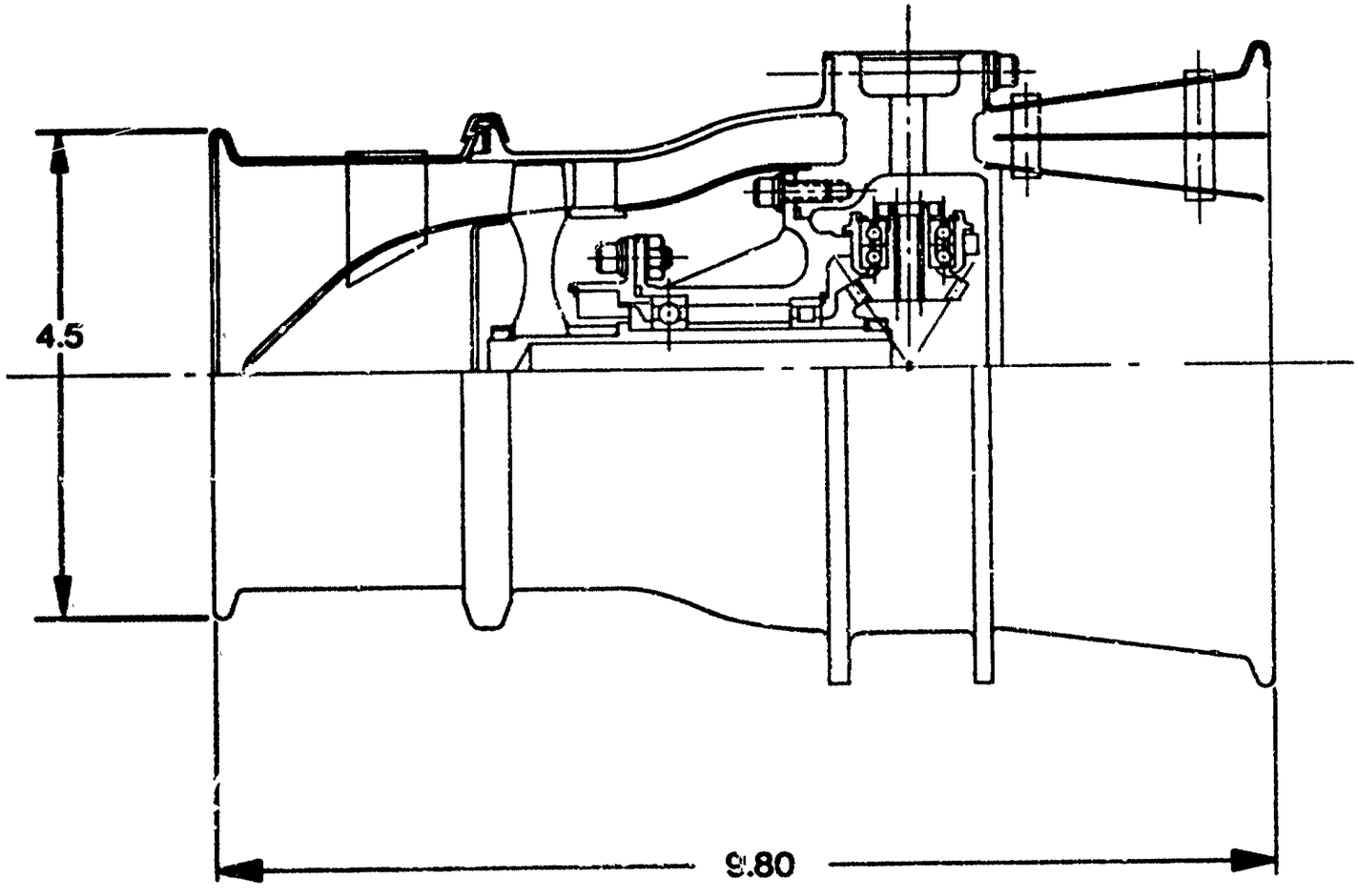

Figure 1. Conventional Blower Design.

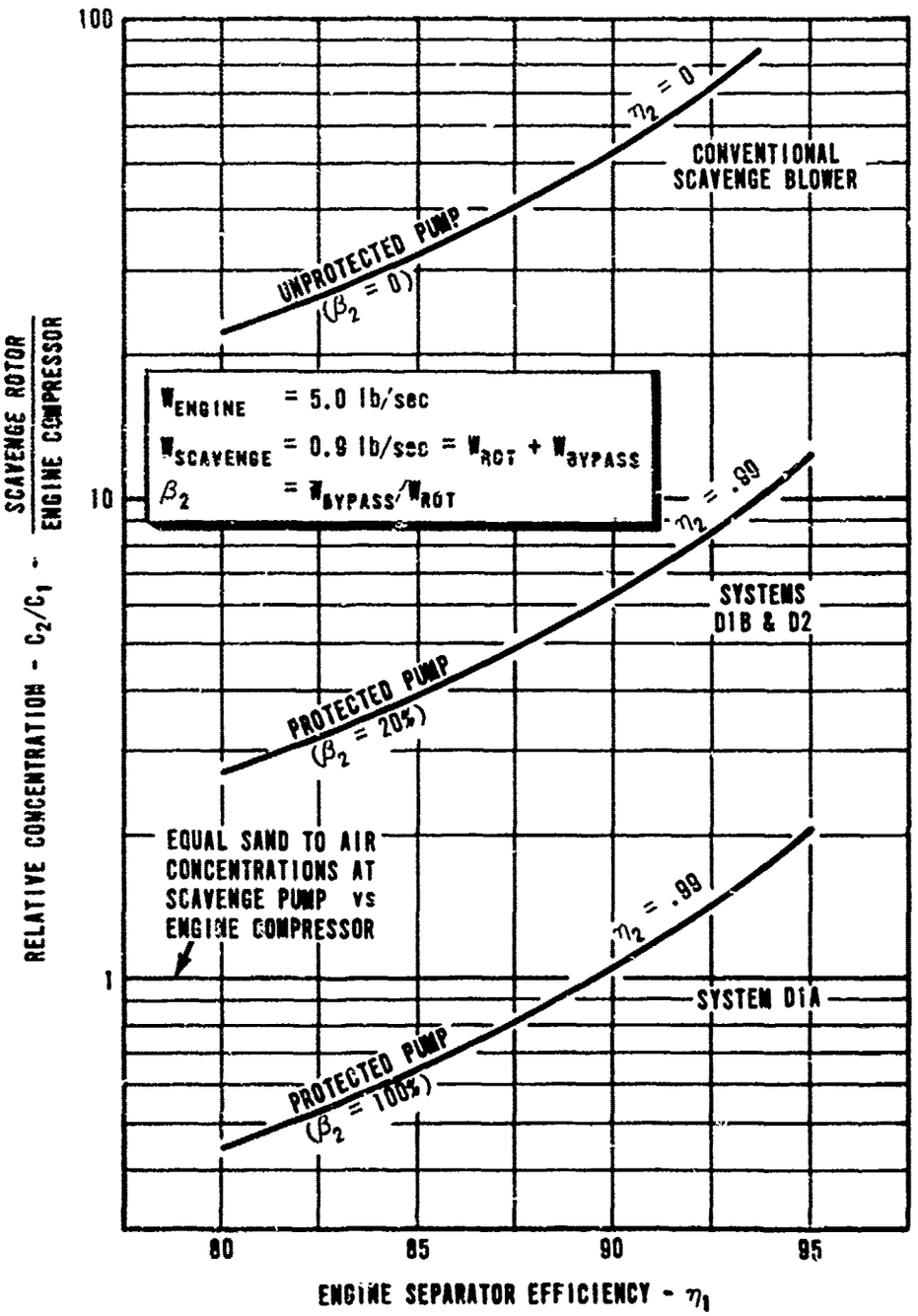

Figure 2. Relative Sand Concentrations as a Function of Engine Separator Efficiency.

CONCEPT FEASIBILITY STUDIES (TASK I)

GENERAL

The prime consideration throughout this program centered upon the aspect of durability, however, not to the exclusion of power consumption reliability, physical size, etc. This paraphrases the requirement that the scavenge pump should be a practical device in terms of application to an aircraft gas turbine. Overall practicality motivated the study of various design approaches, with careful attention to the weighting of relative merits as well as disadvantages.

In Task I, feasibility studies were conducted on several innovative concepts for engine particle separator scavenging systems. Based on aerodynamic studies for each system, flow path definitions and assessments of engine power penalties were evolved. Preliminary design layout drawings for each concept were prepared with sufficient detail to permit a competitive evaluation. In certain cases, particle trajectory analyses were used to provide an estimate of sand separation efficiency. The impact of engine/system integration was studied by using a typical advanced technology gas turbine as a basis.

For purposes of subsequent reference, the proposed systems are designated by alphanumeric prefixes according to the following definitions:

D1A - Self-Bypassing System (Mixed Flow Rotor)	Dynamic Systems (Primary)
D1B - Self-Bypassing System (Axial Rotor)	
D2 - Externally Bypassed System (Protected Fan)	
D3 - Vortex Tube Assembly	
S1A - Single Tube Ejector	Static Systems (Alternate)
S1B - Multiple Tube Ejector Assembly	
S2 - Engine Tailpipe Eductor	

The above systems are categorized into three groups for purposes of subsequent comparative discussion:

1.	Mechanically Driven	(D1A & D1B)
2.	Composite Mechanically Driven and Engine Flow Powered	(D2 & D3)
3.	Engine Flow Powered	(S1 & S2)

SELF-BYPASSING DESIGN CONCEPT

A preliminary design for a "self-bypassing" type of separator scavenging unit is shown in Figure 3. The salient features in this type of design are the utilization of an inertial bypass inlet to afford erosion protection to the rotor, and the use of an annular ejector (powered by the rotor exit flow) to expel the contaminated bypass air through the system exhaust. Prior to describing the specific details of two designs (D1A & D1B) that incorporate this feature, the concept will be discussed on a more general basis in terms of advantages or disadvantages which result when key system parameters are varied.

This type of system can be designed for a wide range of bypass ratios, that is, ratio of flow pumped by the ejector to that which is passed through the rotor. As the bypass flow rate is increased, the total pressure supplied to the ejector primary nozzle, and the required rotor input power, must also increase. The off-setting advantage, which results from high bypass is that sand separation efficiency is improved, thus favoring rotor durability. A trade-off results between power requirements and rotor durability, depending upon the bypass ratio selected for the system.

Figure 4 shows this trade-off expressed in terms of bypass ratio specifically for the two self-bypassing designs which were studied, namely Systems D1A and D1B. The vertical asymptote represents the extreme case of zero bypass ratio, and zero sand separation efficiency wherein all of the scavenged airflow is passed through the rotor as in the case of most scavenge blowers in use today. The only input power required is for sufficient headrise to overcome losses in exhausting the flow. For this purpose, a rotor pressure ratio of 1.08, at a rotor adiabatic efficiency of 0.70 was assumed. The low efficiency is consistent with a simple rotor design having relatively few blades, thick cross sections, blunt leading and trailing edges, and with castable tolerances.

As the bypass ratio is increased, progressively higher pressures are required at the ejector primary nozzle, but with the inherent advantage of continually improving the sand separation efficiency. At the labled design points, the magnitude of pressure ratio required classifies the type of rotor to be designed (based on 70-percent rotor adiabatic efficiency) as mixed flow for System D1A, and axial flow for System D1B. In all instances the total inlet airflow to the system is 0.9 lb/sec.

SYSTEM D1A - SELF-BYPASSING SYSTEM (MIXED FLOW CENTRIFUGAL)

This design (Figure 3) uses an inertial bypass inlet with a 1:1 rate of bypass flow, to afford substantial erosion protection to the mixed-flow compressor. An accelerating vane row downstream of the impeller serves to turn the flow to the axial direction where it provides primary air to the annular ejector.

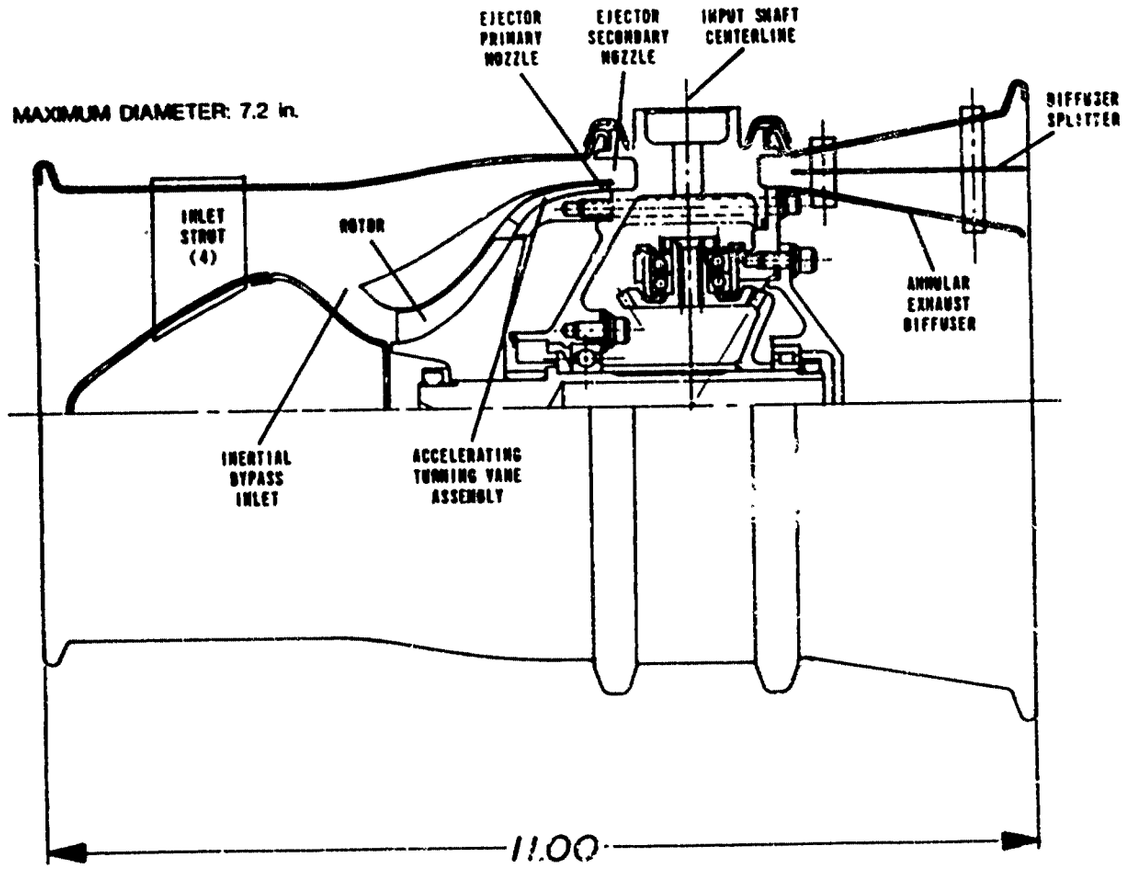

Figure 3. Preliminary Design - System D1A.

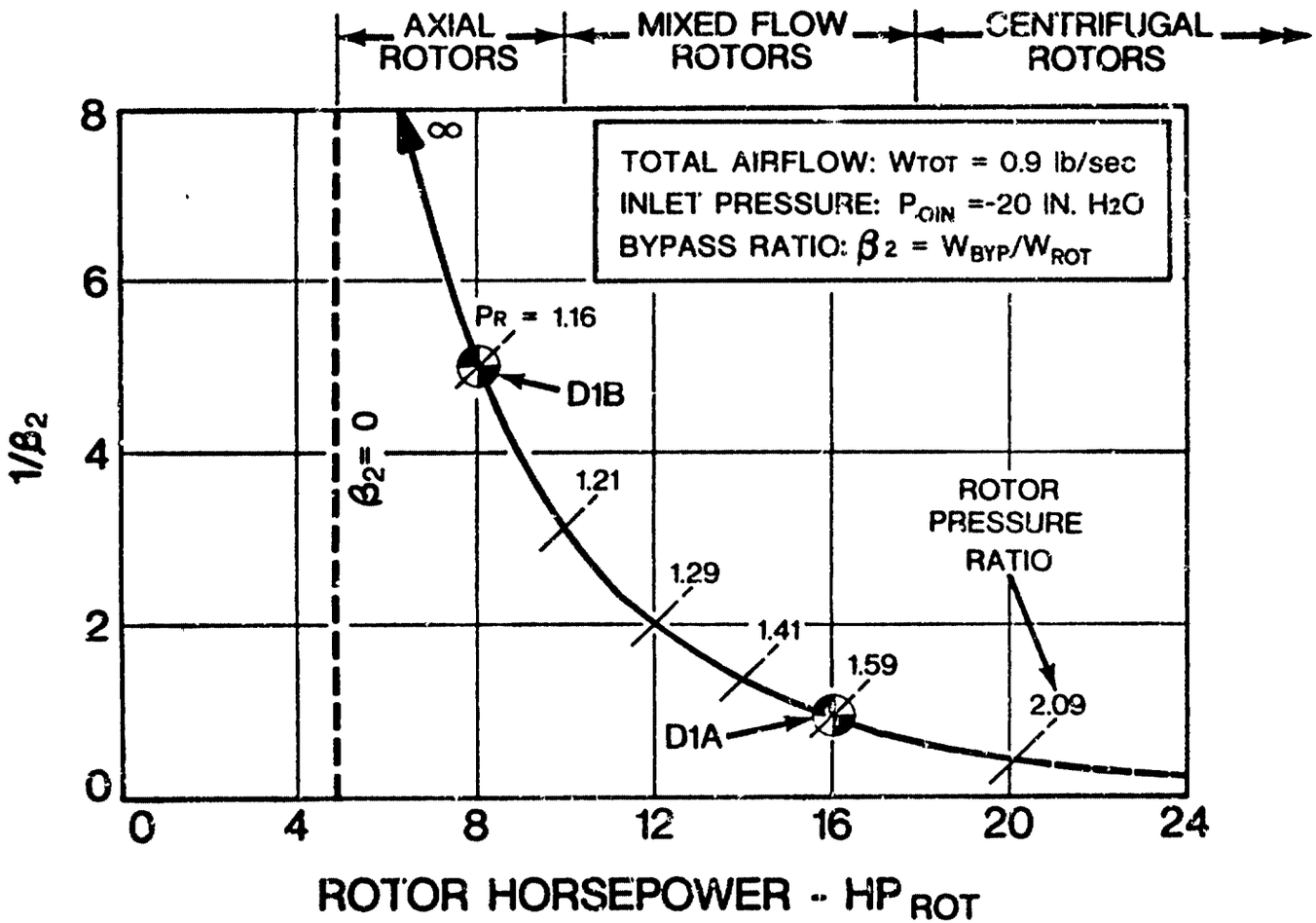

Figure 4. Bypass Ratio/Power Trade-Off (Self-Bypassing Design).

Analytical studies were made to determine the ejector performance as a function of mixing tube and diffuser geometry. Initially, the ratio of secondary flow area to primary flow area was varied (for fixed primary airflow conditions) until a sufficiently high secondary flow velocity was obtained, that is, adequate margin from recirculation of the secondary flow in view of the high headrise requirements of the ejector. Next, the length of the mixing tube was optimized for maximum secondary flow. Numerically, this optimum condition was found to occur at a mixing tube length which was approximately three times the tube hydraulic diameter. L/D_H values (length to hydraulic diameter) up to 5.0 were studied. Final adjustments to the system pumping capacity were made by varying the L/D_H and the exit area of the diffuser. From these studies, the following parameters were evolved:

Ejector Area Ratio - A_s/A_p	3.5
Primary Nozzle Mach Number - M_p	0.78
Mixing Tube L/D_H	3.0
Diffuser Area Ratio	3.8
Diffuser Recovery	0.78

The overall performance characteristics for this system are summarized in Table 1.

Nominally, this system is designed for a 1:1 bypass ratio; since only 50 percent of the inlet airflow passes through the rotor, this feature will favor high sand separation efficiency and durability, though at the expense of some increase in drive power as the ejector is now required to pump more flow. (Refer also to Figure 4.)

In order to obtain an estimate of the sand separation efficiency of the system inlet, a series of particle trajectories were computed, and the results are shown in Figures 5 through 9. From this analysis, it appears that particles which are above 15 μ in size will maintain sufficient inertia as to bypass the intake to the rotor. On that basis, the following calculated sand and dust separating efficiencies result:

MIL-E-5007C	AC COARSE	AC FINE
(Mean Size = 200 μ)	(Mean Size = 25μ)	(Mean Size = 7μ)
η_{SEP} =99%+	η_{SEP} = 92%	η_{SEP} = 80%

The above data is based on bypassing all particles above 15μ in diameter (from the trajectory analysis) and 50 percent of those particles under 15μ (based on 1.0 bypass ratio). This type of analysis generally results in optimistic efficiency prediction.

TABLE 1. PERFORMANCE CHARACTERISTICS - SYSTEM D1A

Total Inlet Flow	0.9 lb/sec
Inlet Total Pressure	-20 in. H_2O (13.98 psia)
Inlet Total Temperature	518.7°R
Bypass Flow	0.45 lb/sec
Rotor Flow	0.45 lb/sec
Bypass Ratio	1.0
Rotor Pressure Ratio	1.59
Engine Power Loss	2.1%
Rotor Speed	50,000 rpm
Ejector Primary Pressure	20.75 psia

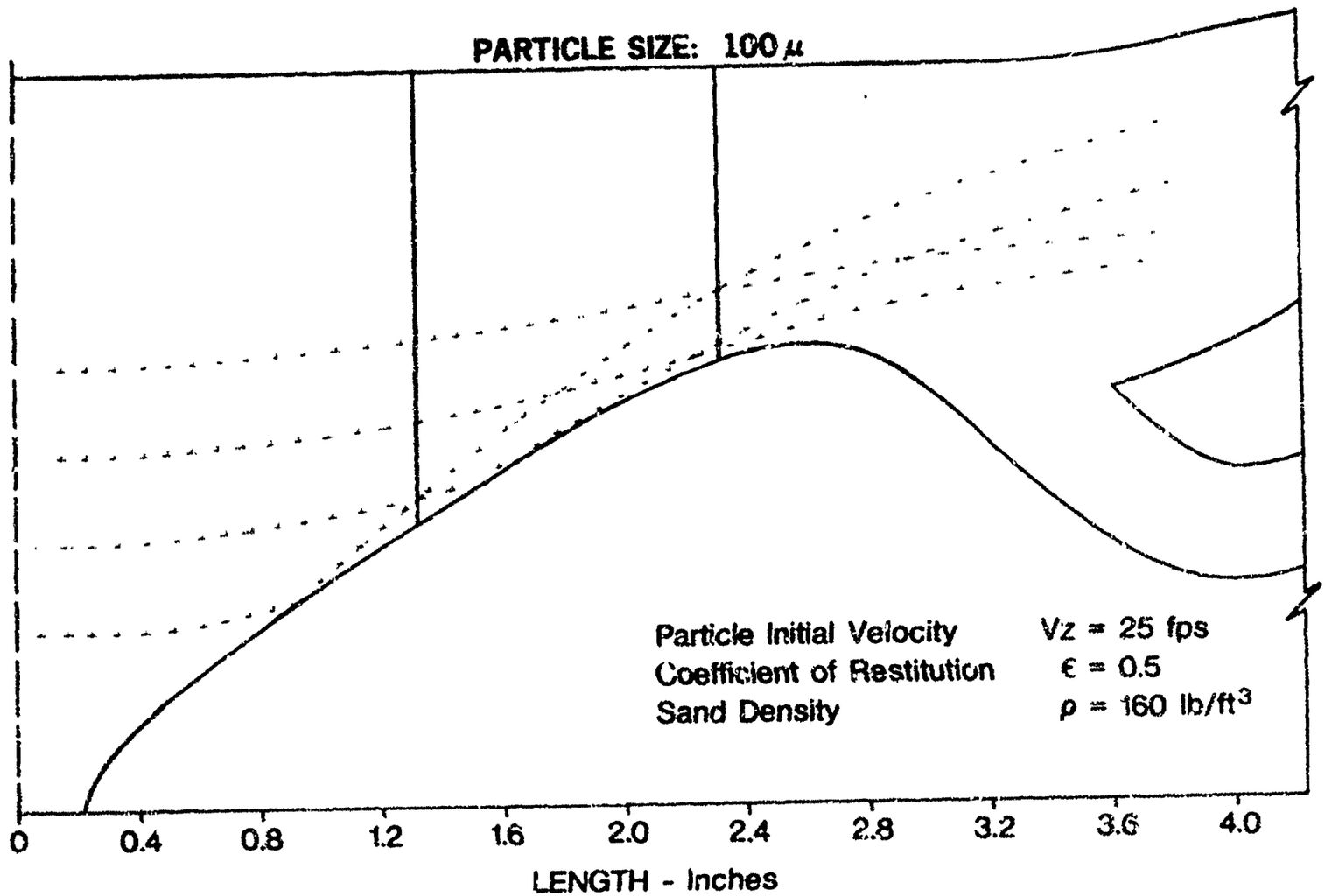

Figure 5. Particle Trajectory Analysis System DIA (100μ).

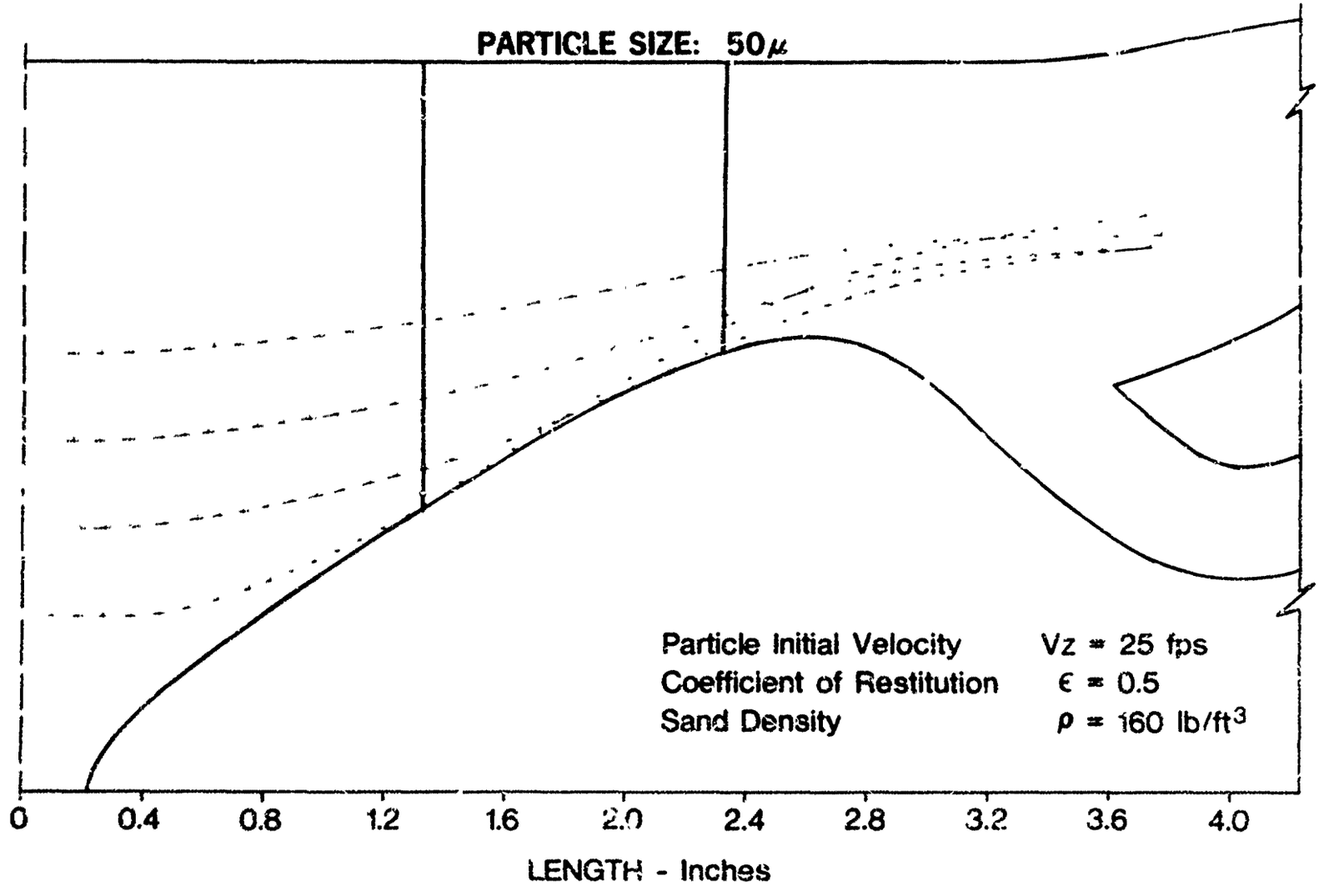

Figure 6. Particle Trajectory Analysis System D1A (50μ).

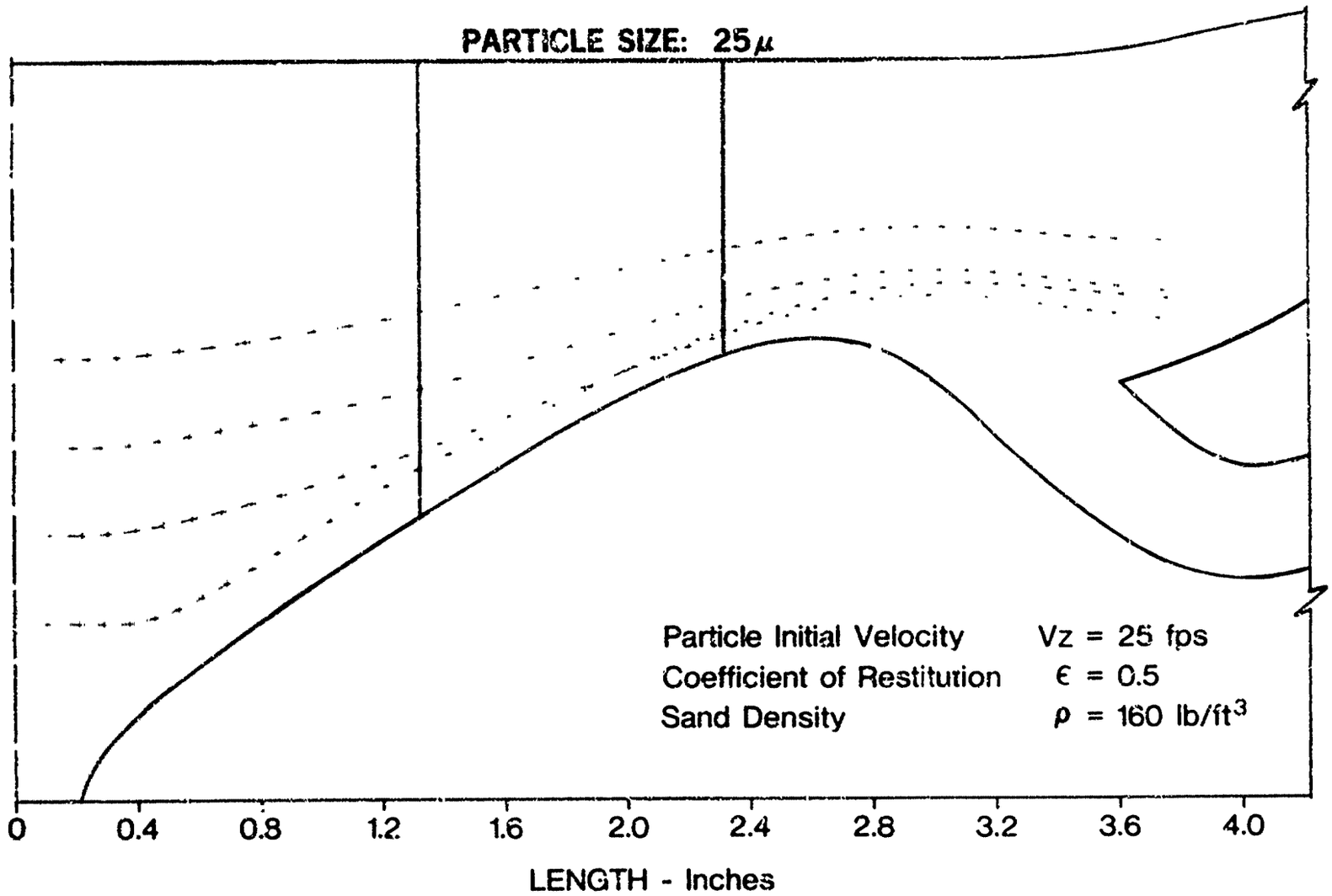

Figure 7. Particle Trajectory Analysis System D1A (25μ).

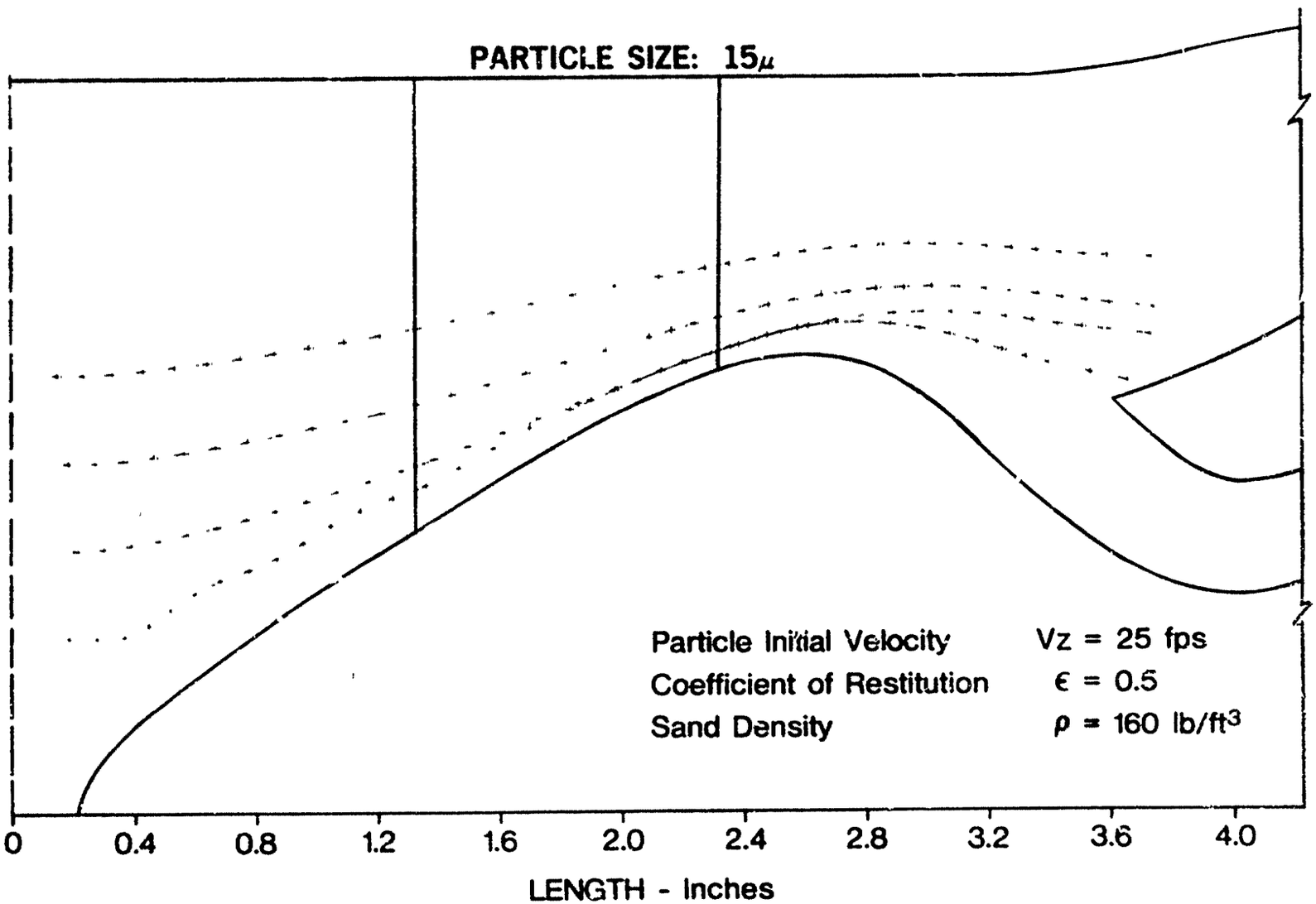

Figure 8. Particle Trajectory Analysis System D1A (15μ).

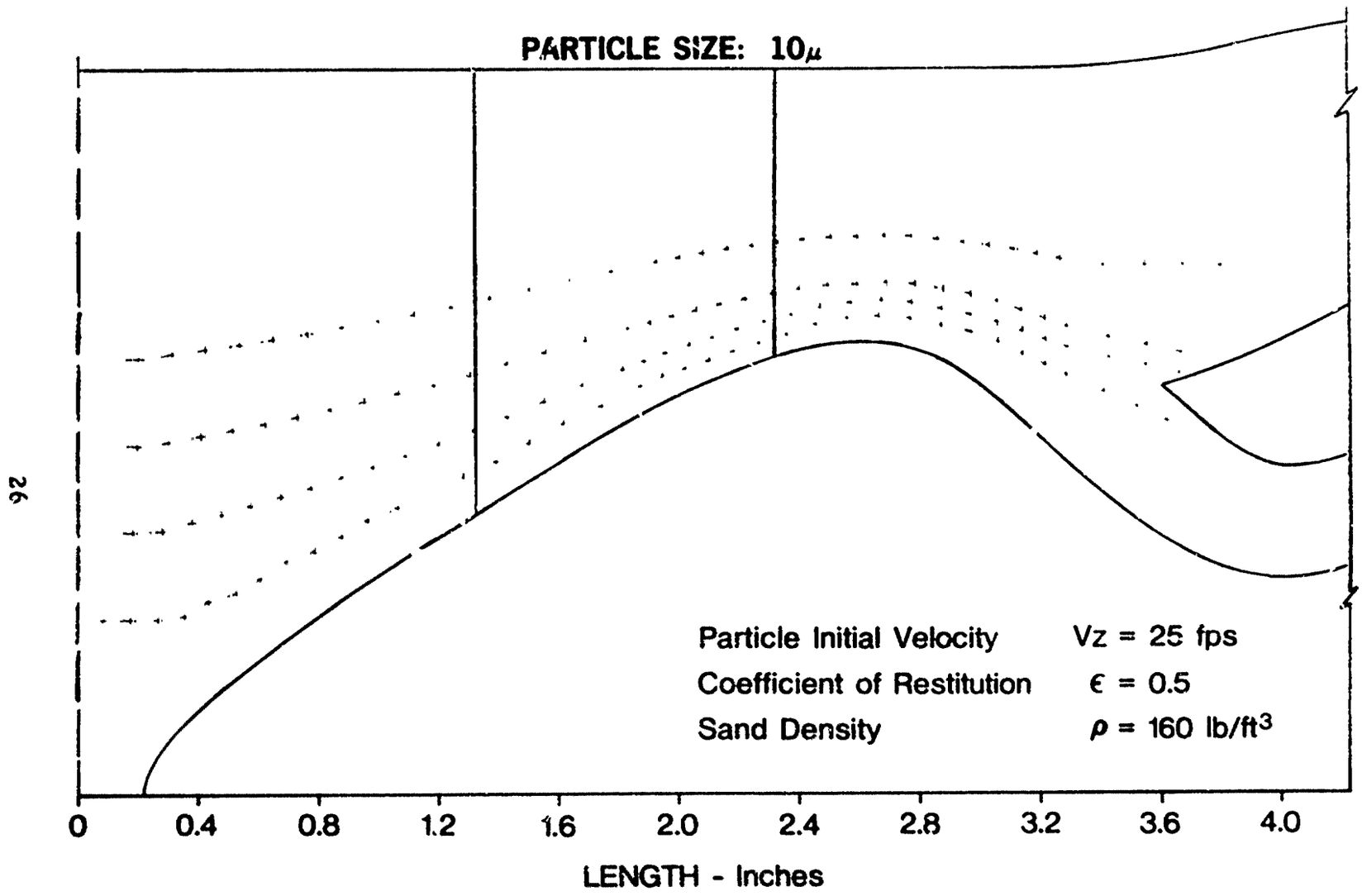

Figure 9. Particle Trajectory Analysis System D1A (10μ).

A mechanical drive arrangement using bevel gears is shown in Figure 3. As an alternative scheme, the feasibility of an axial flow air turbine drive was considered. On the basis of a simplified matching study, it was found that turbine blade heights became unreasonably small (under 0.100 in.) for rates of engine bleed air on the order of 2% (6.4% engine power loss). Conversely, to achieve more realistic channel heights (0.200 in.) would require low, off-optimum blade speeds of approximately 400 fps with a bleed air supply of 3.2% (10.2% engine power loss). Each of the preceding cases applies to a supersonic impulse turbine, restricted to only 15-percent partial admission. From this study, consideration of an air turbine drive appeared impractical.

The fundamental disadvantage to this design, relative to other concepts, lies in technical risk. The self-bypassing feature inherently involves interaction between the bypass airflow and the rotor airflow, with no means available to independently vary these parameters. Thus, uprating the system performance for development purposes requires major hardware changes. By contrast, a system whose bypass flow is independently controllable, might only require (as an example) an increase in bleed airflow to effect the required performance change. Another aspect of technical risk, particular only to the D1A design, is the small size of the channel height at exit from the turning vanes (0.075 in.). It was found that the ejector performance is sensitive to changes in nozzle channel height of approximately $\pm$.005 in., which is of the same order as the manufacturing tolerances on each wall contour ($\pm$.002 in.).

In summary, a prime advantage in this design is rotor durability, owing to high bypass ratio. Other significant advantages include relatively low power requirement, and compactness of the design in terms of minimal impact upon the engine envelope.

SYSTEM D1B - SELF-BYPASSING SYSTEM (AXIAL ROTOR)

This configuration (Figure 10) is similar to System D1A, except that the centrifugal stage is replaced with an axial rotor and stator assembly. By reducing the quantity of bypass air to be pumped by the annular ejector, this concept requires the least input power of all systems studied. Performance characteristics for this system are listed in Table 2.

The objective in formulating this particular concept was to obtain the required system pumping capacity of 0.9 lb/sec by utilizing the relatively low pressure ratio available from a single-axial stage. This would then require a high rate of mass flow through the ejector primary nozzle, but at a much lower velocity relative to the D1A design.

In analyzing the ejector, it was determined that for a secondary-to-primary area ratio of 0.84, and at a primary airflow of 0.75 lb/sec, the secondary airflow was 0.15 lb/sec, or 20-percent bypass flow. The total pressure required at the primary nozzle would be 15.80 psia, for a secondary supply pressure 20 in.H_2O below ambient (13.98 psia).

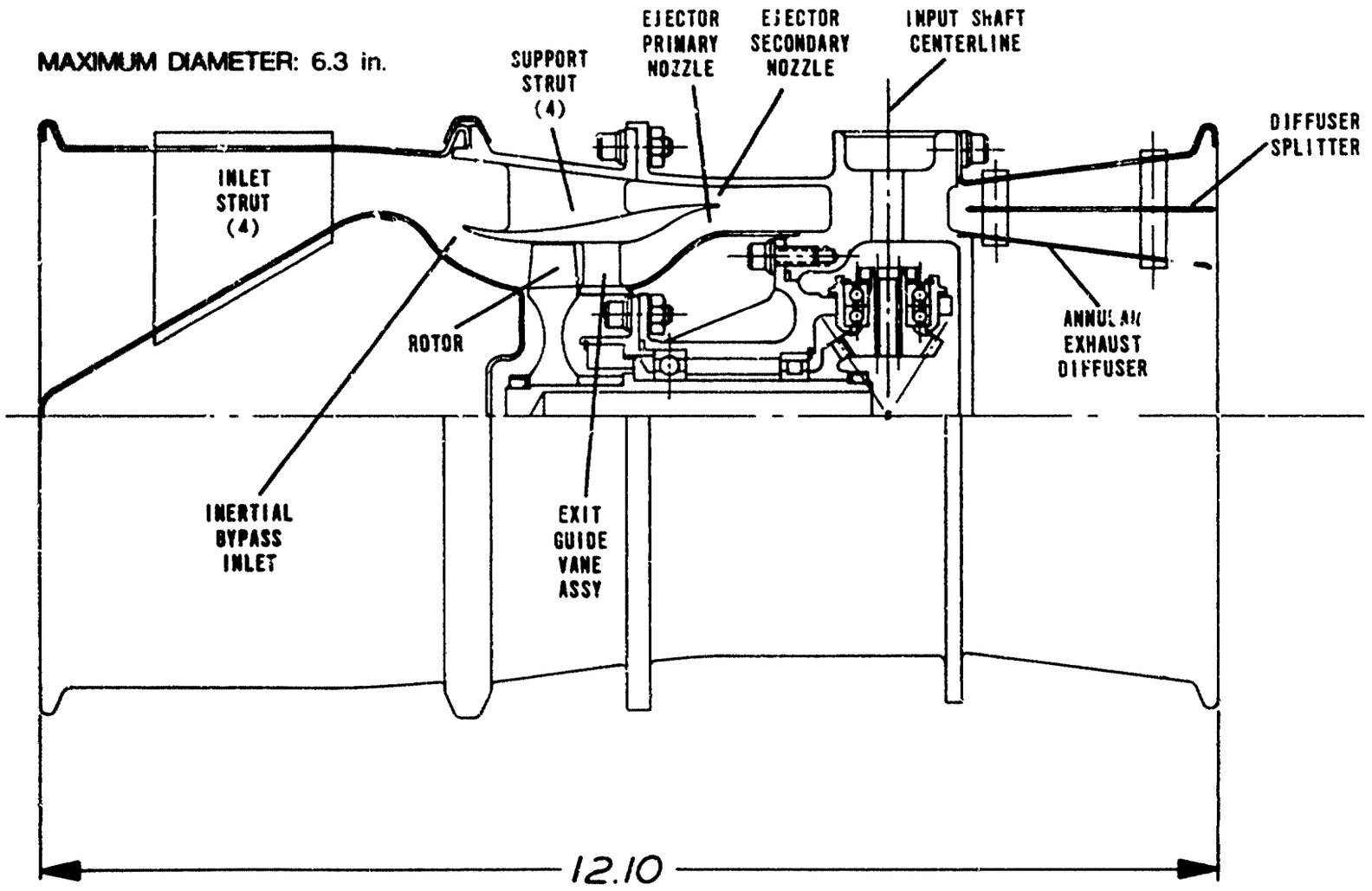

Figure 10. Preliminary Design - System D1B.

A general comparison of key rotor and ejector parameters for the D1A and D1B self-bypassing designs is given below:

PROPERTY	SYSTEM D1A	SYSTEM D1B
Primary Airflow - lb/sec	0.45	0.75
Primary Total Pressure - psia	20.75	15.80
Primary Mach Number	0.78	0.44
Primary Velocity - fps	910	507
Secondary Airflow - lb/sec	0.45	0.15
Bypass Ratio	1.0	0.20
Area Ratio - A_s/A_p	3.5	0.84
Rotor Exit Pressure - psia	22.23	16.22
Rotor Inlet Pressure (Secondary Supply Pressure) - psia	13.98	13.98
Rotor Pressure Ratio	1.59	1.16

For purposes of computing rotor power requirements (Tables 1 and 2), a rotor adiabatic efficiency of 70 percent was assumed in both cases.

By effecting a trade-off in power input and bypass ratio, system D1B would not exhibit the rotor durability characteristics of the high-bypass design of System D1A. However, in terms of cost, volume, and weight, the D1B design is more favorable. In considering other comparative criteria such as reliability, system failure impact, technical risk, maintainability, on/off and all-weather capabilities, and noise level, both designs are very similar.

Additional comments pertinent to the comparison of the self-bypassing designs to other concepts are given under "Rating Technique and Concept Selection", later in this report.

SYSTEM D2 - EXTERNALLY BYPASSED SYSTEM (PROTECTED FAN)

This design is the first of two concepts (D2 and D3) which require a combination of mechanical drive input and compressor discharge air. A preliminary design is shown in Figure 11. The design is similar to systems D1A and D1B, except that the compressor discharge air is used to power three ejectors, which motivate the bypass air.

TABLE 2. PERFORMANCE CHARACTERISTICS - SYSTEM D1B

Total Inlet Flow	0.9 lb/sec
Inlet Total Pressure	-20 in. H_2O (13.98 psia)
Inlet Total Temperature	518.7°R
Bypass Flow	0.15 lb/sec
Rotor Flow	0.75 lb/sec
Bypass Ratio	0.20
Rotor Pressure Ratio	1.16
Engine Power Loss	1.1%
Rotor Speed	50,000 rpm
Ejector Primary Pressure	15.80 psia

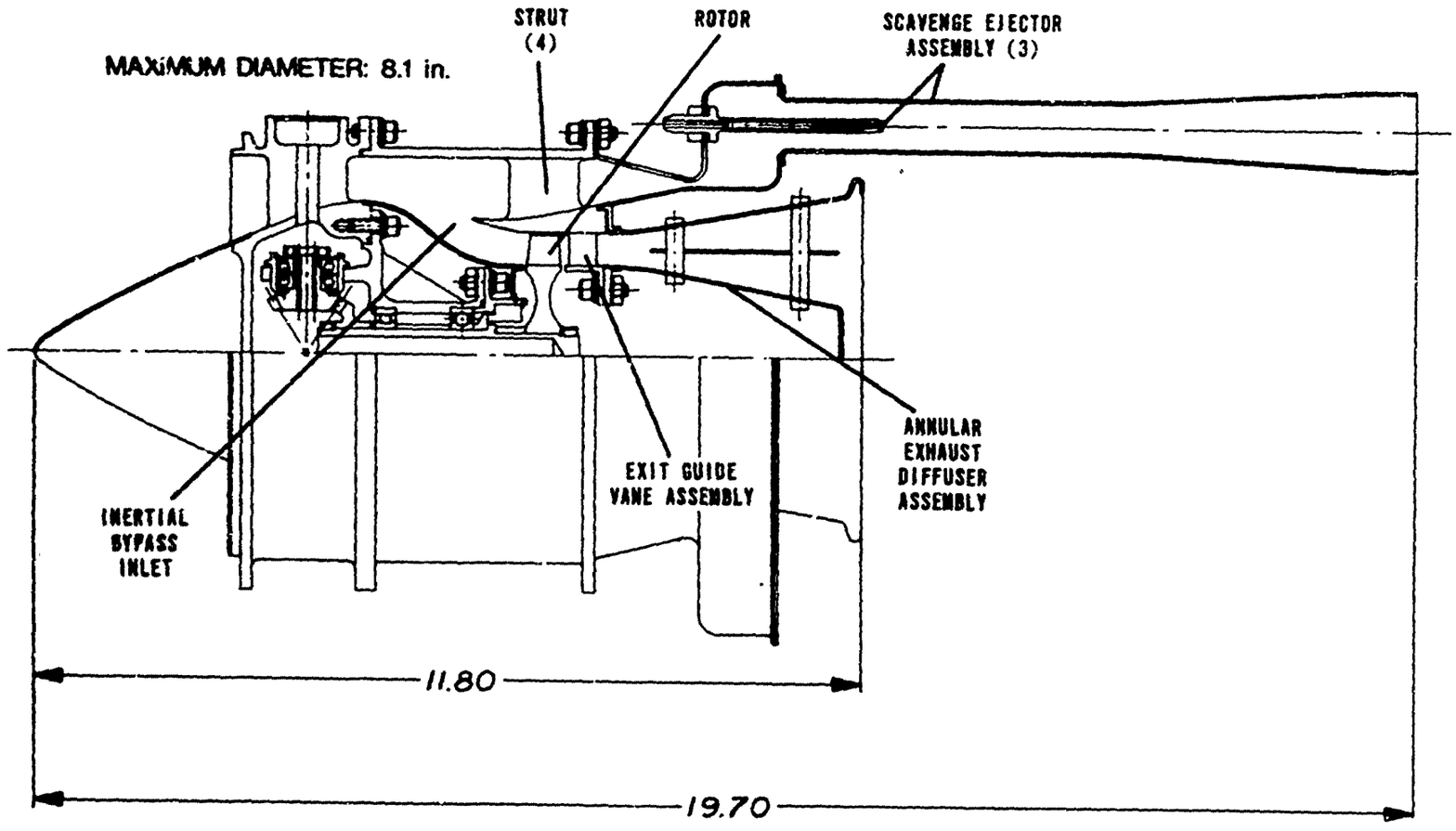

Figure 11. Preliminary Design - System D2.

The system flow characteristics for this design are based upon existing engine separator technology. Consequently, technical risk is low in that components of known performance are used. On that basis, it has been demonstrated that 90-percent sand separation efficiency can be achieved in an inertial bypass separator using 15-percent of the total flow as bypass air. Further, the inherent segregation of primary and bypass air in this type of design provides a relatively clean air exhaust which may be applied for various cooling purposes.

Power requirements for this type of system will be somewhat higher than the "self-bypassing" designs since engine air bleed is utilized. (Refer to Table 3.)

Although a reasonably high sand separation efficiency is attainable, durability would be compromised. If 90-percent efficiency is assumed for both engine separator and scavenge system, then for a given quantity of sand ingested by the engine, 10 percent will reach the compressor, 9 percent will pass through the scavenge rotor, and 81 percent will be discharged through the ejectors. (Refer to Figure 2.) However, the concentration of sand to air is six times higher at the scavenge pump than at the engine compressor for the specific airflows involved; in order for the relative concentrations to be equal, a 98-percent efficiency would be required in the scavenge system. Higher separation efficiencies could also be achieved in the "externally bypassed" system by increasing the bypass ratio analogous to the D1B versus D1A "self-bypassing" designs. Improvements in durability could be attained, but at substantial engine power penalties since the bleed rate must be increased.

The ejectors which are used to pump the overboard bypass air are scaled from the single-tube ejector design discussed subsequently under System S1.

Principal advantages offered by this design approach are clean air exhaust availability, moderate power requirements for low rates of bypass, and low technical risk. Durability, however, is compromised due to the low bypass ratio. Since in effect, two independent subsystems are present, reliability must be judged as lower than the self-bypassing designs, and markedly lower than the simplistic designs which utilize ejectors alone. (Refer also to "Rating Technique and Concept Selection".)

SYSTEM D3 - VORTEX-TUBE ASSEMBLY

This concept, shown in Figure 12, can be designed to mate directly to any specified annular engine particle separator. An annular arrangement of vortex tubes is used to separate out the contaminants, which are then collected and discharged by three ejectors, while the clean air is exhausted by means of a conventional blower.

TABLE 3. PERFORMANCE CHARACTERISTICS - SYSTEM D2

Total Inlet Flow	0.9 lb/sec
Inlet Total Pressure	-20 in. H_2O (13.98 psia)
Bypass Flow	0.15 lb/sec
Rotor Flow	0.75 lb/sec
Bypass Ratio	0.20
Rotor Fressure Ratio	1.10
Engine Power Loss	2.7%
Rotor Speed	50,000 rpm
Bleed Rate	0.6%
Ejector Primary Pressure	184 psia
Ejector Primary Temperature	1210°R

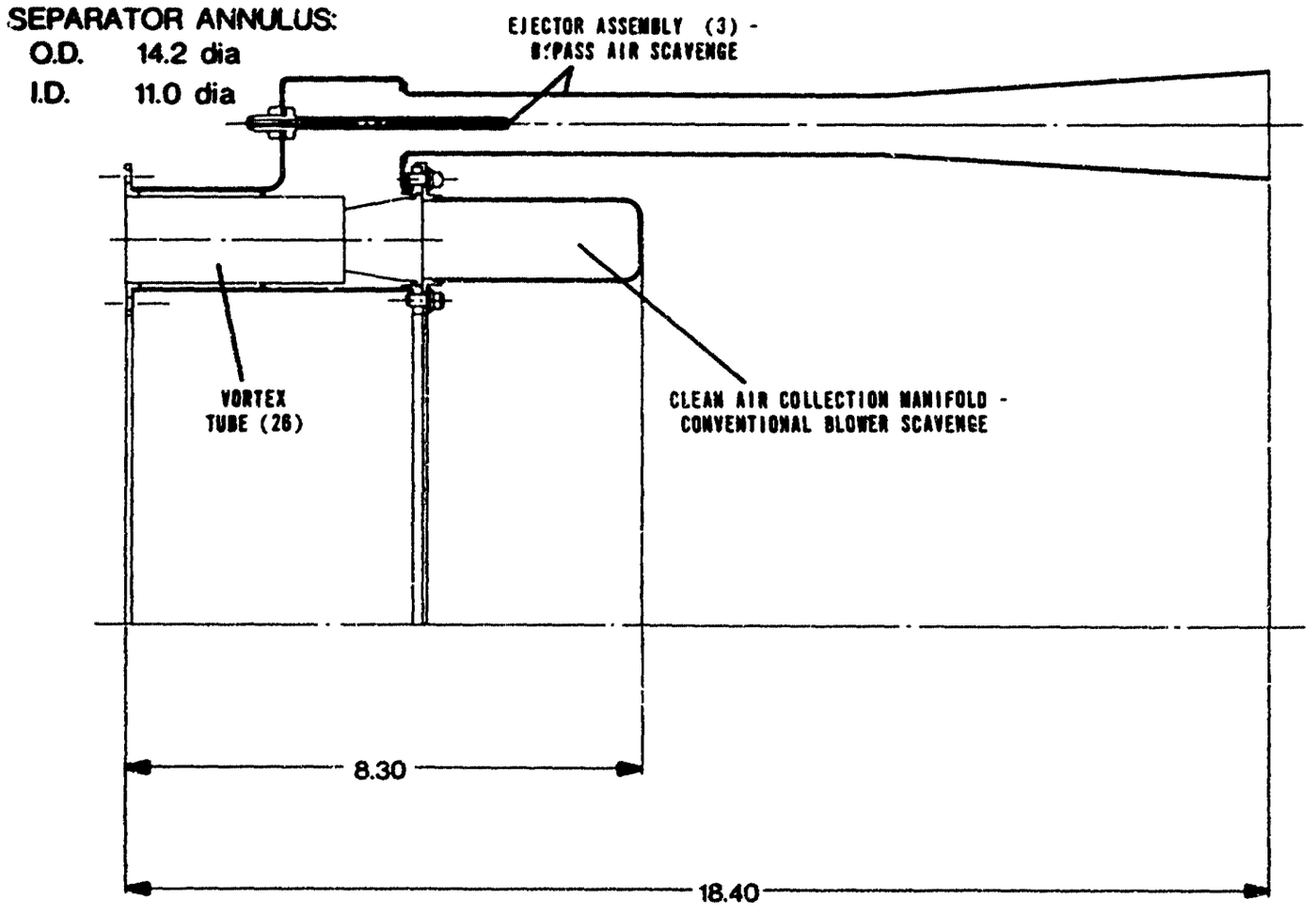

Figure 12. Preliminary Design - System D3.

The individual vortex tubes are 1-1/2 inches in diameter by 4 inches in length. At a total inflow of 0.9 lb/sec (760 cfm at 13.98 psia), 26 tubes are required, with a resulting pressure loss of 8 inches of water. Minimum requirements for the clean air scavenge blower would be 0.8 lb/sec (675 cfm) pumping capacity, at a headrise of 28 in. H_2O.

System drive power requirements are comparable to Configuration D2. (Refer to Table 4.) In relation to all other systems, engine power penalty is intermediate. Since all components in this system utilize existing technology, little technical risk is involved. As with System D2, clean air exhaust is also available for cooling purposes.

One disadvantage to this system lies in all-weather operation. Materials used in the fabrication of vortex tubes preclude the possibility of anti-icing.

SYSTEMS S1A AND S1B - SINGLE-TUBE/MULTIPLE - TUBE EJECTOR ASSEMBLY

This concept (the first of two designs which are solely engine-flow powered) utilizes a single-tube, supersonic ejector of high bypass ratio, or an equivalent multiple-tube assembly, in order to provide the required separator scavenge flow rate. Preliminary mechanical designs for this configuration are shown in Figures 13 and 14, and the performance characteristics appear in Table 5.

Based on the fundamental simplicity of the ejector concept, many advantages are offered, among which are low cost and weight, high reliability and durability, inherent on/off capability, and minimal noise addition to the engine.

Its disadvantages stem from the relatively high rate of bleed required, resulting in high power penalty and, in the event of failure, potentially significant effect upon the compressor operating point. Maintainability is considered to be low with respect to other systems, since (excepting the primary nozzle) repairs will require virtual replacement of the entire unit.

The aerodynamic studies of the ejector followed the same general sequence as described earlier under the D1A and D1B designs. The primary nozzle is axisymmetric and is designed for an exit Mach number of 2.53. Choice of Mach number was based upon achieving slightly under-expanded conditions at the nozzle exit, that is, a slightly higher primary nozzle static pressure relative to the pressure within the secondary nozzle. Under these conditions, maximum primary velocity is sustained. Higher Mach numbers, by comparison, could cause shock waves to be present within the system, resulting in a reduced secondary flow.

TABLE 4. PERFORMANCE CHARACTERISTICS - SYSTEM D3

Total Inlet Flow	0.9 lb/sec
Inlet Total Pressure	-20 in. H_2O (13.98 psia)
Vortex Tube Scavenge Flow	0.1 lb/sec
Rotor Flow	0.8 lb/sec
Rotor Pressure Ratio	1.10 lb/sec
Engine Power Loss	2.4%
Rotor Speed	50,000 rpm
Bleed Rate	0.5 %
Ejector Primary Pressure	184 psia
Ejector Primary Temperature	1210°R

MAXIMUM DIAMETER: 6.1 in.

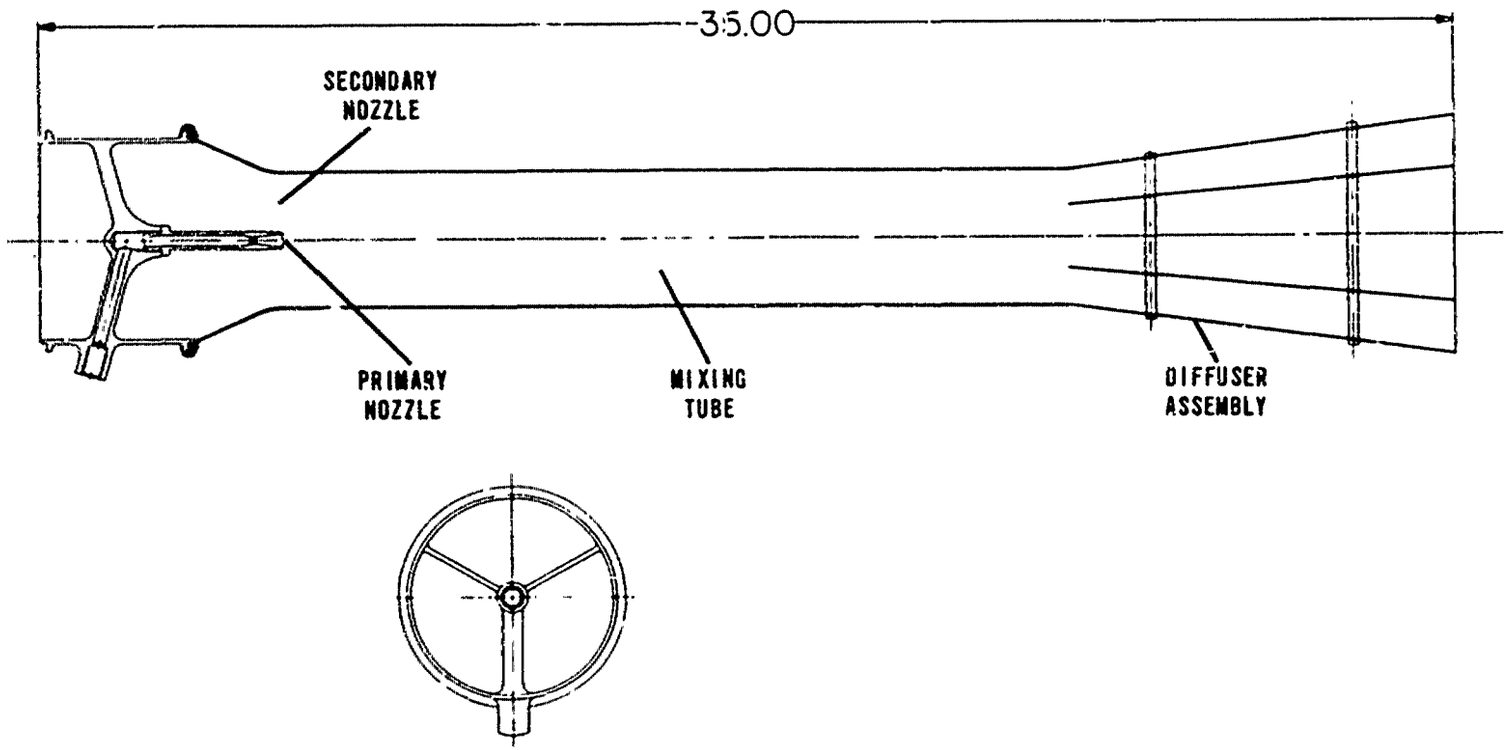

Figure 13. Preliminary Design - System S1A.

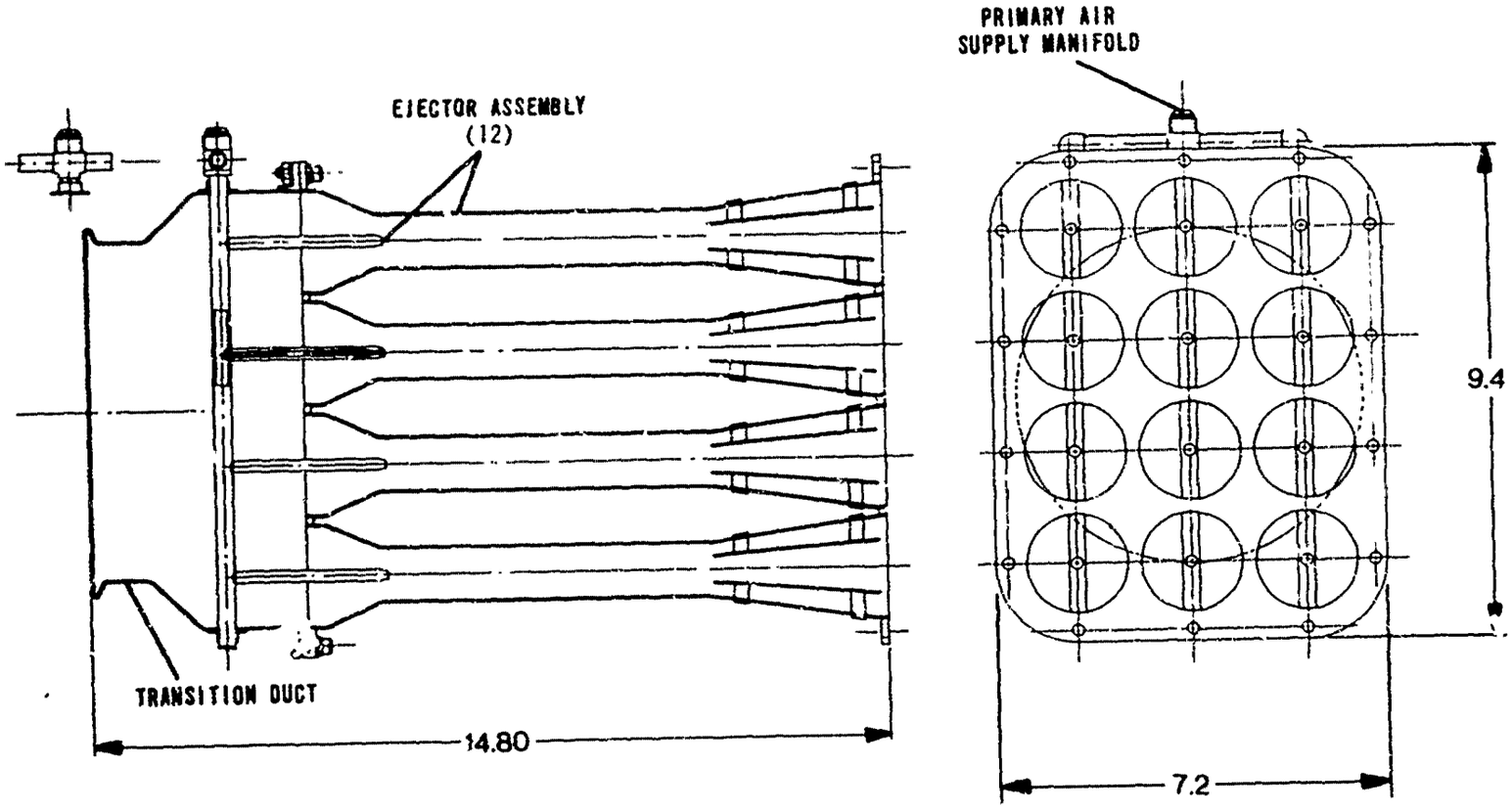

Figure 14. Preliminary Design - System S1B.

TABLE 5. PERFORMANCE CHARACTERISTICS - SYSTEM S1	
Secondary Flow Rate	0.9 lb/sec
Secondary Supply Pressure	-20 in. H_2O (13.98 psia)
Primary Flow Rate	0.1 lb/sec
Engine Power Loss	6.4 %
Bleed	2.0%
Primary Supply Pressure	184 psia
Primary Supply Temperature	1210°R

Analysis of the ejector indicated that for the available supply conditions, the optimum mixing-tube length is approximately six times the hydraulic diameter. In summary, the following key parameters resulted from the system study:

Primary Airflow - lb/sec	0.1
Primary Total Pressure - psia (Given)	184
Primary Total Temperature - ^{o}R (Given)	1210.
Primary Nozzle Exit Mach Number	2.33
Primary Nozzle Exit Velocity - fps	2775.
Secondary-to-Primary Air Ratio - A_s/A_p	100
Secondary Airflow - lb/sec	0.9
Entrainment Ratio	9.0:1
Mixing Tube L/D_H	6.0
Diffuser Area Ratio	3.5
Diffuser Recovery - (One Splitter)	0.75
Diffuser Exit Velocity - fps	160.

In Figure 15, the secondary flow pumped by the ejector is shown as a function of percentage of bleed. For a given percentage of bleed, an influence coefficient for determining engine power decrement is obtained from the data given in Figure 16.

After the aerodynamic design is established for the single-tube ejector, an equivalent multiple-tube design is obtained by directly scaling the primary and secondary airflows, maintaining the same area ratios, and the mixing tube length to the hydraulic diameter.

As the number of tubes is increased, the limiting criterion becomes the throat diameter of the primary nozzle. If this minimum diameter is set at 0.060 in., then 12 tubes would be the maximum. Figure 17 shows a relationship between nozzle throat diameter and number of tubes, for fixed primary pressure and flow rate.

Relative to the single-tube unit, the multiple-tube assembly offers a high degree of flexibility in that any number of compact packaging arrangements are possible.

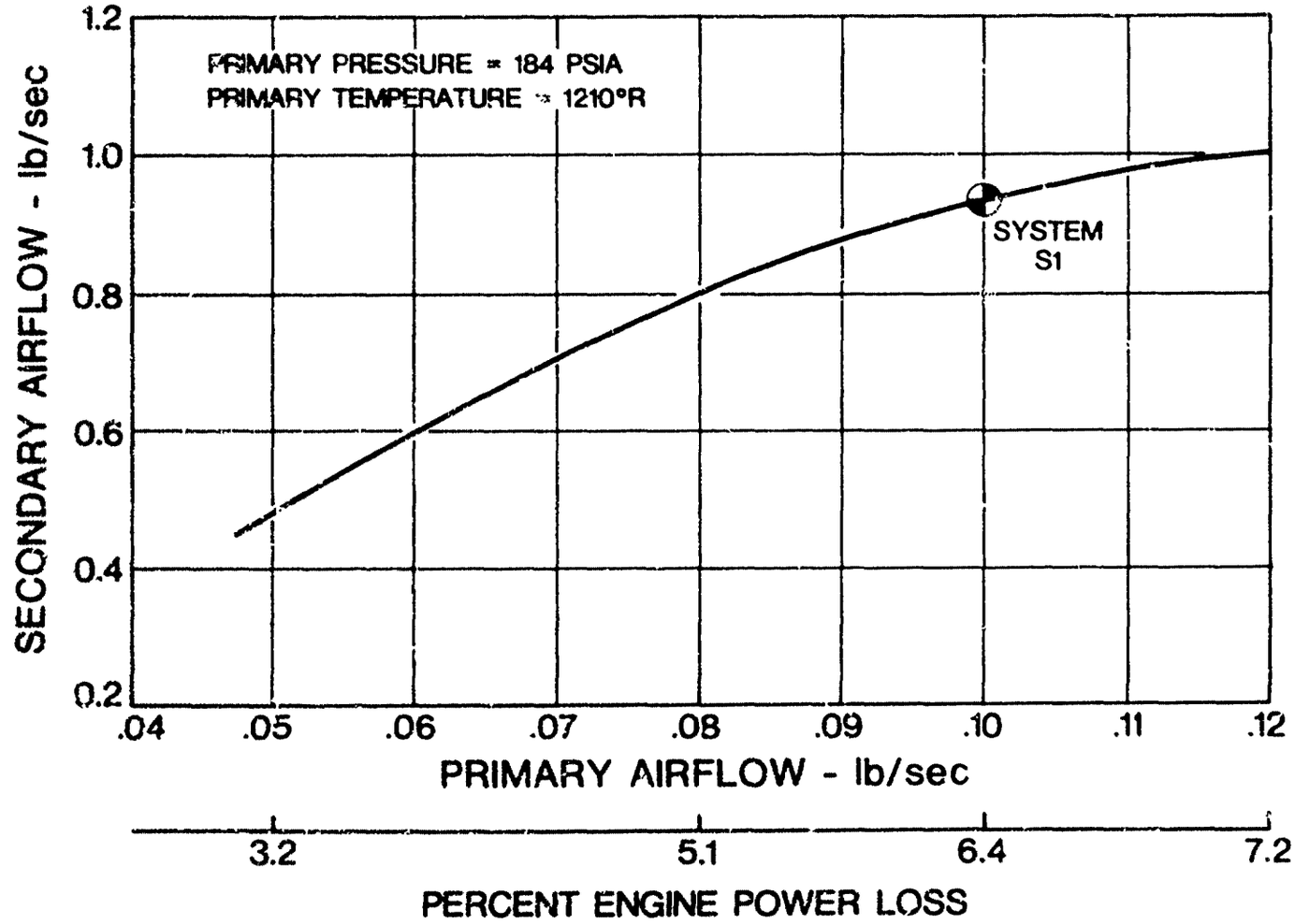

Figure 15. Ejector Study - System S1.

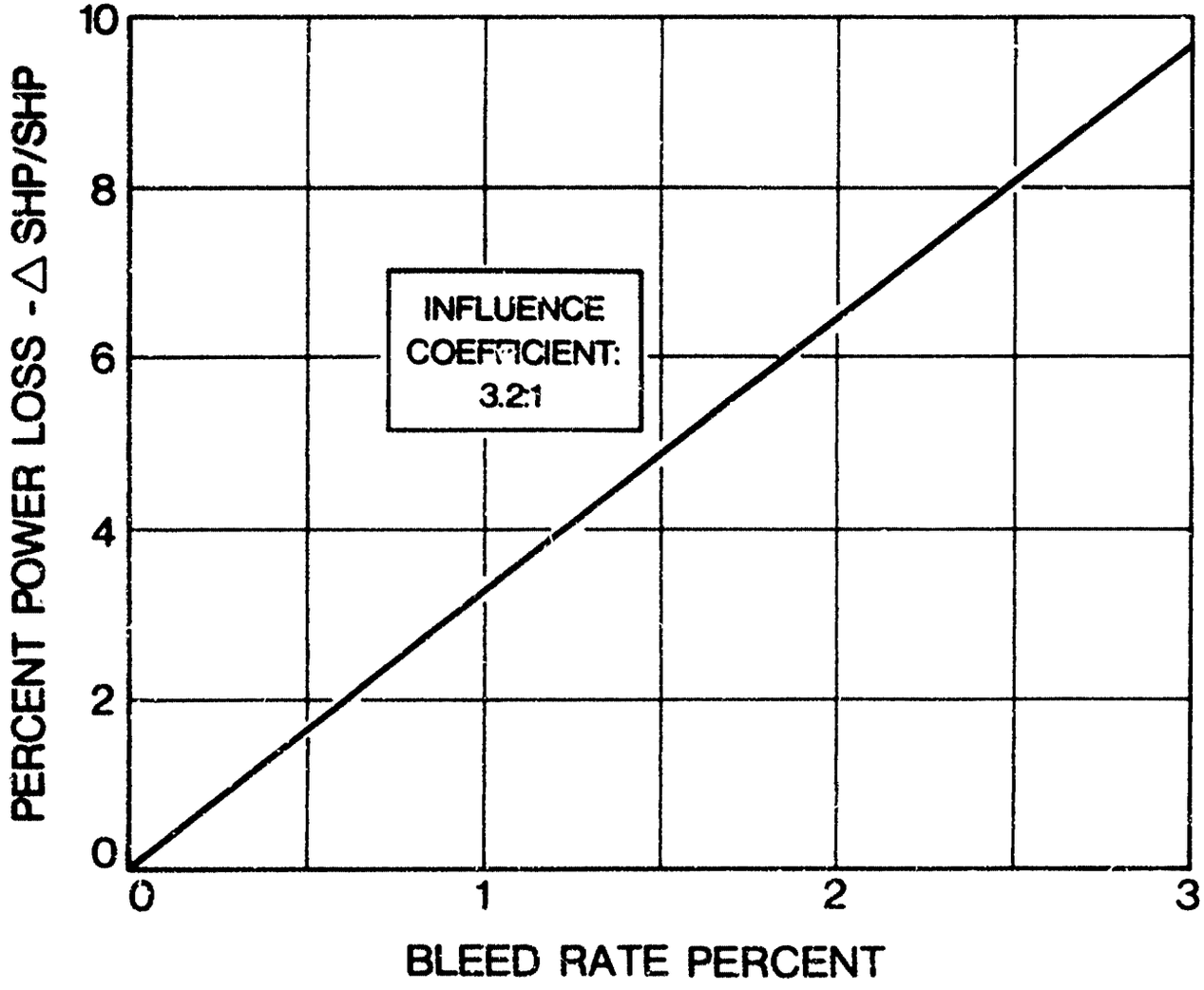

Figure 16. Bleed Effect on Engine Power.

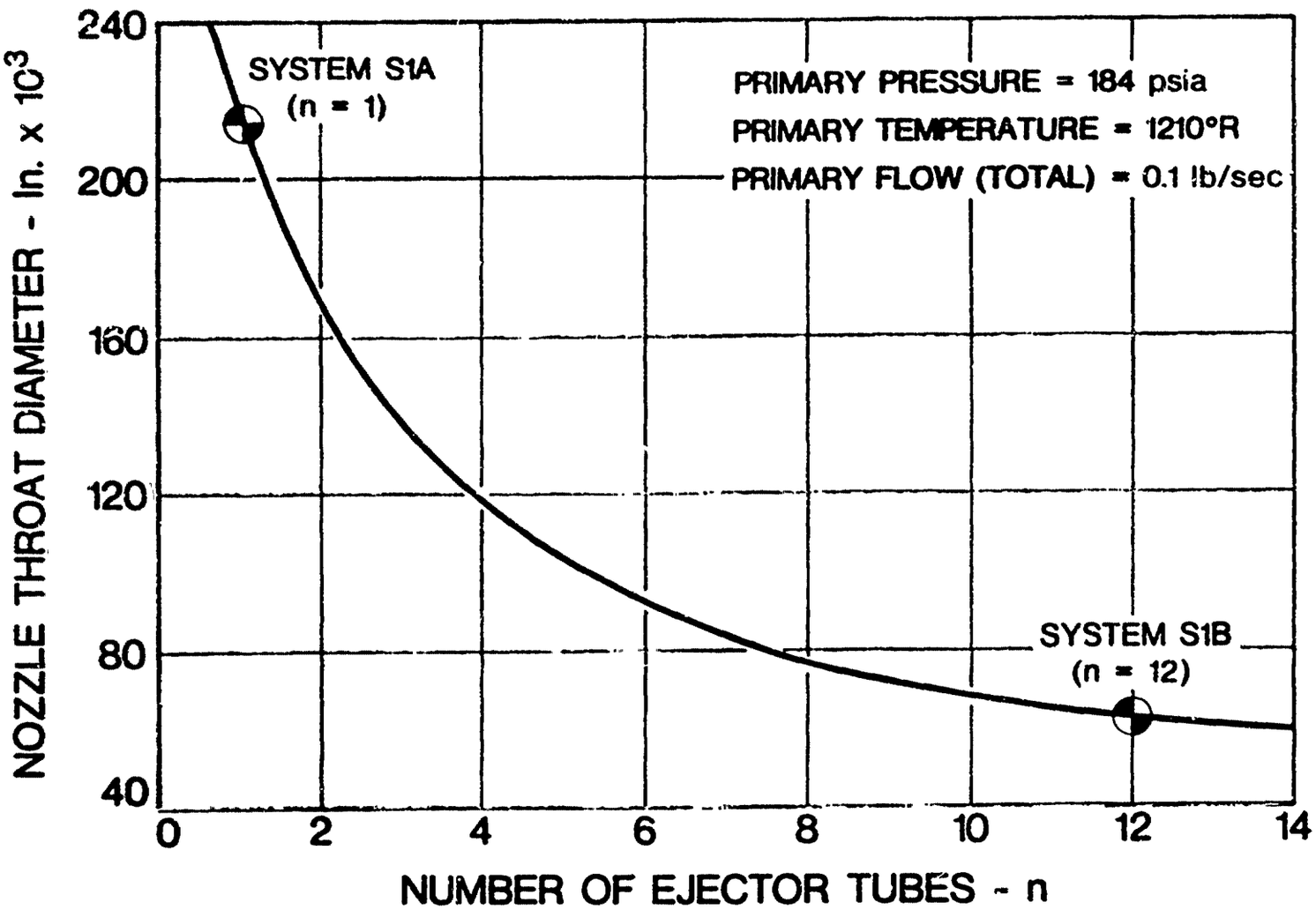

Figure 17. Nozzle Throat Diameter Liminations - System Si.

SYSTEM S2 - ENGINE TAILPIPE EDUCTOR

Utilization of an engine exhaust driven ejector, as shown in Figure 18, offers considerable advantages in terms of reliability, durability, low technical risk, and noise level addition to the engine.

In general, this type of system is best applicable where headrise requirements are low. Since the scavenge unit under consideration must pump against a minimum of 20 in. H_2O headrise, the required power turbine exit pressure results in high power penalty to the engine. (Refer to Table 6.)

The power loss in Table 6 is based upon the percentage difference between power turbine exit total pressure, and the ambient air static pressure. The net figure is more realistic in that it represents the additional loss which the eductor would cause, over and above a "standard" engine equipped with a diffuser having 3-percent (typically) total pressure loss.

Summarizing the design point parameters for the eductor:

Primary Gas Flow Rate - lb/sec	5.06
Primary Total Pressure - psia	15.95
Primary Total Temperature - ^{o}R	1550.
Primary Mach Number	0.48
Primary Velocity - fps	904.
Secondary Airflow - lb/sec	0.9
Secondary-to-Primary Area Ratio - A_s/A_p	0.49
Mixing Tube L/D_H	2.5
Diffuser Area Ratio	3.6
Diffuser Recovery	0.73

Although the overall length of the system was minimized by addition of splitters to the diffuser and by optimizing the mixing tube length, the engine envelope is still increased on the order of 100 percent if the eductor is treated as part of the engine, rather than a given installation.

Other significant disadvantages to this approach appear in cost (material and fabrication), weight, and poor maintainability.

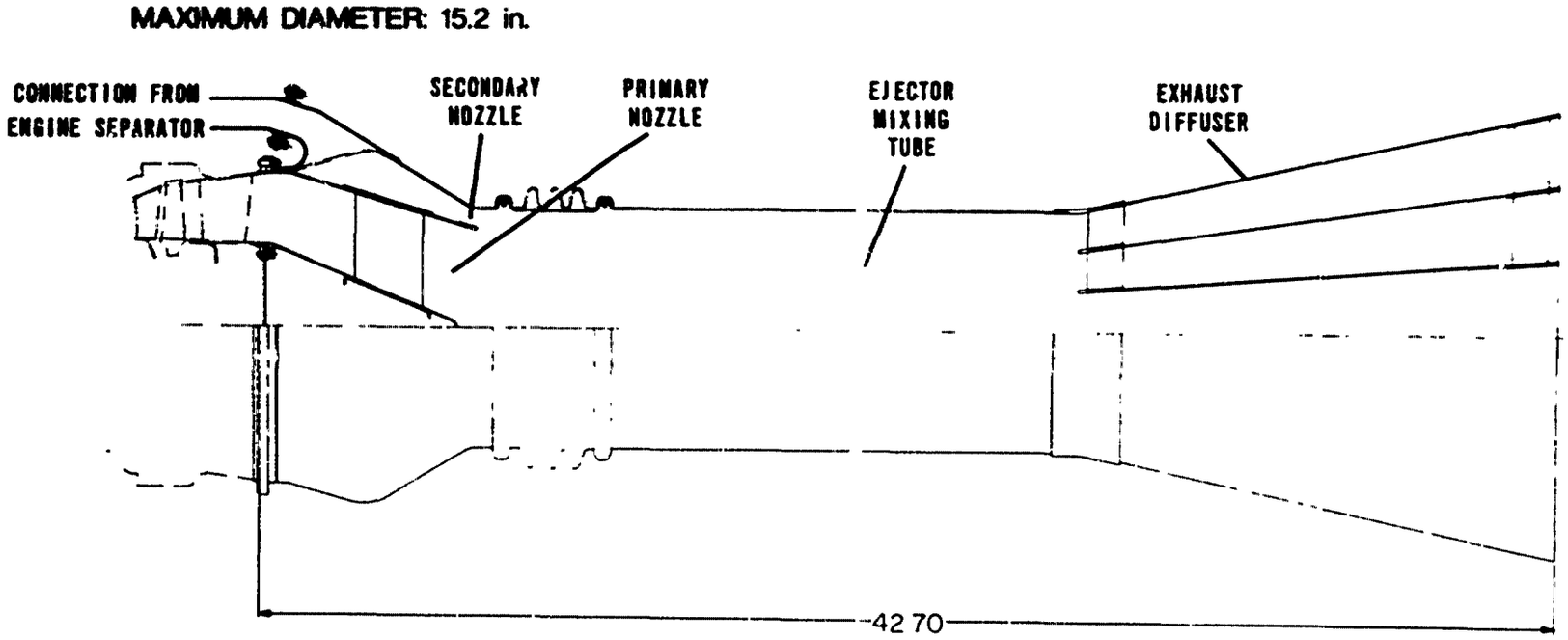

Figure 18. Preliminary Design - System S2.

TABLE 6. PERFORMANCE CHARACTERISTICS - SYSTEM S2

Secondary Flow Rate	0.9 lb/sec
Secondary Supply Pressure	-25 in. H_2O (13.80 psia)
Primary Flow Rate	5.06 lb/sec
Engine Power Loss	8.2% (5.2% Net)
Primary Supply Pressure	15.95 psia
Primary Supply Temperature	1550°R

MECHANICAL DESIGN - SYSTEMS IN GENERAL

The types of components common to all mechanically driven systems are summarized below, with comments as to materials, and proposed methods of fabrication:

	COMPONENT	METHOD OF FABRICATION
1.	Inlet Ducting	Formed sheet metal; flow-path defined by inner and outer shrouds.
2.	Rotor	Investment casting
3.	Support Housings	Investment casting
4.	Drive Elements	Machined
5.	Exhaust Diffusers	Seam-welded tubing, brazed support struts; splitters treated with tungsten carbide wear coating.

For the static systems:

	COMPONENT	METHOD OF FABRICATION
1.	Ejector Primary Nozzle	EDM internal nozzle contour; externally hard-coated.
2.	Ejector Secondary Nozzle	Seam welded, formed sheet metal tubing.
3.	Mixing Tube	Seam welded, formed sheet metal tubing.

In general, consideration has been given, where possible, to the removal of structural members from the flow path, or to structuring them such that wear has little or no ill effect upon integrity or flow efficiency.

INTEGRATION/INSTALLATION CONSIDERATIONS

Figure 19 shows the approximate envelope requirements for the six systems under investigation. All systems, except D3, which will mate directly to an annular separator exhaust, require transition ducting from the separator to the scavenge pump inlet.

For the concept study, mechanically driven systems or subsystems are engine oil lubricated, bevel gear driven, and configured with an axial

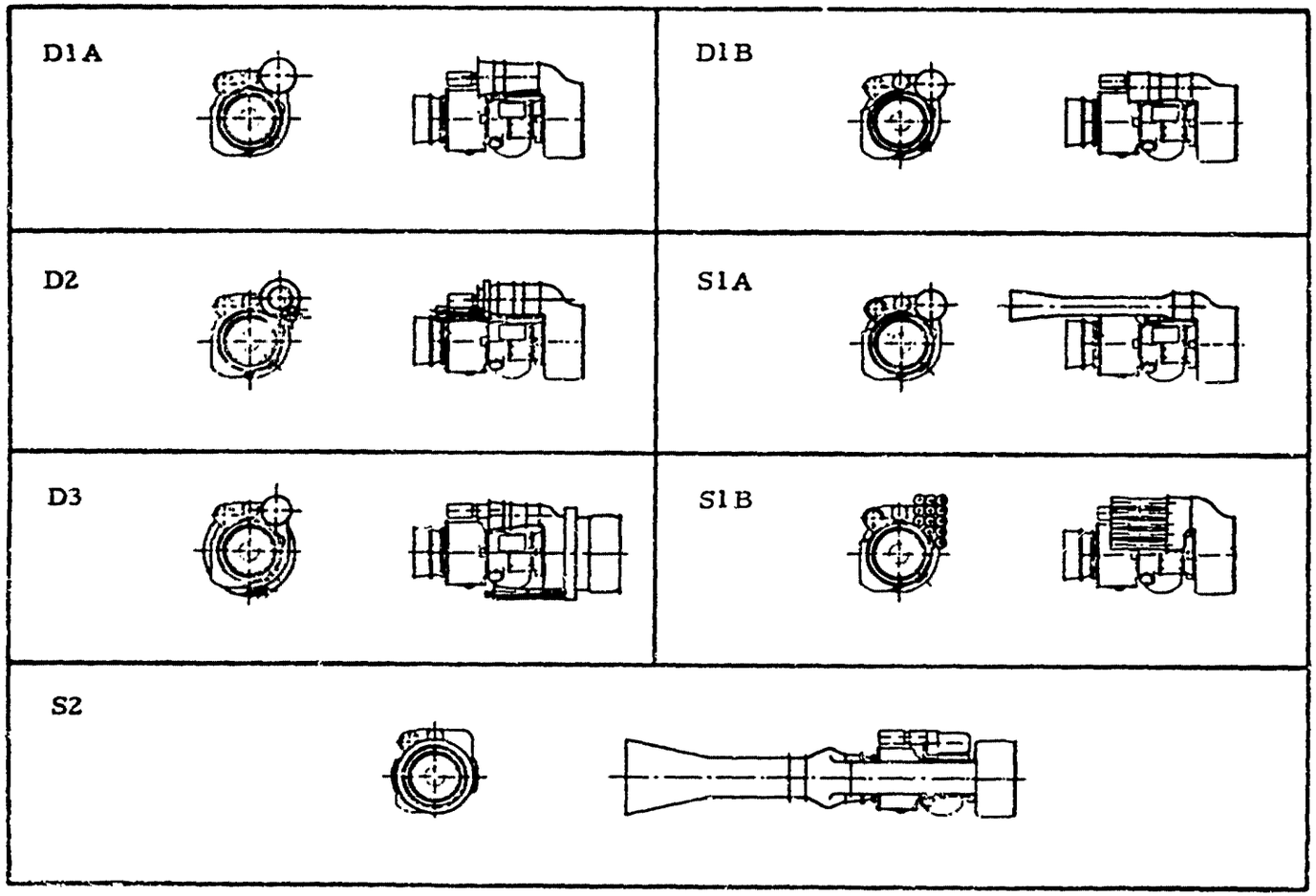

Figure 19. Scavenge System Installation.

inlet and exhaust. At installation, each of these units is located approximately at mid-engine, and is driven by the gas generator shaft through an accessories gearbox. As an alternative, a geared mechanical drive from the engine output shaft is also possible.

On-off capability is inherent in the bleed-air powered designs, with the addition of a valve in the supply line. Decoupler or clutches for the mechanically driven systems were nominally considered, but were determined to be beyond the scope of the basic investigation.

System failure modes were examined for their potential effect upon mission completion. Generally, dynamic systems would be designed to contain failures, and would employ a shear section in the input shaft system. Bleed-powered systems automatically become inoperative when the supply in interrupted. Composite systems would provide some engine contaminant protection as long as the dynamic component remains operative. Therefore, scavenge system failures are not anticipated to affect mission completion, but would potentially expose the engine to high erosion.

Comparative data on volume and weight for all systems is given in Figures 20 and 21, with specific numerical data given in Table 7. Clearly, the tailpipe eductor (S2) incurs substantial penalties in these two criteria, while most remaining systems are generally comparable.

Engine power penalties are compared in Figure 22. As is indicated, the engine-flow powered systems are highest in power requirements, and the purely mechanically driven systems require the least.

Finally, the cost data (shown in Figure 23 and Table 8) were not based on any rigorous analysis owing to the preliminary nature of the designs; thus the data presented are estimates only.

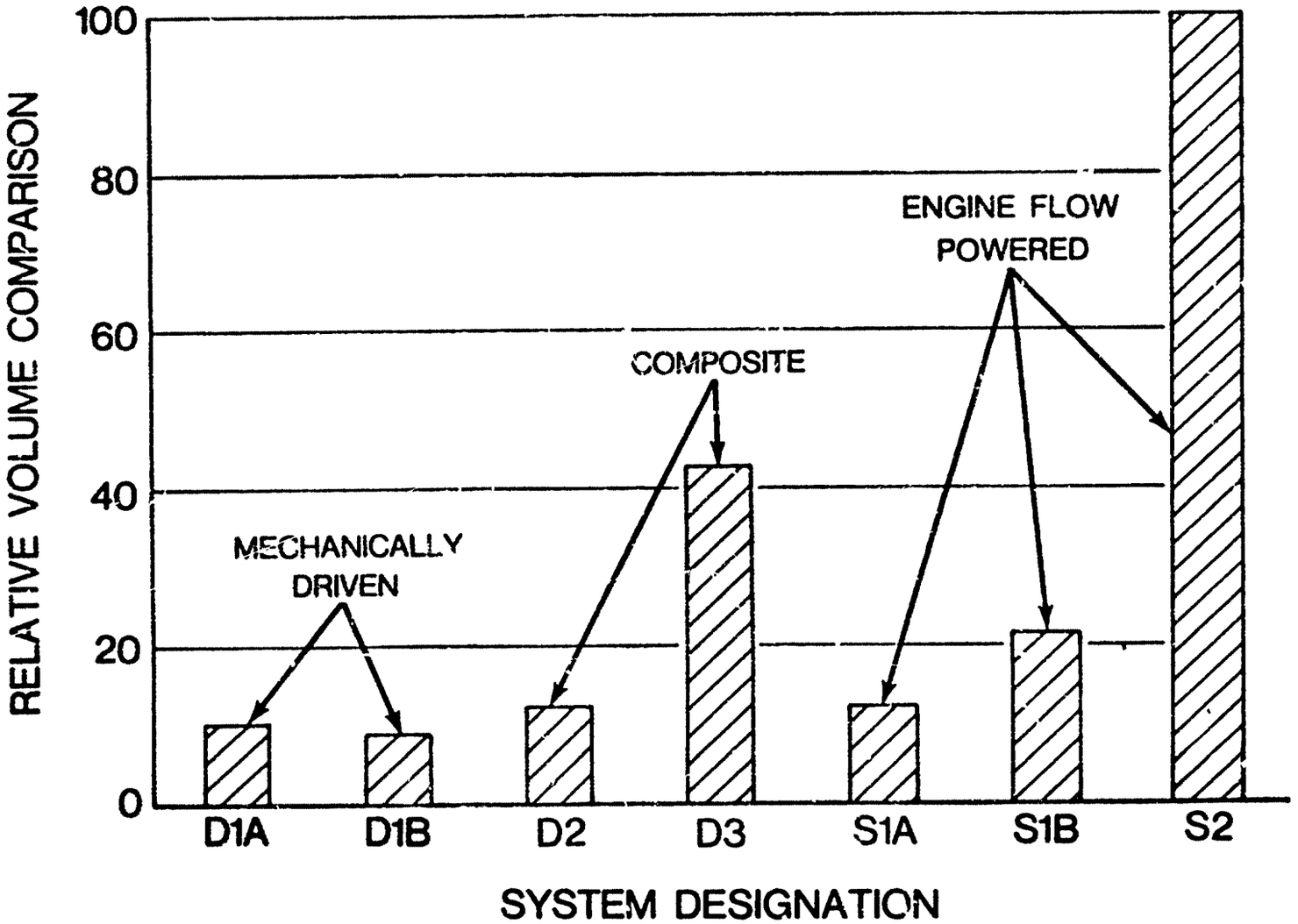

Figure 20. Relative Volume Comparison.

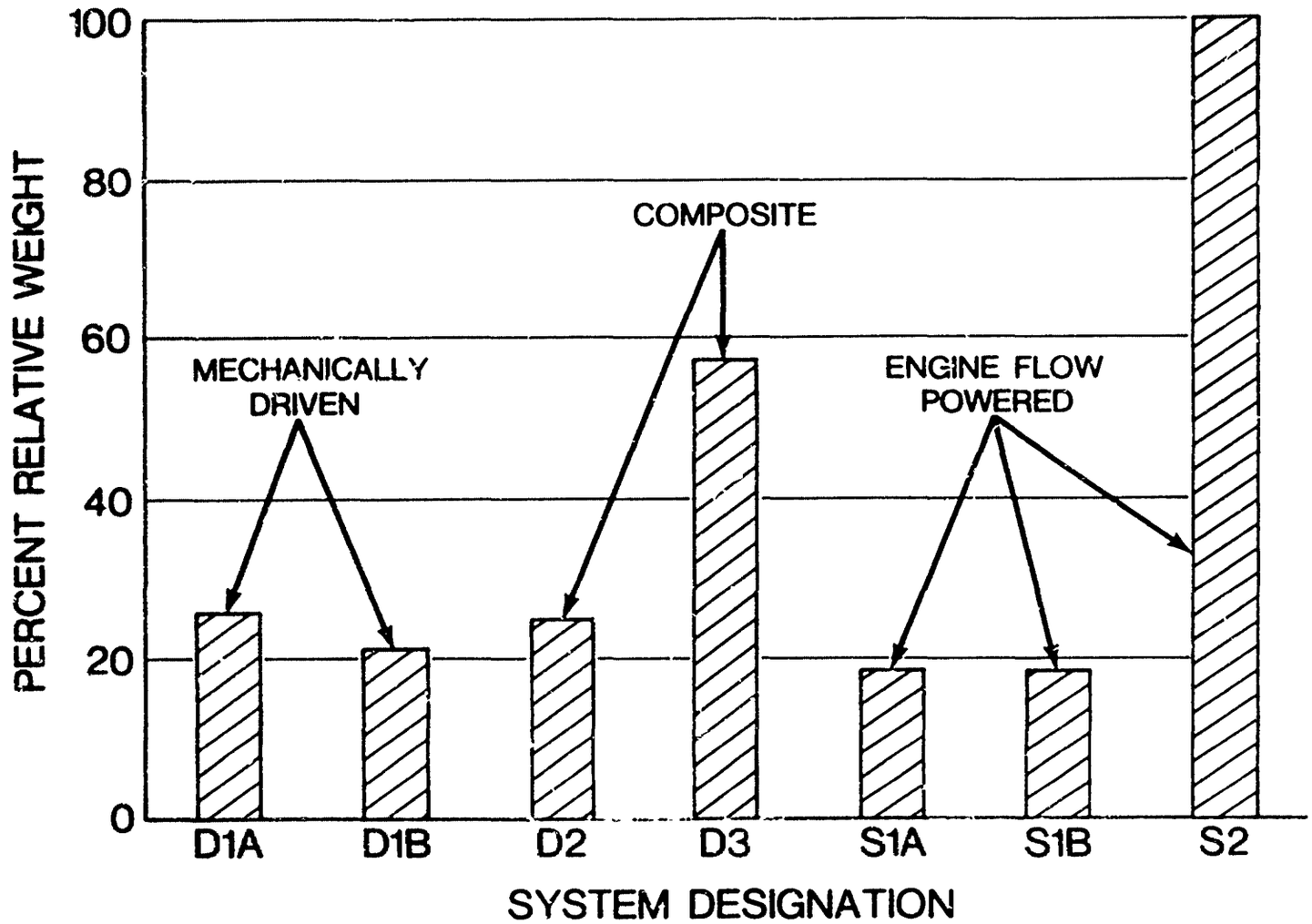

Figure 21. Relative Weight Comparison.

TABLE 7. PHYSICAL CHARACTERISTICS SUMMARY

Configuration	Weight (lb)	Dimensions (in.)		Volume (in^3)
		Length	Diameter	
D1A	9.7	11.0	7.2	336
D1B	7.8	12.1	6.3	298
D2	9.4	19.7	8.1	400
D3	21.0	18.4	-	1399
S1A	6.8	35.0	6.1	500
S1B	6.6	14.8	9.4	700
S2	36.9	42.7	15.2	3360

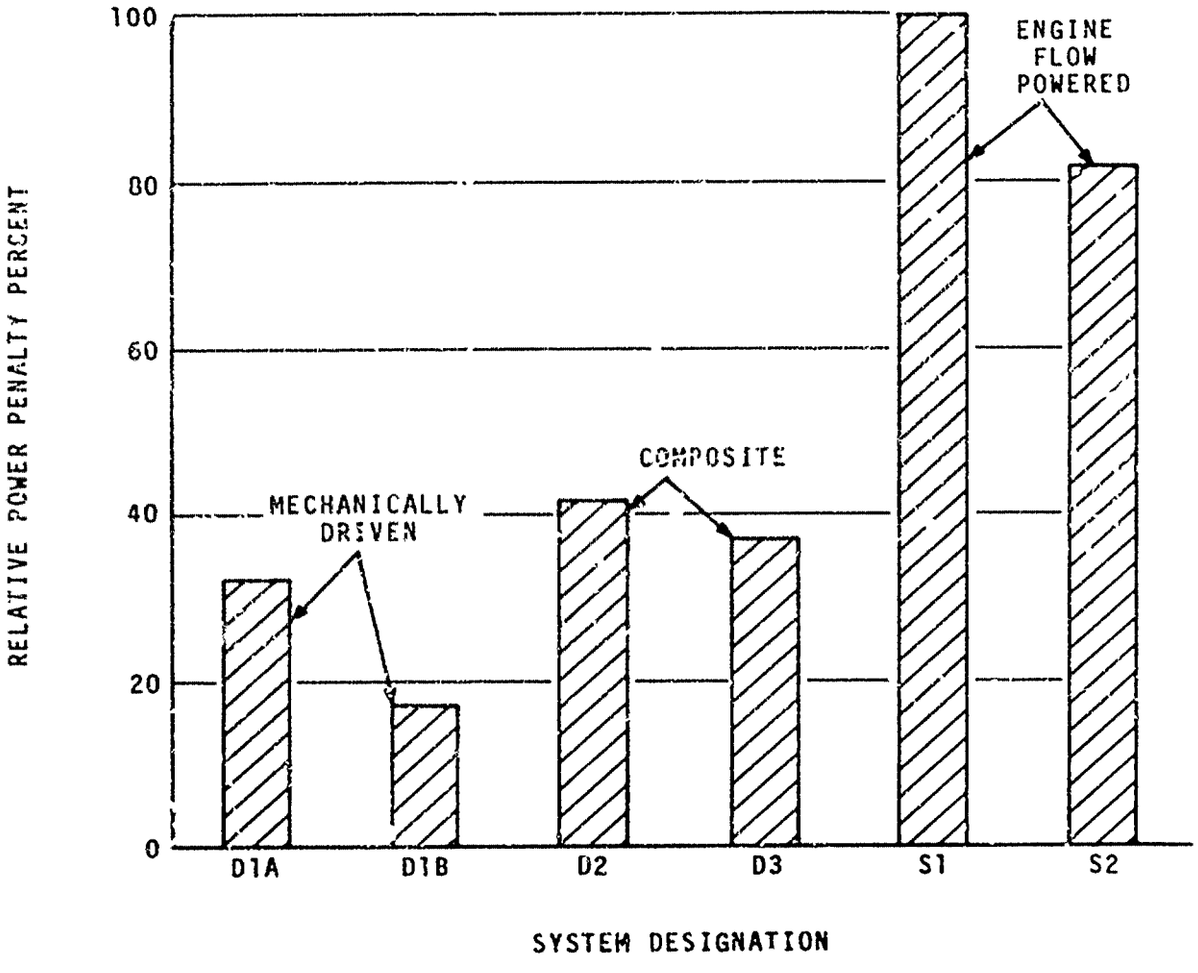

Figure 22. Relative Comparison - Engine Power Penalty.

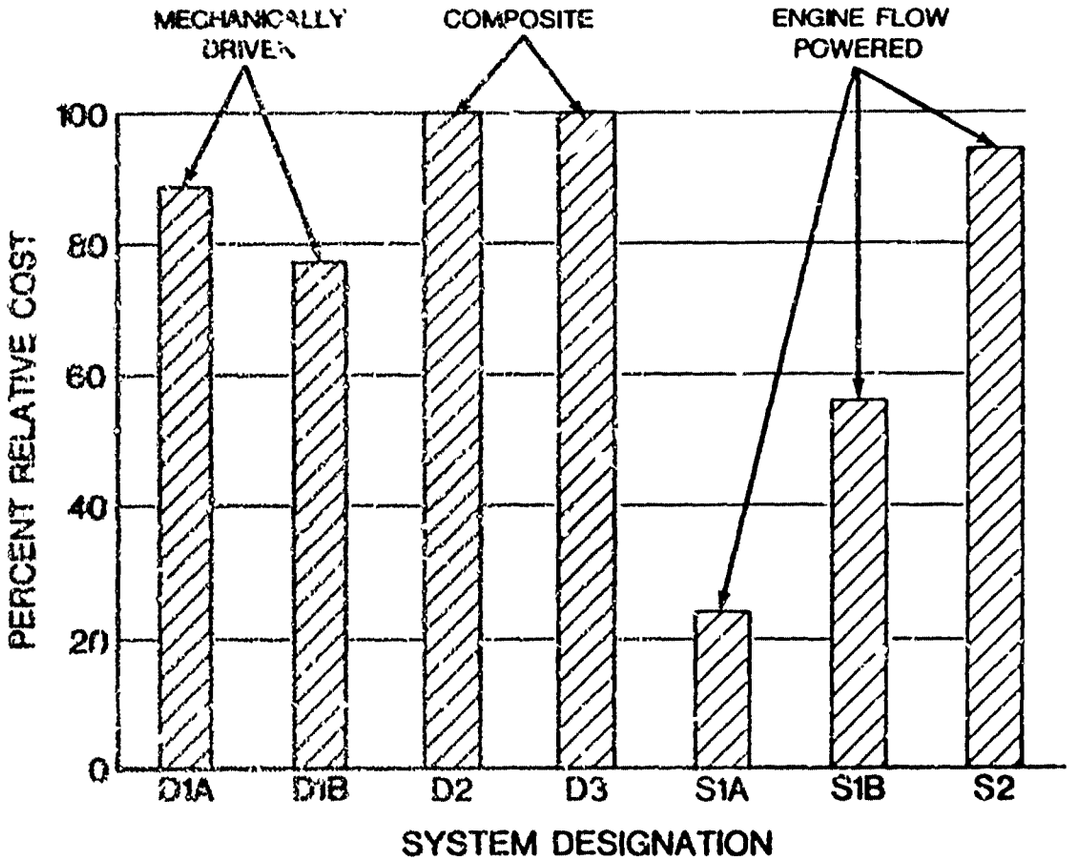

Figure 23. Relative Cost Comparison.

TABLE 8. ESTIMATED COST DATA (1974 DOLLARS)

System	Unit Cost*
D1A	$1060
D1B	$ 945
D2	$1200
D3	$1220
S1A	$ 290
S1B	$ 680
S2	$1160

*Tooling Costs Prorated over 500 Units

RATING TECHNIQUE AND CONCEPT SELECTION

In Task I, aerodynamic and mechanical studies were conducted on six scavenge systems concepts. Additionally, integration studies addressed system weight, effect upon engine envelope, cost, weight, method of power extraction, power required, effect of system failure on the engine, and potential usage of the exhaust air. The data generated from these studies was used to furnish input for selection of two concepts, on the basis of the following factors: Engine power penalty, reliability, volume, durability, system failure impact, technical risk, maintainability, weight, on/off capability, all-weather capability, cost, noise level, and surge impact.

Weighting factors for each of the preceding categories were arrived at by using a binary technique of forced decisions, which is described in detail in Reference 1. According to this method, each category is compared individually to all other categories, and is judged on the basis of relative importance. For each positive decision that is made (e.g., cost versus weight, etc.), a one is assigned. If a decision is negative as to relative importance, then a zero is assigned. The weighting given to each rating category is then the sum of the number of positive decisions made. A summary of the resulting rating factor weight values is listed in Table 9.

The individual concepts were then evaluated with respect to each other in each of the above categories, using the same binary method of forced decision. The resulting concept evaluation rankings (numerically, a digit from 0 to 6, with the six denoting highest, or most favorable ranking within a category) were then multiplied by the weighting values to obtain a mathematical ranking of the separator concepts. In any instances where two (or more) designs are considered as ranking equally in a given category, then ties are permitted, and decimal values result. For example, if two designs are ranked highest, but equal, in a given category, then a value of 5.5 is assigned to each, as opposed to arbitrarily assigning "5" to one design, and "6" to the other. The results of the rating system are summarized in Table 10.

Prior to discussing these results, it should be emphasized that the rating system used does not provide an indication of the relative degree to which one system is better, or worse than another. Thus, judgement must be exercised in determining whether or not any overriding factors are present which would alter the conclusions so indicated.

---

1. Fasal, J., FORCED DECISIONS FOR VALUE, Product Engineering, 12 April 1965

As an example, from Table 10 the tailpipe eductor (System S2) is ranked last in point score under the "volume" (impact or engine envelope) category. But regardless of the total point score achieved by this design on the merits of other considerations, the concept could not be recommended based singularly on the fact that the eductor virtually doubles the length of the engine.

TABLE 9. RATING FACTOR WEIGHT VALUES

Number	Factor	Weight
1	Engine Power Penalty	12
2	Reliability	11
3	Volume	10
4	Durability	9
5	System Failure Impact	8
6	Technical Risk	7
7	Maintainability	6
8	Weight	4
9	On/Off Capability	4
10	All-Weather Capability	3
11	Cost	2
12	Noise Level	2
13	Surge Impact	0

TABLE 10. CONCEPT RATING SUMMARY

WEIGHTING FACTOR	12	11	10	9	8	7	6	4	4	3	2	2	-		
	ENGINE POWER PENALTY	RELIABILITY	(IMPACT ON VOLUME ENGINE ENVELOPE)	DURABILITY	SYSTEM FAILURE IMPACT	TECHNICAL RISK	MAINTAINABILITY	WEIGHT	ON/OFF CAPABILITY	ALL WEATHER CAPABILITY	COST	NOISE LEVEL	SURGE IMPACT	TOTALS	
SELF BYPASSING - D1A (MIXED FLOW CENTRIFUGAL)	60	27.5	50	45.0	44	3.5	33	8	14	7.5	6	6	-	304.5	DYNAMIC
SELF BYPASSING - D1B (AXIAL ROTOR)	72	27.5	60	4.5	44	3.5	33	16	14	7.5	8	4	-	294.0	
EXTERNALLY BYPASSED - D2 (PROTECTED FAN)	36	11	40	4.5	20	38.5	15	12	6	3	2	2	-	190.0	
VORTEX TUBE ASSY - D3	48	0	10	22.5	20	38.5	15	4	6	0	2	0	-	166.0	
EJECTOR (SINGLE) - S1A	6	55	30	45.0	12	17.5	3	20	22	15	12	9	-	246.5	STATIC
EJECTOR (MULTIPLE) - S1B	6	44	20	45.0	12	17.5	3	24	22	15	10	9	-	227.5	
TAILPIPE EDUCTOR - S2	24	66	0	22.5	0	28.0	0	0	0	15	2	12	-	169.5	

Another drawback to the system lies in the fact that it is, at least to some extent, dependent upon opinion. This is particularly true in deciding the relative weights to be assigned to each rating factor.

Recognizing the preceding qualifiers, the rating system still establishes certain well-defined boundaries in assessing the relative merits of all systems concerned. A qualitative discussion of the results, by individual category, is given below.

Engine Power Penalty - (Weighting Factor = 12)

The power requirements for each system are well-known, and thus the ranking order is established. As indicated earlier in this report, the self-bypassing designs with only mechanical drive input require the least power. At the other extreme are the engine flow-powered systems. The composite designs receive intermediate scores.

Reliability - (Weighting Factor = 11)

Relative merit is judged on the basis of fundamental system simplicity, or complexity and upon the number of "subsystems" present. The engine-flow systems (S1 and S2) are ranked highest, while the composite designs would be considered least favorable, based upon the quantity of independent components which comprise the system.

Volume - (Weighting Factor = 10)

Under this category, the general impact upon engine envelope is considered. Specific data is available for each design (Table 7), and thus a ranking order is established. The self-bypassing designs (D1A and D1B) are the most compact and require the least modification to the engine envelope. (Refer also to Installation Drawing, Figure 18.)

Durability - (Weighting Factor = 9)

Assessment of durability is made on a relative, rather than on an absolute basis, since the minimum design goal for all systems is to satisfy a 50-hour military sand ingestion test, with no more than a 10-percent degradation in flow.

On a relative basis, the general considerations from which rankings were evolved are the degree of protection afforded to the rotor as determined by the bypass ratio, or the sand separation efficiency of the unit. Thus among the dynamic systems, D1A is ranked highest ($\eta_{SEP} = .99+$), followed by D3 ($\eta_{SEP} = 0.93$), D1B ($\eta_{SEP} \cong .90$), and D2 ($\eta_{SEP} \cong .90$). Additional considerations taken into account are whether or not the system contains any other key wear points such as diffuser splitters, or ejector secondary flow nozzles.

System Failure Impact - (Weighting Factor = 8)

Other than the loss of all, or part of scavenging capability, the factors which have been considered are debris scatter, influence upon the engine operating point, and potential for backflow into the engine separator. The last item is a problem common to all systems, and its solution will be addressed in the detailed design phase to follow. On the question of potential for debris scatter, it is assumed that all dynamic systems will be designed so as to contain a rotor failure. Thus, the remaining criterion becomes the extent to which the engine operating point is shifted, as a result of scavenge pump failure. The sole exception to this is the tailpipe eductor; it is ranked last because of its potential for debris scatter in the event of failure, although that possibility is rather remote. The remaining designs are then ranked according to the amount of compressor bleed which is required; none for the self-bypassing systems (ranked highest), intermediate for the composite designs, highest bleed rate for the ejectors (ranked lowest).

Technical Risk - (Weighting Factor = 7)

Under this category, a particular design is rated according to the extent that existing technology (or components of known performance) is employed. The composite designs (D2 and D3) are either patterned after existing engine separators or utilize commercially available components with well-defined performance characteristics. Hence, these designs pose minimal technical risk. Likewise the eductor concept is widely applied, although most effectively where secondary flow losses are low. Clearly, the self-bypassing designs are the most innovative of all concepts considered, and as such represent the highest risk. Specific examples of risk elements were discussed under "Concept Feasibility Studies", D1A and D1B designs.

Maintainability - (Weighting Factor = 6)

Maintainability is gaged in terms of relative ease, or difficulty incurred in replacement of major systems components. Systems D1A and D1B are designed for ready access to rotors in the event of required replacement. At the other extreme the ejector designs are essentially integral units, and maintenance implies replacement of the entire unit.

Weight - (Weighting Factor = 4)

Self explanatory - ranking is based upon data in Table 7.

On/Off Capability - (Weighting Factor = 4)

Relative merit is assigned on the basis of the degree of difficulty in providing this feature to each design. In descending order, the ejector designs (S1A and S1B) require only a modulating valve. The self-bypassing designs (D1A and D1B) require mechanical decoupling, whi the com-

posite designs require both of the preceding devices. Finally, the tailpipe eductor (S2) would require variable geometry in a high-temperature, erosive environment in order to be efficient in both modes of operation.

All-Weather Capability - (Weighting Factor = 3)

Ejector designs are only subject to icing upstream of the secondary flow nozzles. Self-bypassing designs are subject to inlet icing and potential shedding, but the inertial bypass feature should afford adequate rotor protection. Least desirable, from an icing viewpoint, is the vortex-tube assembly (D3).

Cost - (Weighting Factor =2)

Self-explanatory - ranking is based upon data in Table 8 and Figure 23.

Noise Level - (Weighting Factor =2)

All systems are designed for low discharge velocities, on the order of 150 fps, thereby eliminating jet noise as a factor. Minimum noise addition would be expected in the eductor design; noise associated with the supersonic jets present in several of the ejector designs tends to be highly directional, and also considerably attenuated due to immersion in a lower velocity surrounding fluid. In general, dynamic systems are least favored in this category, depending upon blade passing frequencies and rotor-to-stator axial clearances. Rotor designs would require a minimum of 14 blades in order to produce passing frequencies in excess of the audible range at 50,000 rpm.

With reference again to Table 10, the self-bypassing designs (D1A and D1B) are seen to be the best overall choice, based upon all of the preceding criteria. Within this concept, the recognizable trade-offs involve durability versus power, compactness and cost.

The second choice, resulting largely from inherent simplicity is the ejector concept (Systems S1A and S1B). In considering these two systems, the latter (multiple-tube assembly) affords a high degree of flexibility in terms of potential packaging arrangements, and is thus recommended over the single-tube unit.

FEASIBILITY STUDY CONCLUSION

On the basis of the Task I feasibility study, the "self-bypassing" concept was selected as the primary scavenge system for subsequent detail design, procurement, and evaluation. Optimization of this design, with respect to type of rotor, pressure ratio, bypass ratio, separation efficiency, power input, etc., was accomplished in the Task II phase of the program.

The alternate system, selected for critical component design and evaluation is the Multiple-Tube Ejector, System S1B.

OPTIMIZATION OF THE BYPASSING DESIGN CONCEPT (TASK II)

GENERAL

At the conclusion of the feasibility study, the bypassing blower was selected as the dynamic system approach to an advanced scavenging means for a gas turbine engine integral particle separator. Since there is considerable latitude of choice as to how this type of blower may be configured for a given application, it is the purpose of this section to consider those factors which influence design parameters and then to select a configuration which is optimum for the given program goals.

Two variations of the bypassing design were presented earlier, and these were designated as configurations D1A and D1B. These cases may be considered as extremes since the first (D1A) uses a very high rate of bypass (100%) in order to achieve rotor durability via high inlet separation efficiency. Accordingly, input power required is also high. In contrast, Configuration D1B uses much less bypass air, would achieve more modest levels of rotor protection, but requires substantially less (approximately 50-percent) drive power.

The power versus durability aspects of these designs were weighed in detail, including other relevant factors such as type of rotor, inlet blade speed, choice of material, etc.

COMPARISON OF D1A AND D1B IN TERMS OF EJECTOR CHARACTERISTICS

Configurations D1A and D1B are compared on the basis of their component performance in Figure 24. This figure illustrates a series of operating lines for an ejector/diffuser combination, exhausting to standard day ambient conditions. Each operating line pertains to a specific geometry which relates the primary flow area of the ejector to the mixing tube area. Parameters that have been held constant in this computation (mixing tube nondimensional length, diffuser efficiency, primary nozzle temperature, secondary supply pressure, and friction factor) were assigned values as listed in Figure 24.

Superimposed on the ejector performance map are the two specific design points considered. The two designs differ considerably in terms of the required primary pressure (i.e., level of rotor output), the flow ratios delivered, and the relative sizing of the primary and secondary flow areas. For an inlet pressure of 13.98 psia (-20 in. H_2O), the required stage pressure ratios are:

	D1A	D1B
Stage Pressure Ratio = $\frac{P_{o\ PRIM}}{P_{o\ IN}}$	1.48	1.13

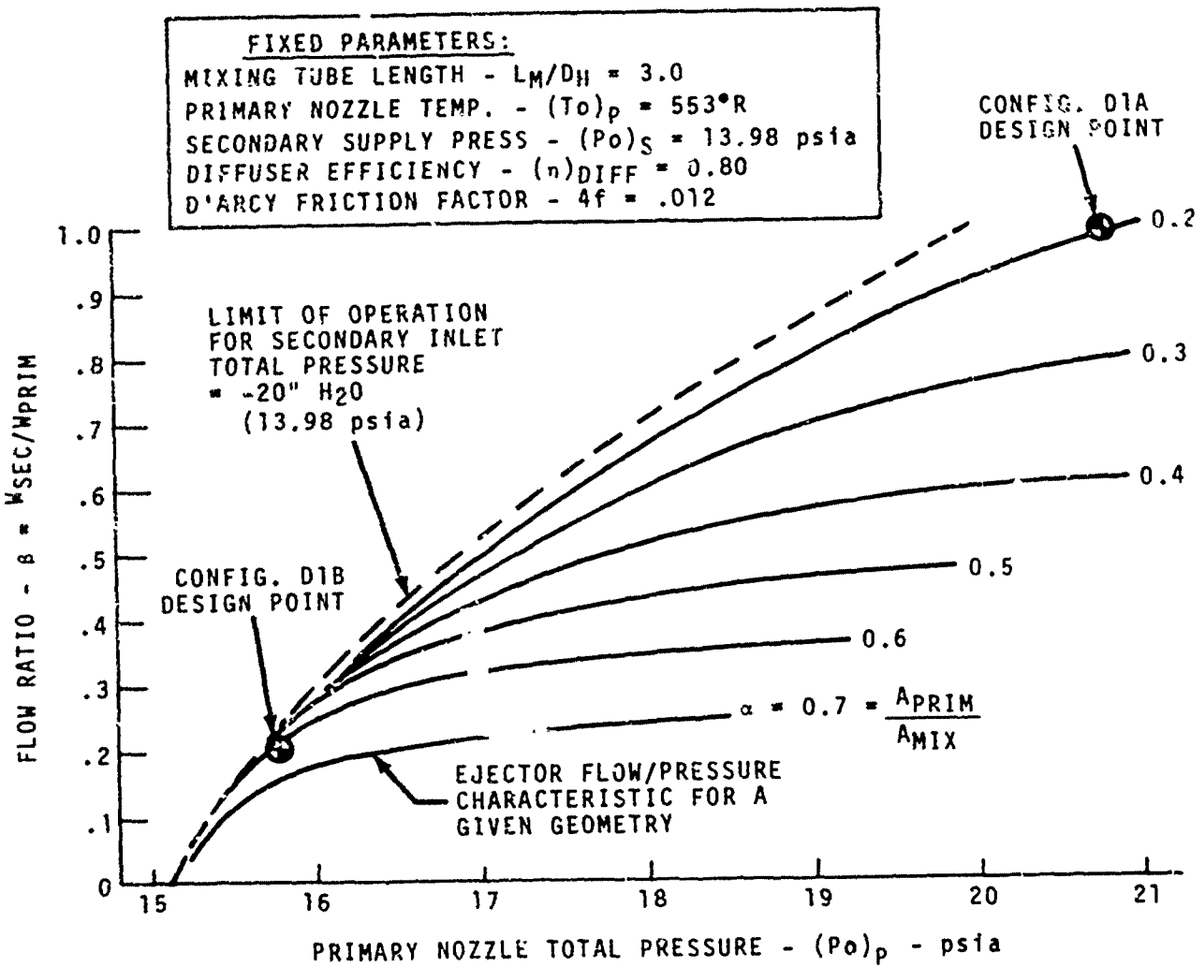

Figure 24. Comparison of Study Configuration D1A and D1B on the Basis of Ejector Performance.

Deducting pressure losses across turning vanes (Figures 3 and 10) consistent with the respective flow Mach numbers:

	D1A	D1B
Rotor Pressure Ratio = Pr_{ROT}	1.59	1.16

For an assumed rotor polytropic efficiency of 0.70 in each case, and with a total flow of 0.9 lb/sec, * the input power requirements are:

	D1A	D1B
Rotor Power = HP_{ROT}	16.1 HP	8.2 HP

Thus, the computed power requirements are different, in this instance, by a factor of two. (Figure 4 also summarizes this conclusion.)

Since the drive power is a direct function of bypass ratio, once a total airflow has been specified it becomes critical to choose a minimum level of bypass that is consistent with a desired inlet separation efficiency. In turn, the separation efficiency must afford the required rotor durability.

CLASSIFICATION OF D1A AND D1B ACCORDING TO SPECIFIC SPEED

In determining a design point on Figure 24, it is necessary to consider the general class of rotor which will be required to deliver specific conditions at the ejector primary nozzle. A prime factor in determining the rate of wear of the rotor will be the inlet blade speed, which (from an erosion viewpoint) should be kept as low as practical.

Given a total pressure ratio (isentropic headrise) and a flow rate to be delivered (volumetric flow rate), then for a particular design rotational speed, the specific speed N_s may be used to classify the type of rotor required:

$$N_s = \frac{N\sqrt{Q}}{(\Delta h_o')^{.75}}$$

*NOTE: $W_{TOT} = W_{ROT}/(1 - \beta_2)$ where β_2 is found on Figure 4, and W_{ROT} is the fraction of the total used to calculate power.

Where N is the design rpm = 50,000 rpm

Q is the volume flow rate = ft^3/sec

$\Delta h_o'$ is the ideal head = $C_p J T_{o\ IN} (Pr_{ROT}^{.286} - 1)$

The units for ideal head are ft lb_f/lbm

In Figure 25, the D1A and D1B design points are superimposed on a plot of specific speed versus volumetric flow rate. As indicated, Configuration D1A would be a centrifugal design, while an axial rotor could be used for Configuration D1B. Of the classes of rotors, an axial rotor is least favorable from the viewpoint of required blade speed. Figure 26 shows the mean blade speeds for an axial design as a function of total pressure ratio based upon an assumed efficiency of 0.70. (The low efficiency level reflects an "after wear" state of the rotor.) Depending on the inlet meridional velocity, mean blade speeds of 600 to 800 fps are required (Configuration - D1B) to achieve a 1.16:1 total pressure ratio. If a blade speed of 500 fps is taken as a preferred maximum, then axial rotors could only be used in bypassing designs where the total pressure ratio required is about 1.10; in terms of bypass ratio, this would result in $\beta_2 \cong 8\%$.

Further comments on the effect of blade speed on erosion appear later in this section.

CRITERIA FOR INLET SEPARATION EFFICIENCY (η_2)

Determination of the bypass ratio necessitates an estimate of the blower inlet requirements for separation efficiency. The basic criterion for establishing an inlet separation efficiency was to fix the maximum quantity of sand to be ingested by the rotor in a 50-hour operating period, in conjunction with given airflow characteristics for an associated engine and particle separator. That maximum quantity has been set at 5.0 pounds sand for 50 hours of operation with a 5.0-lb/sec engine whose particle separator requires 18 percent scavenge, at an efficiency of 0.95 for MIL-E-5007C sand. Sand-to-air concentration at the engine separator inlet is 1.5 mg/ft^3. In this instance, the choice of 5 pounds as a limit is based upon previous experience with a scavenge blower of "conventional" design where the effect upon performance of a given quantity of sand ingestion was known. From the preceding data, the required inlet separation efficiency is found to be 88.4 percent by weight, for 50 hours of operation with "C" Spec sand, in order that the rotor ingest no more than 5.0 pounds of sand.

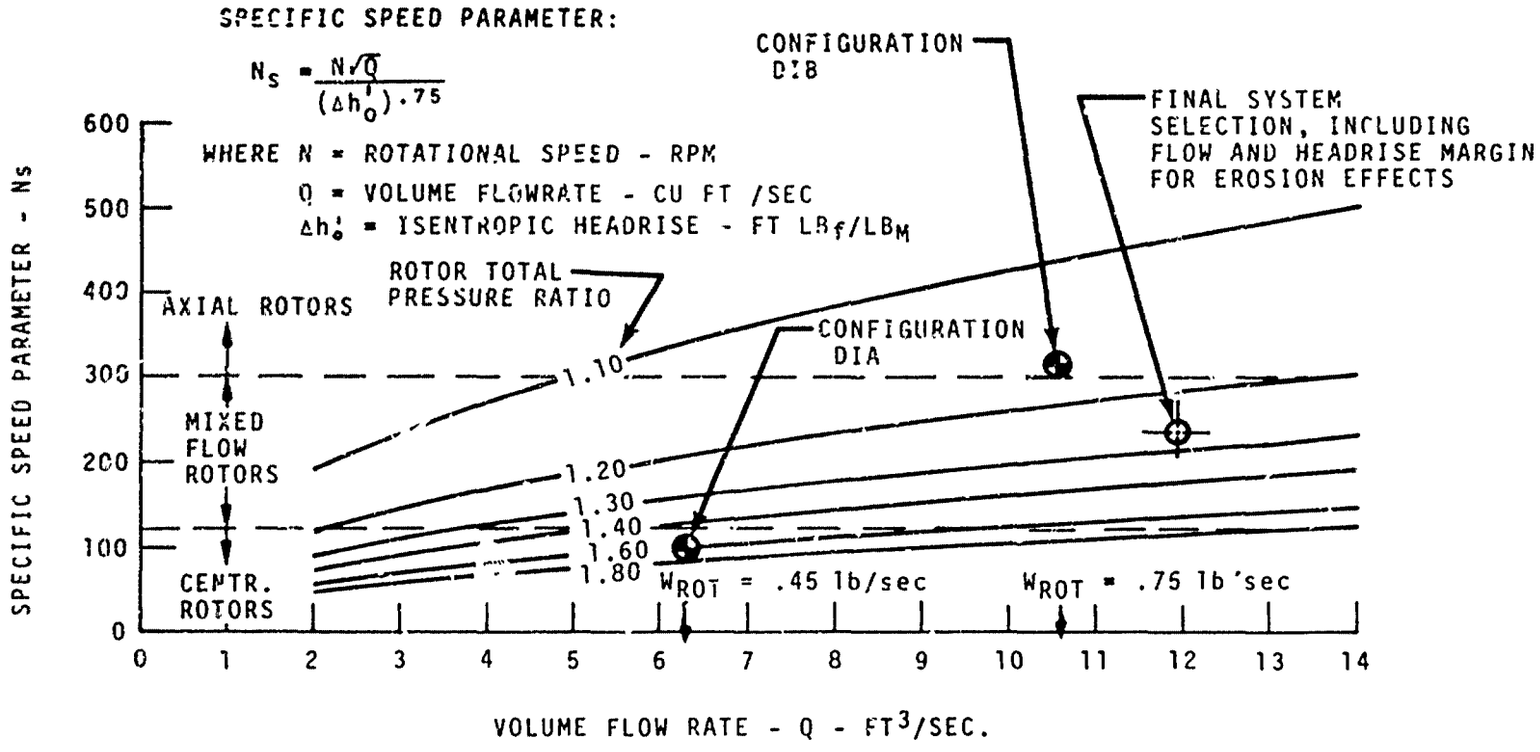

Figure 25. Specific Speed Classifications for Scavenge Blower Study Configurations.

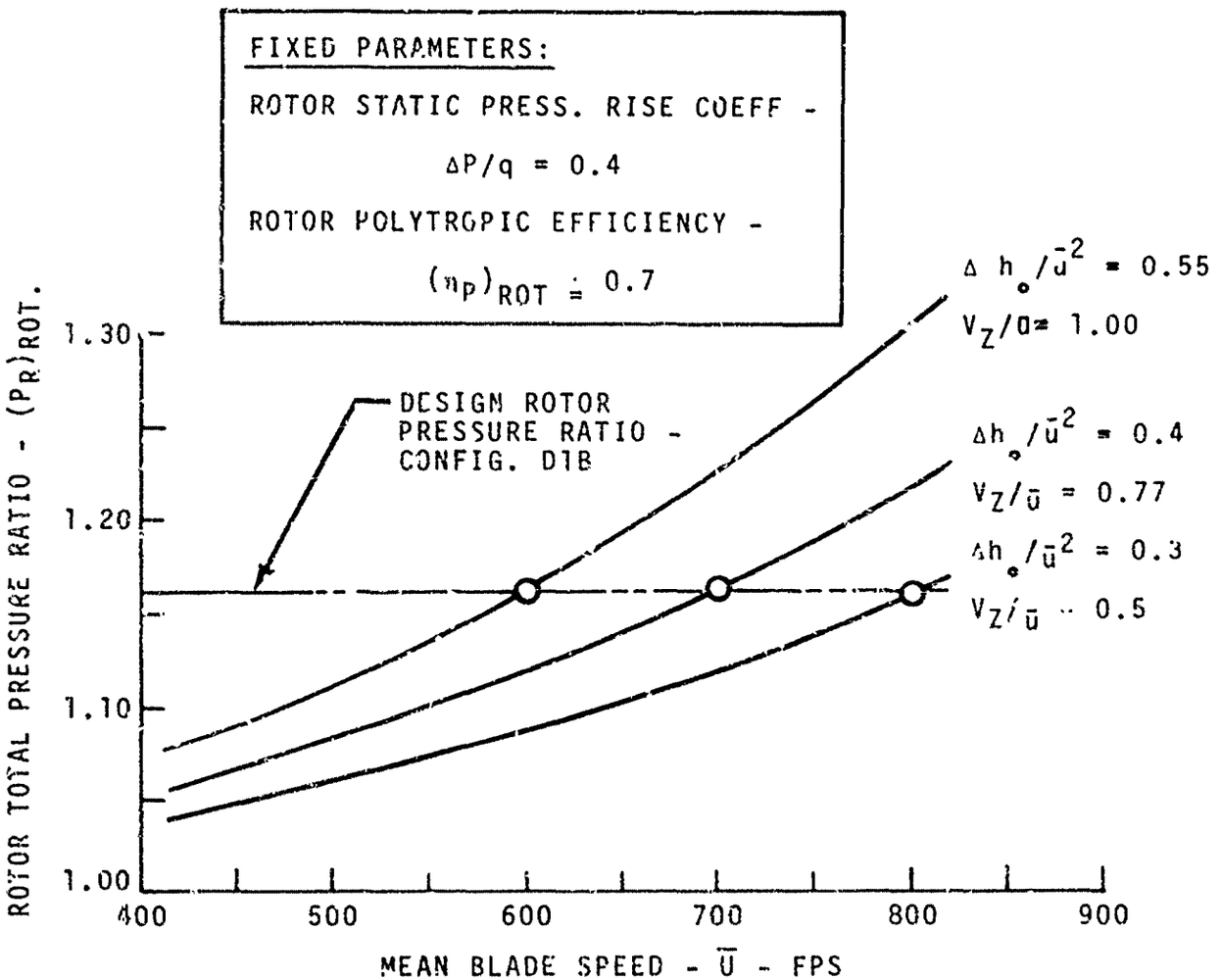

Figure 26. Mean Blade Speed Requirements for an Axial Blower Configuration (D1B).

BLADE SPEED INFLUENCE ON INLET EFFICIENCY REQUIREMENTS

Suppose that we next consider the extent to which the first estimate of η_2 is modified if we introduce another variable, namely blade speed. To do this, redefine the maximum quantity of sand to be ingested by the rotor as being a function of the blade speed level, using 500 fps as a reference datum. If X denotes the maximum quantity of sand to be ingested by the rotor over a 50-hour period,

$$X = 5.0/F_1$$

Where F_1 is a factor that describes the variation in wear rate as a function of blade speed. If $F_1 = 1.0$ is taken at a datum of 500 fps, then at 800 fps, $F_1 \cong 2.7$ (Reference 2). This increase in wear rate is quite significant in terms of effect upon blower inlet separation efficiency. From Figure 27, η_2 is increased to 0.957 for 50 hours of operation, where the rotor may now only ingest $(5.0/F_1)$ pounds of sand.

MATERIALS INFLUENCE ON INLET SEPARATION EFFICIENCY

A similar analysis may be made for various materials as was done for blade speed, by incorporating a second factor, F_2, which describes wear rate relative to a selected datum material. The amount of sand ingested by the rotor then becomes

$$X = \frac{5.0}{F_1 F_2}$$

If $F_2 = 1.0$ for AL 2024, then typical values for other materials include 0.70 for titanium and 0.42 for stainless steel. By analogy to Figure 27, the use of both of these factors yields a range of inlet separation eificiencies of 0.725 to 0.957 for 50 hours of operation, depending upon material and blade speed.

2. MECHANISM OF SAND AND DUST EROSION IN GAS TURBINE ENGINES, Solar Div., International Harvester Co., USAAVLABS Technical Report 70-36, Eustis Directorate, U. S. Army Air Mobility Research and Development Laboratory, Fort Eustis, Virginia, August 1970, AD 876584.

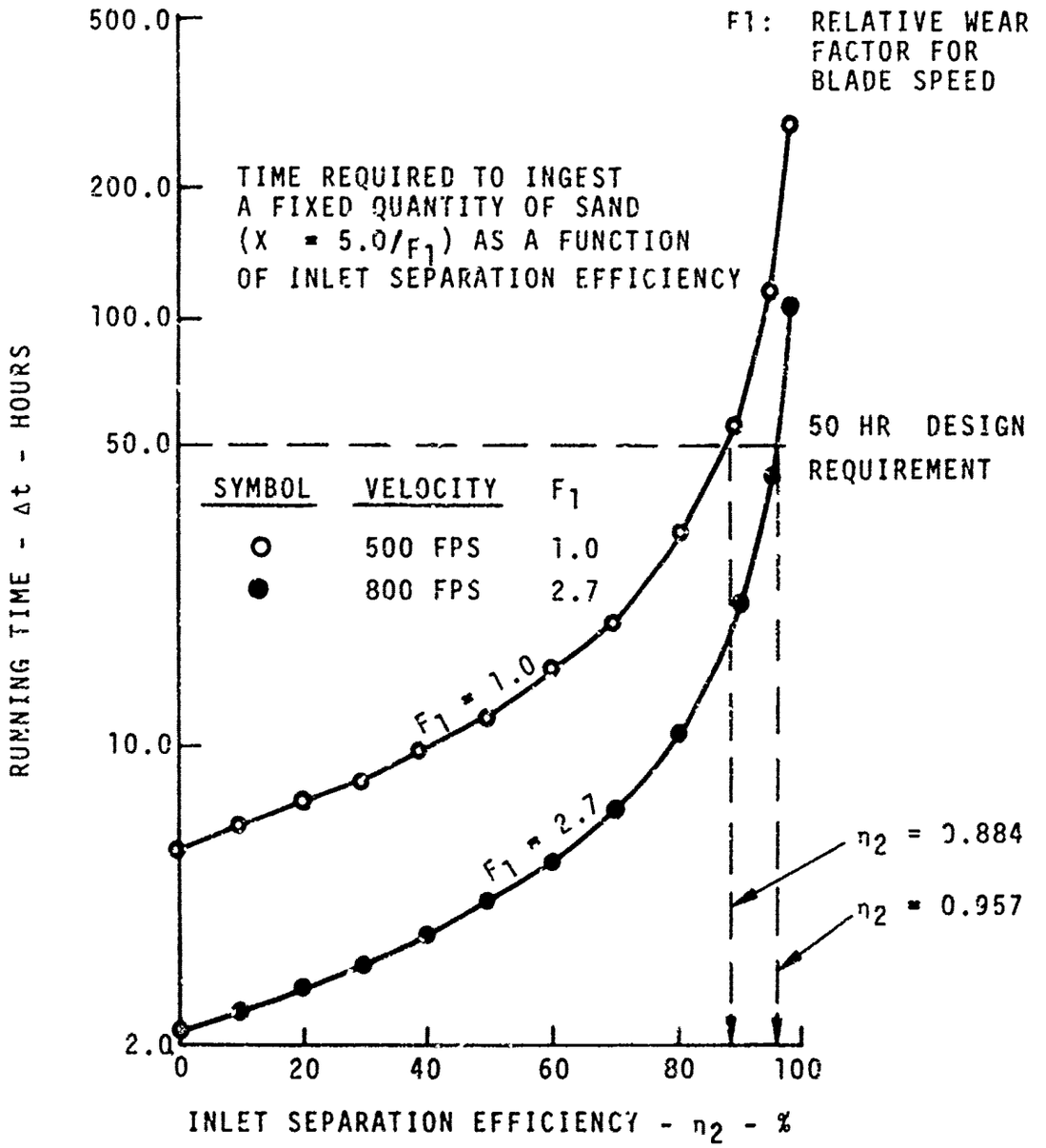

Figure 27. Separation Efficiency Versus Operating Time for $5.0/F_1$ Pounds Sand Ingested by the Rotor.

In summary, an inlet separation efficiency of about 72 percent would afford adequate protection to a stainless steel rotor, if the blade speed is on the order of 500 fps. From the assumed criteria, the equivalent amount of sand ingested by the rotor over 50 hours would be:

$$X = \frac{5.0}{F_1 F_2} = 11.90 \text{ lb sand @ } \eta_2 = 0.72$$

The value of 0.72 for η_2 should be readily attainable from the inlet inertial separator, and requirements for bypass ratio are not excessively high. The restriction on blade speed will necessitate a mixed flow design, since an axial design limited to U = 500 fps will produce insufficient output for all but the lowest bypass ratios ($\beta_2 < 8\%$).

DETERMINATION OF BYPASS RATIO

Based on previous in-house experience in the design of inertial particle separators, the minimum inlet efficiency goal of $\eta_2 = 0.72$ should be attainable with a bypass rate of 10 percent ($\beta_2 = 0.10$).* To fix a design point on the ejector map (Figure 24), it is necessary to consider performance decay, as a result of erosion. Since a fraction of the total flow extracted by the blower is due to bypass air which is in turn pumped by the primary flow, some allowance must be made for deterioration in rotor airflow and headrise due to erosion damage. The 10-percent bypass after 50 hours of operation was selected as the objective.

If a 5-percent allowance (current practice is typically 8 to 10 percent) is made for loss of rotor airflow, then

$$W_{TOT} = 0.90 \text{ lb/sec (with no margin)}$$

$$W_{ROT} = \frac{W_{TOT}}{1+\beta_2} = .818 \text{ lb/sec (with no margin)}$$

$$\boxed{(W_{ROT})_{DES} = 1.05\,(W_{ROT}) = 0.860 \text{ lb/sec}}$$

In Figure 28, an ejector operating characteristic (extracted from Figure 24) is shown for a value of $\alpha = 0.6$, where $\alpha = A_{PRIM}/A_{MIX}$ specifies the ejector geometry. If a 5-percent allowance is made for decrease in primary pressure due to erosion, then to arrive at a 10-percent bypass after 50 hours, an initial value of $\beta_2 = 25\%$ is required.

* Using MIL-E-5007C sand, 200 μ mean particle diameter.

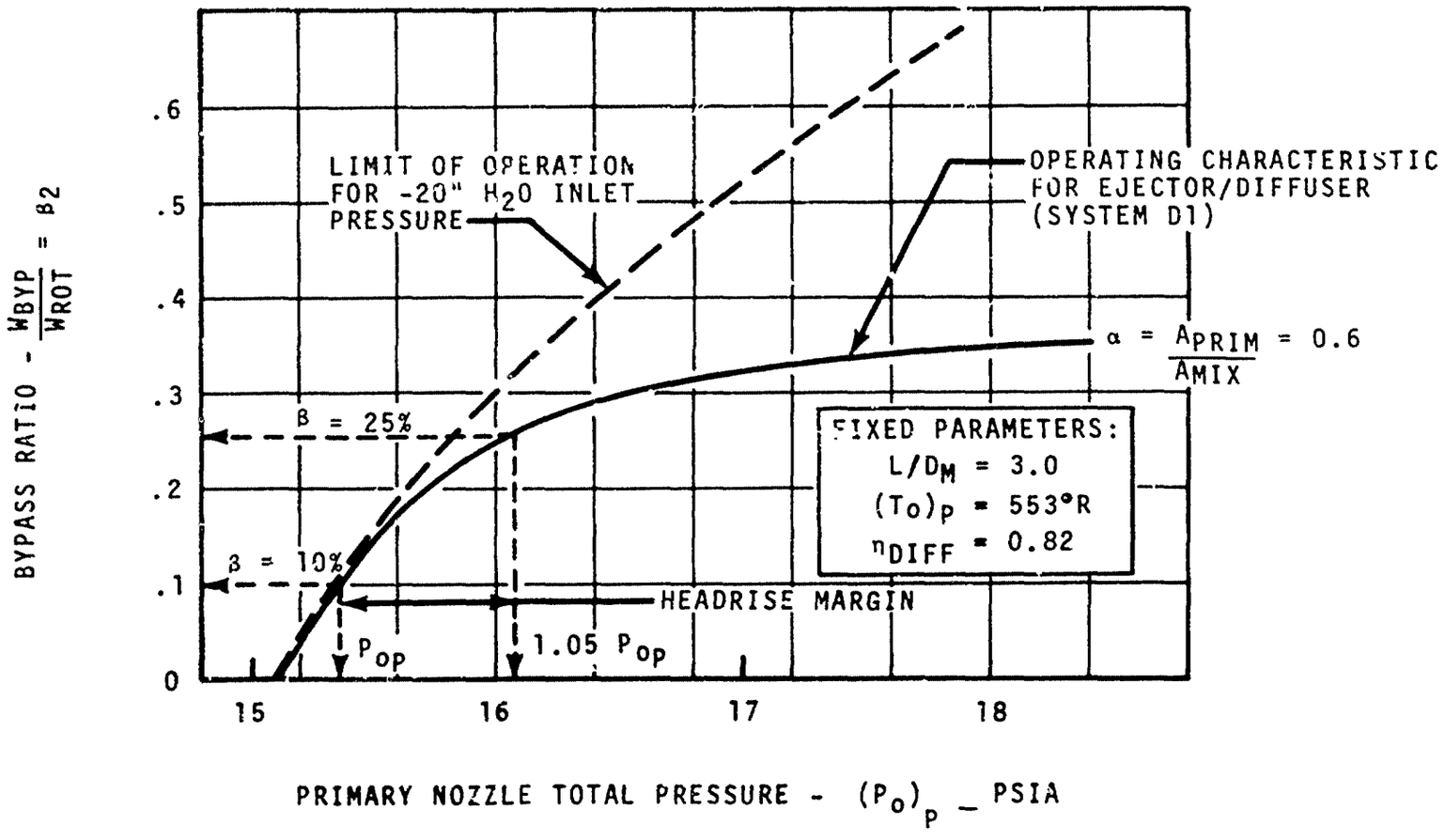

Figure 28. Margin in Headrise for Performance Loss Due to Erosion.

Taking the flow and pressure margins together will determine what the initial (or design) total airflow must be:

$$(W_{TOT})_{DES} = (W_{ROT})_{DES} \times (1 + \beta_{2_{DES}})$$

Includes 5% margin for flow

Includes 5% margin in pressure

$$(W_{TOT})_{DES} = 1.075 \text{ lb/sec}$$

SUMMARY OF OVERALL DESIGN PARAMETERS

Based on the preceding analysis, the following is a summary of key parameters that form the basis for detailed aerodynamic and mechanical design of the primary system, designated as System D1:

Total Airflow	-	W_{TOT}	= 1.075 lb/sec
Rotor Airflow	-	W_{ROT}	= .86 lb/sec
Bypass Ratio	-	$W_{BYP} / W_{ROT} = \beta_2$	= .25
Bypass Airflow	-	W_{BYP}	= .215 lb/sec
Inlet Total Pressure	-	$P_{o\ IN}$	= 13.98 psia
Inlet Total Temperature	-	$T_{o\ IN}$	= 518.1 ^{o}R
Rotational Speed	-	N	= 50,000 rpm
Rotor Type	-	Mixed flow	
Rotor Material	-	Stainless steel	
Inlet Blade Speed	-	U_{mean}	= 500 fps
Minimum Inlet Separator Efficiency	-	η_2	= 0.72
Total Sand to Blower		- 50 hours	= 43.3 lb
Maximum Sand Ingested by Rotor		- X	= 11.9 lb

After 50 hours of operation, minimum design goals are

Total Airflow	-	W_{TOT}	= 0.90 lb/sec
Bypass Ratio	-	β_2	= 0.10

AERODYNAMIC DESIGN - SYSTEM D1

GENERAL

In this section, the details of the aerodynamic design of the bypassing blower, designated as system D1, are presented. The overall design was approached on a component basis, according to the following sequence:

1. Detailed design of the annular ejector and diffuser, including refinements for inlet total pressure loss, mixing tube length, strut blockages, and ejector splitter thickness.

   The required pressure ratio to be delivered across the rotor/vane stage evolves from this phase of the design.

2. One-dimensional analysis of the rotor/turning vanes interfacing with the ejector.

3. Potential flow analysis of the inlet separator.

From items 1 through 3 above, with intervening iterations as required, the aerodynamic flow path of the entire blower is evolved.

4. A detailed particle trajectory analysis of the inlet separator to determine the separation efficiency in relation to the previously established minimum efficiency goal.

5. Impeller internal flow analysis to ascertain acceptable diffusion rates consistent with available separation criteria.

6. Turning vane aerodynamic design/cascade analysis.

7. Translation of r, θ, z impeller coordinates into blading manufacturing cross sections.

EJECTOR/DIFFUSER THERMODYNAMIC DESIGN

The general method of approach which has been used in ejector design is to specify a particular geometry and primary airflow, followed by application of the conservation equations to determine the amount of bypass (secondary) flow induced, and the required level of primary pressure. Examples of this computation, carried out for several different geometries, were shown in Figure 24.

In Figure 28, the required primary nozzle total pressure for a 25-percent bypass ratio was shown; two parameters however, which are indicated as fixed, namely mixing tube nondimensional length (L/D_M = 3.0) and secondary nozzle supply pressure ($P_o)_{SEC}$ = 20 in. H_2O), warrant further consideration.

The -20 in. H_2O value has been fixed as the total pressure at the blower inlet flange; prior to this time, that pressure has been presumed constant through the bypass channel up to the ejector secondary nozzle. (Refer to Figure 3 for nomenclature.) For final design purposes, this assumption is unrealistic, and some allowance for total pressure loss should be incorporated. To assign a more realistic secondary supply pressure to the ejector, the assumed pressure loss was taken as 5 in. H_2O, i.e.,

$$(P_o)_{SEC} = -25 \text{ in. } H_2O, \text{ or } 13.80 \text{ psia.}$$

In general, the secondary flow induced by an ejector will be a function of the available length of mixing tube. An "optimum" length is attained by allowing the static pressure to reach a maximum value, beyond which frictional effects override and no further improvments result from an increase in the mixing chamber length. However, this "optimum" length, depending upon the flow rate and the area ratio of the ejector, can be up to 6 to 8 times the hydraulic diameter of the mixing tube (subsonic ejectors), thereby adding considerable length to the overall unit.

Since the impracticality of fully optimizing the ejector length was recognized, studies were made on the effect of various mixing tube lengths that were progressively shorter, and the increase in primary pressure associated with each was assessed. It was concluded that an (L/D_M) value of 2.0 represented a length consistent with objectives for a maximum overall length of the blower, yet without the introduction of undue power penalty.*

Combining the effects of using a mixing tube whose length is twice the inlet hydraulic diameter, and a secondary supply pressure of -25 in. H_2O, produced the increase in primary total pressure that is shown in Figure 29.

The point labled as "A" in Figure 29 represents the ejector design point for a 25-percent bypass design, allowing a 5-in. H_2O inlet loss, and using a ratio of primary-to-mixing tube area of 0.6.

By refining the value of primary nozzle total temperature and by adjusting the value of $\alpha = A_{PRIM}/A_{MIX}$ to include a finite thickness splitter separating the primary and secondary channels, the ejector/diffuser design point parameters were generated (Table 11).

Values of particular importance in this table are the total pressure headrise and the required input drive power.

* Preliminary Designs D1A and D1B used an $(L/D_M) = 3.0$.

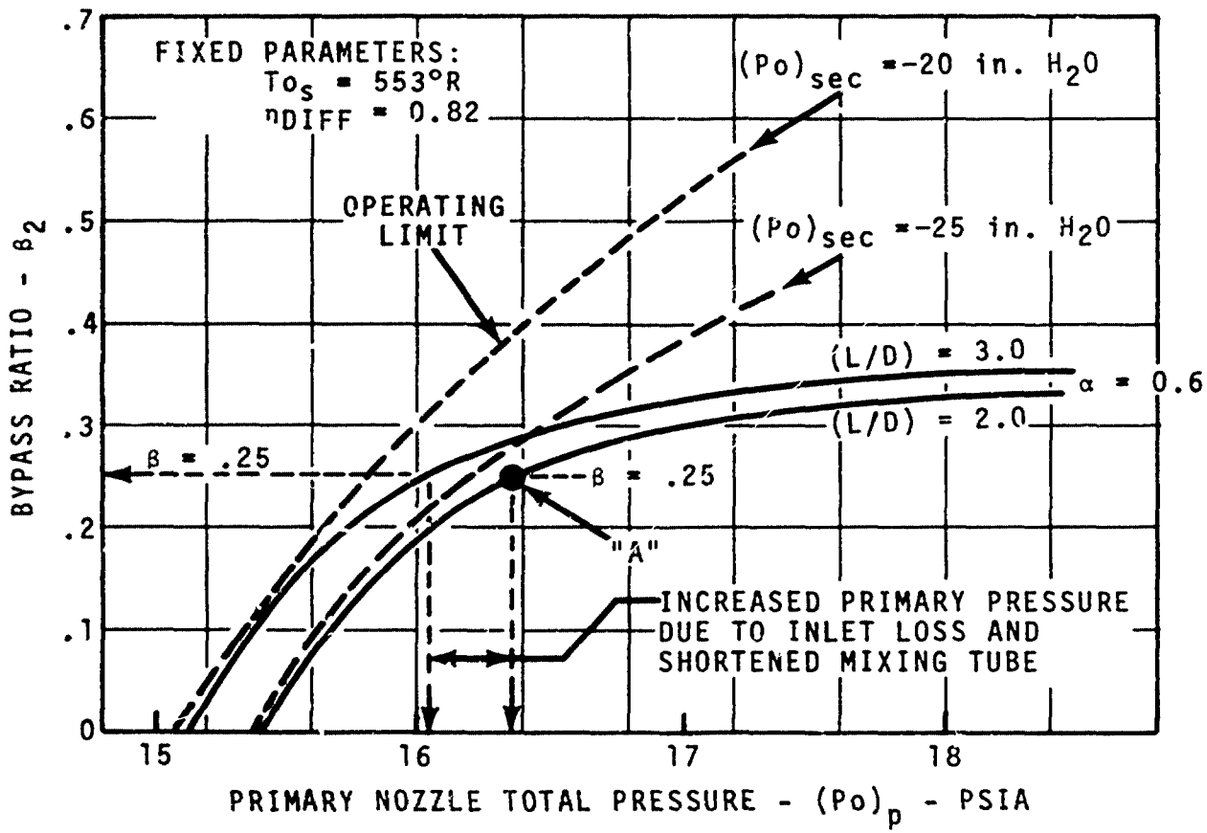

Figure 29. Effects of Inlet Loss and Mixing Tube Length on Ejector Primary Pressure.

TABLE 11. EJECTOR/DIFFUSER DESIGN POINT PARAMETERS

Area Ratio (A_p/A_M*)	.52
Flow Ratio	.25
Momentum Correction Factor*	1.13
Mixing Tube Nondimensional Length*	3.00
D'Arcy Friction Factor*	.012
Diffuser Area Ratio*	2.50
Diffuser Efficiency*	0.82
Diffuser Actual Recovery	0.69
Primary Flow Parameters	
Flow Rate	0.860 lb/sec
Mach Number	.562
Total Pressure	16.332 psia
Static Pressure	13.178 psia
Total Temperature	572°R
Effective Flow Area	2.93 in^2
Secondary Flow Parameters	
Flow Rate	0.214 lb/sec
Mach Number	.258
Total Pressure*	13.80 psia
Static Pressure	13.178 psia
Total Temperature*	518.7°R
Effective Flow Area	1.95 in^2
Mixing Tube Exit Parameters	
Flow Rate	1.074 lb/sec
Mach Number	.351
Total Pressure	15.070 psia
Static Pressure	13.840 psia
Total Temperature	561.4°R
Effective Flow Area	5.63 in^3
Diffuser Exit Parameters	
Total Pressure	14.884 psia
Ambient Pressure	14.696 psia
Total Temperature	561.4°R
Velocity Head	5.1 in. H_2O
Blower Headrise (Flange to Flange)	25.1 in. H_2O
Blower Horsepower	15.57

* Input Parameters

EJECTOR/DIFFUSER FLOW-PATH SPECIFICATION

To generate a geometric flow path for the ejector/diffuser section of the bypassing blower, the assumption is made that the effective flow areas (A_p, A_s) that were determined by analyzing a "concentric" ejector may be transformed into equivalent annular areas, as is required by the basic design concept, once a reference inner wall radius is specified.

In computing the physical length of the mixing tube, the hydraulic diameter term in ($L/D_M = 2.0$) is taken to be that of an annulus, i.e., four times the mixing tube channel height. In so doing, the "wetted perimeter" of the annular ejector is equated to the concentric analytical model, and frictional similarity is maintained.

The geometric flow area at the primary nozzle is based upon allowing 15% aerodynamic blockage ($\tau_p = .85$) and area compensation for 20 turning vanes of .032 inch trailing-edge thickness. The thickness of the splitter separating the primary and secondary channels was set at .060 inch.

Design of an annular diffuser to exhaust the flow from the blower is based upon the empirical data for static pressure recovery (CP_s) given in Reference 3. For a given area ratio diffuser, a nondimensional length ($L_D/\Delta r$) may be selected such that the static pressure rise through the diffuser is maximized. By placing a conical flow splitter at the entrance to the diffuser, the inlet channel height (Δr) is effectively reduced, and for the same area ratio and recovery, the overall length is accordingly shortened.

Figure 30 shows the resulting geometric flow path for the ejector and diffuser sections of the blower. The four support struts in the ejector mixing tube are of double circular arc profile, with a 1/8-inch maximum thickness. Placement of the exhaust diffuser splitter has been biased somewhat towards the inner flow channel in order to compensate for change in recovery due to diffuser flow curvature. Empirical data relating meanline flow curvature to loss in recovery is given on pages 590 to 592 of Reference 4.

MEANLINE ANALYSIS OF THE ROTOR AND TURNING VANES

Thermodynamic conditions at the exit from the compressor stage have been established through the ejector/diffuser design, in conjunction with preceding considerations on rotor and bypass flow requirements.

3. Sovran, G., FLUID MECHANICS OF INTERNAL FLOW, 1967 pp. 270-319.

4. Schlicting, H., BOUNDARY LAYER THEORY, 1968, pp. 590-592.

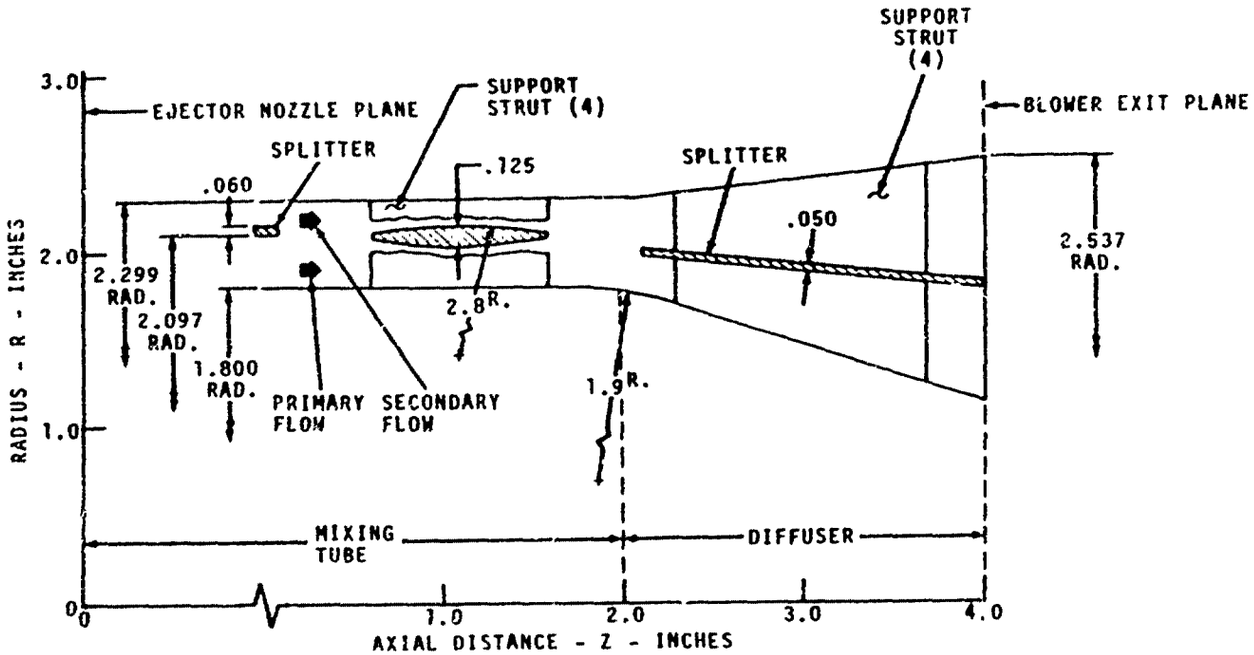

Figure 30. Ejector/Diffuser Flow Path - System D1.

Table 12 summarizes the stage performance requirements and the physical characterisitcs thus far determined.

In addition to the performance requirements given in Table 12, the following general considerations were applied to the rotor design:

TABLE 12. ROTOR AND TURNING VANE DESIGN REQUIREMENTS

Rotor Airflow, Actual	-	W_{ROT}	= 0.86 lb/sec
Blower Inlet Pressure	-	$P_{o\ IN}$	= 13.98 psia=20in. H_2O
Blower Inlet Temperature	-	$T_{o\ IN}$	= 518.7°R
Rotor Airflow, Referred	-	$\left(W_{ROT}\sqrt{\theta}\right)_{IN}$	= .904 lb/sec
Rotor Inlet Pressure	-	$P_{o\ IN}$	= 13.80 psia*=25in. H_2O
Inlet Prewhirl	-	α_1	= 0°
Design Rotational Speed	-	$N/\sqrt{\theta}_{IN}$	= 50,000 rpm
Maximum Inlet Blade Speed (Goal)	-	(U_{TIP})	= 500 fps
Rotor Type	-	Mixed Flow	= - - -
Primary Nozzle Total Pressure	-	P_{oP}	= 16.33 psia
Primary Nozzle Mach Number	-	M_P	= 0.56
Primary Nozzle Effective Area	-	$(A_p)_{EFF}$	= 2.93 in^2
Primary Nozzle Geometric Area	-	$(A_p)_{GEO}$	= 3.636 in^2
Primary Nozzle Outer Wall Radius	-	$(r_o)_P$	= 2.097 in
Primary Nozzle Inner Wall Radius	-	$(r_i)_P$	= 1.800 in
Primary Nozzle Aerodynamic and Vane Blockage	-	---	= 20%
Stage Total Pressure Ratio	-	$(Pr)_{STG}$	= $P_{o\,P}$ / $P_{o\ IN}$ = 1.183
Rotor Assumed Polytropic Efficiency	-	$(\eta_{poly})_{ROT}$	= 0.700

*Assumed inlet pressure drop of 5 in. H_2O from the blower inlet plane to the rotor leading-edge plane.

1. The rotor blading configuration should be as simple as possible, with relatively few blades and radially exiting meanlines.

2. Blunt leading edges, with relatively thick blade profiles, and only modest goals for efficiency and slip factor.

A meanline analysis, from which the meridional flow path is established, was conducted by the use of a one-dimensional performance procedure for a stage consisting of a centrifugal rotor, a vaneless space, and a diffusing vane row.

Basic one-dimensional compressible flow relations are used in computing the velocity triangles and the thermodynamic performance; inlet conditions are specified, along with the rotor and vane geometry, and the resulting stage performance was calculated.

Conditions at the impeller outlet are calculated by iterating on the exit meridional velocity, until continuity and work are satisfied, using input values for rotor efficiency and slip factor. Internal calculations of the slip factor, based upon the number of blades, and the trailing-edge metal angle are also provided for purposes of correlation against the assumed value, which are used in calculating the exit velocity triangle.

Application of the compressor meanline design program was an iterative procedure that interfaced with mechanical constraints, e.g., a specified overall length for the rotor/vanes and a minimum permissible rotor inlet hub radius consistent with bearing and shafting requirements.

The final velocity triangles and thermodynamic state parameters are given in Figures 31 and 32 and Tables 13 and 14. Based upon a 70-percent rotor polytropic efficiency and a slip factor of 0.9, the total pressure ratio across the rotor is 1.271, at a mean exit radius of 1.450 inches. With vaneless space and vane losses as stated in Table 14, the overall total pressure ratio for the stage is 1.190.

A layout of the rotor and turning vane flow path is shown in Figure 33; overall length from leading edge to the ejector interface plane is 3.00 inches.

INLET SEPARATOR POTENTIAL FLOW ANALYSIS

The specification of the inlet section to System D1 requires essentially the design of an inertial particle separator. The following design parameters have thus far been established for the inlet separator:

1. The total flow is 1.074 lb/sec, with .214 lb/sec bypassed (25-percent bypass ratio).

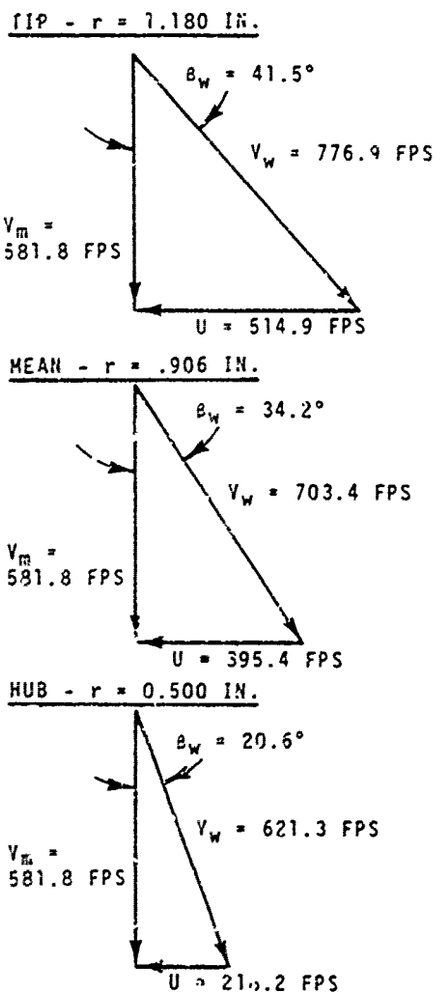

AIRFLOW - W_{ROT} = 0.860 lb/sec
SPEED - N = 50000 RPM
TOT. PRESS - P_o = 13.80 psia
TOT. TEMP. - T_o = 518.7 psia
BLOCKAGE FACTOR - τ = 0.95

Figure 31. Velocity Triangles at the Impeller Inlet.

ROTOR EXIT MEAN
RADIUS = 1.450 IN.

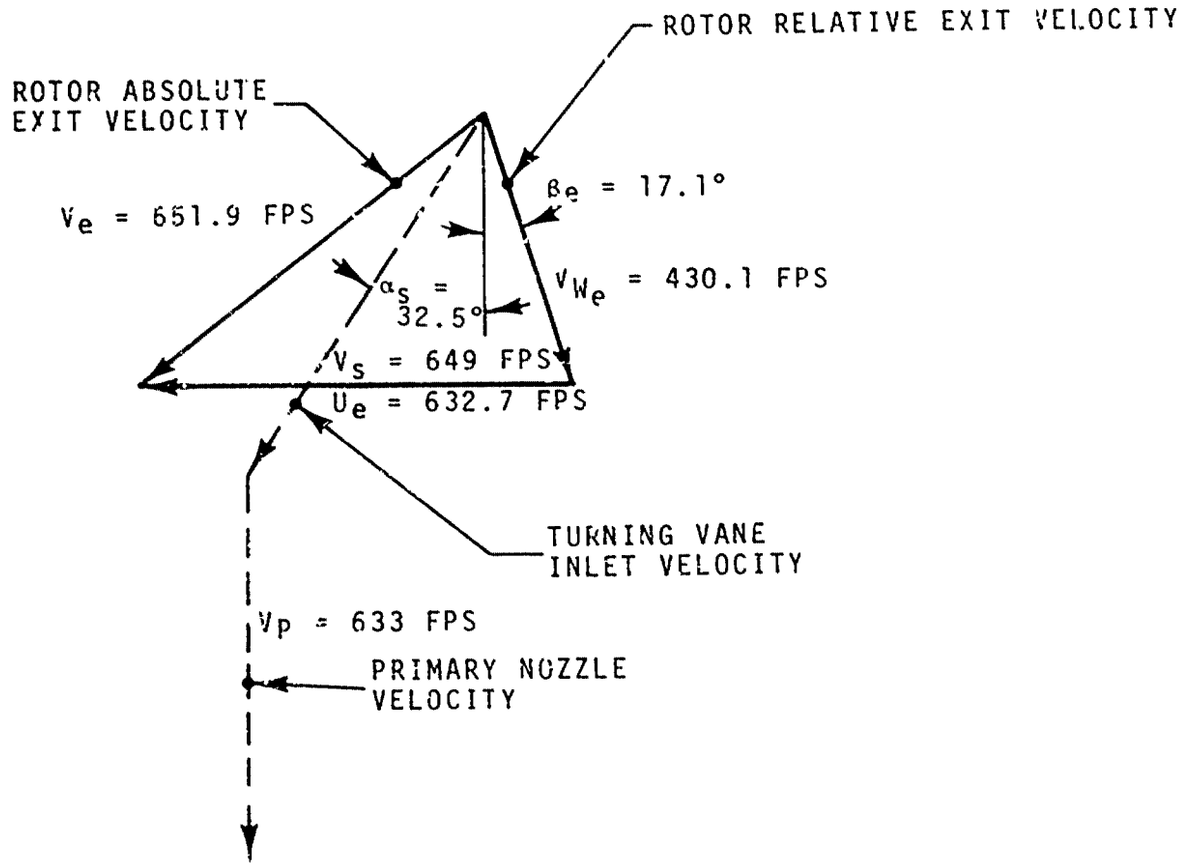

Figure 32. Rotor Exit and Turning Vane Velocity Triangles.

TABLE 13. VELOCITY TRIANGLE DATA FOR ROTOR AND TURNING VANES

	SYMBOL	IMPELLER INLET			IMPELLER DISCHARGE	TURNING VANE INLET	VANE EXIT (PRIMARY NOZZLE)
		TIP	MEAN	HUB			
RADIUS - INCHES	r	1.180	.906	.500	1.450 (MEAN)	2.097-1.800	2.097-1.800
BLADE SPEED - FPS	U	514.9	395.4	218.2	632.7		-
RELATIVE VELOCITY	Vw	776.9	703.4	621.3	430.1	-	-
MERIDIONAL VELOCITY	Vm	581.8	581.8	581.8	411.1	547.0	632.7
ABSOLUTE VELOCITY	V	581.8	581.8	581.8	551.9	648.8	632.7
TANGENTIAL VELOCITY, ABS.	Vu	0	0	0	506.2	349.5	0
ABSOLUTE AIR ANGLE	α	0	0	0	50.9	32.6	0
RELATIVE AIR ANGLE	βw	41.5	34.2	20.6	17.1	-	-
RELATIVE MACH NUMBER	Mw	.715	.648	.573	.379	-	-
ABSOLUTE MACH NUMBER	M	.540	.540	.540	.574	.571	.556
BLOCKAGE FACTOR	λ		.95		.90	.90	.85

SLIP FACTOR (ASSUMED)	S.F. - 0.8 = $[Vu/U]_{IMP.EX.}$ FOR RADIAL BLADES
SPEED	N - 50,000 rpm
HUB/TIP RATIO	r_H/r_T - 0.424
NUMBER OF BLADES	n - 8
RELATIVE VELOCITY RATIO	$(Vw_{TIP})_{IN}/(Vw)_{EX}$ - 1.806

TABLE 14. THERMODYNAMIC STATE PROPERTIES, ROTOR AND TURNING VANES

	SYMBOL	IMPELLER INLET	IMPELLER DISCHARGE	TURNING VANE INLET	VANE EXIT (PRIMARY NOZZLE)
TOTAL PRESSURE - psia	P_o	13.80	17.537	17.214	16.426
TOTAL TEMPERATURE - °R	T_o	518.7	572.28	572.28	572.28
STATIC PRESSURE - psia	P	11.35	14.027	13.799	13.316
STATIC TEMPERATURE - °R	T	490.8	536.92	537.26	538.98
DENSITY - lbm/ft^3	ρ	.0624	0.0705	0.0693	0.0667
TOTAL PRESSURE RATIO	PR	-	1.2708	1.2474	1.1903
TOTAL TEMPERATURE RATIO	TR	-	1.1027	1.1027	1.1027
ADIABATIC EFFICIENCY (CUM)	η_{AD}	-	0.689	0.634	0.497
POLYTROPIC EFFICIENCY (CUM)	η_{POLY}	-	0.700	0.646	0.509
ACTUAL WORK - Btu/lbm	Δh_o	-	12.79	-	-
SPECIFIC HEAT RATIO	γ	1.3998	1.3995	1.3995	1.3995

STATIC PRESSURE RISE COEFFICIENTS:

IMPELLER MEAN - $CPR = \frac{\Delta P}{(P_o)_{in} - P} = 0.123$

VANELESS SPACE - $CPR = \frac{\Delta P}{P_o - P} = -.076$

TURNING VANES - $CPR = \frac{\Delta P}{P_o - P} = -.142$

TOTAL PRESSURE LOSS COEFFICIENTS:

VANELESS SPACE - $CPL = \frac{\Delta P}{P_o - P} = 0.092$

TURNING VANES - $CPL = \frac{\Delta P_o}{P_o - P} = 0.230$

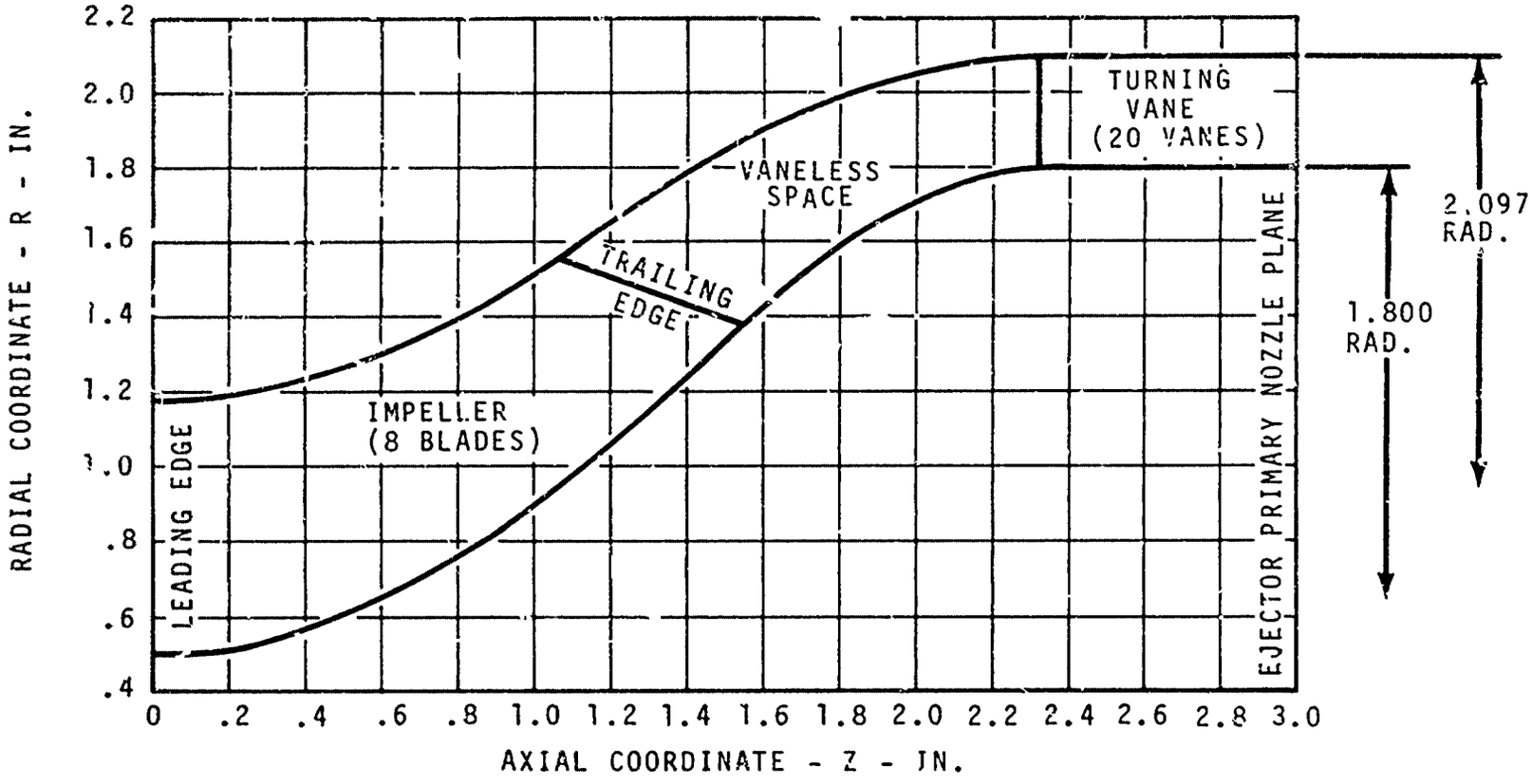

Figure 33. Rotor and Turning Vane Flow Path.

2. The minimum separation efficiency for MIL-E-5007C sand is 0.72.

3. The maximum total pressure loss from inlet plane to secondary nozzle and from inlet plane to rotor leading edge is 1.3 percent or 5 in. H_2O.

In addition to the above, an axial length of 3 inches was imposed for the inlet, which gives an overall unit length of 10 inches; this is consistent with goals established during the earlier feasibility studies.

Of the two key design parameters (namely, separation efficiency and pressure loss), the latter was considered to be the more stringent requirement for the present application, because of the use of an ejector downstream of the separator. For a fixed bypass ratio, the power requirements to the blower will increase rapidly as a function of losses in the primary and secondary channels.

Initially, a constant-diameter outer wall shape was considered, possibly in conjunction with the use of swirl vanes, at the inlet. However, in view of the rather modest efficiency goal ($\eta_2 = .72$), the use of swirl vanes was not warranted, considering the additional pressure loss, cost, complexity, and potential for erosion damage that would be introduced.

A separator configuration with a constant OD, or a diverging outer wall, would favor high separation efficiencies due to the large capture area, but at the expense of increased losses in both the scavenge and the core channels.

By an iterative application of potential flow analysis, followed by particle trajectory analysis, the bypass channel "catch area" was gradually reduced until the flow path shown in Figure 34 was obtained. The estimated bypass channel total pressure loss for this configuration is 3 in. H_2O, which is within design objectives. A discussion of trajectory analysis results is given below.

The blunt centerbody shape (Figure 34) was introduced primarily as a length consideration, accepting the small pressure loss penalty associated with an abrupt inlet contraction, and some adverse impact on local separation efficiency for those radii where the wall contour is steep.

INLET PARTICLE TRAJECTORY ANALYSIS

The purpose of a particle trajectory analysis was to obtain an estimate of separation efficiency; in this particular instance, 200 μ mean particle diameter MIL-E-5007C type sand was used. The analysis required a knowledge of the fluid properties (velocity and density) at all

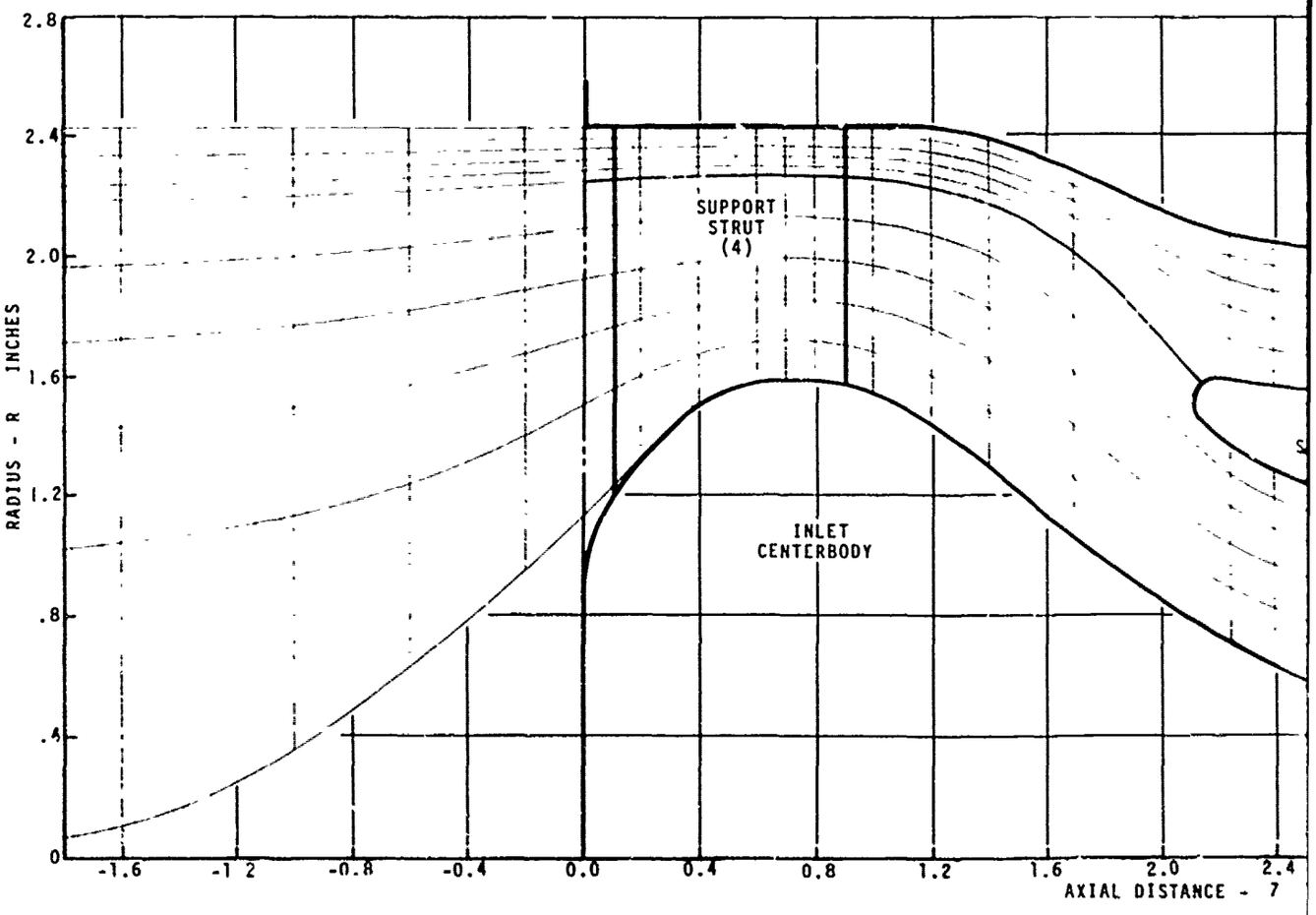

Figure 34. Potential Flow Analysis of the Blower Inlet.

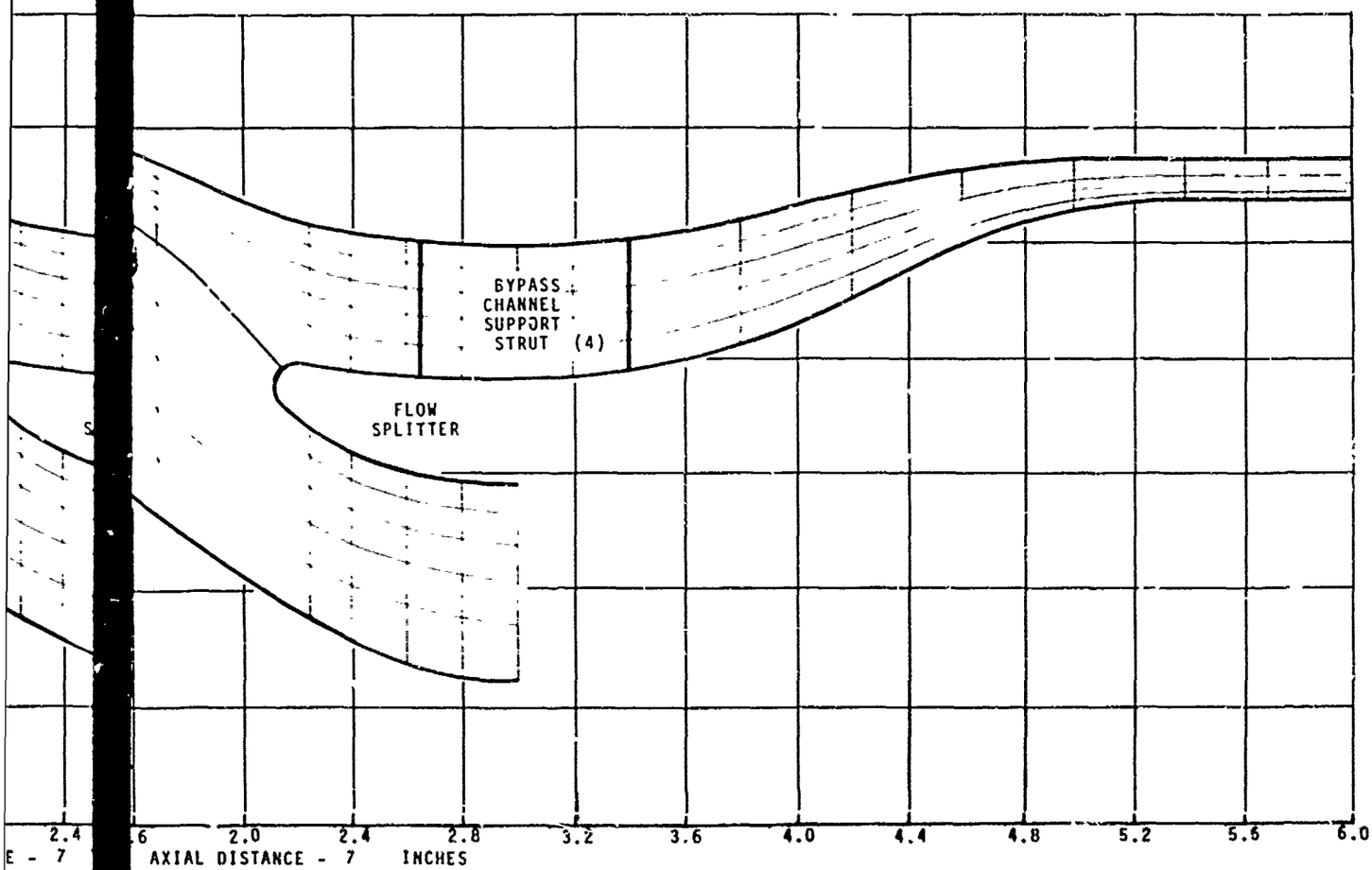
BYPASS
CHANNEL
SUPPORT
STRUT (4)
FLOW
SPLITTER
2.4
6
2.0
2.4
2.8
3.2
3.6
4.0
4.4
4.8
5.2
5.6
6.0
E - 7
AXIAL DISTANCE - 7 INCHES

2

points in the flowfield, the configuration geometry, and the initial conditions, of the sand particles (velocity and position).

Throughout this analysis, the following assumptions were made:

1. The forces acting on the particles are due to drag and gravity.

2. For purposes of calculating the drag coefficient, and the wall rebound characteristics, the particles are assumed to be spherical in shape.

3. Wall rebounds are treated as semi-elastic collisions with a constant value of coefficient of restitution, $\epsilon = 0.5$.

Particle diameters ranging from 1 μ up to 1000 μ were introduced at various inlet radii, from 0.6 inch to 2.200 inches in each case at 50 fps axial velocity, zero radial velocity. The initial position for the particle trajectory analysis was taken $Z = -2.000$ inches relative to the blower inlet flange.

Other fixed parameters included:

Sand Particle Density	$- \rho_s$	=	160 lb_m/ft^3
Air Absolute Viscosity	$- \mu$	=	3.5×10^{-7} $lb_f sec/ft^2$
Total Airflow Rate	$- W_{TOT}$		1.074 lb/sec

A typical series of resulting trajectories is given in Figure 35. In actuality, considerably more trajectories were run. The particle position computation terminates at the splitter leading edge, and particles are judged as bypassed or ingested on the basis of the last position relative to the center of the splitter leading-edge radius.

If we summarize the results of all trajectories, listing by radius, the range of particles ingested, versus the size range of particles bypassed, the results are as given in Table 15.

Through use of the percentages by weight of MIL-E-5007C which lie within the ranges of particle diameters bypassed, the separation efficiency by weight may be calculated at any specified radius.

Finally, by plotting this distribution of efficiencies versus radius (Figure 36), an integrated value may be found that represents the average separation efficiency for "C-Spec" sand, for the assumptions made.

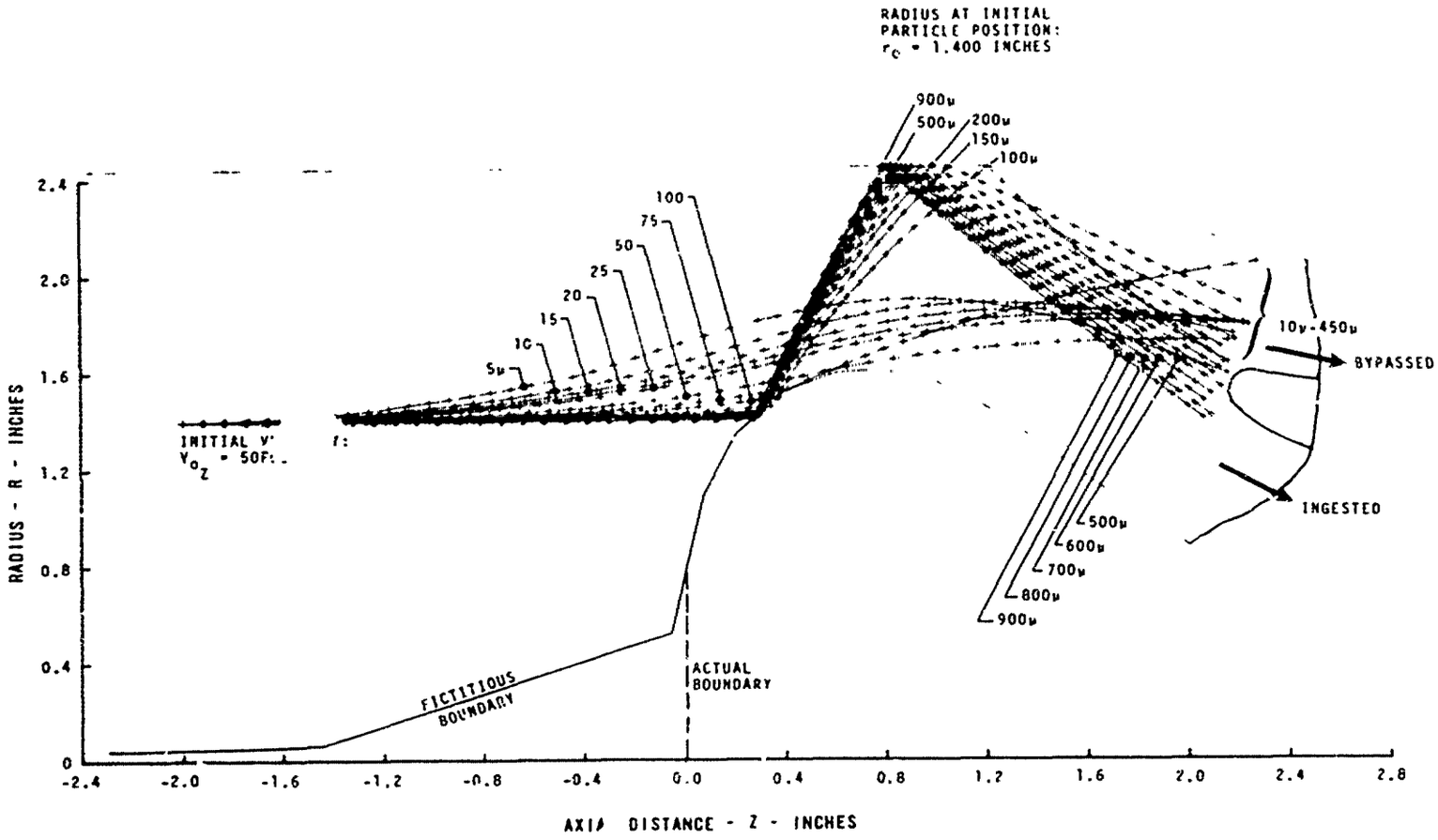

Figure 35. Composite Trajectory Analysis at r_o = 1.400 Inches.

TABLE 15. TRAJECTORY ANALYSIS SUMMARY - SCAVEN[illegible] LOWER INLET

RADIUS (inches)	PARTICLES INGESTED	PARTICLES BYPASSED (1)	% OF MIL-E-5007C BY WEIGHT LYING BETWEEN RANGES OF PARTICLE DIAMETERS GIVEN IN (1)	SEPARATION EFFICIENCY BY WEIGHT η_{sep}
.600	1μ-7μ 176μ-210μ	8μ-175μ >210μ	44.5% 43.5	88%
.700	1μ-7μ 176μ-215μ	8μ-175μ >215μ	45.0% 42.0	87%
.800	1μ-6μ 161μ-215μ	7μ-160μ >215μ	38.0% 43.0	81%
.900	1μ-6μ 146μ-210μ	7μ-145μ >210μ	33.0% 43.0	76%
1.000	1μ-6μ 141μ-215μ	7μ-140μ >215μ	31.0% 42.0	73%
1.050	1μ-6μ 141μ-215μ	7μ-140μ >215μ	31.0% 42.0	73%
1.100	1μ-6μ 115μ-250μ	7μ-115μ >250μ	22.0 33.0	55%
1.200	1μ-5μ 116μ-280μ	6μ-115μ >280μ	20.0% 28.0	48%
1.300	1μ-5μ 181μ-285μ	6μ-180μ >285μ	46.0% 26.0	72%
1.400	1μ-5μ >500μ	6μ-500μ	92.0%	92%
1.500	1μ-4μ >500μ	5μ-500μ	92.0%	92%
2.200	<4μ	>4μ	100.0%	100%

FIXED PARAMETERS

RADIAL VELOCITY - $(Vo)_R$	0
AXIAL VELOCITY - $(Vo)_Z$	50 fps
INITIAL POSITION - Z_0	-2.000 in
SAND PARTICLE DENSITY	150 lbm/ft^3
AIR VISCOSITY - μ	3.5E-07 lb$_f$ sec/ft^2
COEFFICIENT OF RESTITUTION - ϵ	0.5
AIR FLOWRATE - W_{tot}	1.074 lb/sec

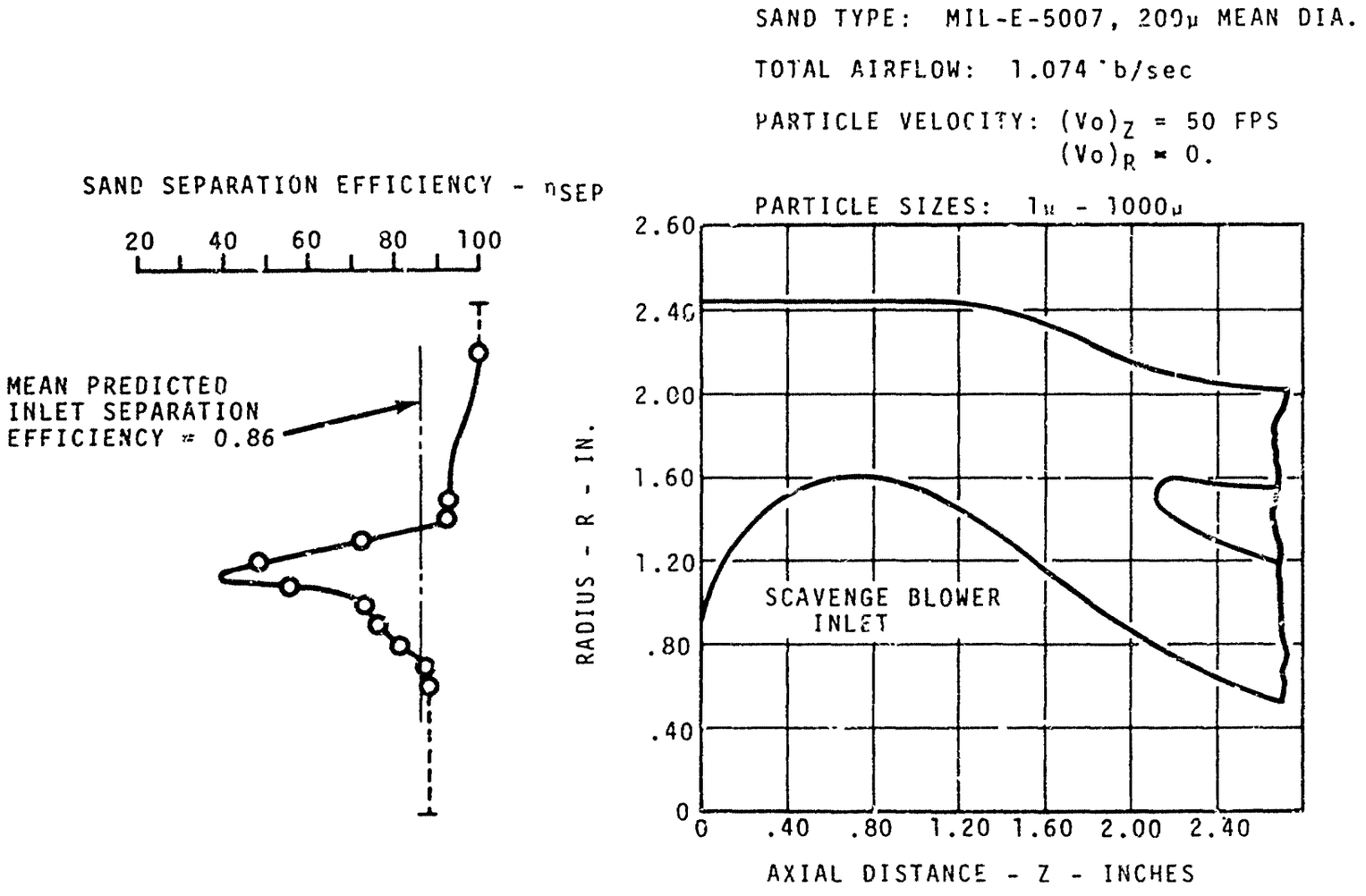

Figure 36. Estimated Distribution of Sand Separation Efficiency in the Blower Inlet.

The value thus obtained is as follows:

$$\eta_{SEP} = \eta_2 = \frac{\text{Weight of sand bypassed}}{\text{Total weight of sand into blower}}$$

$$\eta_{2\ CALC} = 0.86$$

The actual level of separation efficiency achieved is fundamental to the durability of the blower. Past experience in correlating the analytics of efficiency prediction with test data has generally shown discrepancies that can be up to 10 points in magnitude, with the prediction being optimistic. The same problem is pointed out in Reference 5, page 230, with respect to trajectory analysis results in general.

In the analysis above, the two prime sources of error are considered to be a failure to achieve the assumed initial conditions (i.e., a real world set of initial conditions that can be much more random in initital velocity and direction than the assumed-constant values) and a lack of adequate statistical treatment of the actual rebound characteristics, considering the true polyhedral shape of the particles as opposed to the assumed spherical shape.

Although we recognize some measure of optimism in the estimated efficiency, the stated design goal of 72 percent is still considered to have sufficient margin to proceed with the inlet flow path as specified at this point without modification for further efficiency improvement.

OVERALL FLOW-PATH SPECIFICATION

The approach taken in the aerodynamic design of the scavenge blower was to consider the major components separately, interfacing each in sequence, with iterations as required, to obtain specified overall performance goals. Summarizing these components:

Inlet separator section	-	3 inches in length	- inlet to rotor leading edge

5. Duffy, R. J., and Shattuck, B. F., INTEGRAL ENGINE INLET PARTICLE SEPARATOR, Vol. II, DESIGN GUIDE, General Electric Co., USAAMRDL TR-75-31B, Eustis Directorate, U. S. Army Air Mobility Research and Development Laboratory, Fort Eustis Virginia, August 1975, AD AO15064.

Rotor and turning vanes	-	3 inches in length	- rotor leading edge to ejector primary nozzle plane
Ejector/Diffuser section	-	4 inches in length	- nozzle plane to blower exit plane.
Total length	-	10.00 inches	

The overall flow path definition appears in Figure 37, with the point-for-point coordinate specification of channel boundaries given in Table 16.

TURNING VANE DESIGN

Design of the turning vane assembly in the primary airflow channel was based upon NACA -65 series airfoil strip stock, A=1 meanline shape, with a maximum thickness of 10-percent chord.

Given the geometry for the -65 series airfoil, the cascade solidity, and the required amount of turning (refer to the data below), then the objective of this phase of the design is to generate a recambered airfoil which provides the required turning at an acceptable level of deviation angle.

Number of Vanes	-	20
Airfoil Type	-	-65 Series, A=1 Meanline
Tip Radius	-	2.097 in.
Hub Radius	-	1.800 in.
Mean Radius	-	1.954 in.
Chord Length	-	0.694 in.
Solidity (Mean)	-	1.124 in.
Inlet Angle	-	32.3 deg
Inlet Mach Number	-	0.57
Exit Air Angle	-	0 deg

Using a vane cascade selection program, the camber was determined to be 39.9 degrees or 7.6 degrees past axial for 0 degrees incidence. The resulting vane profile shape is shown in Figure 38.

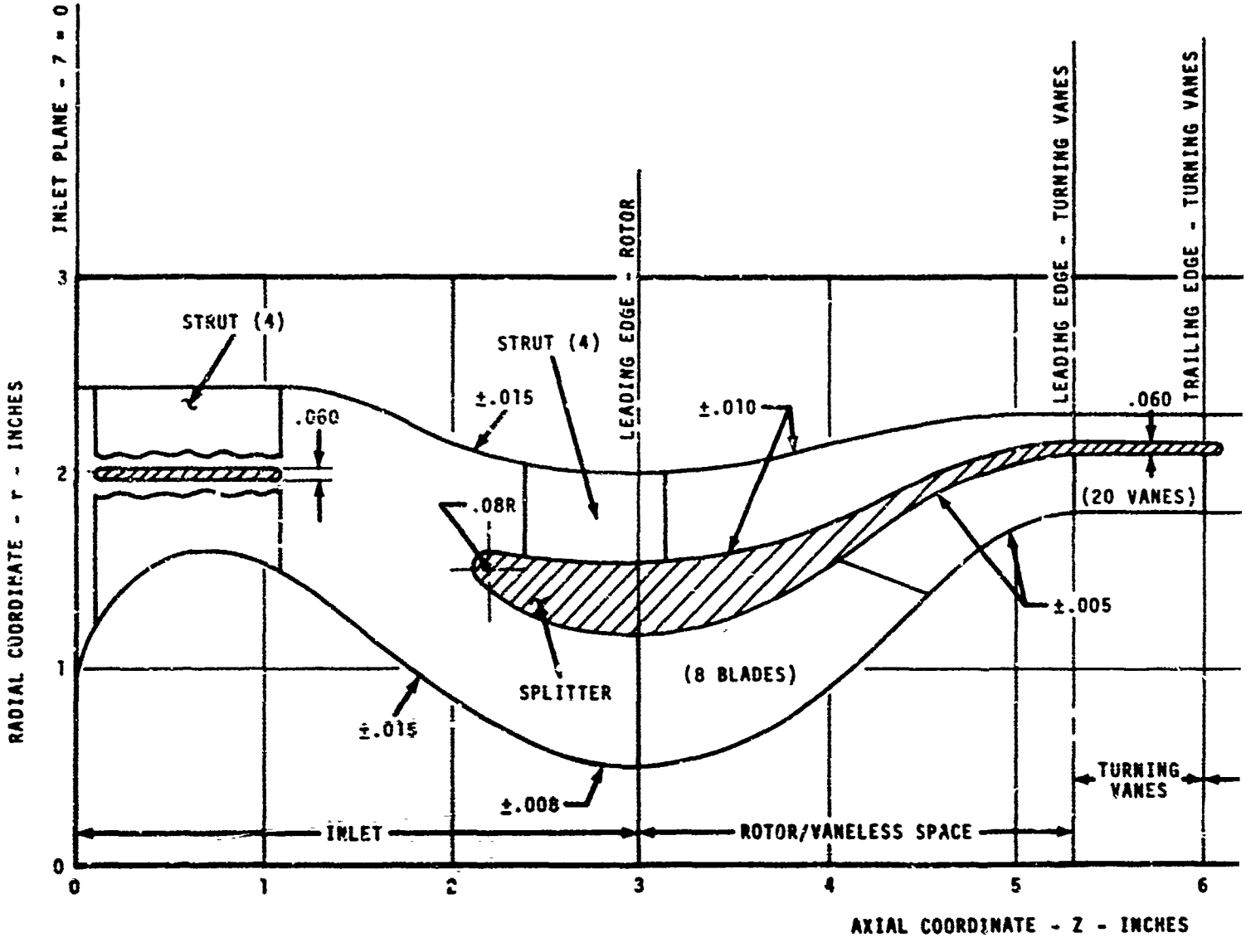

Figure 37. Overall Flow Path for Bypassing Blower (System D1).

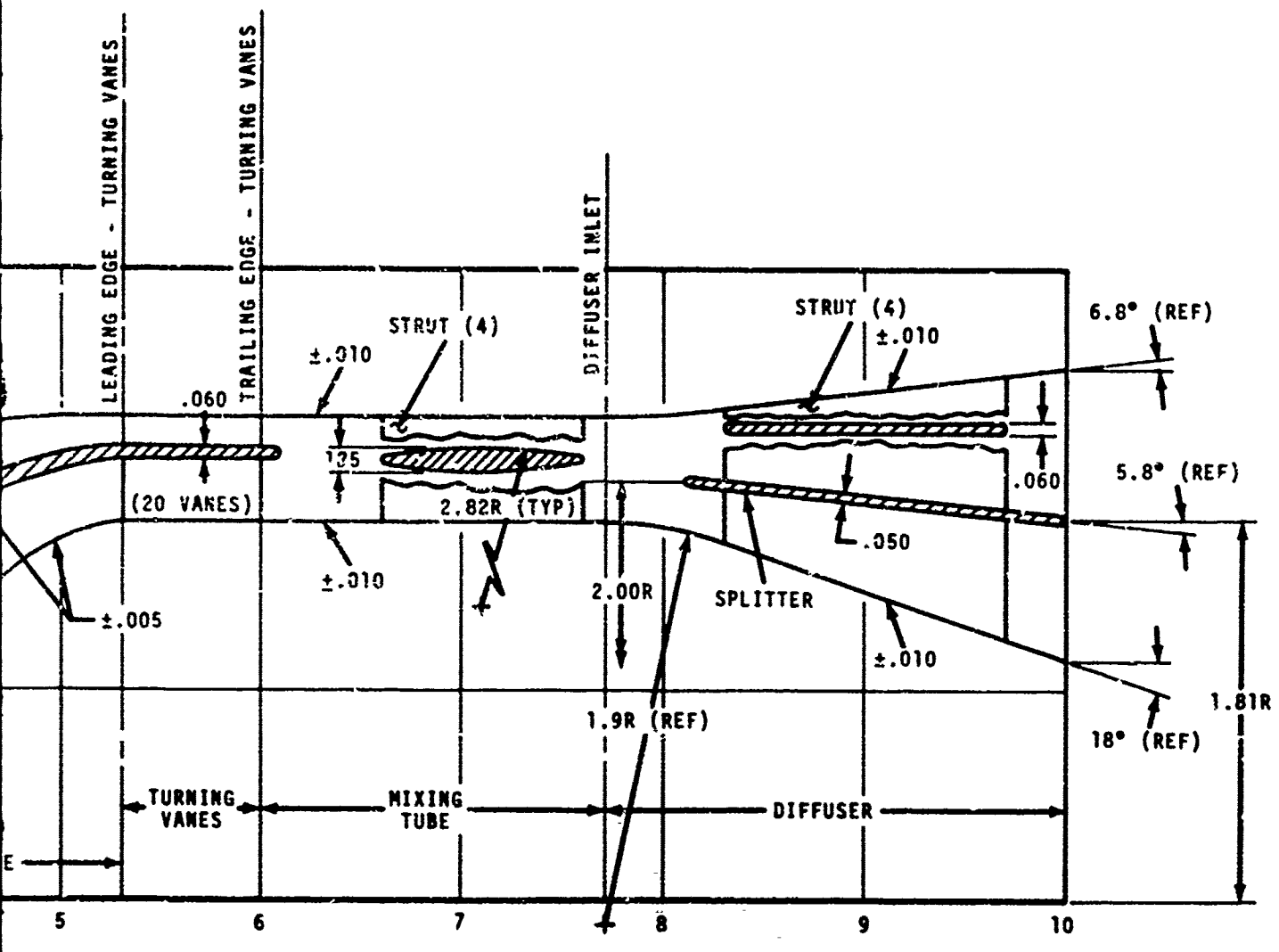
LEADING EDGE - TURNING VANES
TRAILING EDGE - TURNING VANES
DIFFUSER INLET
STRUT (4)
±.010
.060
(20 VANES)
.135
2.82R (TYP)
±.010
±.005
2.00R
1.9R (REF)
STRUT (4)
±.010
6.8° (REF)
.060
5.8° (REF)
.050
SPLITTER
±.010
1.81R
18° (REF)
TURNING VANES
MIXING TUBE
DIFFUSER
5
6
7
8
9
10
DINATE - Z - INCHES

2

TABLE 16. SYSTEM D1 FLOW-PATH COORDINATES

AXIAL LENGTH	HUB RADIUS	SHROUD RADIUS
z	r_i	r_o
0.000	0.900	2.440
0.200	1.340	2.440
0.400	1.538	2.440
0.600	.592	2.440
0.700	.600	2.440
0.800	1.597	2.440
1.000	1.550	2.440
1.200	1.445	2.438
1.400	1.305	2.398
1.700	1.078	2.295
2.250	0.715	2.076
2.400	0.640	2.050
2.600	0.557	2.005
2.800	0.508	2.010
3.000	0.500	2.000
3.200	↑	2.008
3.400	SEE	2.024
3.800	ROTOR	2.090
4.200	FLOW PATH	2.190
4.600		2.260
5.000		2.296
5.400		2.299
5.700		2.299
6.000	1.800	2.299
6.100	1.800	2.299
7.000	1.800	2.299
7.700	1.800	2.299
7.800	1.797	2.299
7.900	1.789	2.299
8.000	1.776	2.304
8.100	1.757	2.318

--- CONTINUED ---

z	r_i	r_o
8.200	1.735	2.322
8.300	1.702	2.334
8.500	1.637	2.358
8.700	1.573	2.382
8.900	1.507	2.406
9.100	1.442	2.430
9.300	1.377	2.453
9.500	1.312	2.447
9.700	1.247	2.473
10.000	1.150	2.[illegible]

Inner and Outer Wall Flow Path Coordinates

AXIAL LENGTH	SPLITTER LOWER SURFACE	SPLITTER UPPER SURFACE
z	r_{s_L}	r_{s_U}
2.250	1.378	1.592
2.400	1.290	1.572
2.600	1.220	1.555
2.800	1.188	1.545
3.000	1.180	1.542
3.200	↑	1.550
3.400	SEE	1.570
3.800	ROTOR	1.665
4.200	FLOW PATH	1.821
4.600		2.005
5.000		2.120
5.400		2.157
5.700		2.157
6.000	2.097	2.157
6.100	2.127	2.127

Splitter Upper and Lower Surface Coordinates

AXIAL LENGTH	HUB RADIUS	AXIAL LENGTH	SHROUD RADIUS
z	r_{HUB}	z	r_{SHROUD}
3.000	0.500	3.000	1.180
3.004	0.500	3.100	1.184
3.212	0.522	3.200	1.196
3.327	0.551	3.300	1.214
3.464	0.594	3.406	1.238
3.610	0.653	3.508	1.271
3.733	0.722	3.614	1.310
3.862	0.794	3.720	1.360
3.962	0.885	3.826	1.412
4.091	0.971	3.935	1.475
4.220	1.080	4.060	1.560
4.343	1.194	4.265	1.718
4.537	1.377	4.530	1.865
4.754	1.563	4.182	1.991
4.931	1.704	5.104	2.070
5.19?	1.783	5.320	2.097
5.320	1.800	.400	2.097
5.400	1.800	5.700	2.097
5.700	1.800	6.000	2.097
6.000	1.800		

Rotor and Turning Vane Flow Path Coordinates

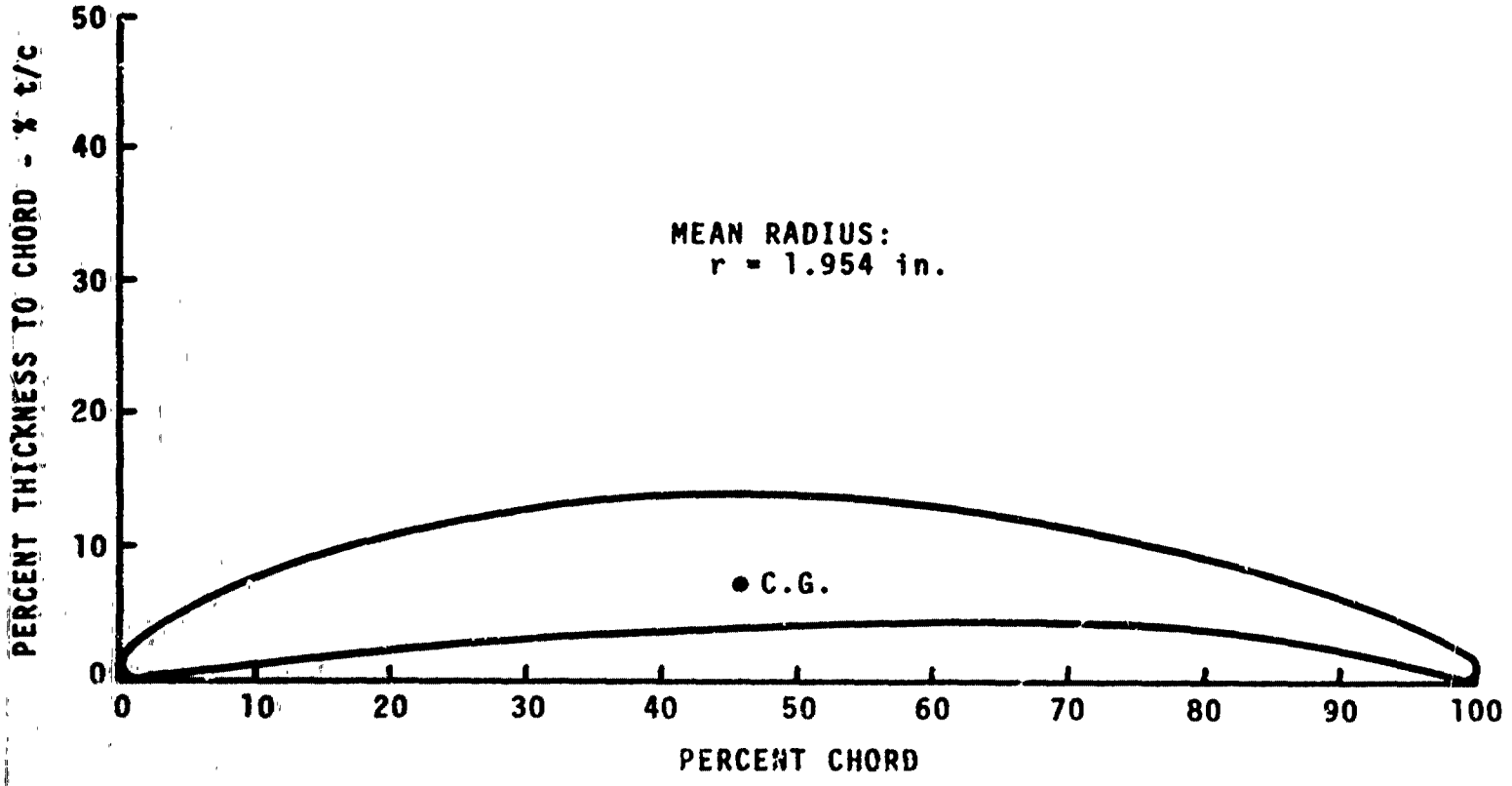

Figure 38. Turning Vane Profile (Percent Chord) - System D1.

IMPELLER FLOW ANALYSIS

The first phase of the impeller design (meanline analysis) established the meridional flow path and the vector triangles, satisfying the required flow and work based on assumed efficiency and slip factor.

The remaining elements to complete the rotor aerodynamic design are as follows:

1. Determine the flow field within the compressor once a blading geometry has been specified.

2. Iterate the blade shape, if required, until acceptable surface velocity distributions are achieved and the previously determined vector triangles are satisfied.

3. Translate the blading coordinates into manufacturing cross sections.

The latter step and the parallel stress analysis are discussed in subsequent sections.

For the internal flow analysis of the impeller, a centrifugal compressor design program was employed which required specification of a distribution of blade angles (mean camberline tangent angles) as a function of axial distance along the rotor. In addition to the blade angle, a thickness distribution normal to the meanline was necessary to complete the blade definition.

At the rotor design speed and flow rate, the mass-weighted average total pressure ratio was calculated to be 1.274, which is in close agreement with the value of 1.271 previously determined from meanline analysis at an exit radius of 1.450.

Relative velocities along the surfaces of the blades were examined with respect to the following:

1. Maximum values along the suction surface (local supersonic flows).

2. Average velocity ratio across the blade row (flow separation)

3. Average channel Mach number (proximity to choking).

The surface and the average velocities at the hub, mean, and tip streamlines were computed; and for the blading configuration that was analyzed, these results were considered to be within acceptable limits with respect to the criteria above. (See Figure 39.)

IMPELLER BLADE MANUFACTURING SECTIONS

In the preceding design analysis of the impeller, all blading definition was along streamtubes and was expressed generally in terms of radius, axial distance, normal thickness, and meanline angle.

The meanline coordinate may also be expressed in terms of the cylindrical coordinate, θ, which is the angle measured with respect to a vertical radial line. The parameter θ is available from the design program output, for each meridional calculation plane and streamtube center. Ten-times size master airfoil charts to be used in manufacturing and inspecting the impeller were prepared from the r, θ, Z, t blading definitions by means of a conversion program that provides horizontal sections (cylinder tangents) calculated from the input cylindrical cordinates.

A composite overlay of the final blade design is shown in Figure 40.

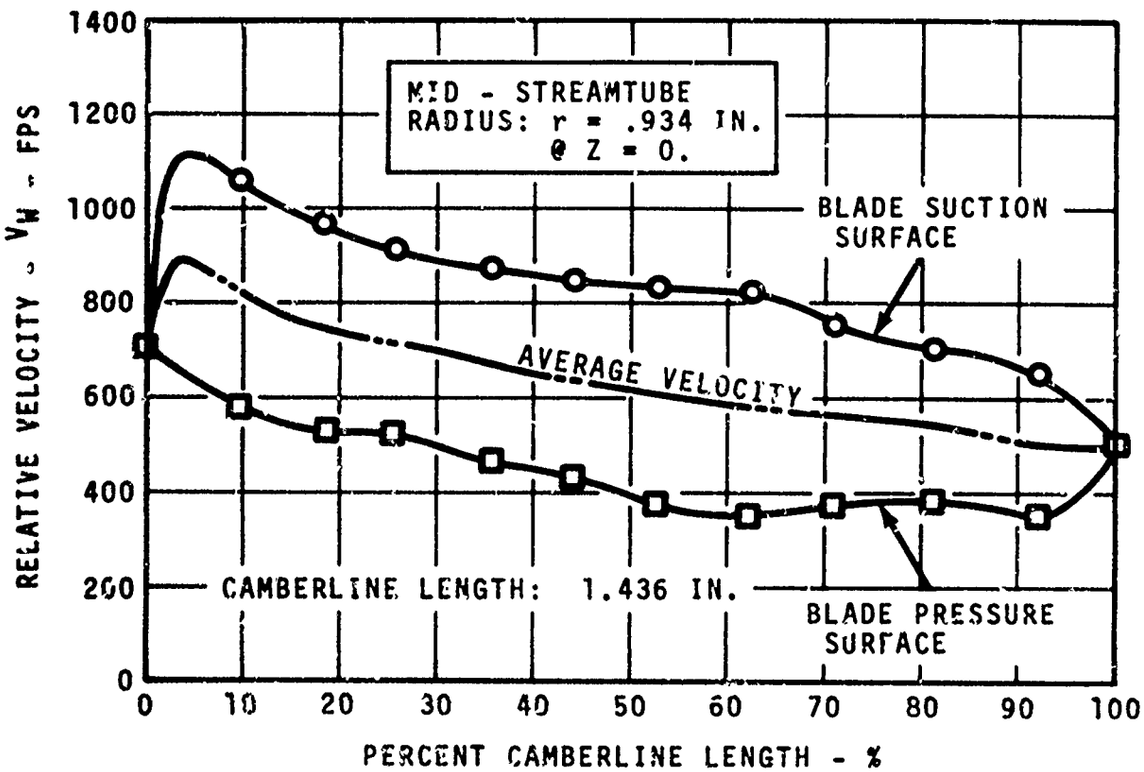

Figure 39. Distribution of Velocities on the Rotor Blade Suction and Pressure Surface (Mean).

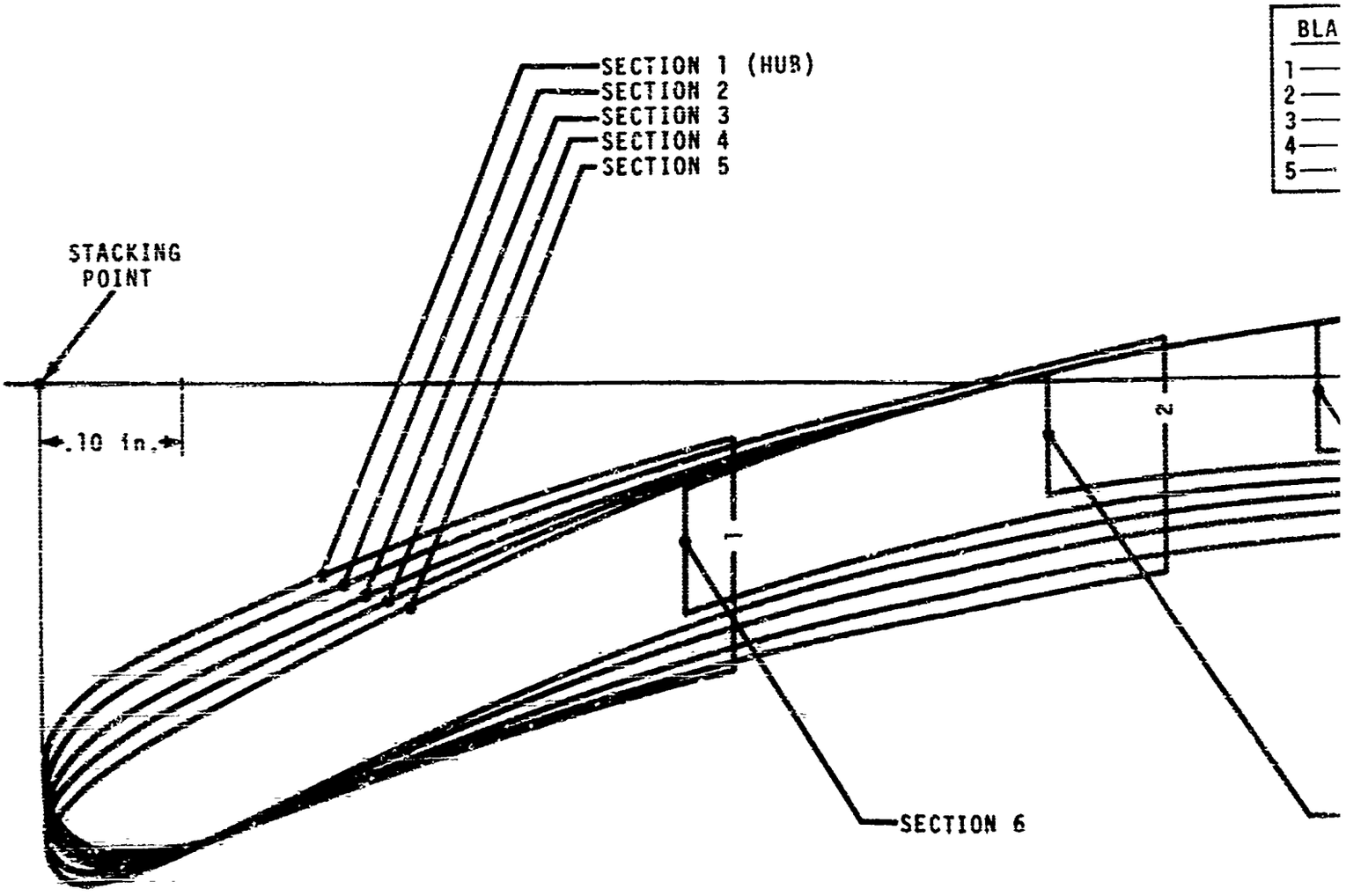

Figure 40. Composite of Impeller Blade Manufacturing Cross Section.

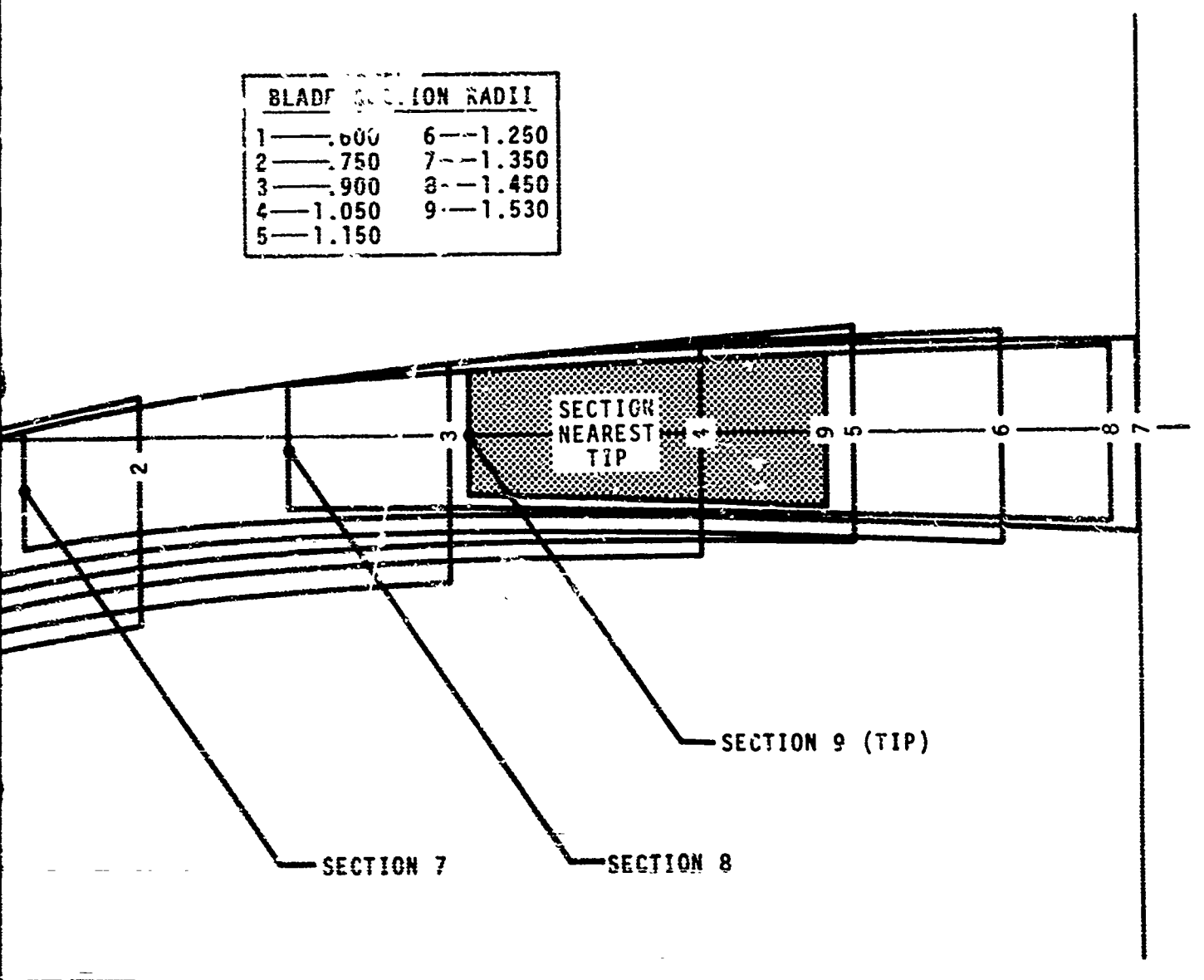
BLADE SECTION RADII
1——.600
2——.750
3——.900
4——1.050
5——1.150
6——1.250
7——1.350
8——1.450
9——1.530
SECTION NEAREST TIP
SECTION 9 (TIP)
SECTION 7
SECTION 8

MECHANICAL DESIGN - SYSTEM D1

GENERAL

The detailed mechanical design of the blower is based upon the aerodynamic flow path, as shown in Figure 37. In addition, the following considerations applied:

1. Use a simple, modular design that permits access at all major components, facilitating development changes if required.

2. Physical similarity to engine-level hardware would apply only insofar as meeting power, durability, and aerodynamic performance requirements.

3. Critical elements, where erosion damage is of potential influence upon performance or mechanical integrity, must be representative of engine-level hardware. The assumed critical element in the present design is the rotor.

4. Methods of fabrication for units produced in quantity have been addressed in the earlier feasibility studies; for present purposes, major components are fully machined where possible. Castings, spinnings, or hydroformed sheet metal components and generally those techniques applicable to quantity production, were not used.

The basic mechanical arrangement which was employed is an overhung integral rotor/shaft, supported by two oil-mist-lubricated 20mm bearings.

A "modular" design approach resulted in a breakdown of components as follows:

1. Inlet housing - This housing contains the separator centerbody, supported by four struts.

2. Air splitter assembly - The inside diameter of the splitter forms the rotor shroud flow path. Four bypass channel struts connect the splitter to the blower outer casing.

3. Turning vane assembly - Twenty NACA Series 65 airfoils are used to remove swirl from the rotor discharge. The exit plane of the vane assembly forms the ejector primary nozzle. No specific provisions have been incorporated into this assembly for erosion protection.

4. Bearing housing/mixing tube assembly - This assembly is the basic structural element of the blower, and transmits rotor/bearing loads through four struts to an external mounting flange. Secondary flow is induced at the inlet plane of the housing flow path.

5. Exhaust diffuser - The exhaust diffuser discharges the mixed flow to ambient, using an efficient, compact arrangement that incorporates a flow splitter. Four struts provide support for the conical splitter.

A detailed layout of the integrated mechanical design for the blower is shown in Figure 41.

DYNAMICS OF THE ROTOR/SHAFT SYSTEM

The design objective was to place the fundamental rotor resonant frequency safely above the 50,000 rpm operating speed. A minimum calculated first critical speed of 60,000 rpm was considered to be satisfactory.

The impeller overhung mass and the positioning of its center of gravity relative to the centerline of the No. 1 bearing is found to be very influential upon the fundamental resonant frequency . (See Figure 42.)

Spring rates are based upon a radial load of 78 lb_f, resulting from 0.5 gm-in. of unbalance at the impeller center of gravity.

The final design weight for the impeller is 1.0 lb, with an overhung center of gravity of 1.10 inches (Figure 42, Dimension A).

For this configuration, the fundamental resonant frequency is an acceptable 62,000 cpm.

STRESS ANALYSES OF THE ROTOR

Stress analyses were performed on the scavenge blower rotor to assure that low operating stress levels would be maintained. In summary, the maximum operating disk stress was kept to 25 ksi, while keeping that of the blade to a maximum of 16 ksi. The maximum calculated radial displacement was under 0.001 inch at design speed.

A two-dimensional finite element analysis was performed to assess both the disk and the blade behavior. The impeller finite-element model consisted of 276 nodes and 243 elements (Figure 43). A portion of the shaft, which is an integral part of the impeller, was included in the analysis to impose the effects of the shaft's shell behavior on the disk. The axial deflection at the end of the shaft was set to zero. Room temperature properties for 17-4 PH steel were used, and the 100-percent speed loading of 50,000 rpm was applied.

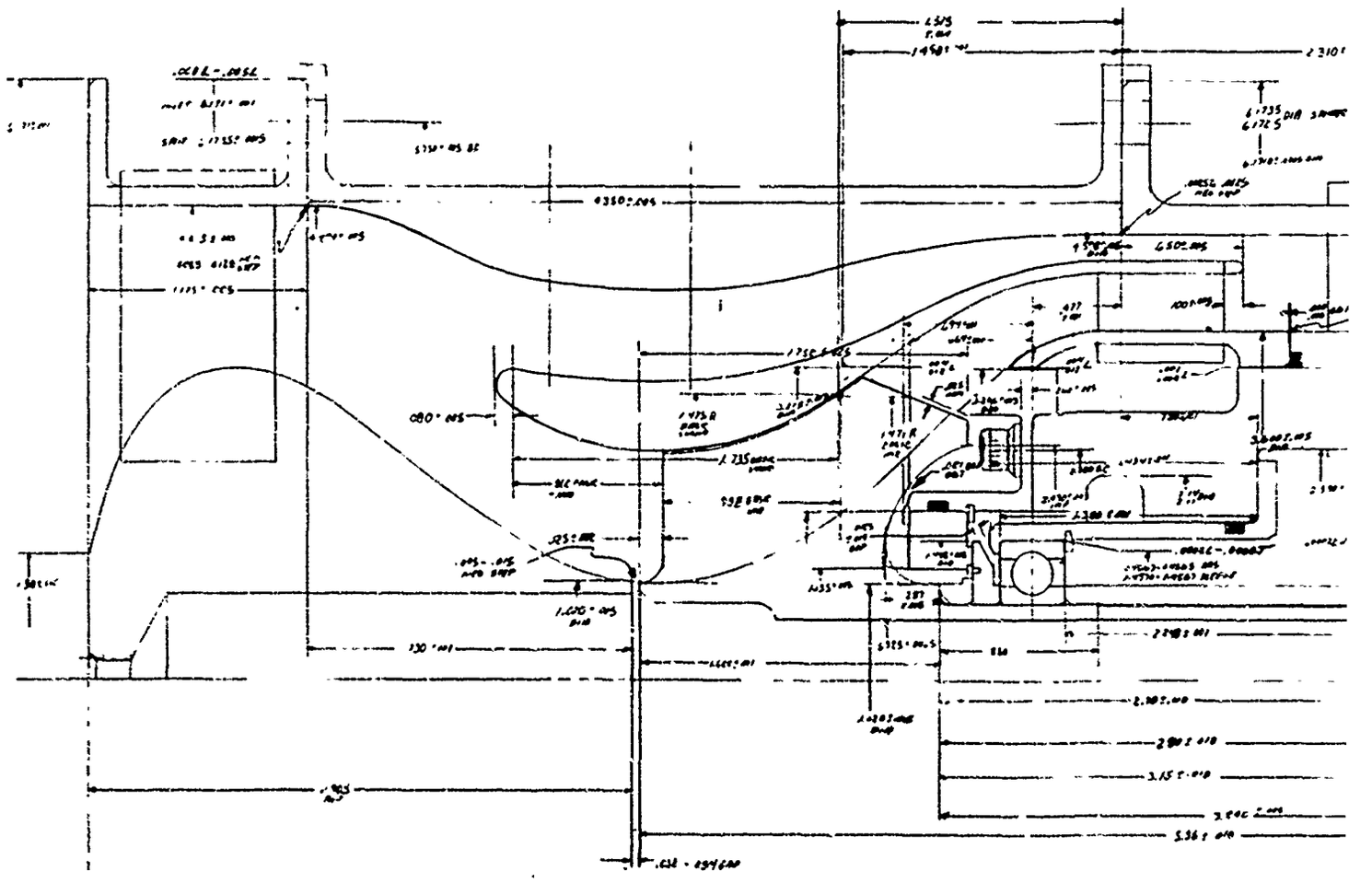

Figure 41. Mechanical Design Layout (System D1).

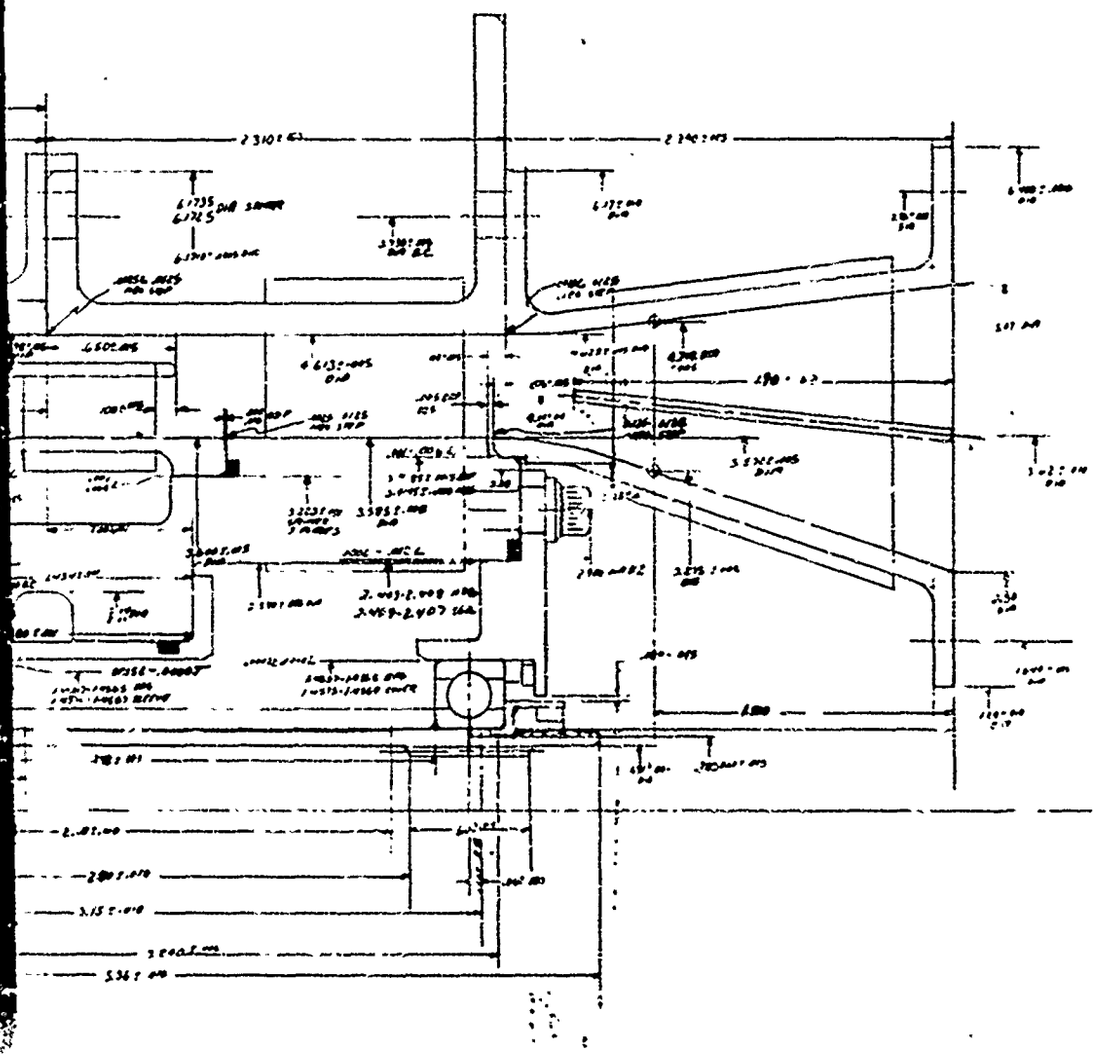

2

BEARING SPRING RATES:

K_1 = 3.2 x 10^5 LB_f/IN.
K_2 = 2.5 x 10^5 LB_f/IN.

SHAFT O.D. = 0.78 IN.
SHAFT I.D. = 0.63 IN.
MATERIAL: 17-4 PH STAINLESS

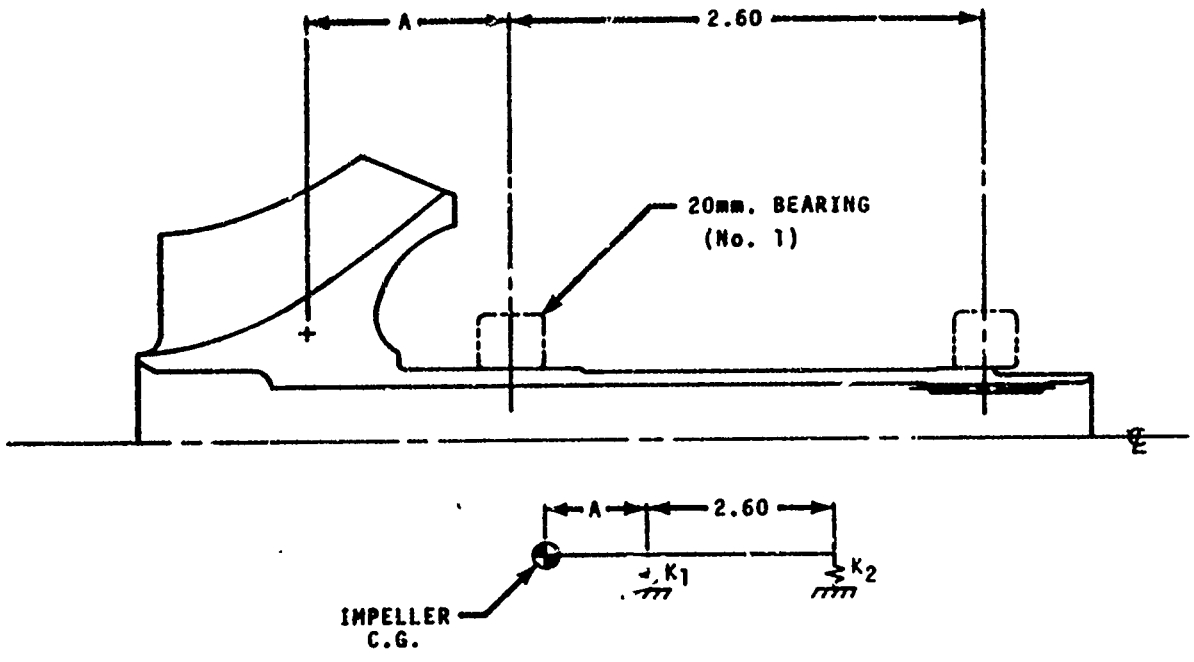

Figure 42. Rotor/Shaft and Bearing Configuration for Dynamics Analysis of System D1.

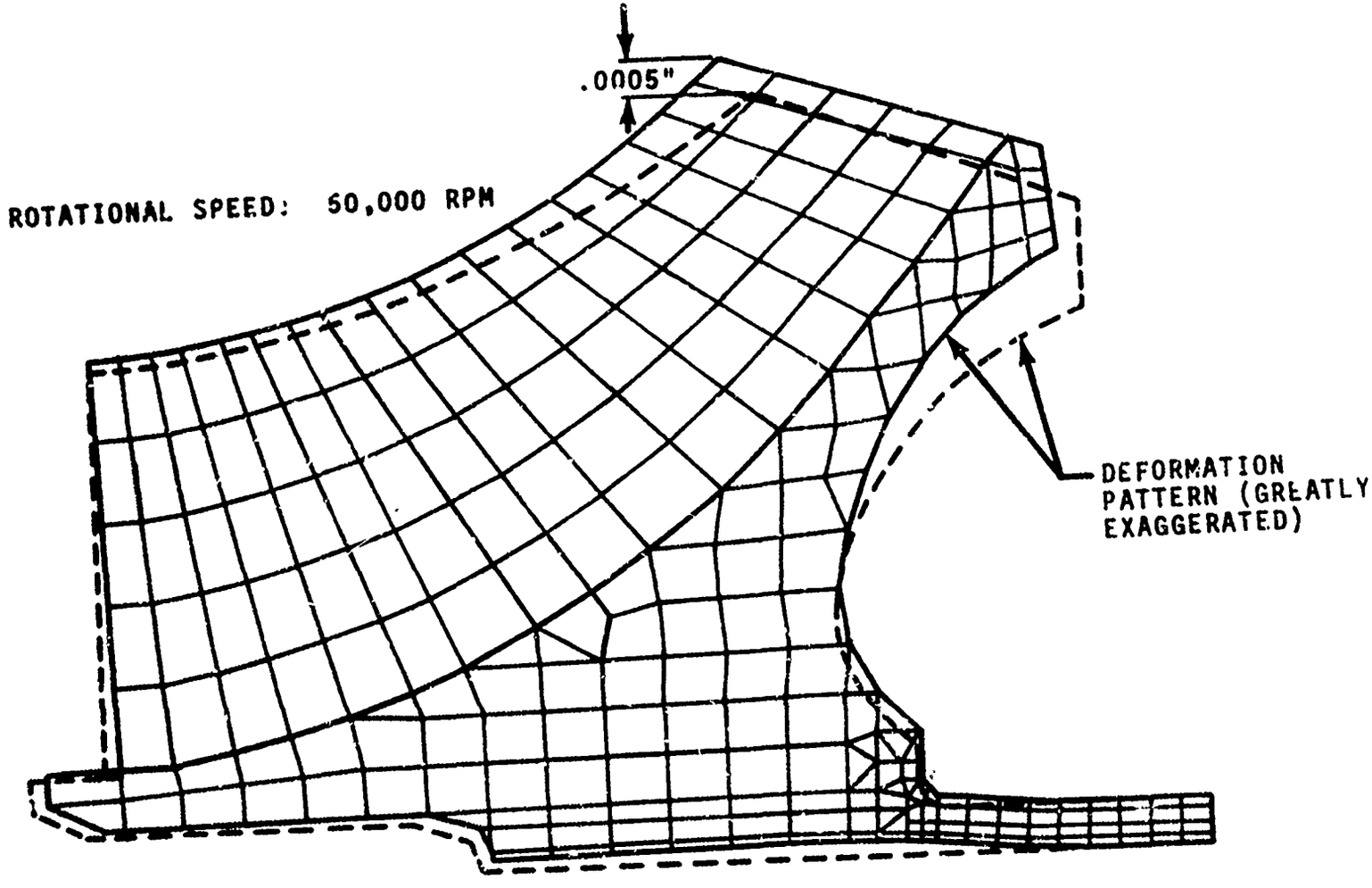

Figure 43. Rotor Disk and Blade Stress Analysis - System D1 (Deformation Pattern).

The resulting deformation and stresses were shown in Figures 43 and 44. Maximum disk stress is 25 ksi, and is located in the bore; the maximum blade stress (assuming a radial blade) is 16 ksi, located at the blade/disk juncture approximately two-thirds up from the leading edge. The negligible slope at the shaft end (Figure 43) confirms that a sufficient portion of the shaft was included in the model to accurately assess the shaft/disk interaction. Aside from blade erosion effects, a disk service life well in excess of 100,000 cycles will result from the above stress levels.

In the analysis of bending stresses at the blade inlet, support given by the more radial sections just downstream of the inlet was neglected. In addition, the direction of centrifugal force loading was fixed along the span to give conservative value for the bending moment. The analysis gave a maximum bending stress estimate of 10.6 ksi at the inlet hub. This bending, when imposed on the nominal inlet blade stress of 5 ksi, as given by the finite element analysis, results in a maximum inlet blade stress of 16 ksi, which provides an adequate margin for blade resonance.

FINAL DESIGN CONFIGURATION

An assembly drawing of the final design configuration for the bypassing blower (System D1) is shown in Figure 45. The physical characteristics and the method of manufacture for key components are summarized below:

INLET HOUSING ASSEMBLY

Material: A-286 stainless steel (AMS 5525B)
Method of Fabrication: Fully machined centerbody and outer casing. Four struts (.093 inch constant thickness) were silver-soldered to form the assembly.

AIR SPLITTER ASSEMBLY

Material: 321 stainless steel (AMS 5645; AMS 5510)
Method of Fabrication: Fully machined splitter, struts, and outer casing. Four bypass channel struts (.125 inch thickness) were welded in position; final contour machining on the splitter ID, following welding operation.

TURNING VANE ASSEMBLY

Material: 321 stainless steel (AMS 5645)
Method of Fabrication: Vanes were coined to final shape from airfoil strip stock (-65 series, A1 meanline, 10% maximum thickness) and furnace brazed to contour-machined inner and outer shrouds.

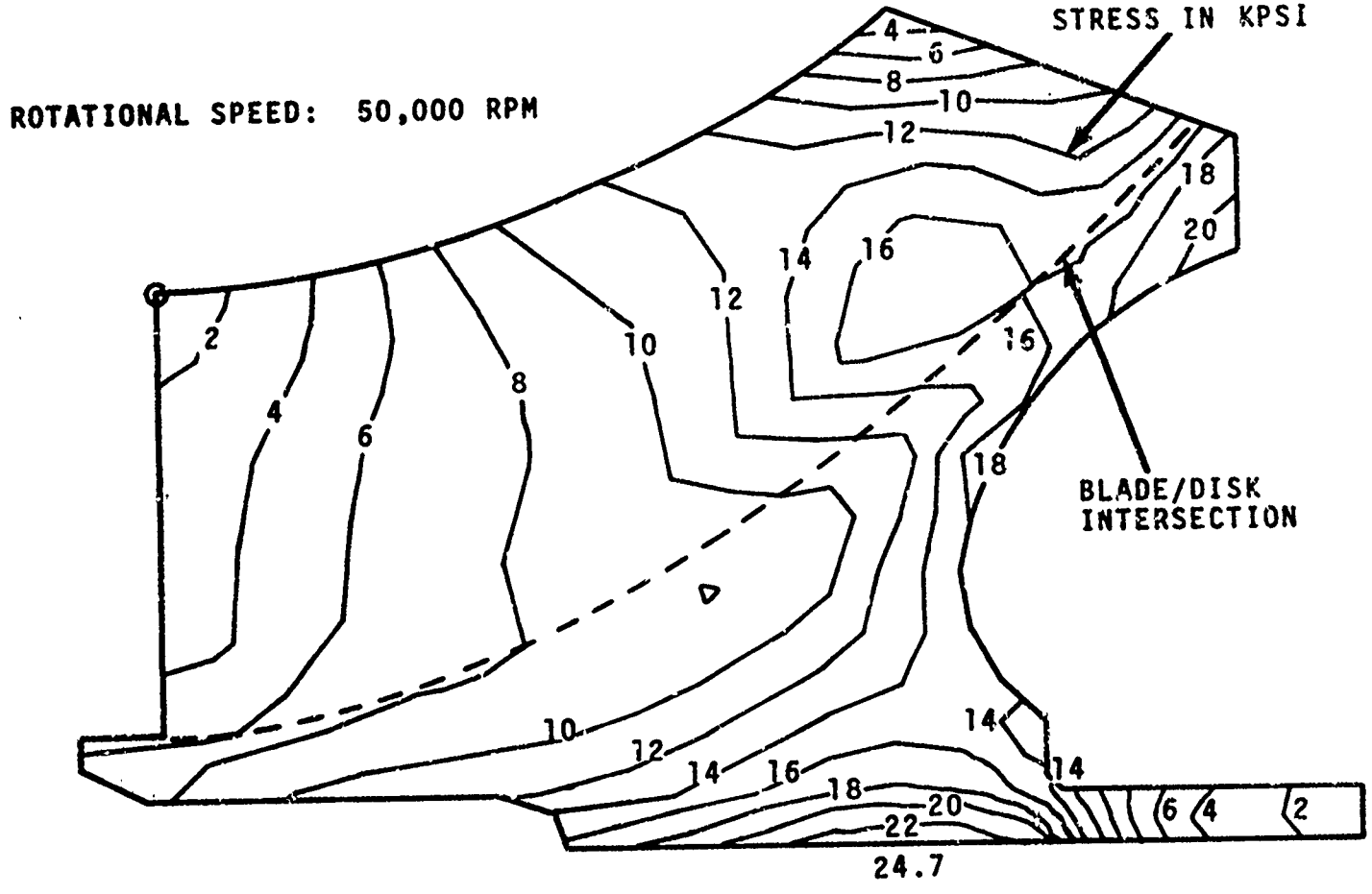

Figure 44. Rotor Disk and Blade Stress Analysis - System D1.

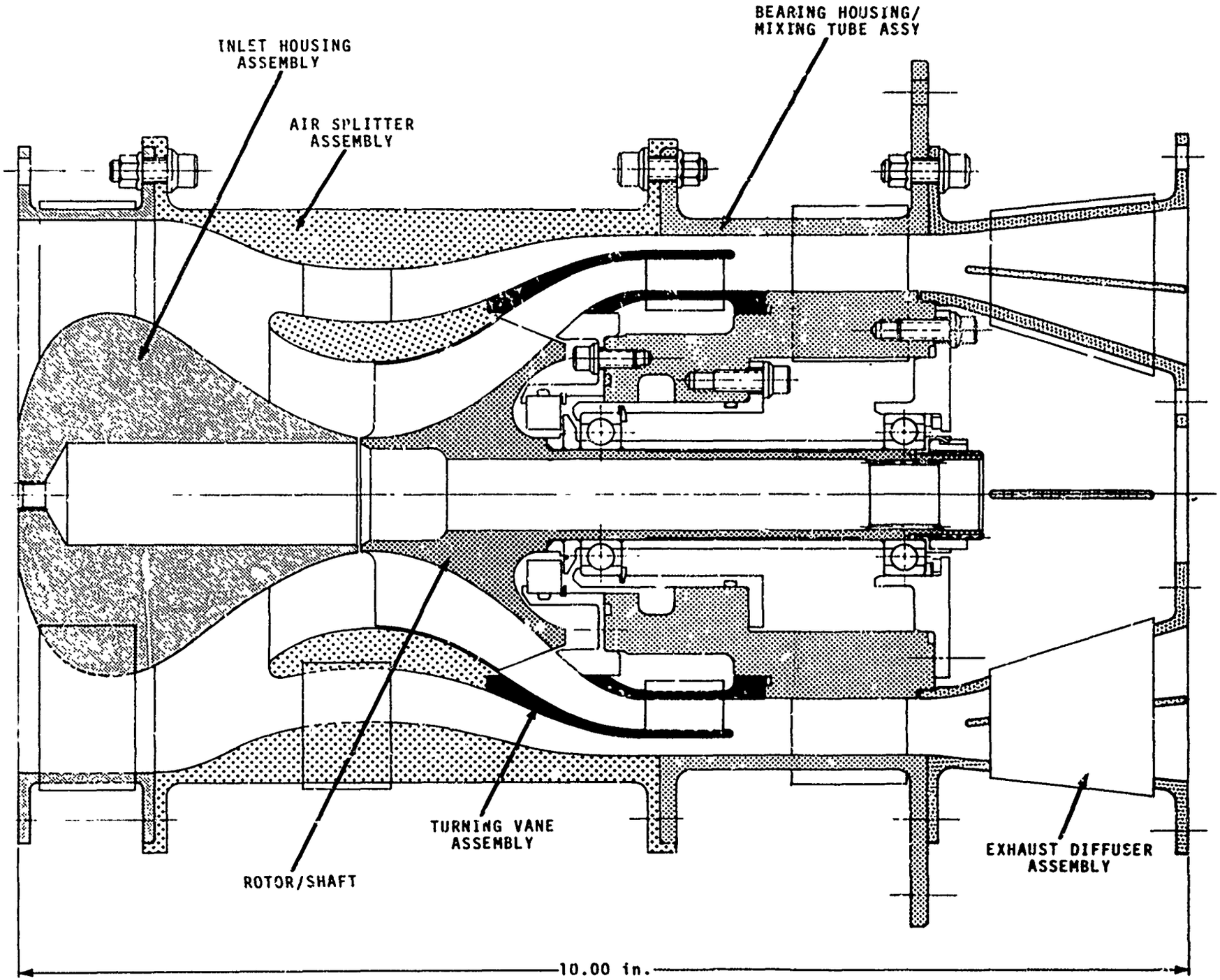

Figure 45. Final Design Assembly - System D1 (Bypassing Scavenge Blower).

ROTOR

Material: 17-4PH stainless steel (AMS 5643J), solution treated at 1900°F, aged in air at 1100°F, for R_C 33-34.
Surface Roughness: 64 microinches, RMS (Max.)
Method of Fabrication: Fully machined integral rotor/shaft; profile-milled rotor blades (Figure 46).

BEARING HOUSING

Material: 321 stainless steel (AMS 5645)
Method of Fabrication: Fully machined; four struts of double circular arc profile (.150 inch maximum thickness) welded to the ID and OD flow path elements

EXHAUST DIFFUSER

Material: 321 stainless steel (AMS 5645)
Method of Fabrication: Machined inner and outer shrouds; 0.060 inch thick struts and splitter; furnace-brazed assembly.

From the stress analysis of the rotor blades and disk, the calculated centrifugal growth (radial) was seen to be less than 0.001 inch. No provisions are made for rotor blade tip protection, in the event of a rub, since any of the typically employed rub materials would be quickly lost from erosion.

Conservatively, the cold static tip clearance (radial) was set at 0.005 to 0.007 inch, anticipating no more than 0.001 inch radial growth under maximum operating conditions.

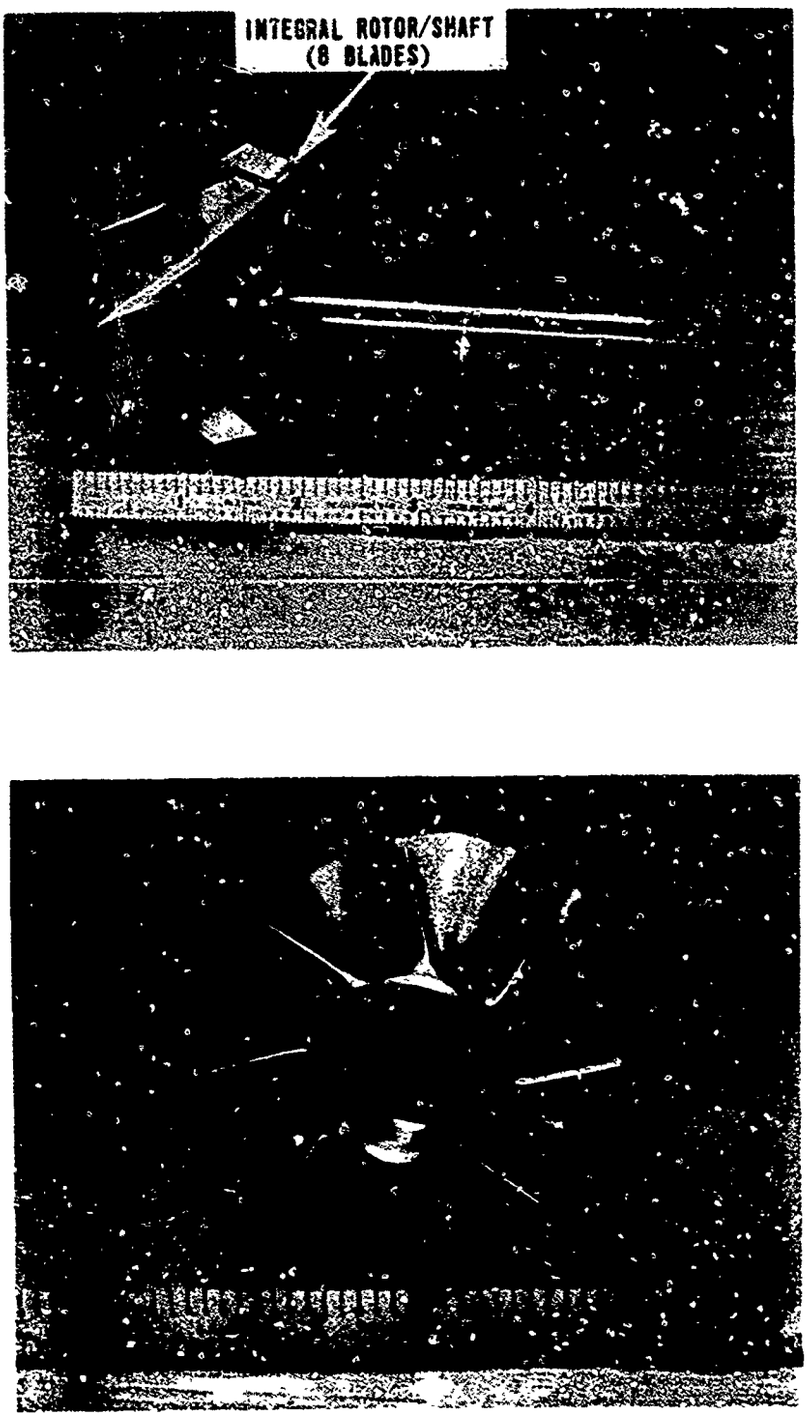

Figure 46. Mixed Flow Impeller - 17.4 PH Steel.

TEST RIG AND INSTRUMENTATION

The test rig shown in Figure 47 was designed to support the separator scavenge blower at the bearing housing mounting flange, and to provide for the aerodynamic and mechanical evaluation of the unit over its full range of possible operating conditions.

Airflow is ducted to the blower from cell ambient, and subsequently collected in an exhaust plenum which contains the pressure and temperature probes for performance measurements. A throttle valve located downstream of the exhaust collector was used to vary the loading on the blower, thus permitting the full stable region of operation to be determined.

Aerodynamic instrumentation was kept at a minimum and designed to provide measurements of total airflow, total pressure, headrise, and rotor horsepower. Inlet conditions were taken as cell ambient, since pressure losses up to the blower inlet flange are negligible.

Total and static pressure measurements in the bypass channel provided an independent measure of bypass channel airflow.

The instrumentation, used for performance measurements, and the test rig location for each type were as follows:

Parameter	Symbol	Quantity	Location
Inlet pressure	$P_{o_{IN}}$	1	Cell Ambient
Inlet temperature	$T_{o_{IN}}$	1	Cell Ambient
Exit total pressure	$P_{o_{EX}}$	6	Exhaust Collector
Exit total temperature	$T_{o_{EX}}$	6	Exit Collector
Bypass total pressure	$P_{o_{BYP}}$	4	Bypass channel, downstream of splitter support struts.
Bypass static pressure	P_{BYP}	4	
Orifice pressure drop	ΔP_{OR}	2	Flow measurement section in the test rig exhaust line.
Orifice upstream pressure	P_{OR}	2	
Orifice temperature	T_{OR}	2	

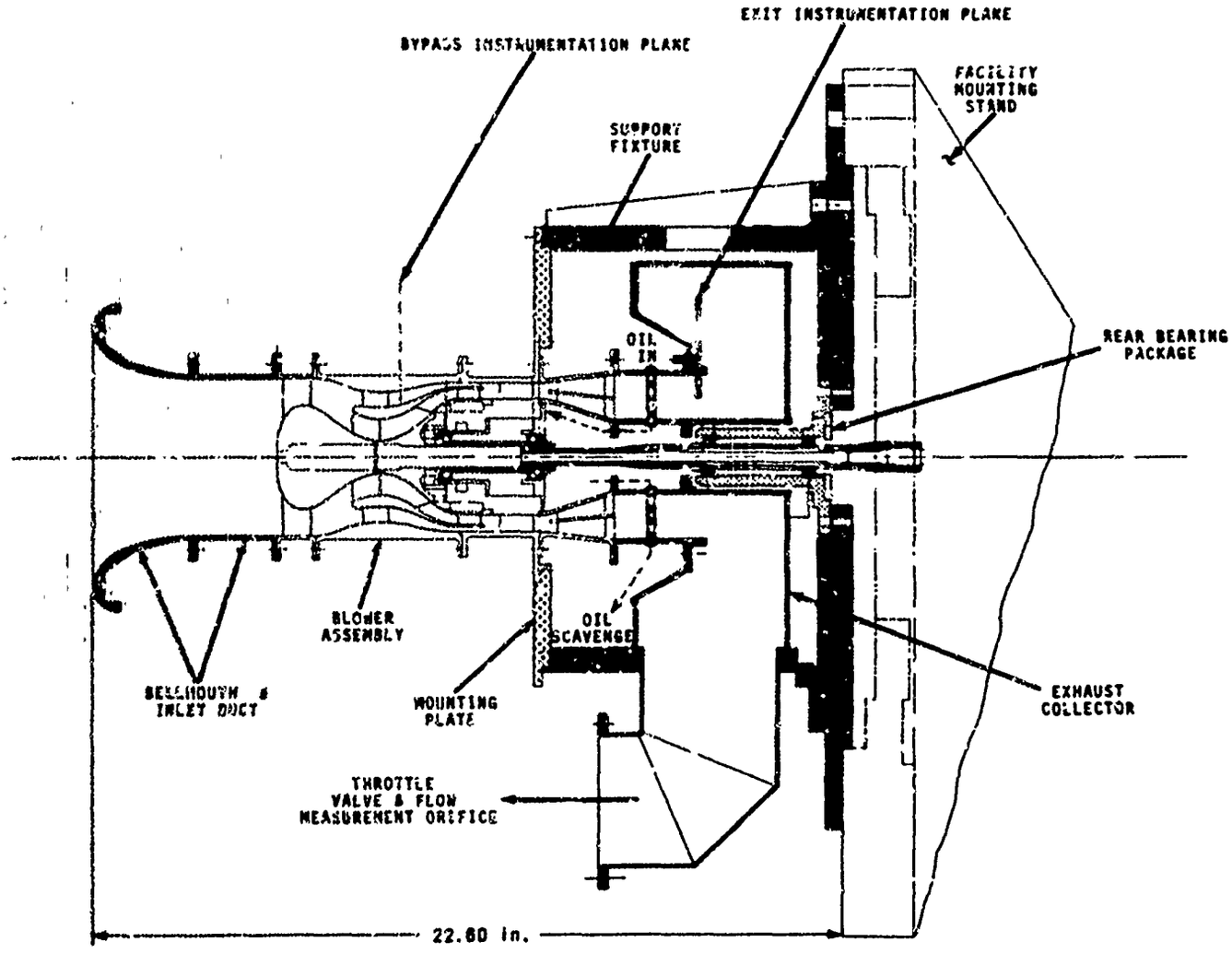

Figure 47. Blower Test Rig Assembly.

The mechanical instrumentation added to the rig was limited to bearing outer race temperatures, rotor tip rub indicators, and vibration pick-ups. Speed was sensed at a location in the facility drive section. The instrumentation and respective locations are given below:

TYPE	QUANTITY	LOCATION
Bearing temperatures	2 per bearing	Outer race, Bearing No. 1, 2, 3, 4
Vibration	2 vertical and horizontal	Externally mounted on the blower casing just aft of the splitter housing upstream flange.
Rub indicators	2 per plane	Impeller shroud, at the leading and trailing edges; staggered depth settings.

Figures 48 and 49 show, respectively, a composite of the major hardware elements, and the blower test rig at a partial assembly point.

A separate inlet module rig (Figures 50 and 51) provided a means of measuring inlet losses and sand separation efficiency by segregating the bypass and main flows. The pressure instrumentation in the bypass channel was also calibrated for flow rate. Each channel is scavenged by a separate facility blower, thus allowing simulation of any total flow, or bypass ratio.

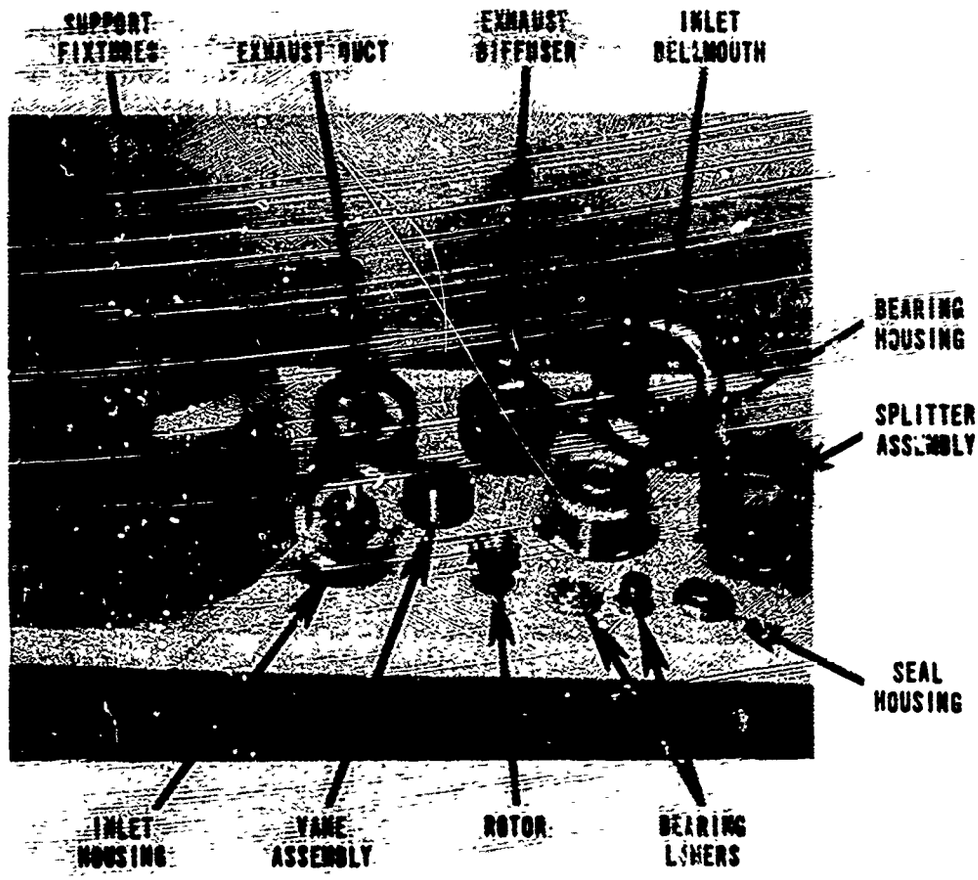

Figure 48. Composite of the Test Rig and Blower Major Components.

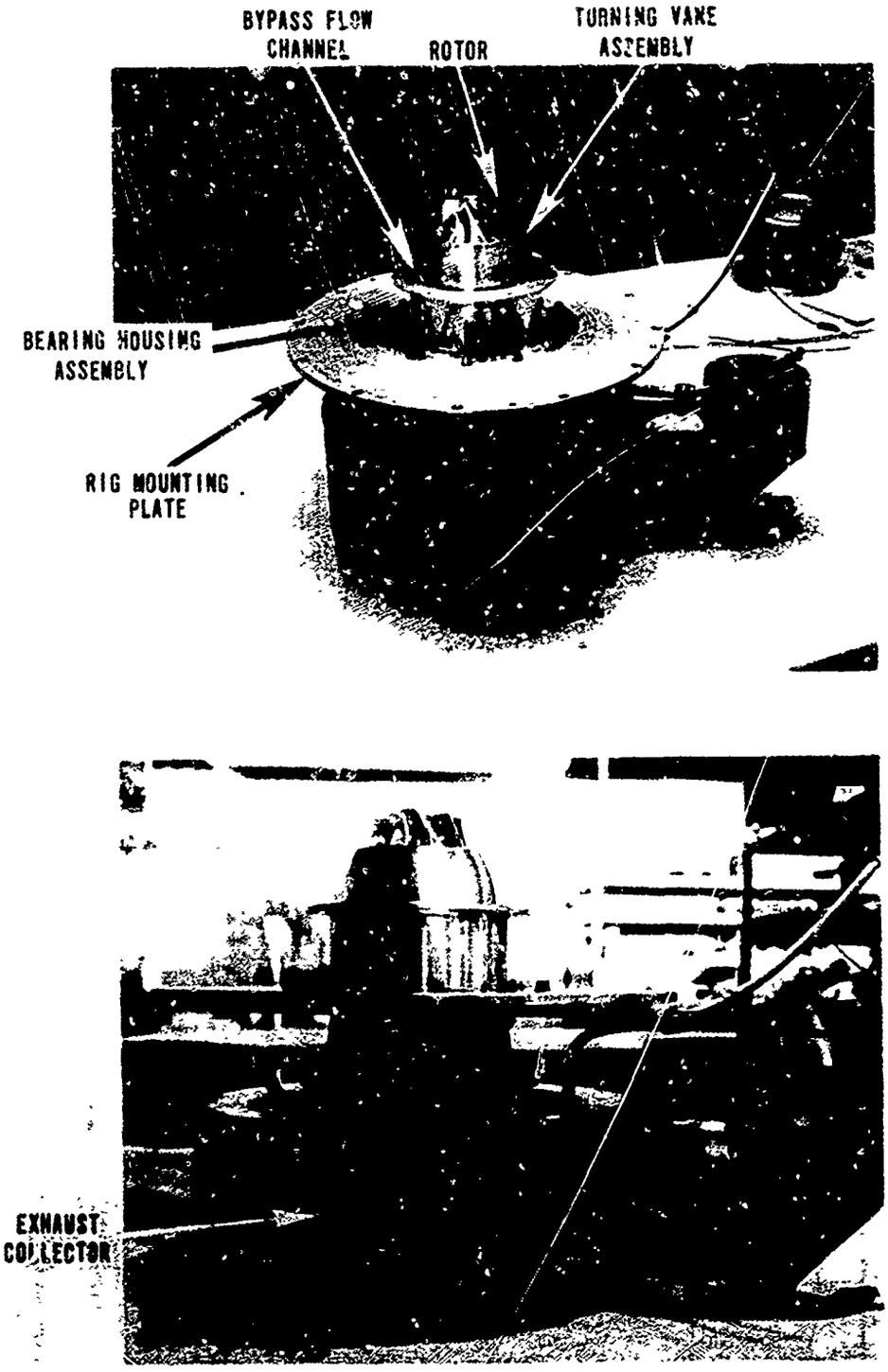

Figure 49. Test Rig Partial Assembly.

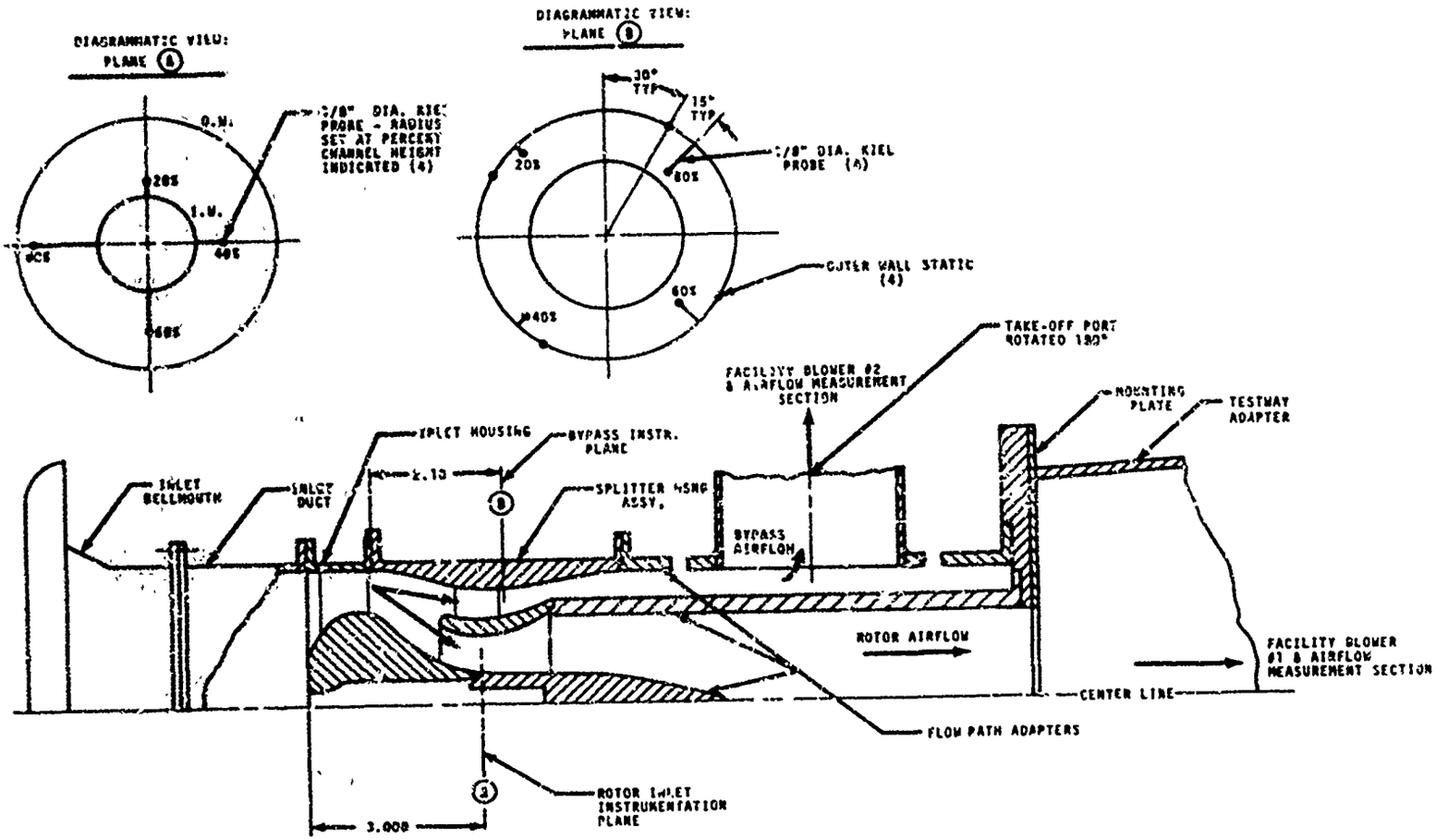

Figure 56. Inlet Module Test Rig Schematic.

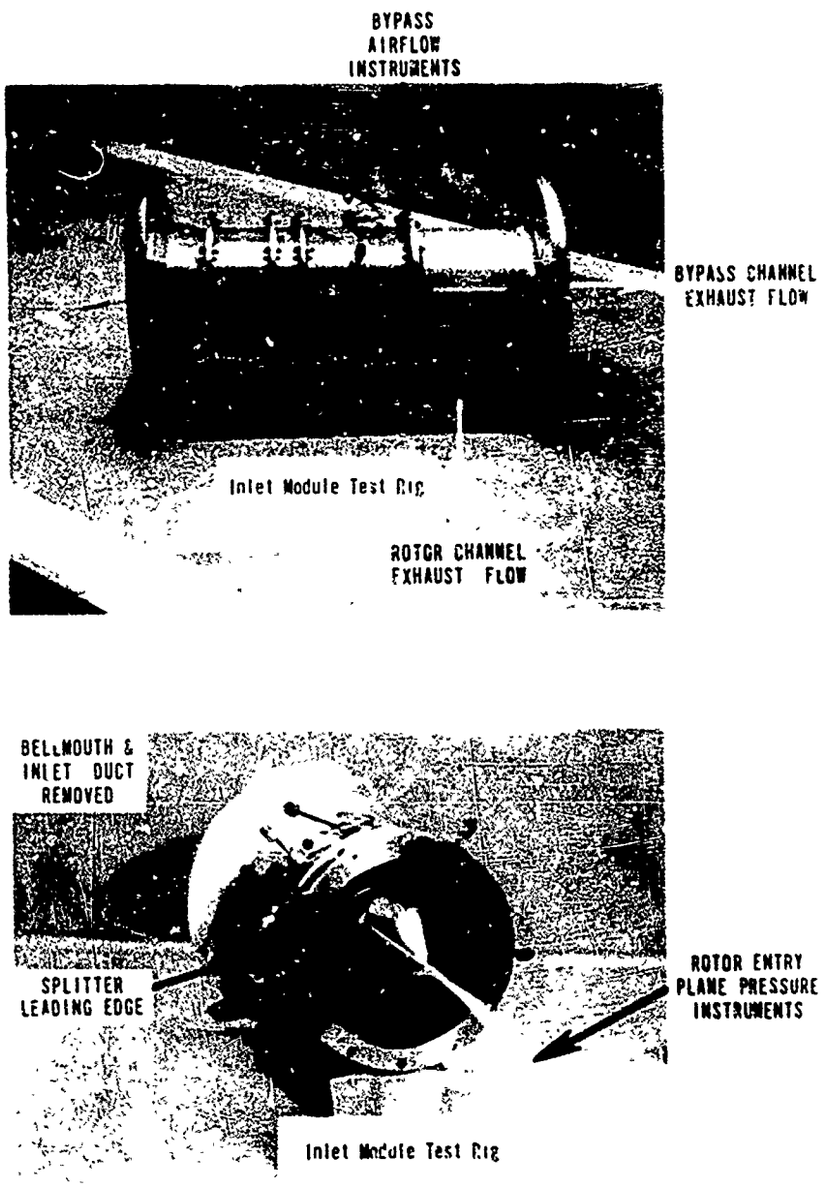

Figure 51. Inlet Module Test Rig.

TEST RIG FACILITY INSTALLATION

The test facility that was used to evaluate the blower provides a speed capability of 0 to 30,000 rpm output from a steam turbine. The drive turbine output speed is increased through a 3.0:1 ratio gearbox, giving an overall capability of 0 to 90,000 rpm. The majority of the tests were conducted at 50,000 to 51,000 rpm, depending upon the cell ambient temperature. The blower test rig is shown installed in the facility in Figure 52.

Pressures from the rig were read through use of a portable, 24-port differential pressure scanner, with digital display of any manually selected value. The following control-room displays were used in monitoring the aerodynamic and mechanical performance of the blower:

Pressures - Digital readout from differential pressure scanning unit.
Temperatures - Honeywell-Brown recorder with individual display of selected inputs.
Speed - Hewlett-Packard preset counter.
Overall pressure ratio - Differential pressure transducer, voltage/frequency converter, preset counter
Rotor tip rubs - Alarm system, activated upon blade contact with wire tip rub indicators.

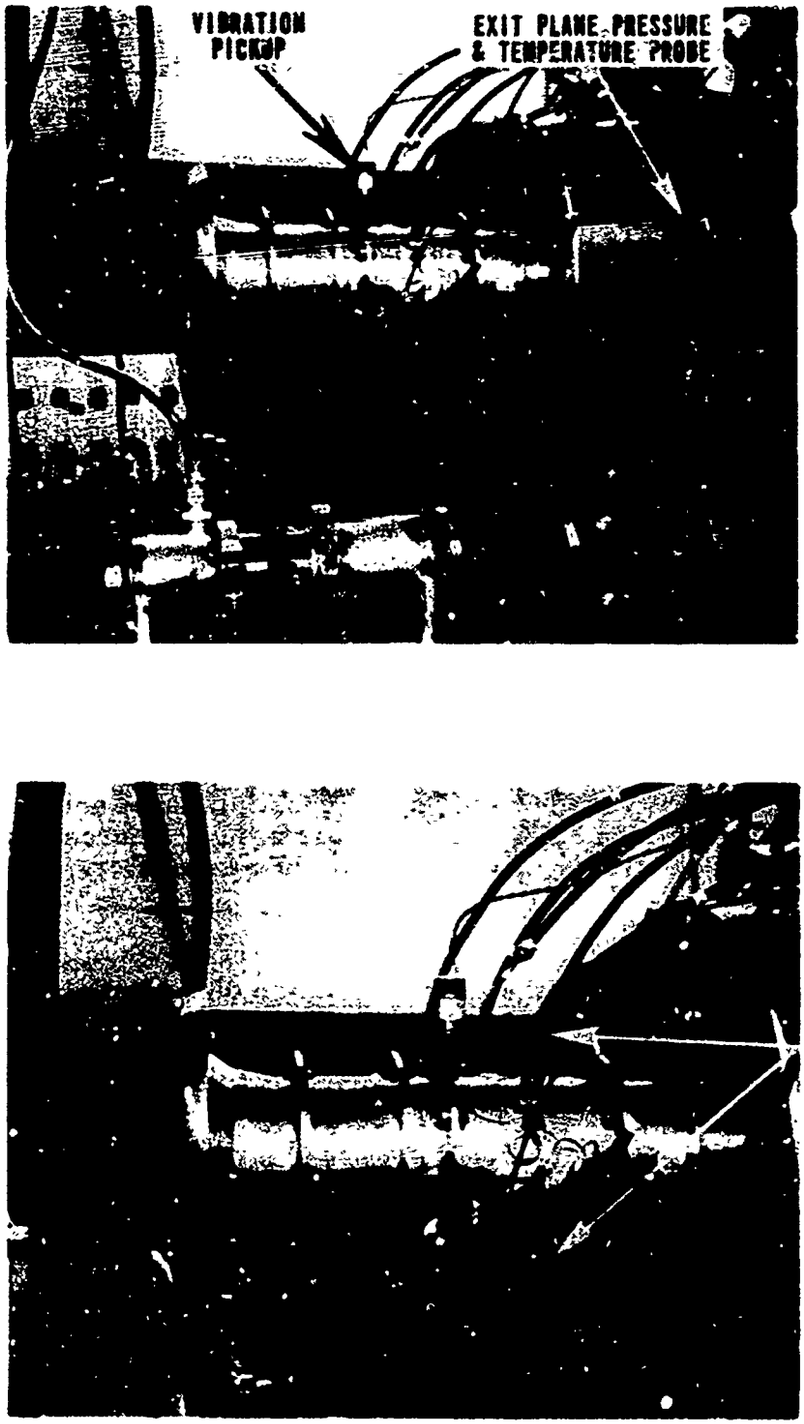

Figure 52. Scavenge Blower Test Rig Installation.

TEST PLAN OUTLINE

The experimental program for evaluating the bypassing blower (System D1) was subdivided into a series of individual tests, with the following objectives:

Test P1 - Inlet System Evaluation

a. Determine the total pressure loss of the blower inlet section.
b. Calibrate the bypass duct instruments against an airflow standard.
c. Determine the extent to which blower flow characteristics are
c influeneced by inlet ice accumulation.

Test P2 - System Efficiency Test

a. Determine the power input requirements over a range of operating conditions, simulating engine idle through full power.
b. Determine the stable operating region by measurements of headrise versus airflow at constant speeds.

Test P3 - Water Ingestion Test

a. Evaluate the effect of water ingestion upon the blower, under both steady-state (design point) and start-up conditions.
b. The water flow rate is based upon ingesting liquid equivalent to 3 percent of the engine airflow, assuming 75 percent water separation efficiency through the particle separator.

Test P4 - Durability Test

The durability test focuses on the prime objective of the entire program:

a. Demonstrate the ability of the blower to operate for a 50-hour period in a sustained erosion environment using MIL-E-5007C sand.
b. The actual test calls for periodic inspections, nominally at 10-hour intervals.
c. At the conclusion of this test, the minimum performance goals are standard day inlet conditions.
d. At the blower design point, the sand feed rate would directly simulate scavenging 18-percent air from a 5.0 lb/sec. engine, whose particle separator is 95 percent efficient by weight. Sand-to-air concentration at the separator inlet is 1.5 mg/ft^3.

Test P5 - Ice Ingestion/FOD Test

The purpose of this test is to qualitatively assess the ability of the system to ingest typical aircraft engine hardware in sizes appropriate to this particular scavenge system design.

EXPERIMENTAL EVALUATION OF THE PRIMARY SYSTEM (TASK IV)

(BYPASSING BLOWER)

TEST P1 - INLET SYSTEM EVALUATION - INLET LOSSES

In accordance with the primary system test plan outlined earlier, test work on the scavenge blower was begun by evaluating the pressure loss and airflow characteristics of the system inlet section, using the inlet module as a test rig. (Refer to Figure 50.)

Total pressure losses in the bypass channel and the rotor (or core) channel were each measured using Kiel probes 90 degrees apart, but staggered radially at 20, 40, 60 and 80 percent of the channel heights. In addition, the bypass channel contained four outer wall statics.

The procedure used was to set a value for rotor flow corresponding to the maximum (or design) value, and then to vary the bypass airflow in increments, thereby simulating a range of bypass ratios. The resulting inlet system losses are shown in Figures 53 and 54.

For the bypass channel, the pressure losses are 1 to 2-1/2 in. H_2O, depending on the bypass ratio. Earlier estimates (based on a simple diffuser analogy, given the area ratio and length) at 25-percent bypass were approximately 3 in. H_2O average loss.

The continually changing shape of the radial profile with bypass ratio shows the tendency for a progressively increasing outer wall flow separation as the bypass ratio is diminished. At 10 percent, the near-flat profile with the free-stream total pressure equal to the wall static shows the flow separation and recirculation. At the design bypass ratio ($\beta = .25$), the 1.5 to 2 in. H_2O loss is well within the 5 in. H_2O maximum allowed for in the design of the ejector.

In the rotor channel (Figure 53), losses were also very low, and only in the extreme case of zero bypass ratio did the mean loss approach any level of significance. For the scavenge blower inlet, losses due to friction in the very short lengths in relation to the channel hydraulic diameters would be negligibly small. Wake losses are induced only in the four centerbody struts which are of .060 inch thickness. Also, the previous inlet potential flow analysis had indicated that flow separations were not expected to be any problem along the hub.

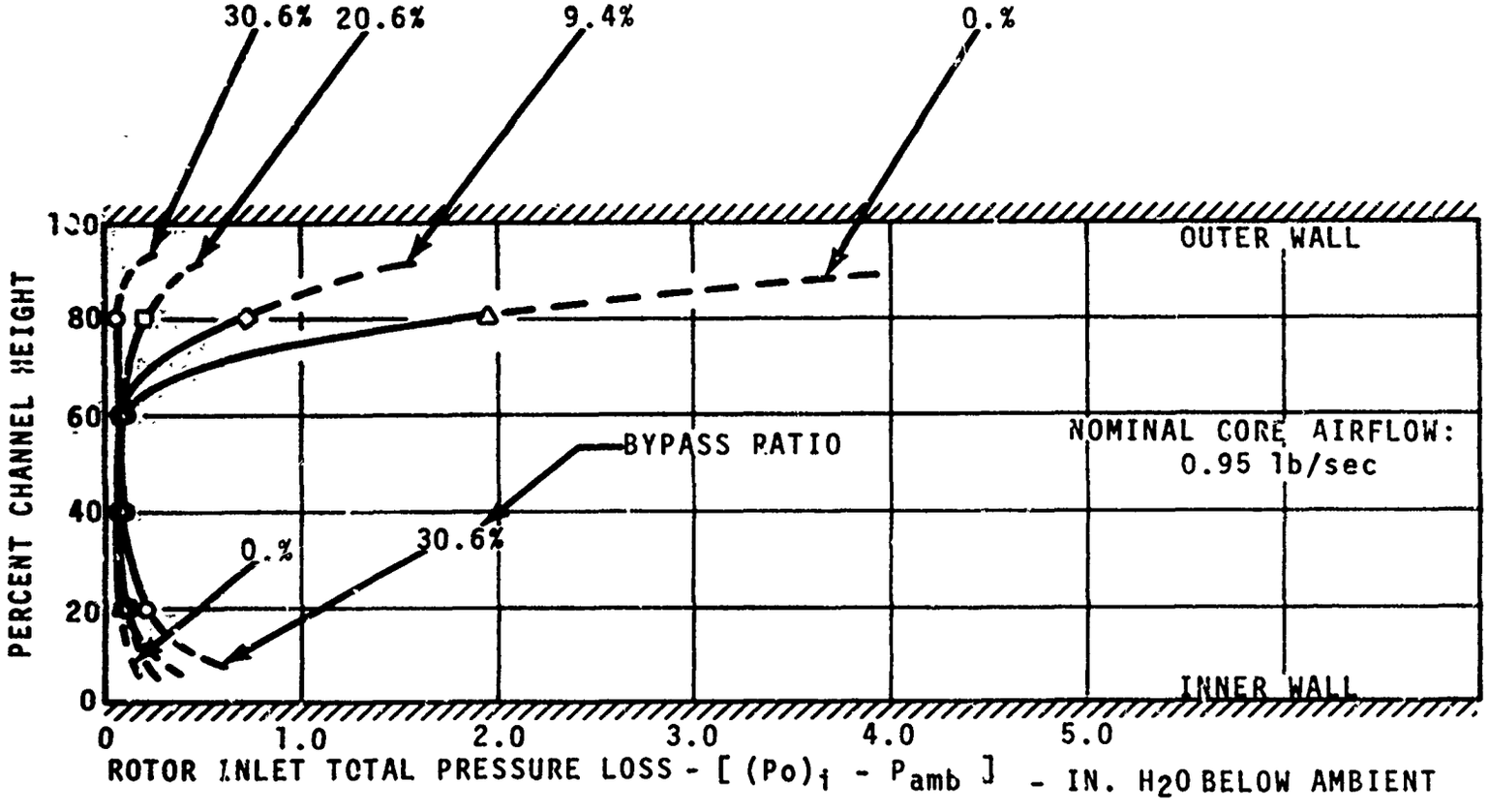

Figure 53. Rotor Channel Pressure Loss Versus Bypass Ratio - Test P1.

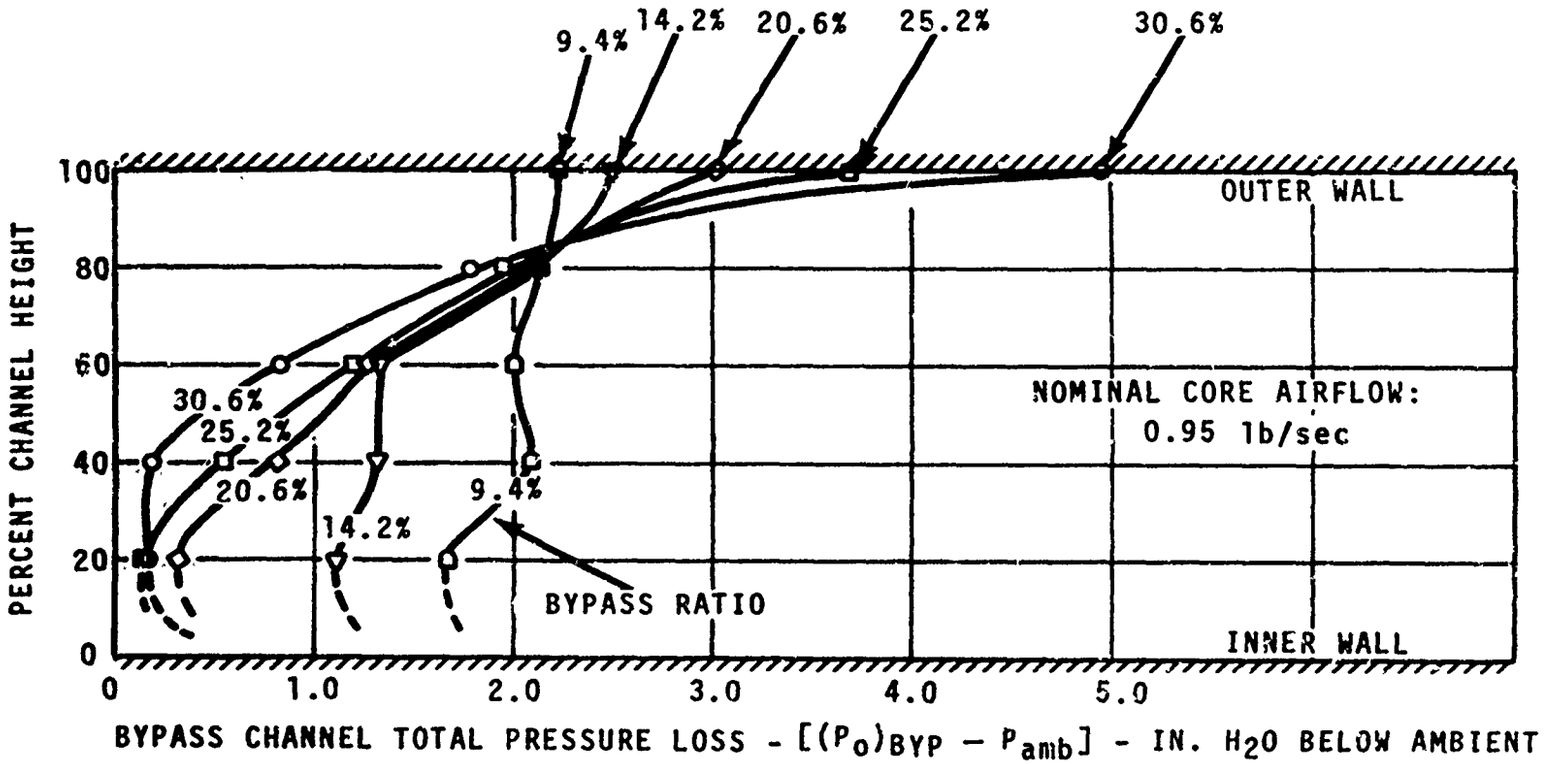

Figure 54. Bypass Channel Total Pressure Loss Versus Bypass Ratio - Test P1.

Along the rotor shroud, the outer channel area reduction and a relatively high bypass ratio provide favorable incidence to the flow splitter. These aspects of the inlet design have minimized the degree of over-acceleration about the splitter nose, which is followed by rapid diffusion and flow separation.

In summary, the emphasis placed on loss minimization during the inlet design appears to be well substantiated by the experimental data obtained.

TEST P1 - INLET SYSTEM EVALUATION - BYPASS FLOW CALIBRATION

The data required for calibration of the bypass channel (airflow vs $P_o - P$) was acquired simultaneously with the loss data using the same test setup referred to previously. By using mean total pressure (simple average), mean wall static pressure, inlet temperature, and the actual airflow from an orifice measurement, the calibration curve shown in Figure 55 was obtained.

TEST P1 - INLET SYSTEM EVALUATION - FLOW VISUALIZATION

The performance of the blower inlet separator in terms of achieving a prespecified minimum level of separation efficiency (72 percent by weight) with MIL-E-5007C type sand is fundamental to the durability of the blower with respect to the 50-hour minimum goal.

By using sparklers as tracers, the results obtained are shown in Figures 56 and 57. Results showed that the vast majority of the particles carried directly into the bypass channel, or of those that bounced, the impact point on the outer wall was downstream of the splitter leading edge, indicating that these particles, as well, were "bypassed".

Based on this simple test, the results were encouraging. The conical fairing shown in Figure 56 had been temporarily added to the rig in order to test for effects on pressure loss. No differences were found, and the fairing was not used in any subsequent test work.

Finally, with the centerbody cone removed, a 1000-gram sample of sand was introduced into the rig inlet with the bypass ratio set at approximately 20 percent.

Of the total sample introduced, 80 percent was recovered, indicating further that the inlet separator performance was satisfactory in view of the established goals.

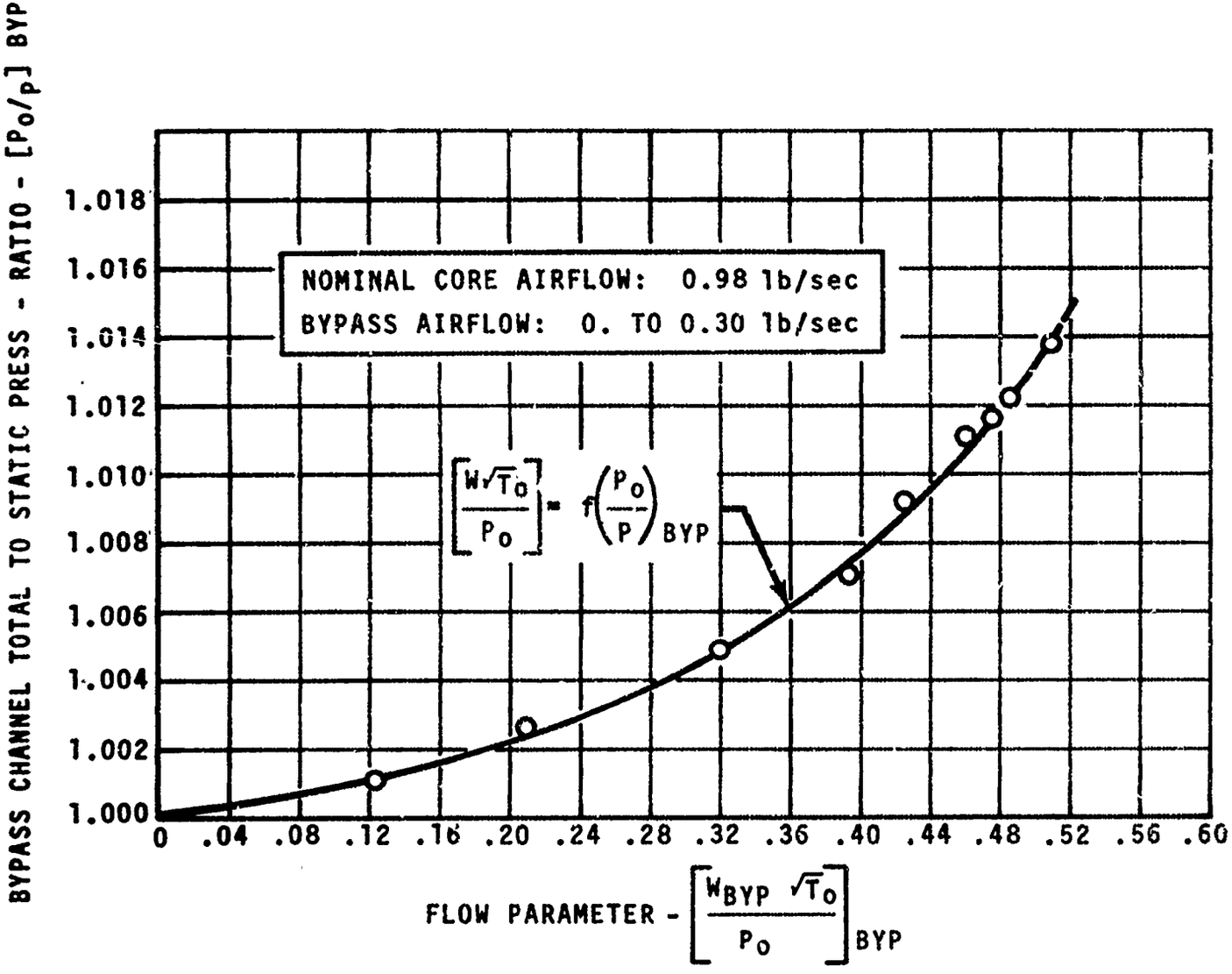

Figure 55. Bypass Duct Airflow Calibration - Test P1.

DEMONSTRATION OF
PARTICLE OUTER-WALL
IMPACT POINTS WITH
RESPECT TO SPLITTER
LEADING EDGE

ROTOR CHANNEL FLOW: .99 lb/sec
BYPASS CHANNEL FLOW: .25 lb/sec
BYPASS RATIO: 25%

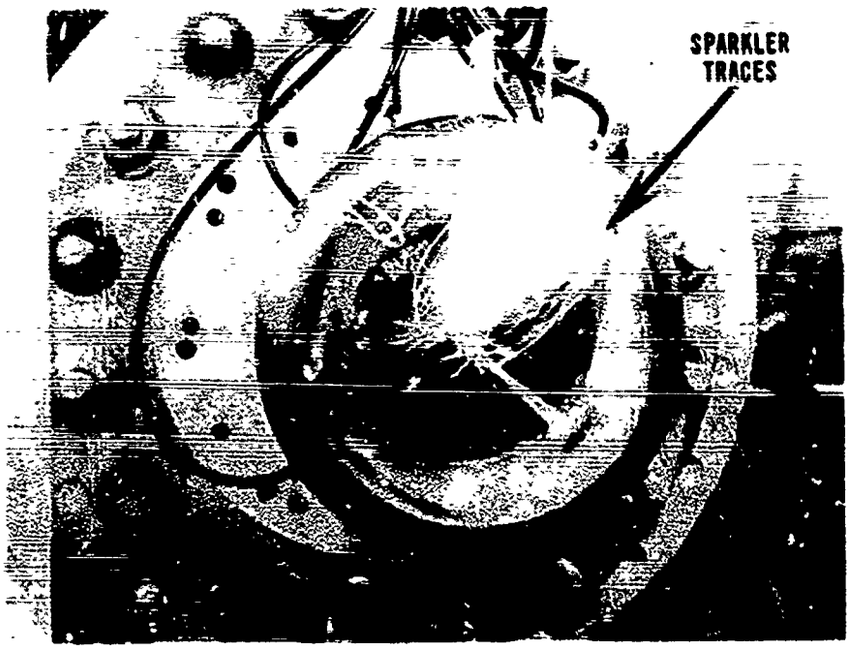

Figure 56. Flow Visualization - Test P1.

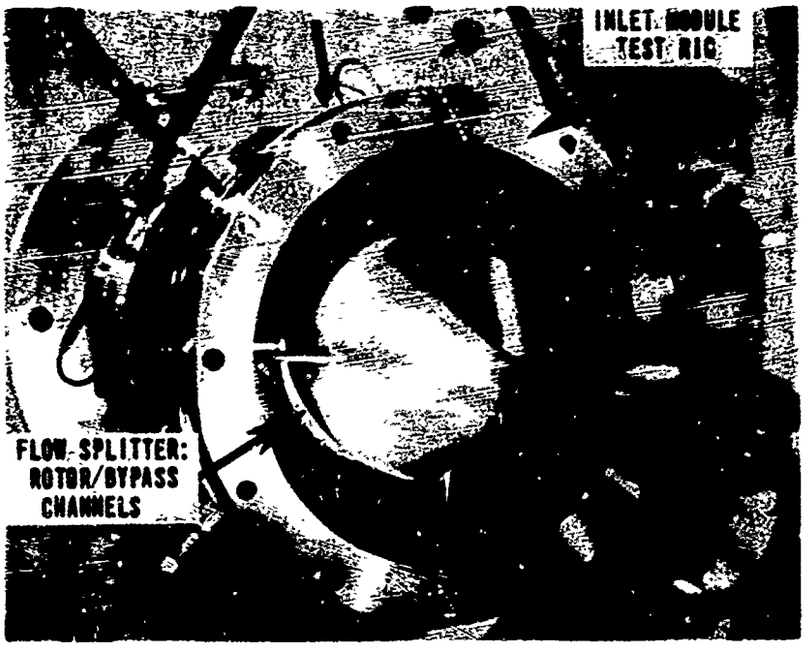

ROTOR CHANNEL FLOW: .99 lb/sec
BYPASS CHANNEL FLOW: .25 lb/sec
BYPASS RATIO: 25%

Figure 57. Flow Visualization - Test P1 (Bellmouth Removed).

TEST P1 - INLET SYSTEM EVALUATION - ICING

To assess the effects of ice buildup upon the blower performance, the inlet module rig was mounted at the downstream end of an icing tunnel into which a variable supply of cold air could be introduced. A spraybar, using one atomizing spray nozzle, was located in the tunnel, approximately 10 feet upstream of the inlet rig.

As in previous tests with the inlet rig, separate facility blowers and orifice sections were used to establish a desired rotor channel and to bypass the channel airflow. The conditions established were:

Total flow to blower =	1.1 lb/sec
Inlet temperature =	+15° to +18°F
Bypass ratio =	25 percent

Under these conditions, the airflow was monitored at 5-minute intervals once a water flow rate of 0.75 gal/hr* had been introduced. A plot of percentage loss in total airflow against time is shown in Figure 58.

At the test conclusion (45 minutes), the regions where ice had accumulated are shown in Figure 59.

Relative to the actual quantity of supercooled water that could physically reach a scavenge blower in an actual engine installation, this particular test would have to be considered as quite severe.

TEST P2 - SYSTEM EFFICIENCY - POWER REQUIREMENTS

Test P2 entails running a "clean inlet" baseline performance test covering the range of possible operating speeds and back pressures. The primary parameters generated from this test at a given speed include:

Total airflow pumped	$\left(W_{TOT} \text{ or } W_{TOT}\sqrt{\theta}/\delta\right)$
Overall headrise	$(\Delta P_{o_s}$ or pressure ratio)
Rotor drive power	$\left(HP_{ROT}, HP/\delta\sqrt{\theta}\right)$

* Liquid Water Content = 2.0 gm/m^3

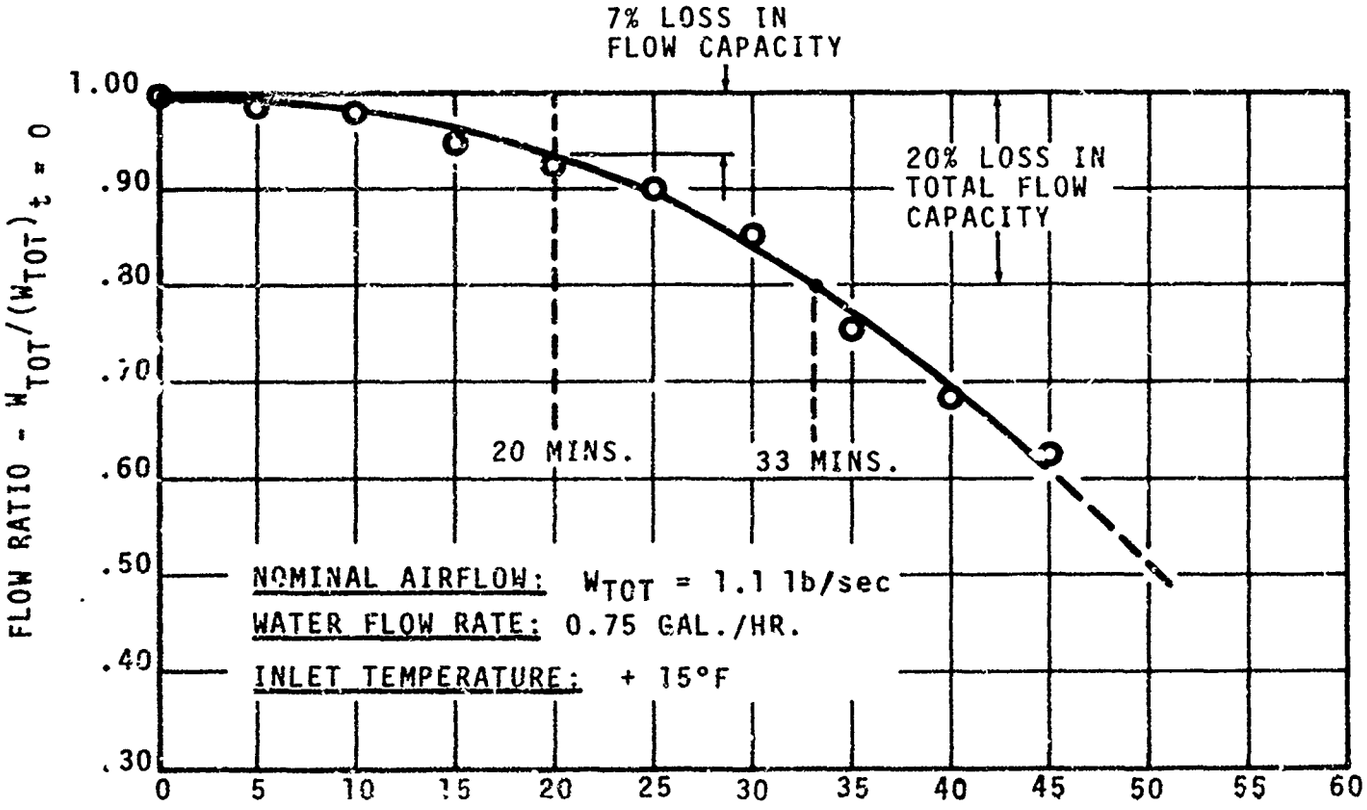

Figure 58. Airflow Reduction as a Function of Running Time Under Icing Conditions - Test P1.

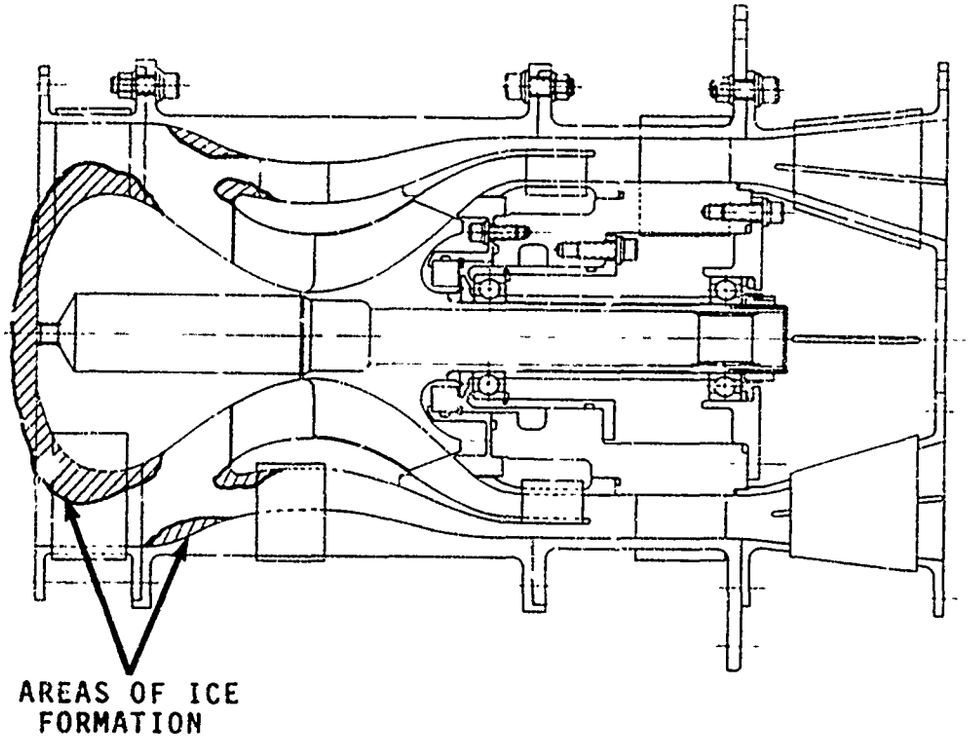

Figure 59. Blower Inlet Ice Formation - Test P1.

Throughout the test data, which is subsequently presented, airflows have been expressed in terms of referred flow, and headrise in terms of pressure ratio. For reference purposes, Table 17 lists actual design point conditions versus the corresponding standard day corrected values. In all cases, the "inlet" station is the blower inlet flange.

The test was run by selecting fractions of design speed, from 50 percent up through 100 percent $N/\sqrt{\theta}$; at each constant speed, the back pressure was varied in increments starting at the lowest attainable, and increasing up to a point where an instability was in evidence. The resulting performance map ($W_{TOT}\sqrt{\theta}/\delta$) versus ($P_{o_{EX}} / P_{o_{IN}}$) is shown in Figure 60.

From the map and Table 17 (design parameters), the 100-percent speed characteristic satisfies the required design point flow and pressure ratio (1.129 lb/sec at Pr = 1.064).

The "stall boundary" is actually a point where a mild instability was seen in various aerodynamic measurements which were monitored during the test. The severity certainly could not be classified as anything resembling a "surge", or even as an audible stall.

The location of the design point in relation to the stall boundary at first appears very unusual, compared with a typical compressor map; generally, that point would be located much nearer to the stall boundary. However, the map represents the overall characteristics of a system which includes an ejector.

If we refer again to Figure 60, then the reason for the design point location becomes apparent. Overlayed on the map are a series of contours that represent calculated bypass ratios; as back pressure is increased along a constant speed line, the result is a rapid reduction in bypass ratio.

Eventually, with sufficient back pressure, the bypass flow is reduced to zero; from that point on, the blower operates "conventionally" although very inefficiently overall, since the flow now "dumps" into the mixing tube and diffuser.

With further throttling, some of the rotor flow actually recirculates back through the bypass channel; and with that outlet, it was never actually possible to cause enough loading on the rotor as to obtain a distinct rotating stall or a surge.

For purposes of this design, since the "bypass" feature is fundamental, the discussion of results will be limited to the "useful" operating region, where some amount of bypass is present, i. e., those points which lie below the line $\beta_2 = 0.$, in Figure 60.

TABLE 17. ACTUAL AND CORRECTED DESIGN POINT PARAMETERS

	FOR COMPARISONS WITH BASELINE TEST RESULTS
DESIGN POINT (CLEAN INLET BASELINE)	
ACTUAL FLOWS FOR: Po_{IN} = -20 in. H_2O = 13.98 psia To_{IN} = 59°F = 518.7°R	CORRECTED FLOWS, REFERRED TO STANDARD DAY INLET:
TOTAL AIRFLOW - W_{TOT} = 1.074 lb/sec	TOTAL AIRFLOW - $(W_{TOT}\sqrt{\theta}/\delta)_{IN}$ = 1.129 lb/sec
ROTOR AIRFLOW - W_{ROT} = 0.860 lb/sec	ROTOR AIRFLOW - $(W_{ROT}\sqrt{\theta}/\delta)_{IN}$ = 0.904 lb/sec
BYPASS AIRFLOW - W_{BYP} = 0.214 lb/sec	BYPASS AIRFLOW - $(W_{BYP}\sqrt{\theta}/\delta)_{IN}$ = 0.225 lb/sec
BYPASS RATIO - β_2 = 25%	BYPASS RATIO - β_2 = 25%
PRESSURE RATIO - 1 + $\Delta Po/Po_{IN}$ = 1.064	PRESSURE RATIO - 1 + $\Delta Po/Po_{IN}$ = 1.064
PRESSURE RISE - (ΔPo) = 25.1 in. H_2O	PRESSURE RISE - (ΔPo) = 26.1 in. H_2O
MINIMUM 50-HOUR OBJECTIVES	
ACTUAL FLOWS: @ -20 in. H_2O @ 59°F	CORRECTED FLOWS: @ 14.696 psia @ 59°F
TOTAL AIRFLOW - W_{TOT} = 0.900 lb/sec	TOTAL AIRFLOW - $(W_{TOT}\sqrt{\theta}/\delta)_{IN}$ = 0.946 lb/sec
ROTOR AIRFLOW - W_{ROT} = 0.818 lb/sec	ROTOR AIRFLOW - $(W_{ROT}\sqrt{\theta}/\delta)_{IN}$ = 0.860 lb/sec
BYPASS AIRFLOW - W_{BYP} = 0.0818 lb/sec	BYPASS AIRFLOW - $(W_{BYP}\sqrt{\theta}/\delta)_{IN}$ = 0.0860 lb/sec
BYPASS RATIO - β_2 = 10%	BYPASS RATIO - β_2 = 10%
PRESSURE RATIO - 1 + $\Delta Po/Po_{IN}$ = 1.052	PRESSURE RATIO - 1 + $\Delta Po/Po_{IN}$ = 1.052
PRESSURE RISE - (ΔPo) = 20.0 in. H_2O	PRESSURE RISE - (ΔPo) = 21.2 in. H_2O
	FOR COMPARISON OF RESULTS FOLLOWING DURABILITY TESTS

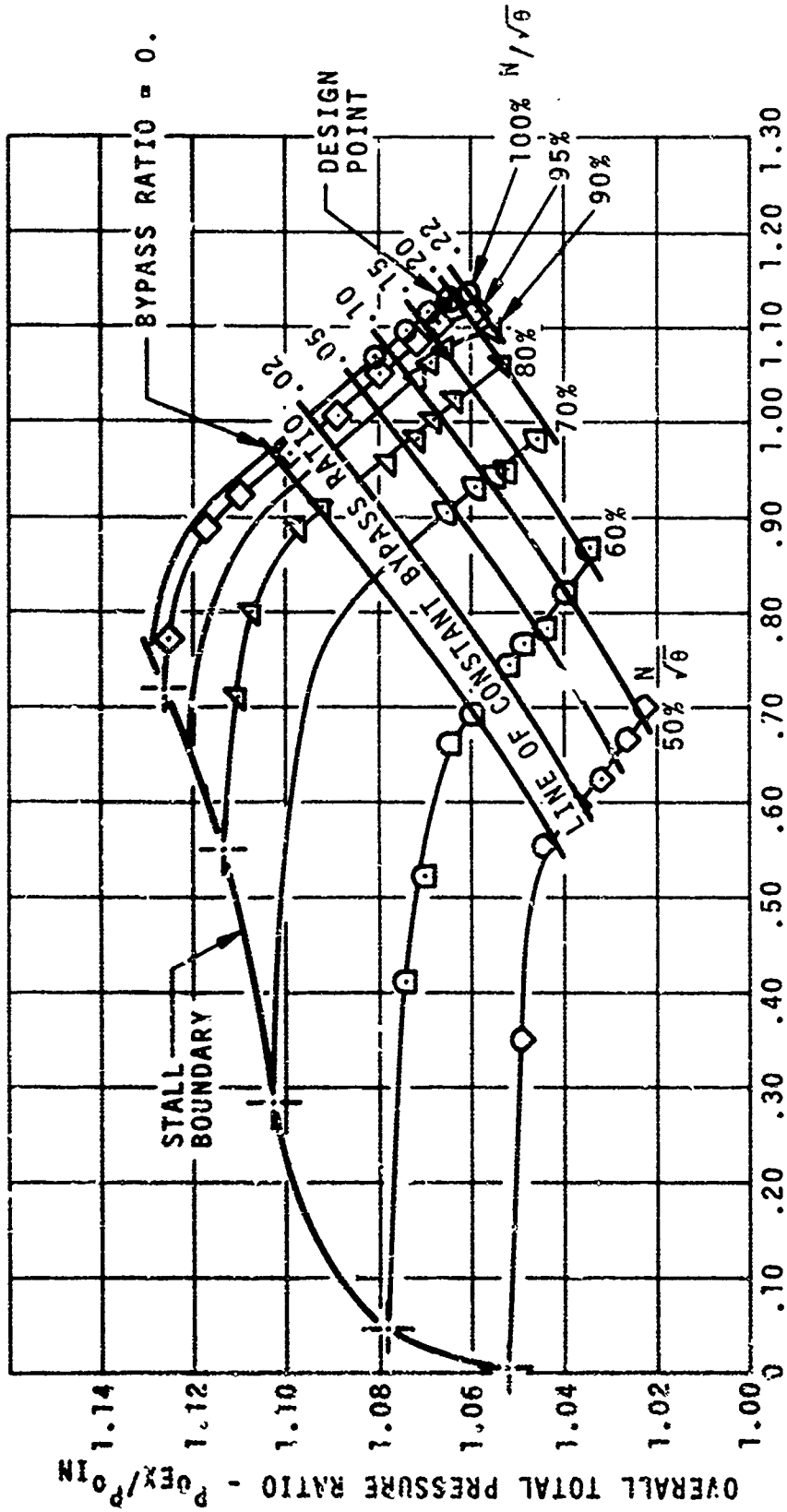

Figure 60. Performance Map Overlay Showing Lines of Constant Bypass Ratio - Test P2.

Another aspect of the performance in general that is indicated in Figure 60 is that at design speed total flow and total pressure ratio, the bypass rate was approximately 20 percent.

Power input to the blower (Figure 61) was computed on the basis of total flow rate and overall temperature rise. (See Appendix A.) From 70% speed and higher, the vertically sloping lines of constant β_2 on Figure 61 are close approximations to operating lines for a blower discharging to a fixed downstream resistance. The 20-percent line, for example, then represents the variation in power as a function of speed along a typical operating line.

At 100-percent speed, the blower requires approximately 15.6 horsepower as determined from test data. The estimated power at 100-percent speed during the design phase was 15.57 horsepower. (Refer to Table 11.)

If we use the independent measurement of bypass channel airflow to compute the performance of the rotor/vane stage, there are no indications of problems in the primary channel, insofar as rotor airflow, rotor pressure ratio, efficiency, or nozzle Mach number is conerned. In fact, the calculated stage efficiency at 100-percent speed (β_2 = 20%) is considerably higher than was assumed during the design phase. (Refer to Figure 62.)

In the bypass channel (Figure 63), losses are about consistent with the inlet module tests but the bypass flow rate is lower than design. (At the design total flow rate and pressure ratio, the bypass ratio is 20 percent compared to the predicted 25 percent.)

An explanation for this is shown in Figure 64, where upon teardown, the turning vane wakes showed a considerable deviation from the axial flow direction, indicating that swirl was present at the mixing tube inlet. The ejector performance is a function of axial velocity and hence for a given rotor output, a somewhat less secondary flow is induced.

In Table 18, a comparison is made between design and test for the significant performance parameters.

We may summarize the Test P2 results by stating that overall flow and headrise requirements were satisfied. The assumed rotor and stage efficiencies proved to be very conservative, and higher performance from the rotor resulted. The swirl problem produced somewhat less bypass flow; however, based on previous particle separator experience, the difference in separation efficiency from 20-percent scavenge to 25 percent scavenge is small, and thus the impact on durability should be minimal.

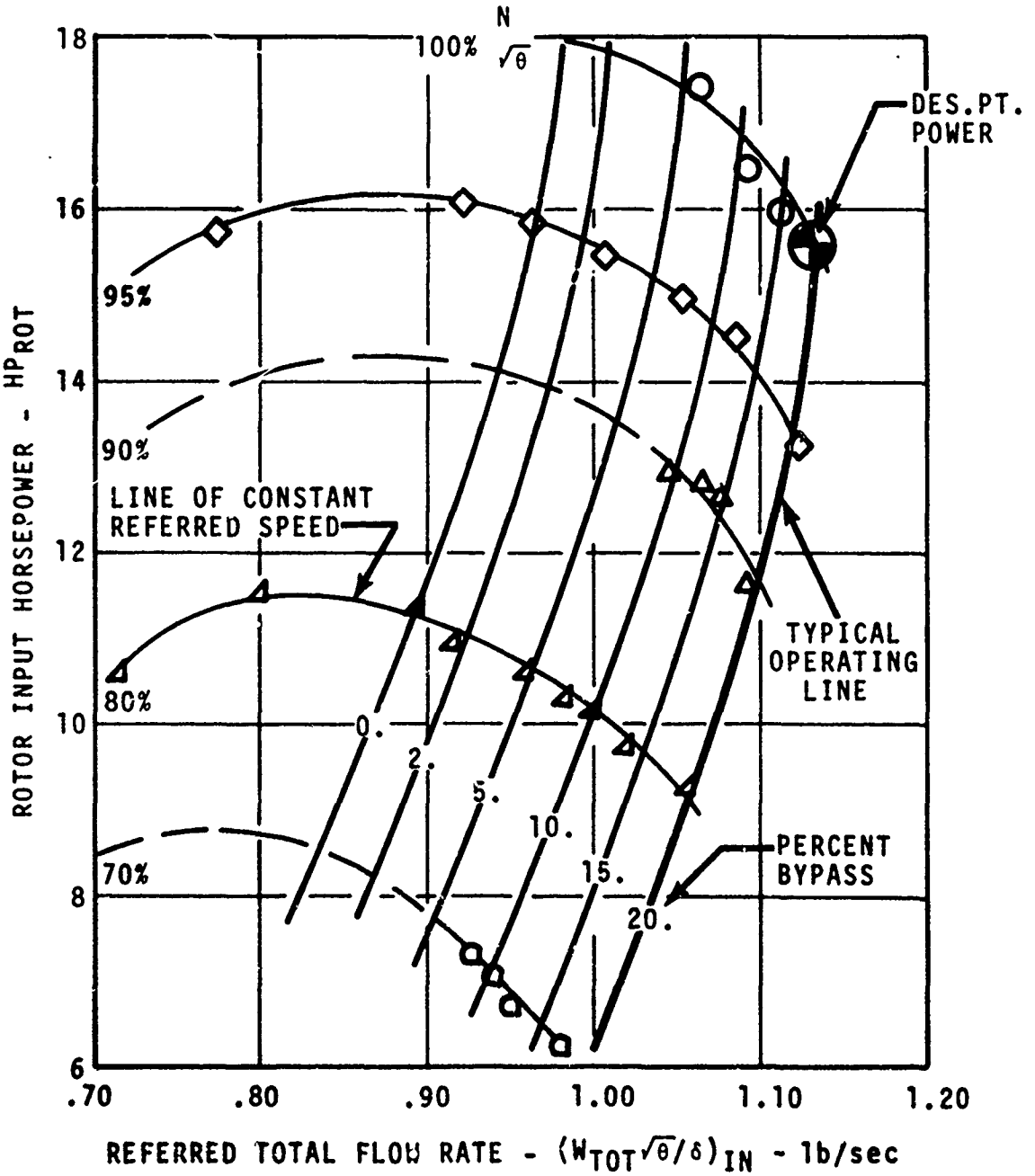

Figure 61. Horsepower Versus Bypass Ratio and Speed - Test P2.

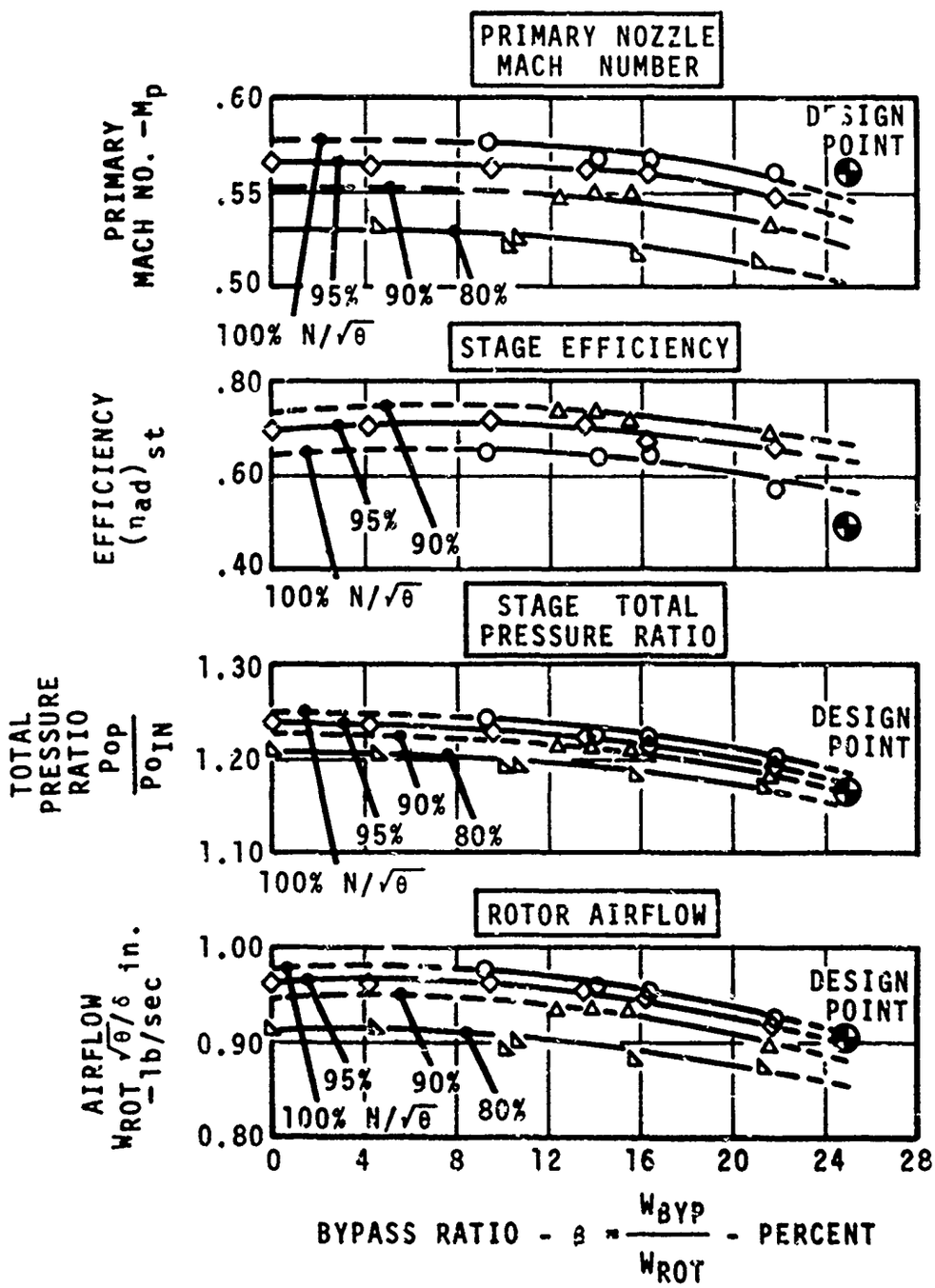

Figure 62. Stage Performance as a Function of Bypass Ratio - Test P2.

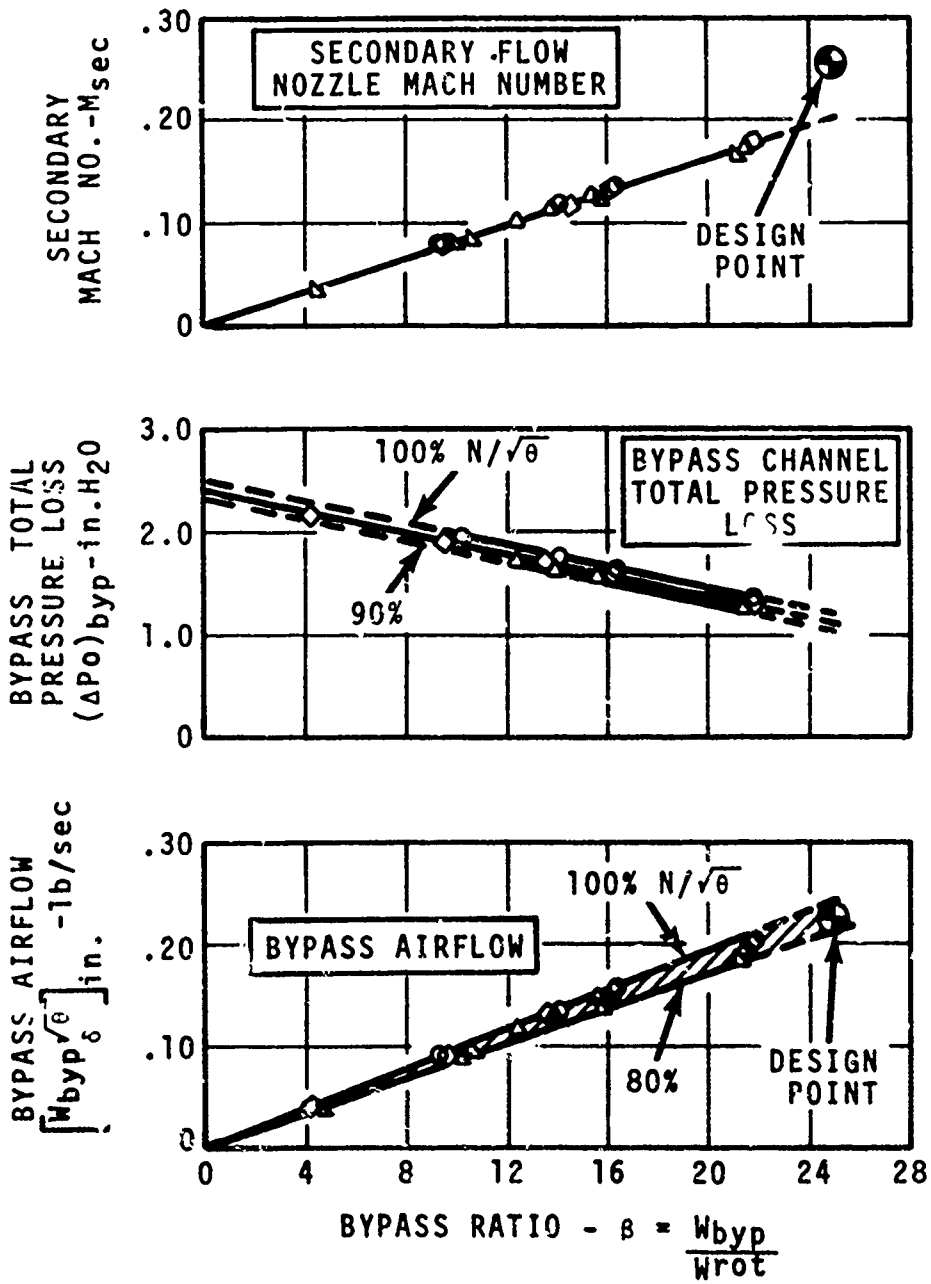

Figure 63. Bypass Channel Flow Parameters - Test P2.

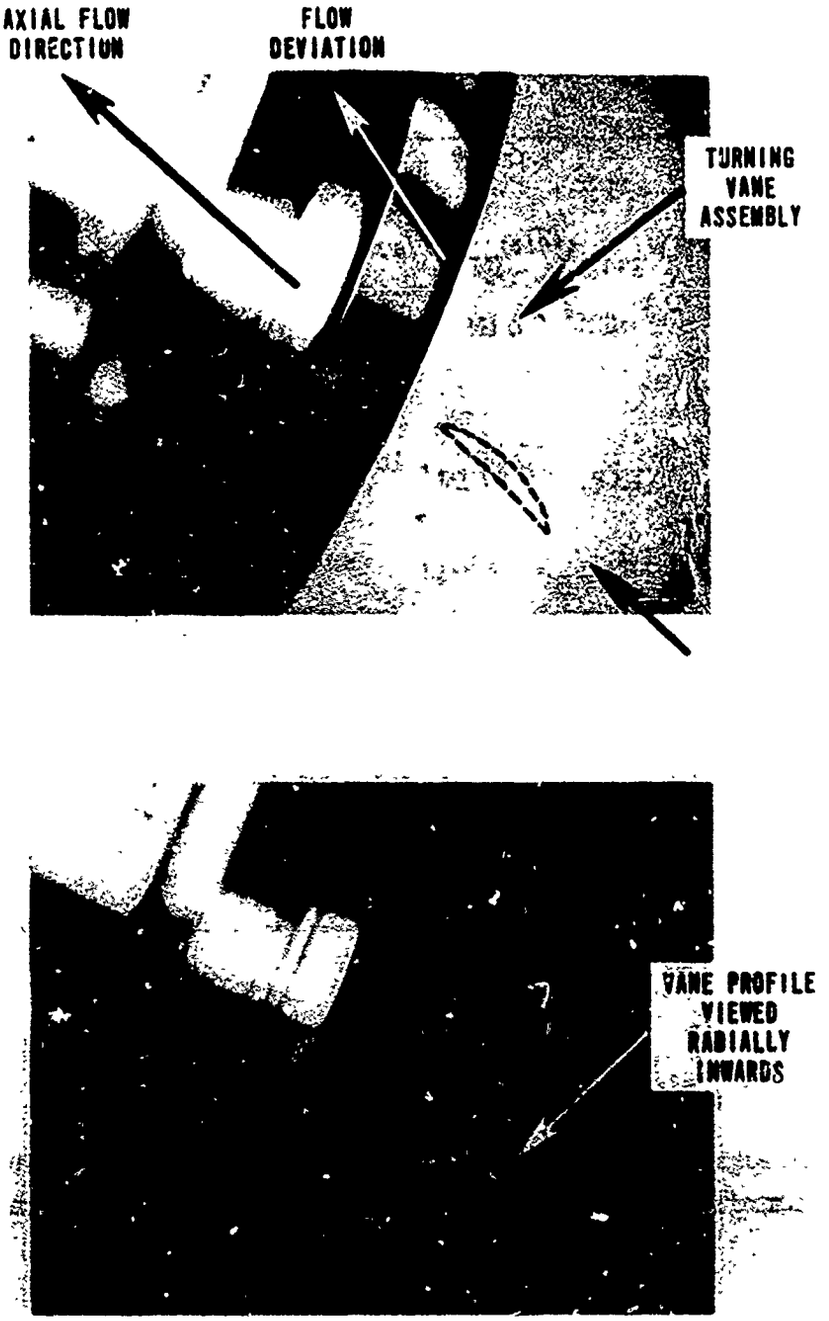

Figure 64. Indication of Swirl at the Ejector Primary Nozzle - Test P2.

TABLE 18. TEST RESULTS VERSUS DESIGN - SYSTEM D1 BASELINE PERFORMANCE

Parameters	Design	Test
Speed - $(N/\sqrt{\theta})_{IN}$, rpm	50,000	50,000
Total Airflow - $(W_{TOT}\sqrt{\theta}/\delta)_{IN}$, lb/sec	1.129	1.13
Pressure Ratio - $P_{oEX}/P_{o\,IN}$	1.064	1.064
Power - HP_{ROT}	15.57	15.6
Rotor Airflow - $(W_{ROT}\sqrt{\theta}/\delta)_{IN}$, lb/sec	.904	.940
Bypass Airflow - $(W_{BYB}\sqrt{\theta}/\delta)_{IN}$, lb/sec	.225	.190
Pressure Ratio - $P_{o_P}/P_{o\,IN}$	1.175	1.215
Pressure Ratio - $P_{o_P}/P_{o\,i}$	1.190	---
Bypass Ratio - $\beta 2$	25%	20%
Stage Efficiency - $(\eta ad)_{STG}$	.497	.600

i = Rotor inlet plane

IN= Blower inlet plane

P = Primary nozzle plane

*This reflects 5 in. H_2O margin on design inlet total pressure.

TEST P3 - WATER INGESTION

The purpose of this test was to evaluate the effects of water ingestion upon the operation of the blower under both transient and steady-state conditions. To simulate operation of the blower in a rainstorm, the water flow rate was based on a 5.0-lb/sec engine which ingests liquid equivalent to 3 percent of the airflow; the engine particle separator was assumed to have 75-percent water separation efficiency.

Under the above conditions, 50 cc/sec would be drawn by the blower at design speed. The test was run as follows:

1. Approximately 100 cc was introduced into the inlet, with the blower at zero rpm. The blower was then accelerated to 25,000 rpm, simulating "start up" while ingesting this slug of water.

2. At 25,000 rpm, water at the rate of 50 cc/sec was introduced continuously for 2 minutes.

3. Continuing with the same flow rate of water, the blower was accelerated up to 50,000 rpm, and was run for approximately 8 minutes.

Throughout this test, there were no observable effects, either mechanical or aerodynamic (for example, vibration level change) other than a very vigorous expulsion of the water from the system exhaust.

TEST P4 - DURABILITY - OVERALL PERFORMANCE

The objective of this phase of the program was to quantitatively measure the operational characteristics of the blower under an erosion environment for 50 hours.

Sand-feed rate to the blower was determined by analogy to a 5.0-lb/sec engine, whose particle separator admits a sand/air concentration of 1.5 mg/ft^3 with a separation efficiency of 95 percent and a scavenge rate of 18 percent. Under these conditions, the blower would extract (nominally) 400 grams of sand (MIL-E-5007C) per hour.

Over the 50-hour duration of this test, inspections were actually performed at the following intervals: 10, 16, 25, 35, 42 and 50 hours.

The 16-hour check was prompted by a somewhat higher than normal outer-race temperature on the No. 2 bearing. This bearing was replaced, as evidence of outer race rotation was present, and the test was resumed. Probable cause was attributed to contamination in the oil mist supply, and the problem was corrected by improving the inlet filtration system.

Up to the 50-hour point, the basic test results can be summarized as follows:

- Excepting one instance (≅16 hours) when the No. 2 bearing ran a higher outer race temperature (215° F versus 190° F), there were no mechanical problems in operating the blower for extended periods of time. Steady-state vibration was low, generally under 0.15 mil.

- Overall performance did not diminish; in fact, a modest improvement in total flow was seen up to about 35 hours

- From periodic inspections, the wear patterns on the rotor were apparent, even after 10 hours running. All erosion took place on the pressure surface of the blade; it was most evident on the leading edge and along the blade shroud.

Figures 65 and 66 show a comparison of the test rotor to a second, unused rotor after 10 hours and after 50 hours. The vane assembly also showed some indication of wear after 50 hours (Figure 66); the erosion occurred towards the outer shroud at the trailing edge, and again, only on the pressure surface of the vane.

Examination of all other flow path components which contain struts or splitters showed no signicant erosion.

At the 50-hour mark, the program objectives were clearly met, and with ample margin remaining on overall performance.

The durability test was then extended for an indefinite number of additional hours with the objective of reaching some definitive aerodynamic and/or mechanical limit. The performance limit, in any event, was taken as the minimum given flow of 0.90 lb/sec at -20 in. H_2O, or 0.946 lb/sec at standard day inlet conditions.

The next three benchmark inspections were at 60, 75, and 85 hours. At 85 hours the wear pattern on the rotor was most pronounced at midspan and towards the shroud (Figure 67).

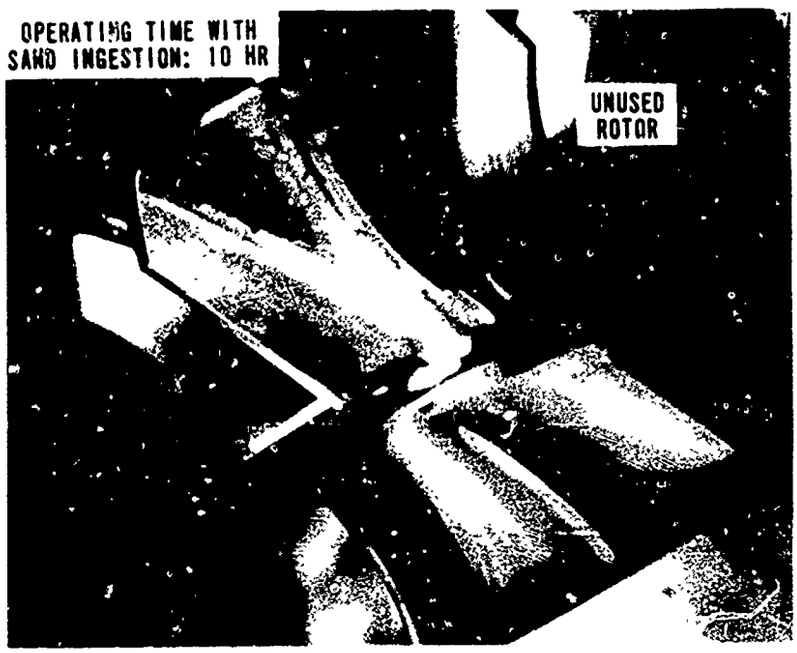

TOTAL AIRFLOW (ACT) = 1.15 lb/sec
ROTOR SPEED = 50,000 rpm
SAND INGESTION RATE = 400 GM/HR
SAND TYPE: MIL-E-5007C

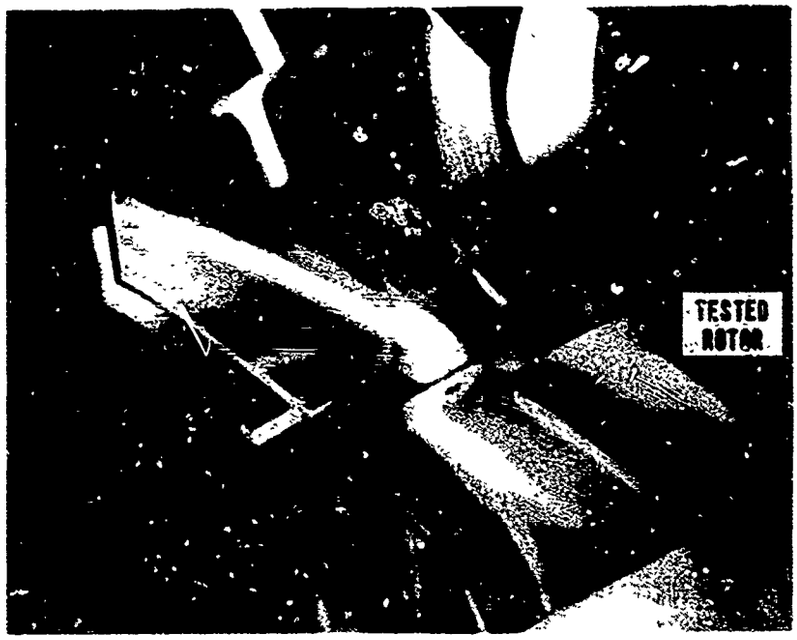

Figure 65. Effect of Sand Ingestion Upon the Rotor - Test P4 - 10 Hours.

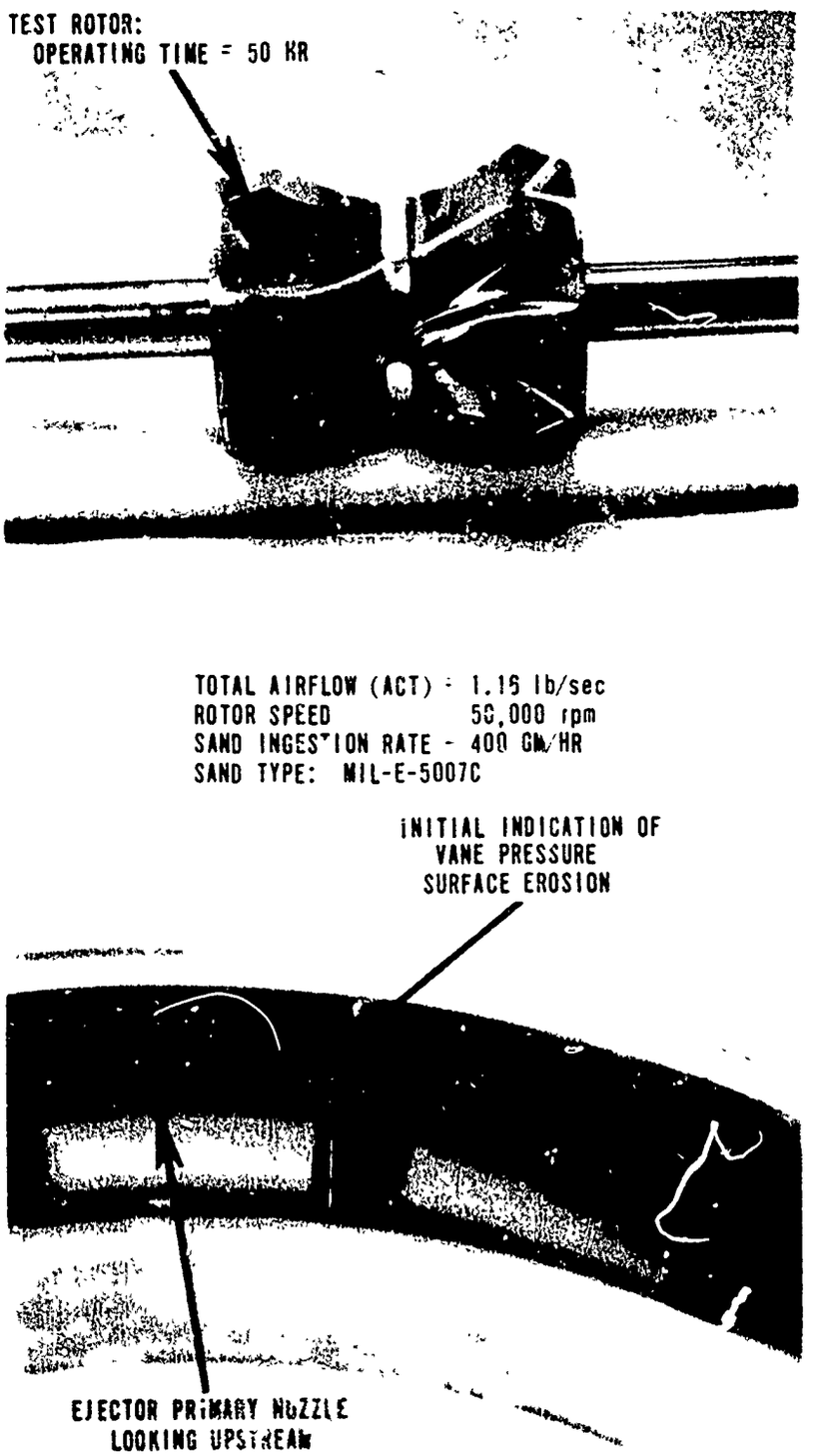

Figure 66. Effect of Sand Ingestion Upon Rotor/Vanes - Test P4 - 50 Hours.

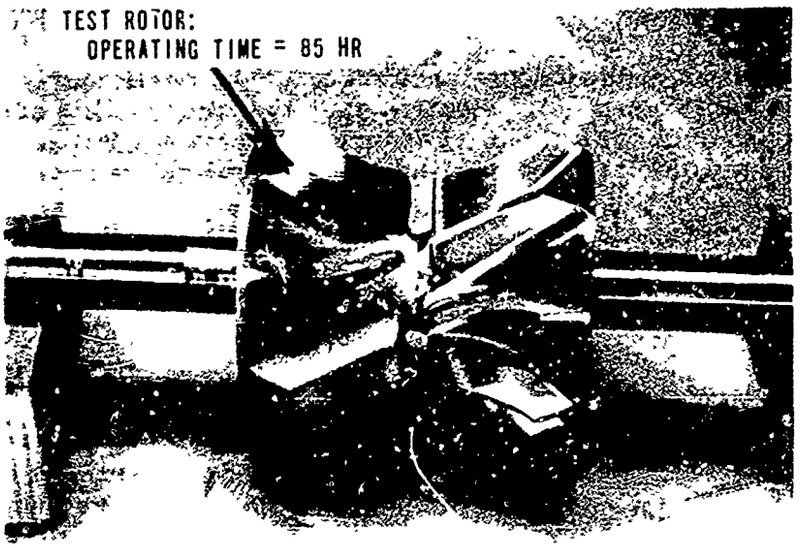

TOTAL AIRFLOW (ACT) 1.15 lb/sec
ROTOR SPEED 13,000 rpm
SAND INGESTION RATE - 400 GM/HR
SAND TYPE: MIL-E-5007C

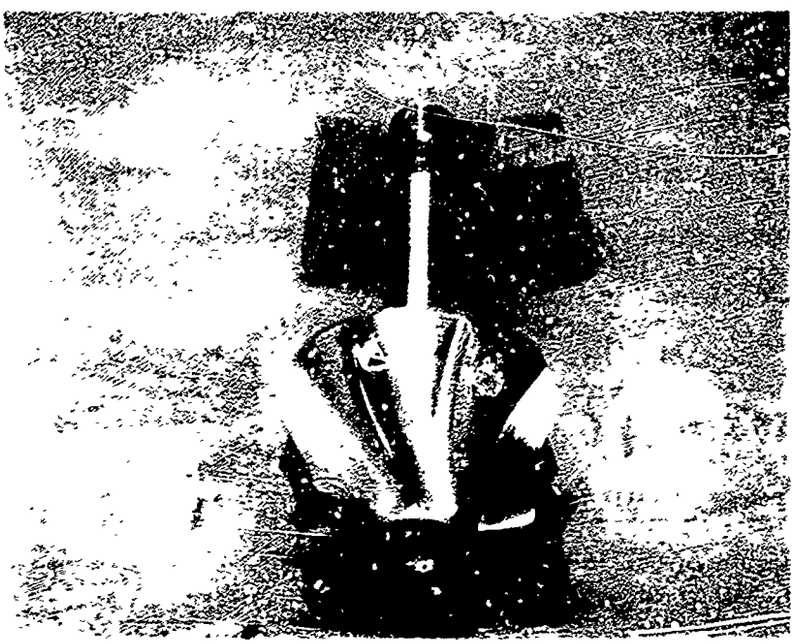

Figure 67. Effect of Sand Ingestion Upon Rotor - Test P4 - 85 Hours.

The turning vanes show some erosion damage, particularly at the trailing edge (Figure 68). Wear is such that the trailing edge is beginning to curl over, from pressure side particle impacts. This condition is worst at the outer shroud and diminishes towards the vane hub.

The testing was terminated after 118 hours due to a bearing failure. Damage from this failure was confined to the rotor bearings and the face seal only.

Photographs of the critical hardware at the 118-hour durability test conclusion are shown in Figures 69 and 70.

In judging the mechanical integrity of these components, it should be emphasized (in the case of the vanes) that no provisions were made for protection from erosion damage, since these were fabricated from standard airfoil strip stock (10-percent maximum thickness) which were then coined to a desired camber. Also, the rotor had no protection (coatings) from the fraction of contaminant admitted by the inlet separator. In view of the preceding, and considering the 50-hour minimum objective, the mechanical performance of these components was very satisfactory, since a factor of 2.4 times the minimum required operation life was achieved with ease.

Figure 71 shows the measured flow and pressure ratio at each data point in relation to the design speed map characteristic at the start of the testing. The effect of erosion upon overall performance was as follows:

- A rise in the total airflow up to about 35 hours.
- An increase in pressure ratio up to 85 hours.
- A decrease in flow and pressure ratio beyond 85 hours.

At the test conclusion, the total flow was 1.081 lb/sec, which is still well above the minimum requirement of 0.946 lb/sec.

TEST P4 - DURABILITY - COMPONENT PERFORMANCE

Performance of the individual blower components in terms of flow, pressure ratio, efficiency, etc., through the durability test indicated a general improvement up to about 35 hours. (Refer to Figures 72 and 73.)

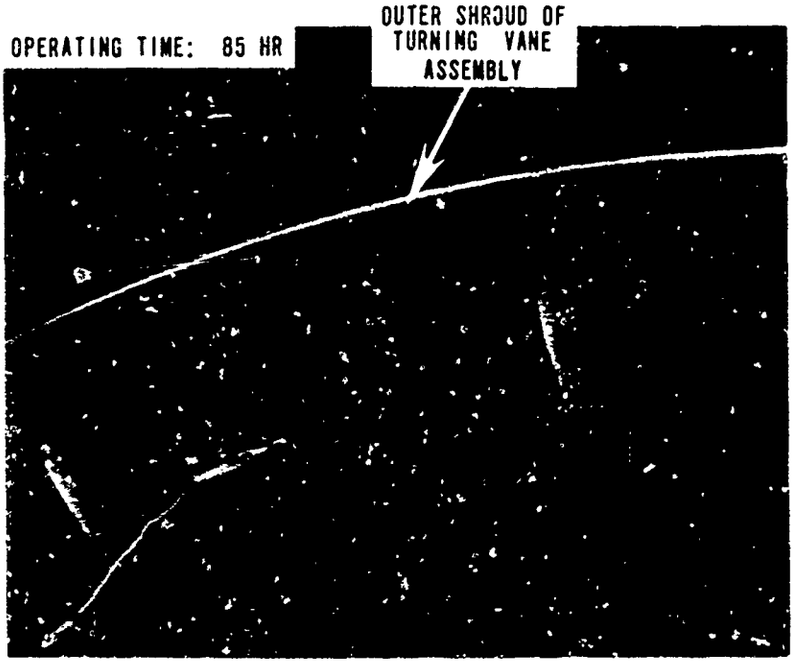

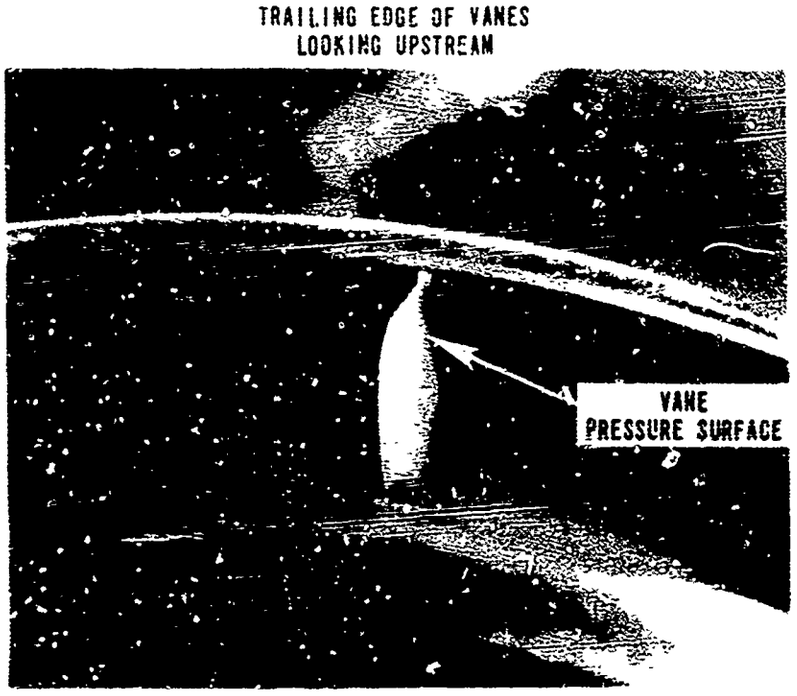

Figure 68. Effect of Sand Ingestion Upon the Turning Vanes - Test P4 - 85 Hours.

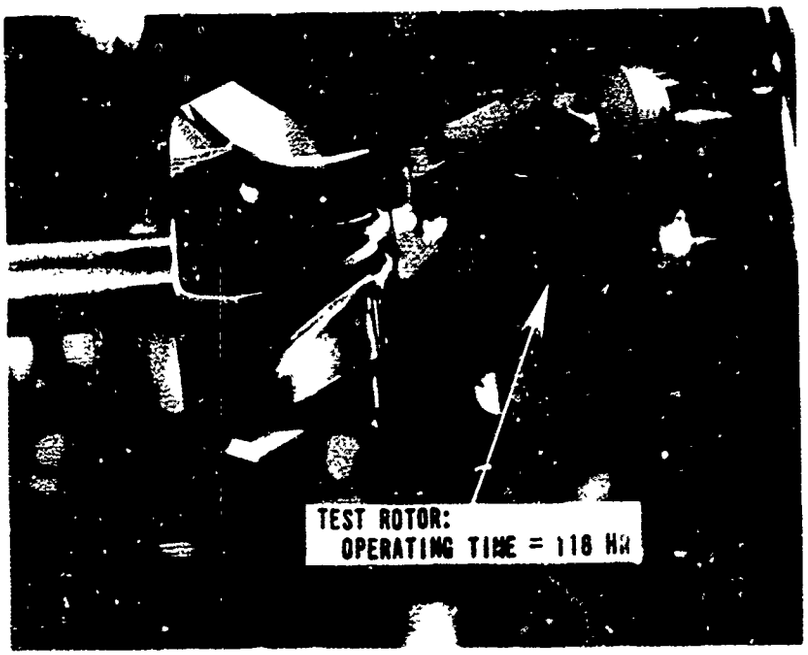

TOTAL AIRFLOW (ACT) = ..06 lb/sec
ROTOR SPEED = 50,000 rpm
SAND INGESTION RATE = 400 GM/HR
SAND TYPE: MIL-E-5007C

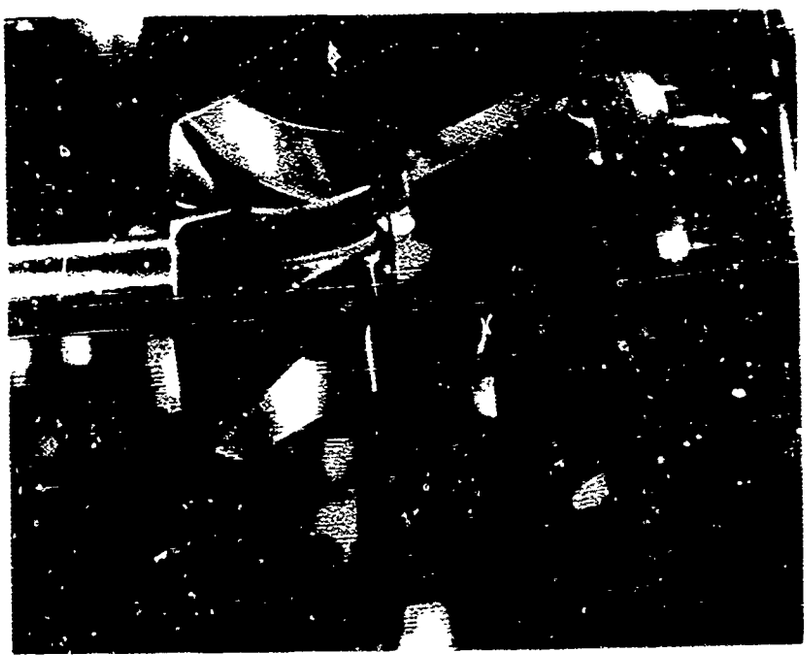

Figure 69. Cumulative Erosion Effect - Test P4 Conclusion - Rotor.

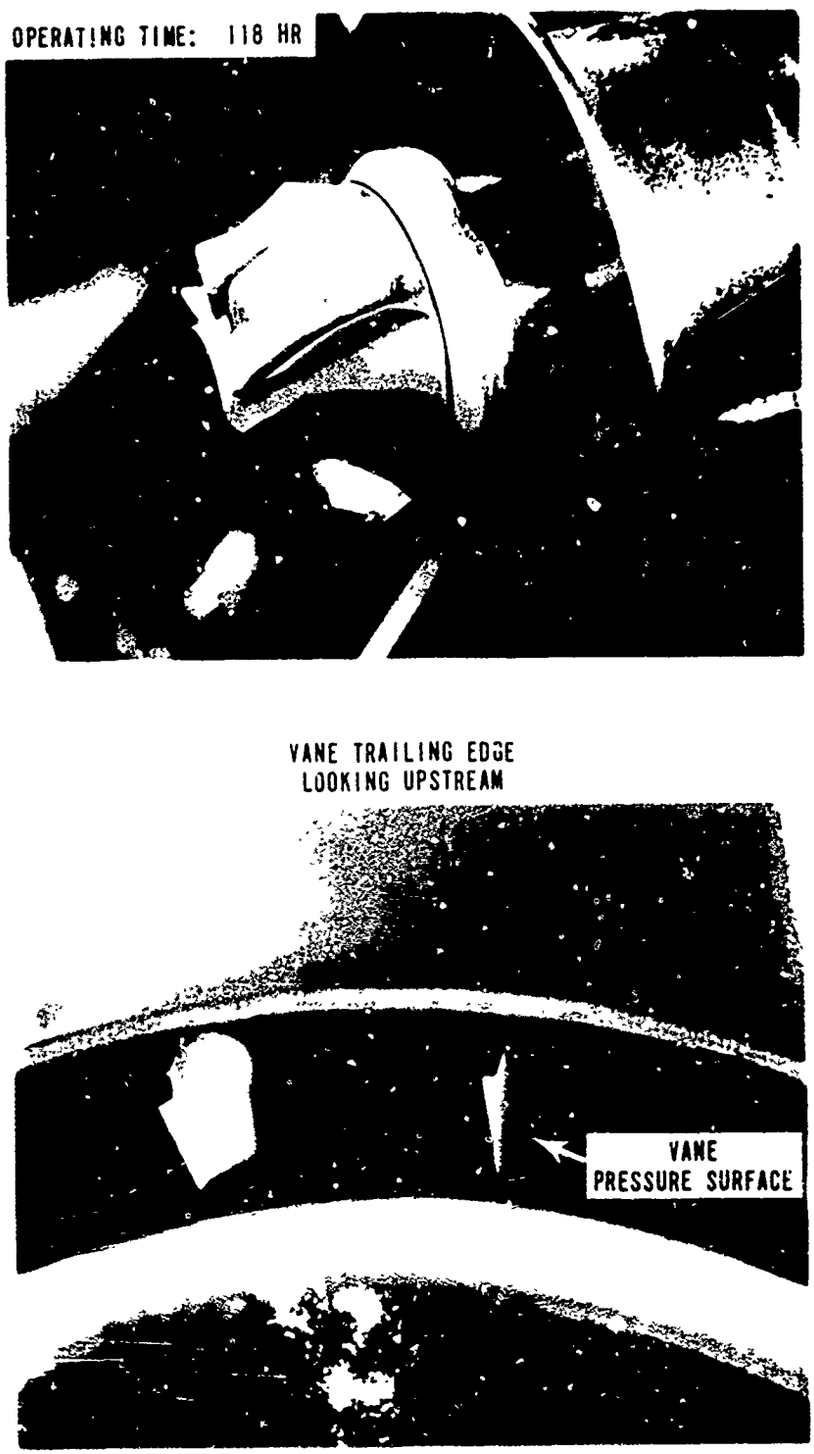

Figure 70. Cumulative Erosion Effect - Tets P4 Conclusion - Vanes.

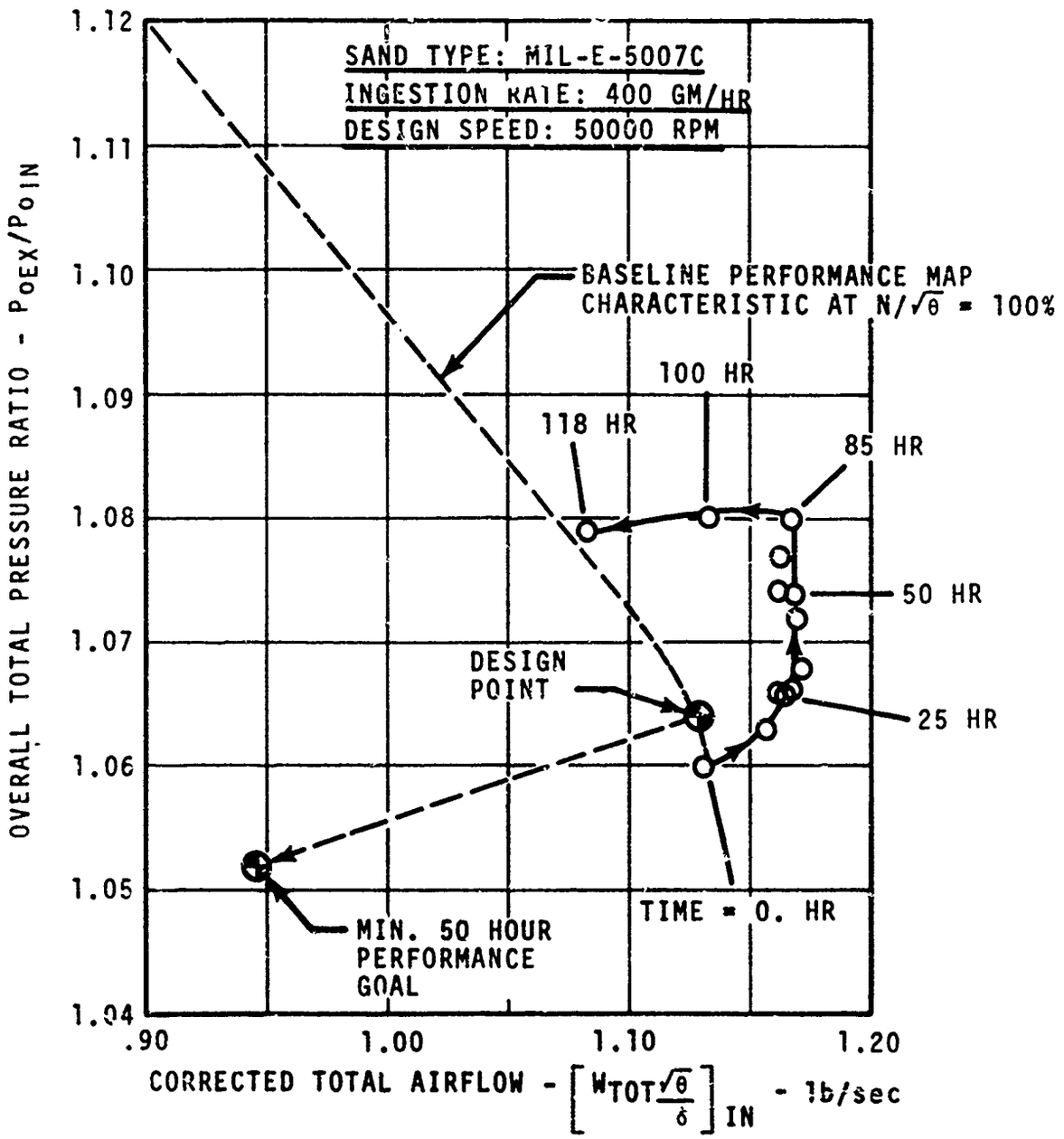

Figure 7.. Effects of Sand Ingestion Upon the Blower Operating Point - Test P4.

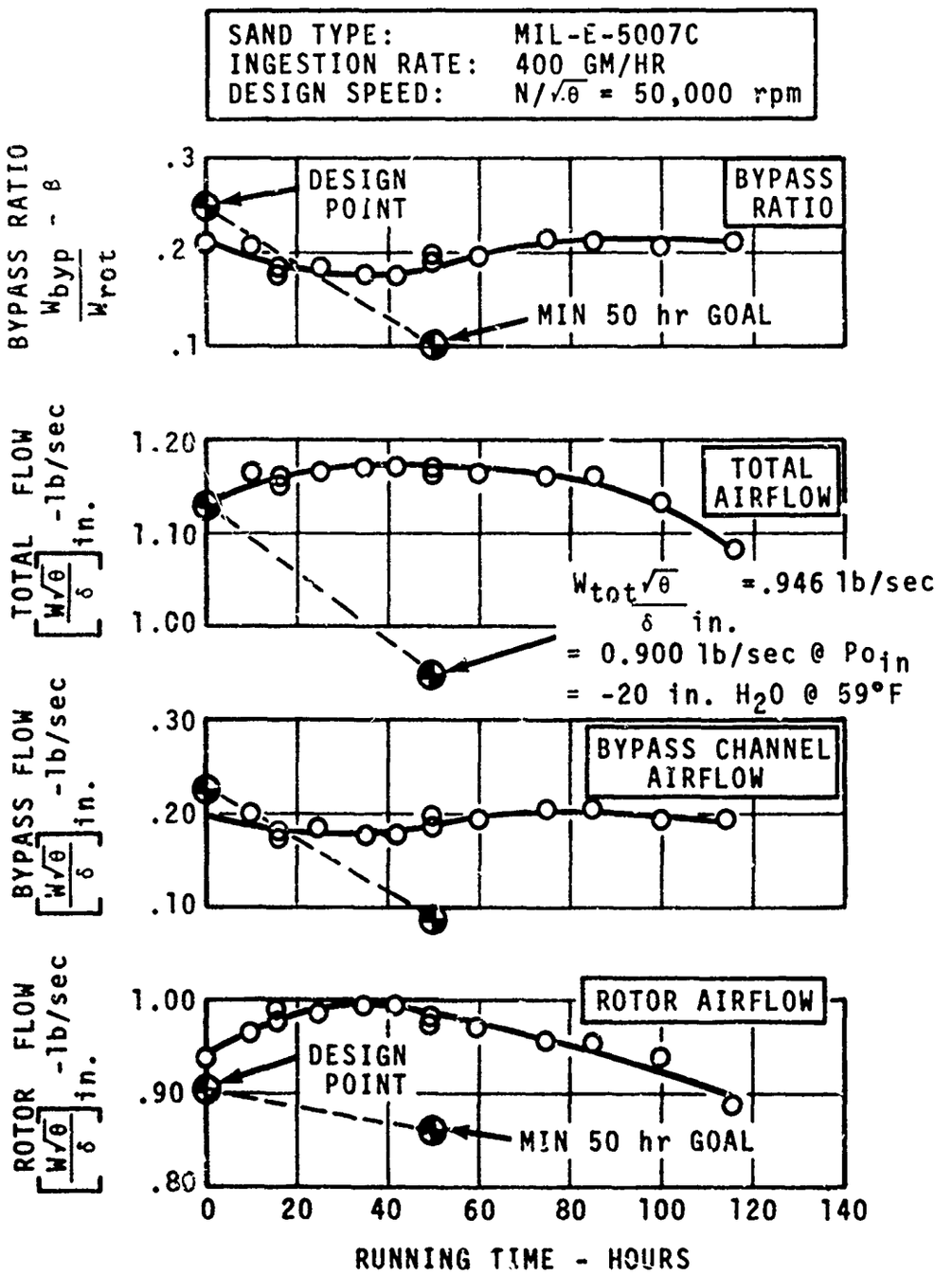

Figure 72. Durability Test Results - Test P4 - Bypass Ratio, Total Flow, Bypass Flow, and Rotor Flow Versus Running Time.

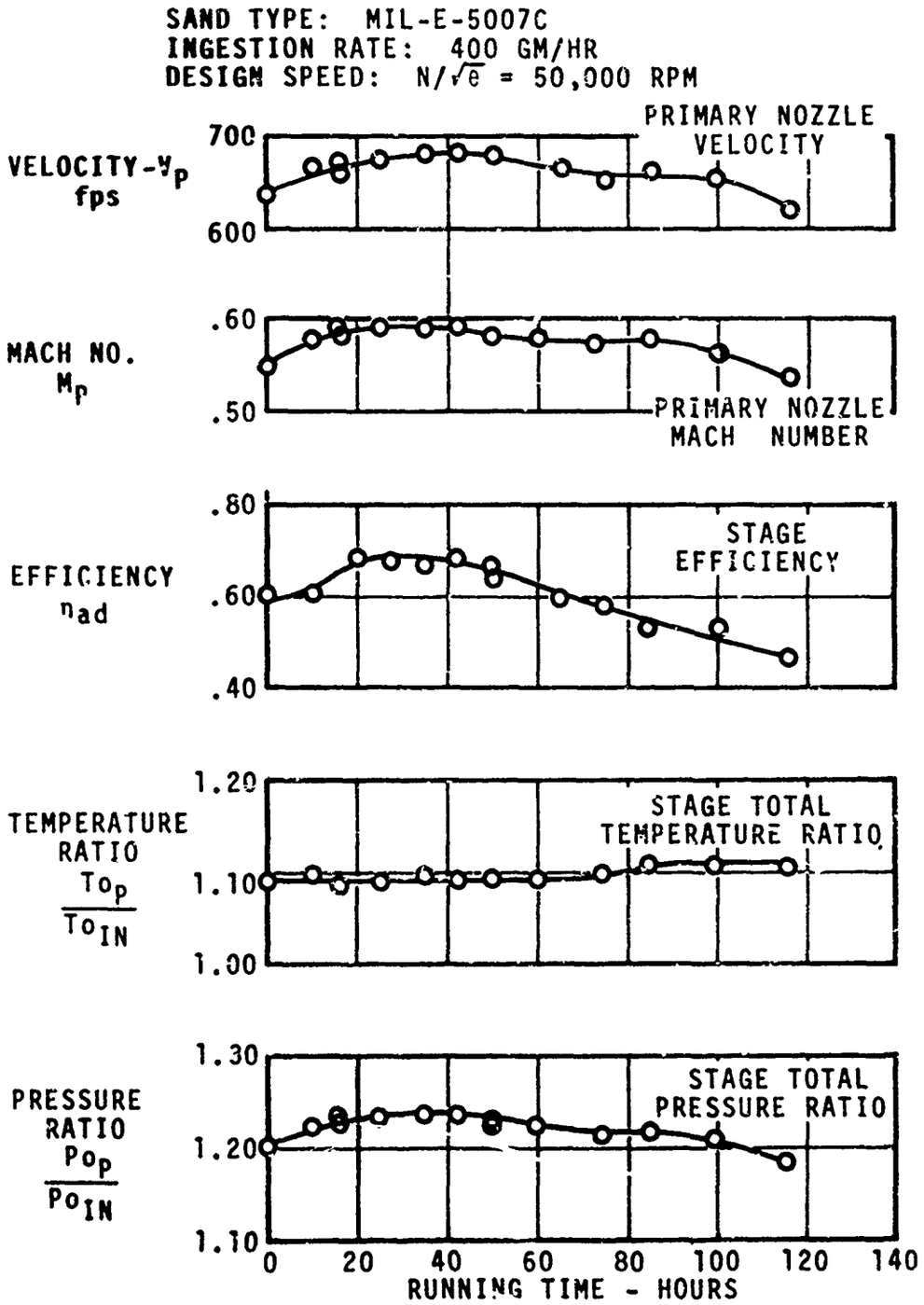

Figure 73. Durability Test Results - Test P4 - Velocity, Mach No., Efficiency, Temperature Ratio, and Pressure Ratio Versus Running Time.

Rotor airflow is a typical example where the effect of erosion is such that the minimum blade passage area is progressively increasing, causing the rotor to move to a new operating characteristic, at higher flow/higher work. From Figures 72 and 73 the trends in rotor flow, pressure ratio, and efficiency all reach peaks near 35 hours, and then begin to decline. (See Appendix A for computational procedure.)

The quantity of bypass flow induced by the primary stream (Figure 72) apparently does not increase, even though more energy is available from the rotor. One possibility is that the stator deviation problem becomes more pronounced as the airflow is increased, and as a consequence, the axial flow component is actually reduced, causing the ejector to pump less bypass air.

The problem is not a significant one, as the 20-percent rate of bypass obviously was an adequate rate of scavenge. However, some modifications to the turning vane design would permit the same amount of bypass air to be induced, but at a somwhat lower rotor output, thereby reducing the power requirements of the blower.

TEST P4 - DURABILITY - MECHANICAL EFFECTS

At the inspection intervals during the durability test, diametral measurements were taken on the rotor near the leading edge and also on the splitter housing. The purpose of these measurements was to determine the nature of the wear rate as a function of time.

From these measurements, it was found that both the shroud (housing) ID and the rotor inlet OD vary linearly as a function of running time (Figure 74). Consequently, the radial tip clearance experienced a fairly linear rate of increase.*

The cold, static radial clearance near the impeller leading edge varied from 0.007 inch at the start of the test to approximately 0.046 inch after 118 hours. The average rate of clearance increase was 0.3 mil per hour of operation under the conditions tested.

---

*NOTE:

(a) Splitter housing material - 321 stainless steel

(b) Rotor material - 17.4 PH stainless, R_C 32-33

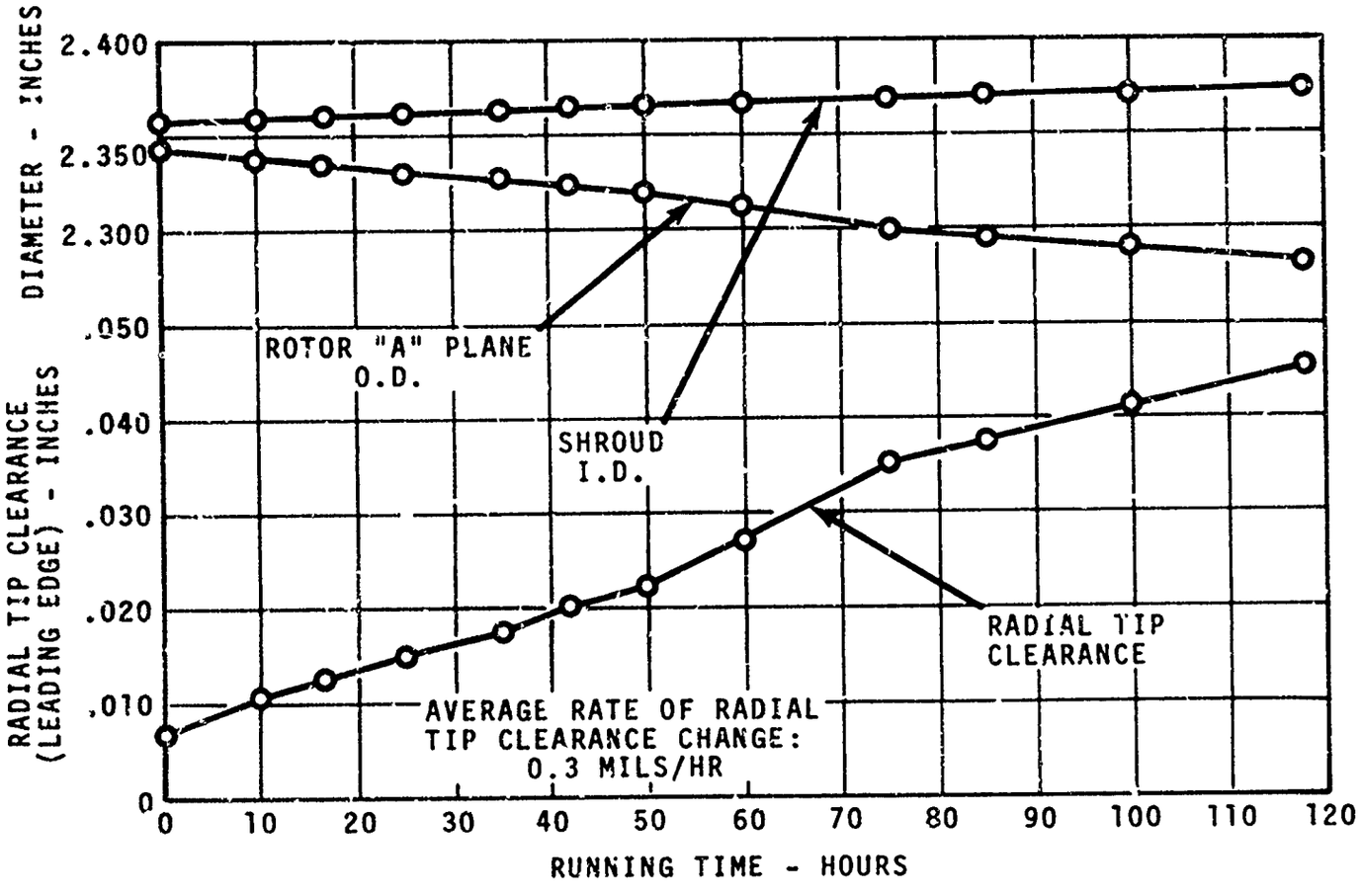

Figure 74. Rotor and Housing Dimensional Changes as a Function of Operating Time - Test P4.

The observed pattern of wear on the blade at the test conclusion is shown in Figure 75. In the view shown, the erosion is fairly uniform along the leading edge and the shroud, with slightly more wear towards the leading-edge hub.

In the cross section, all of the erosion is seen to take place on the blade pressure surface, and the auxiliary view in Figure 75 is typical of sections normal to the flow streamlines at most stations along the blade.

The uniformity of the wear pattern on the rotor is consistent with the relatively slow rate of performance degradation that was observed in the test.

TEST P4 - DURABILITY - OPERATIONAL LIFE CRITERIA

In the preliminary design of this blower, the basic criterion assumed (from related past experience) was that sand ingested by the rotor should be limited to 5 pounds in association with a particular material and rotor inlet blade speed. Translated into equivalent pounds of sand for a steel rotor at 500 fps blade speed, that limit was determined to be 11.9 pounds of sand for a minimum 50-hour operational life. Further, for specified engine and particle separator characteristics (5.0 lb/sec, 18 percent scavenge, 95-percent efficiency, 1.5 mg/ft^3-concentration), 11.9 pounds of sand would be ingested in no less than 50 hours of operation if the blower inlet was a minimum of 72-percent efficient.

We may now modify the above criterion by using the data which was obtained in Test P4.

Assume that the rotor as shown in Figure 70 (P4 conclusion) is taken to represent the maximum operational life of a scavenge blower critical component. This assumption is conservative since the rotor lost less than 5 percent in flow capacity over the duration of the test. For that rotor,

X = pounds of sand through rotor = 20.79 pounds @ t = 118 hours.

By plotting operating time against blower inlet separation efficiency (η_2) for the above quantity of sand then the relationship shown in Figure 76 results.

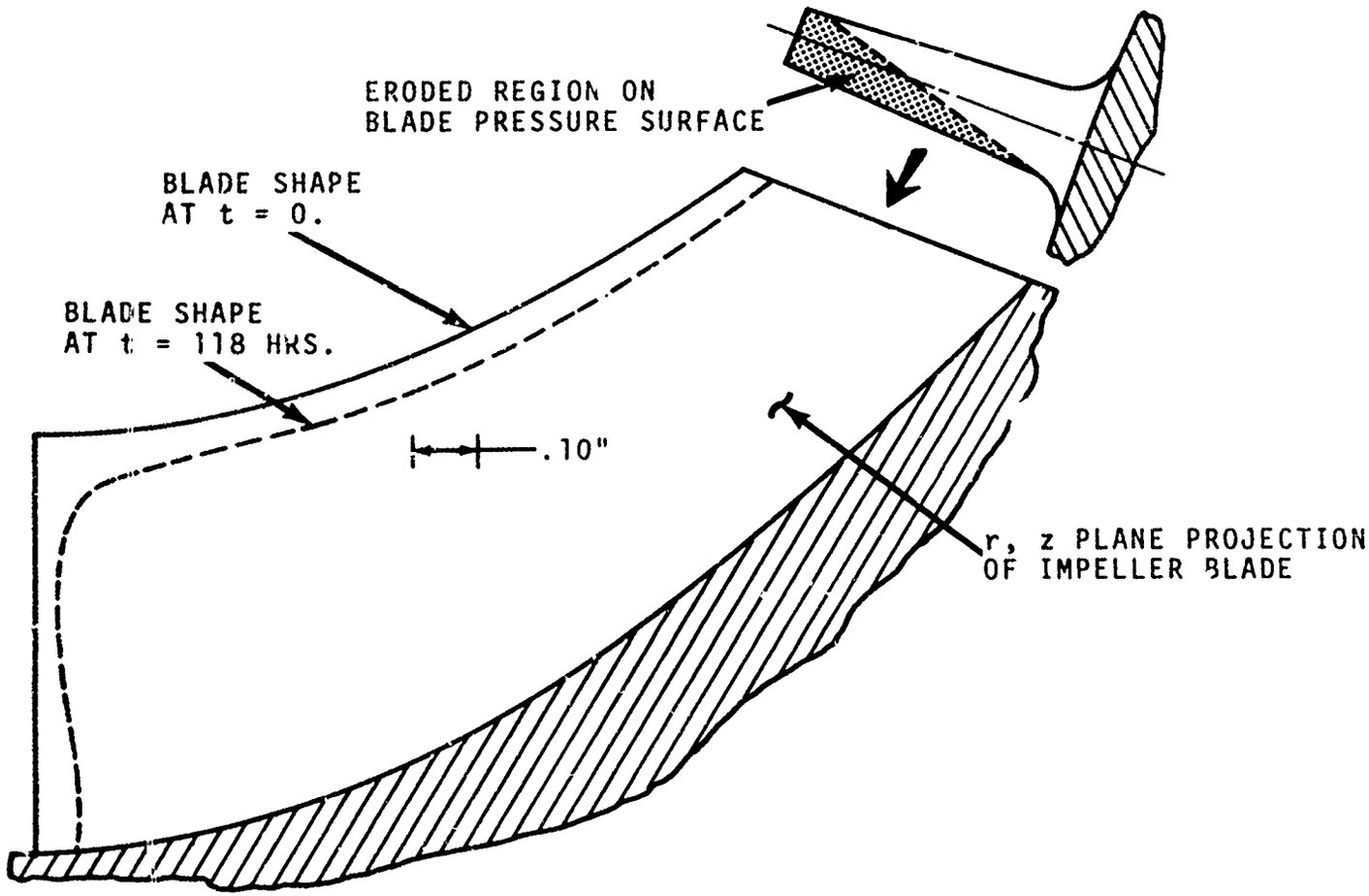

Figure 75. Blade Erosion Pattern at the Durability Test Conclusion - Test P4.

FIXED PARAMETERS:

X = WT. OF SAND THRU ROTOR = 20.79 LB.

η_1 = I.P.S. EFFICIENCY = 0.95

β_1 = I.P.S. SCAV. RATE = 20%

W_{ENG} = ENG. AIRFLOW = 5.0 lb/sec

C_o = I.P.S. SAND/AIR = 1.5 MG./FT^3

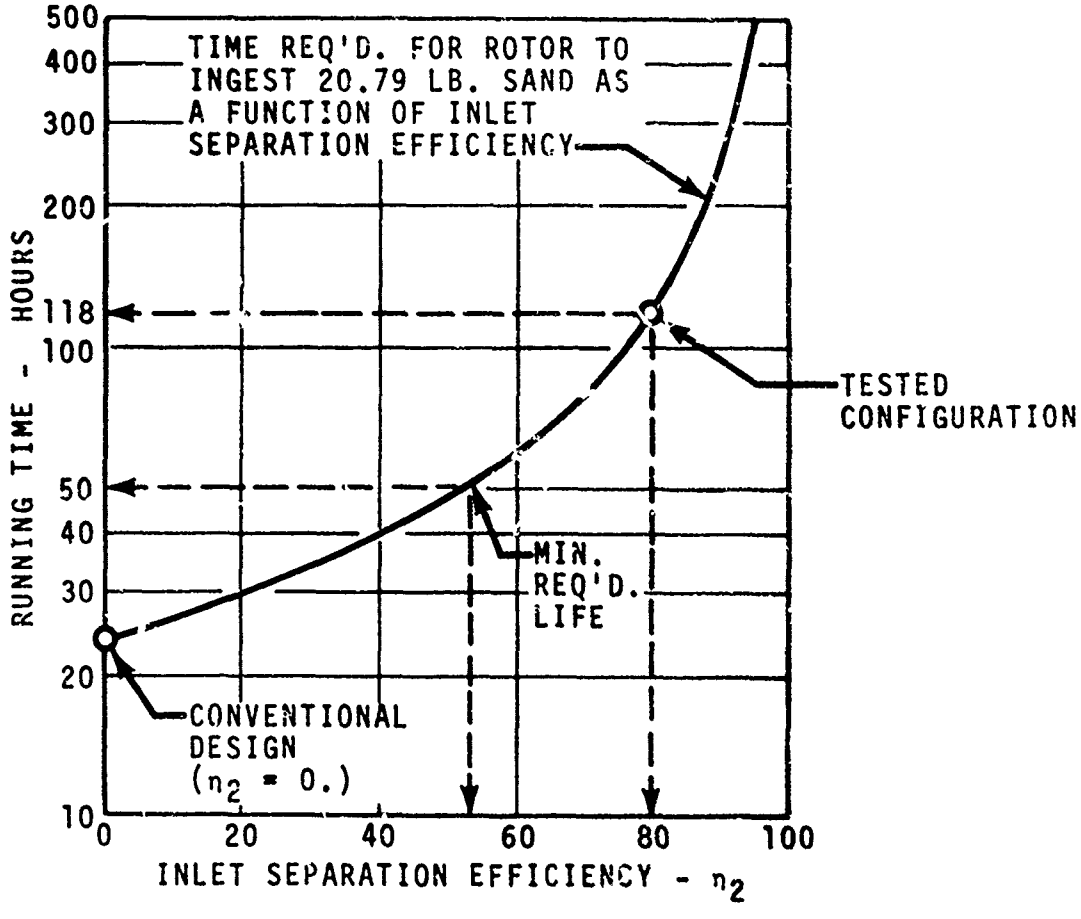

Figure 76. Blower Operational Life as a Function of Inlet Efficiency Based on Test P4 Results.

Clearly for a 50-hour objective, the amount of margin built into the present design can be reduced. By reducing rotor airflow by approximately 4 percent, and rotor pressure ratio also by 4 percent, then the blower input power is 10 horsepower at 60-percent stage efficiency. Bypass ratio becomes 15 percent, which is easily adequate for the required inlet efficiency (η_2) $\simeq$ 0.60 in Figure 75.

TEST P5 - ICE INGESTION/FOD TEST

In the final test of the blower evaluation program, a series of common hardware items were introduced sequentially into the inlet. The objects ranged in size from .33-inch lengths of safety wire, up to No. 8-32 bolts x 1/2-inch length.

Several pieces of ice, nominally 1/2-inch cubes, were introduced as well.

In order that some degree of randomness be present, the objects were directed, under shop air pressure, at the sloped section of a mitered elbow blower inlet flange.

All objects passed through the blower and either were expelled from the exhaust without incident or were trapped in the bypass channel at the reduced area section upstream of the ejector secondary nozzle.

NOTE: The rotor used in this test was a backup (unused) rotor; inspection after the FOD test showed no evidence whatsoever of any damage, indicating that all objects bypassed the rotor completely. Operating point for the test was 50,500 rpm at minimum system back pressure.

AERODYNAMIC DESIGN - SYSTEM S1 (TASK II)

GENERAL

The alternate system (S1) is a second approach to the development of a durable scavenging means for an engine particle separator. From the earlier concept studies, the selected configuration was a multiple-tube ejector assembly. The objective in evaluating this type of design is to achieve high durability, utilizing the inherent additional advantages of extreme simplicity, low cost, reliability, on/off capability, and good potential for a compact design.

For purposes of designing and testing this system, it will be assumed that the conditions available to the primary nozzle are 188 psia at 1250 °R.

The main disadvantage of the ejector approach is that the primary air supply is relatively costly in terms of power penalty to the engine.

In the feasibility study phase of this program, data was presented which related bleed to percent power loss (Figure 16). On the basis of this figure, an influence coefficient of 3.2:1 will be assumed when relating percent bleed (or primary airflow) to power penalty.

The earlier studies also established that for a secondary flow of 0.9 lb/sec, where the ejector (s) must operate with an inlet total pressure depression of -20 in. H_2O, the primary airflow required will be approximately 0.1 lb/sec (2-percent bleed).

NUMBER OF EJECTOR TUBE ELEMENTS

For a specified total quantity of primary airflow (in this case $\cong$ 0.10 lb/sec) that will be required, the maximum number of individual ejector tubes will be limited by the resulting throat area of the nozzle. In general, the overall size of the individual ejector becomes smaller as the size of the primary nozzle is reduced. A practical limitation is reached when the throat size approaches .050 to .060 inch; diameters smaller than this, for a converging/diverging nozzle, would present fabrication problems if conventional machining methods are employed. Also, the nozzle becomes prone to blockage from contamination or from oil film residue at the elevated temperatures present.

To determine the number of tubes in the assembly, the following design point parameters are assumed:

Primary nozzle pressure - $P_{o\,P}$	=	188 psia
Primary nozzle temperature - $T_{o\,P}$	=	1250°R

Total primary flow rate - $\dot{w}_{p\ TOT}$ = 0.1 lb/sec

Specific heat ratio at 1250°R - γ = 1.3663

Blockage factor at the nozzle throat - τ_p^* = 0.97

By using standard compressible flow relationships, the number of tubes as a function of throat diameter may be determined; the results appear in Figure 77.

The 15-tube assembly was selected as yielding the smallest practical throat diameter (D_p^* = .0575 inch) consistent with the specified supply conditions.

Thermodynamic design of the ejector, discussed below, will be based upon analysis of one element of the 15-tube assembly.

EJECTOR THERMODYNAMIC DESIGN

The minimum performance requirements to be satisfied by the ejector assembly are listed below:

Total flow scavenged	-	$W_{s\ TOT}$	= 0.90 lb/sec
Inlet pressure	-	$P_{oIN} = P_{oS}$	= -20 in. H_2O
Inlet temperature	-	$T_{oIN} = T_{oS}$	= 518.7°R
Primary flow rate	-	$W_{p\ TOT}$	= 0.1 lb/sec (2% bleed)
Primary pressure	-	P_{o_P}	= 188 psia
Primary temperature	-	T_{o_P}	= 1250°R

On the basis of <u>one element</u> from the 15-tube assembly:

Secondary flow	-	W_s	= .06 lb/sec at -20 in. H_2O
Primary flow (nominal)	-	W_p	.0068 lb/sec at 188 psia at 1250°R

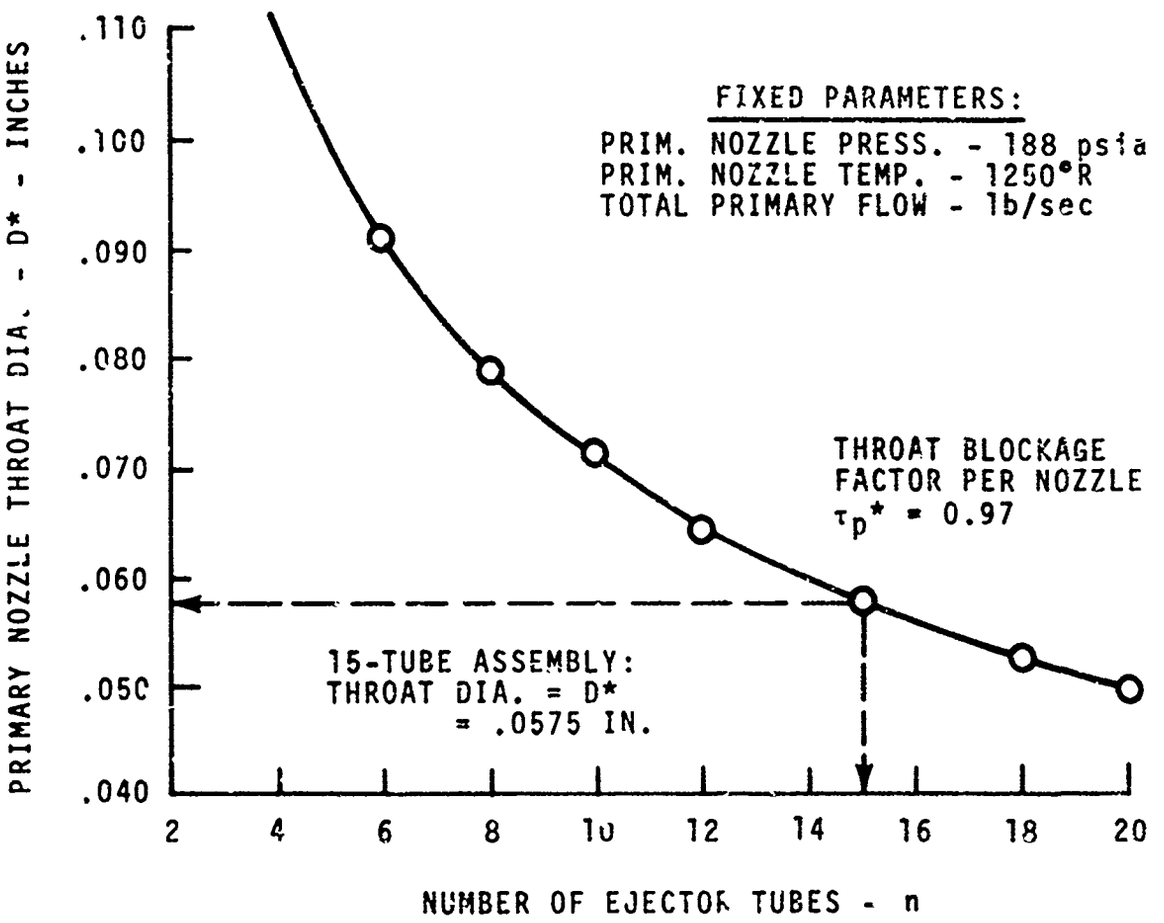

Figure 77. Primary Nozzle Throat Diameter as a Function of the Number of Ejector Tubes.

The computer program which was used to design the ejector is described extensively in Reference 6. Basically, the program can be used to predict the performance characteristics of axisymmetric, single-nozzle jet pumps with variable area mixing tubes, where the primary flow may be supersonic.

The ejector design program was applied to numerous geometric configurations, with the intention of generating a compact unit that requires the minimum bleed air possible to achieve the stated performance objectives. The prime variables that were studied in arriving at a final design configuration were the following:

- Secondary-to-primary area ratio.
- Shape of the mixing tube; for example, converging versus constant diameter.
- Mixing tube length versus diffuser length.
- Diffuser area ratio.

The ejector shown in Figure 78 has an overall length of ten times the mixing tube diameter, and can operate against a static pressure headrise of 50 in. H_2O. In Table 19, the design point thermodynamic characteristics are listed. All areas are effective flow areas. Blockage factors and conversion to geometric flow paths are discussed below.

FLOW-PATH SPECIFICATION

By the assignment of an estimated aerodynamic blockage factor to the areas given in Table 19, the geometric flow path is determined.

A high blockage factor at the nozzle exit was assumed to provide for an overexpanded primary flow. In effect, this provides some margin, where nozzle exit area adjustments could be made in the case where exit effective flow areas were greater than design.

Flow path dimensions for the mixing tube, diffuser, and primary nozzle are shown in Figures 79 and 80.

---

6. Hickman, K., ANALYSIS AND TESTING OF HIGH-ENTRAINMENT SINGLE-NOZZLE JET PUMPS WITH VARIABLE AREA MIXING TUBES, NASA CR-2067, June 1972.

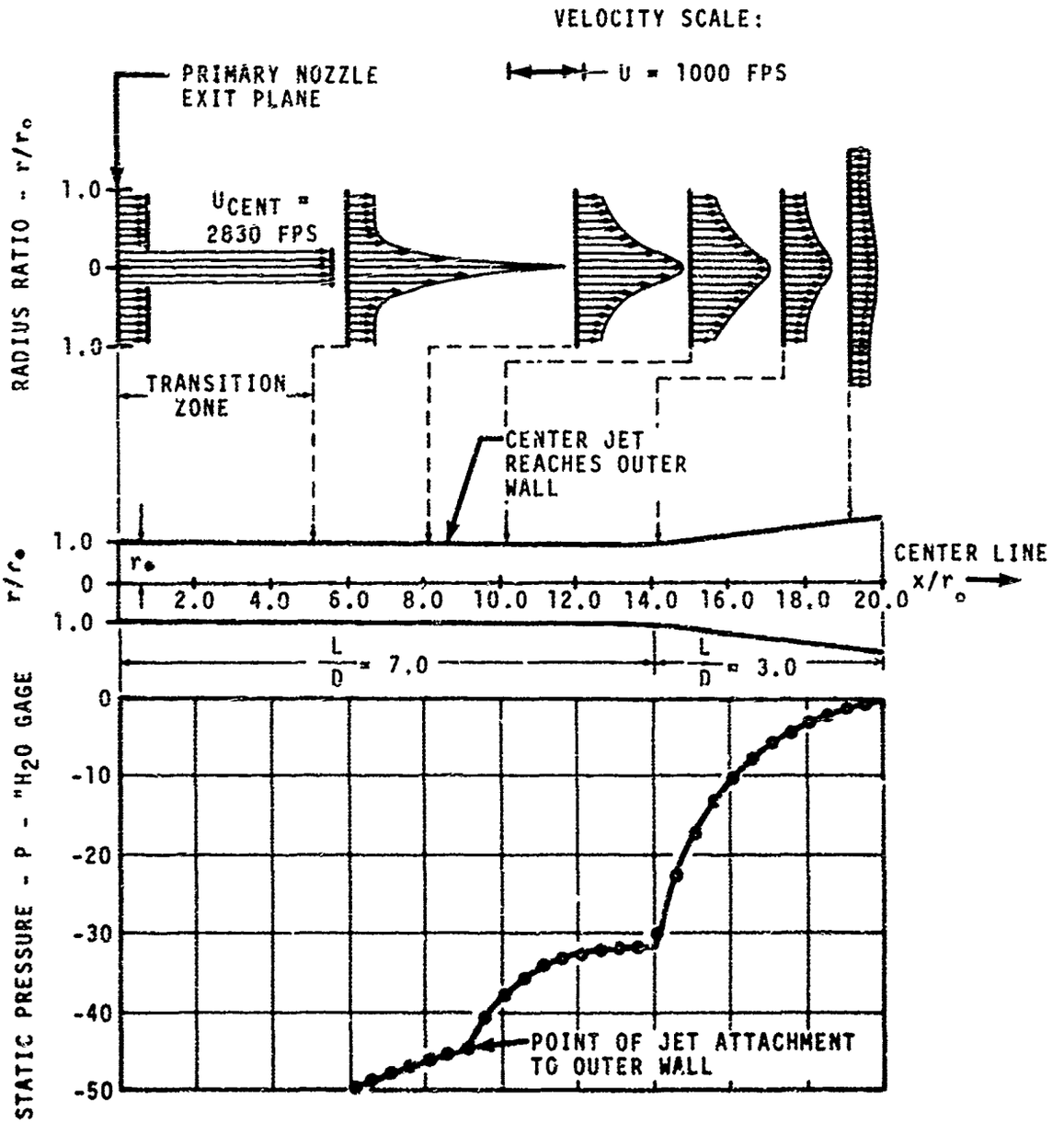

Figure 78. Design Point Static Pressure and Velocity Distributions (System S1).

TABLE 19. SCAVENGE EJECTOR DESIGN POINT

Parameter	Symbol	Units of Measure
Primary Flow		
Flow rate	W_p	.0068 lb/sec
Percent bleed	$\%W_p$	2%
Engine power loss	$\%\Delta SHP/SHP$	6.4%
Total pressure	P_{oP}	188 psia
Total temperature	T_{oP}	1250°R
Nozzle throat area	$A^*_{EFF.}$	.002519 $in.^2$
Nozzle exit area	$A_{P\,EFF}$	.005678 $in.^2$
Mach number	M_P	2.38
Secondary Flow		
Flow rate	W_s	0.06 lb/sec
Flow ratio	W_s/W_p	8.82
Inlet pressure	$P_{o\,IN}$	-22"H_2O=13.91 psia
Inlet temperature	$T_{o\,IN}$	518.7°R
Secondary flow area	A_s	.3543 $in.^2$
Mach number	M_S	0.33
Mixing Tube		
Mixing tube area	A_M	.3509 $in.^2$
Area ratio	A_M/A_p	61.8
Length ratio	L_M/D	7.0
Diffuser		
Area ratio	A_{EX}/A_M	3.0
Length ratio	L_D/D	3.0
Exit Area	A_{EX}	1.057 $in.^2$

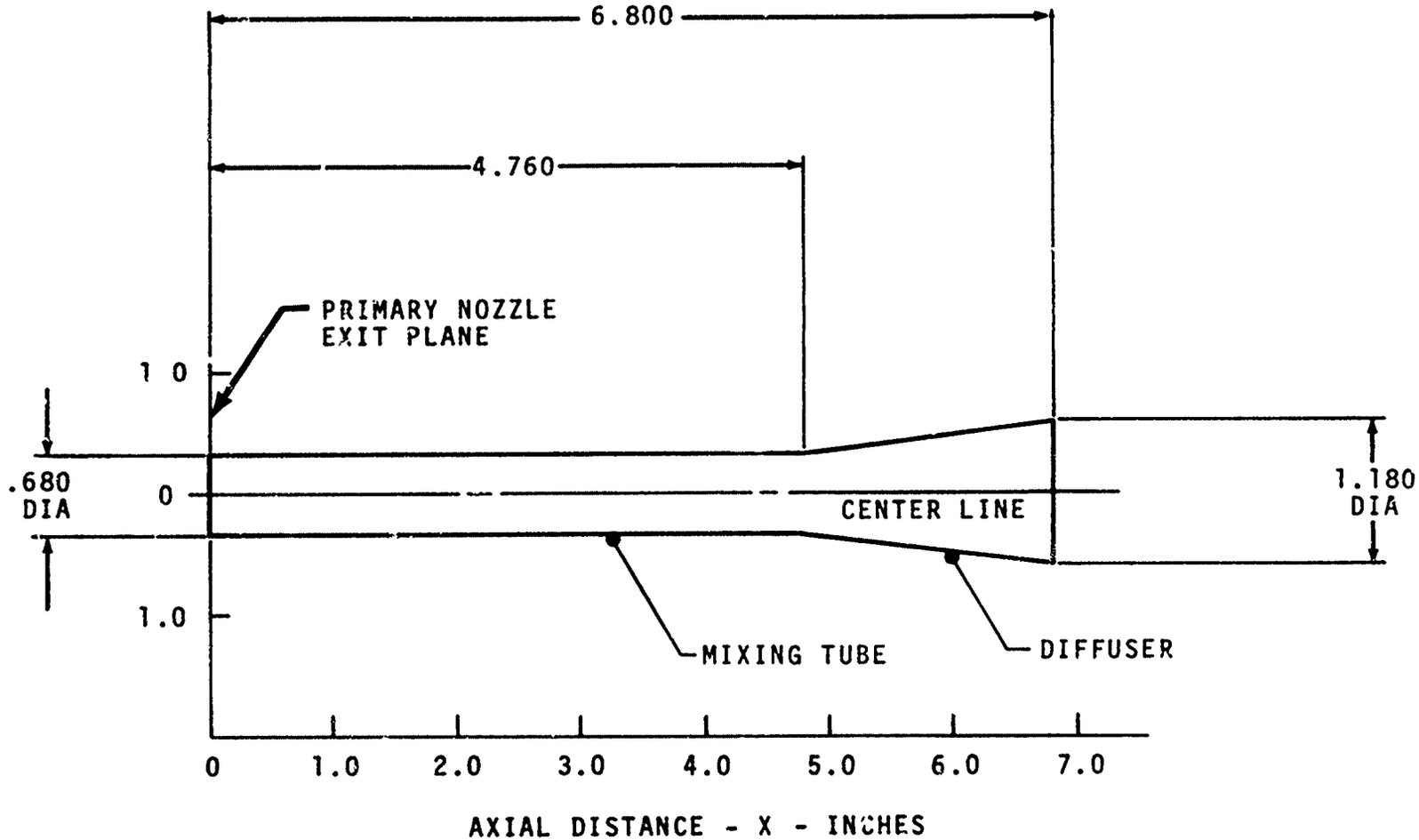

Figure 79. Ejector Mixing Tube and Diffuser Flow Path (S1).

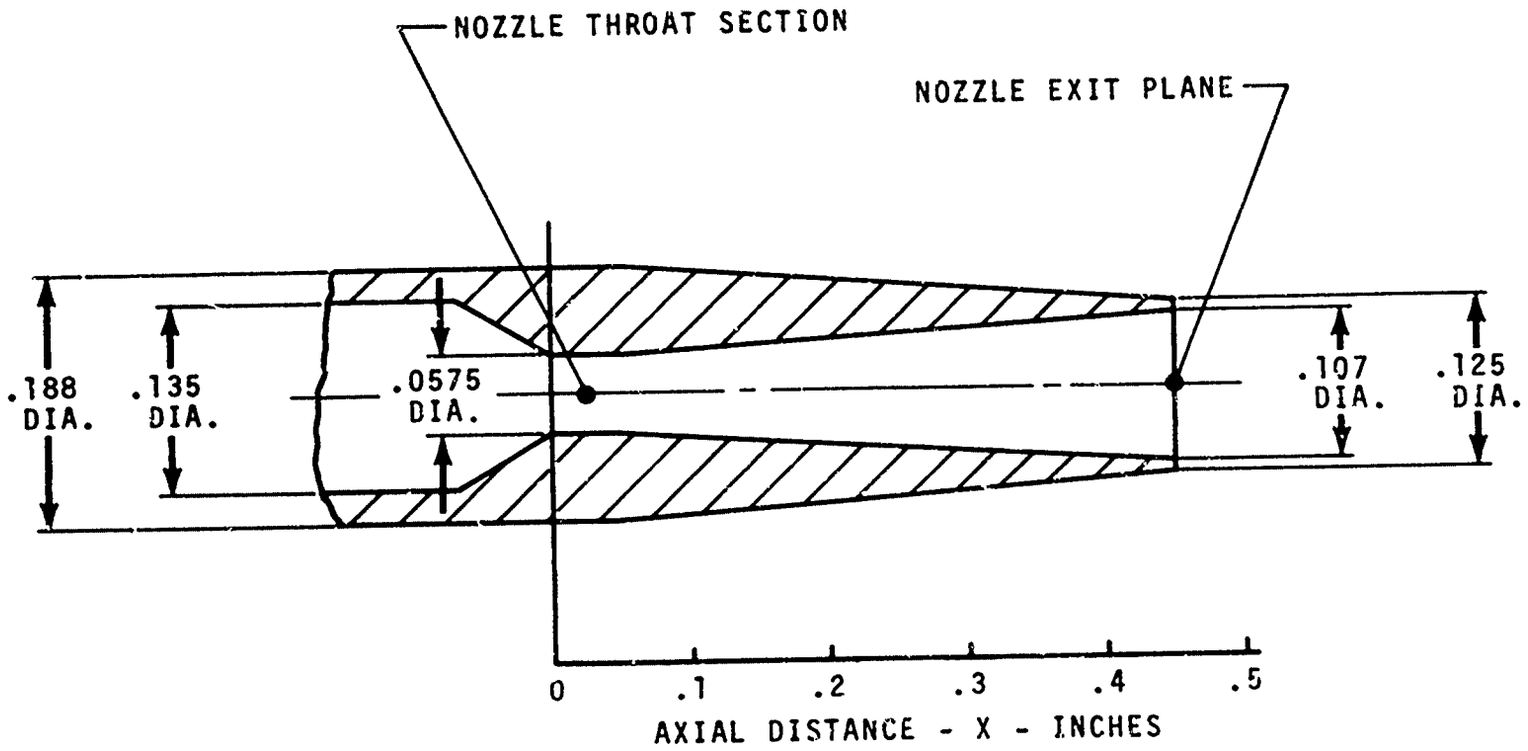

Figure 80. Ejector Primary Nozzle Flow Path (S1).

TEST RIG AND INSTRUMENTATION

The mechanical design of one ejector element was integrated with the design of the test rig. (A typical configuration for the full 15-tube assembly is discussed in the following section.)

Figure 81 shows the rig that was designed along with the primary and secondary performance instrumentation. All flow path elements, including the supply nozzle, were fabricated from 321 stainless steel.

The primary air flow path contains an orifice section (.125-inch orifice/.415-in. duct) followed by a high-pressure manifold to which the nozzle is silver brazed.

In the secondary duct, an inlet throttle is provided to simulate the loss across an engine particle separator. An orifice section (1-inch diameter/2.065-inch duct) is located approximately 25-pipe diameters downstream, allowing for flow stabilization after the valve.

Performance instrumentation was kept to a minimum, including only flow measurements and primary and secondary nozzle inlet conditions. From these measurements, the performance of the ejector was determined under representative suction duct conditions using primary supply air 188 psia at 790°F.

The following measurements were taken:

Primary airflow ΔP	-	(1)
Upstream orifice pressure	-	(1)
Orifice temperature	-	(1)
Inlet pressure	-	(1)
Inlet temperature	-	(1)
Secondary airflow ΔP	-	(2)
Upstream orifice pressure	-	(2)
Orifice temperature	-	(1)
Inlet pressure	-	(1)
Cell ambient pressure	-	(1)
Cell ambient temperature	-	(1)

Photographs of the actual hardware prior to the start of testing appears in Figure 82.

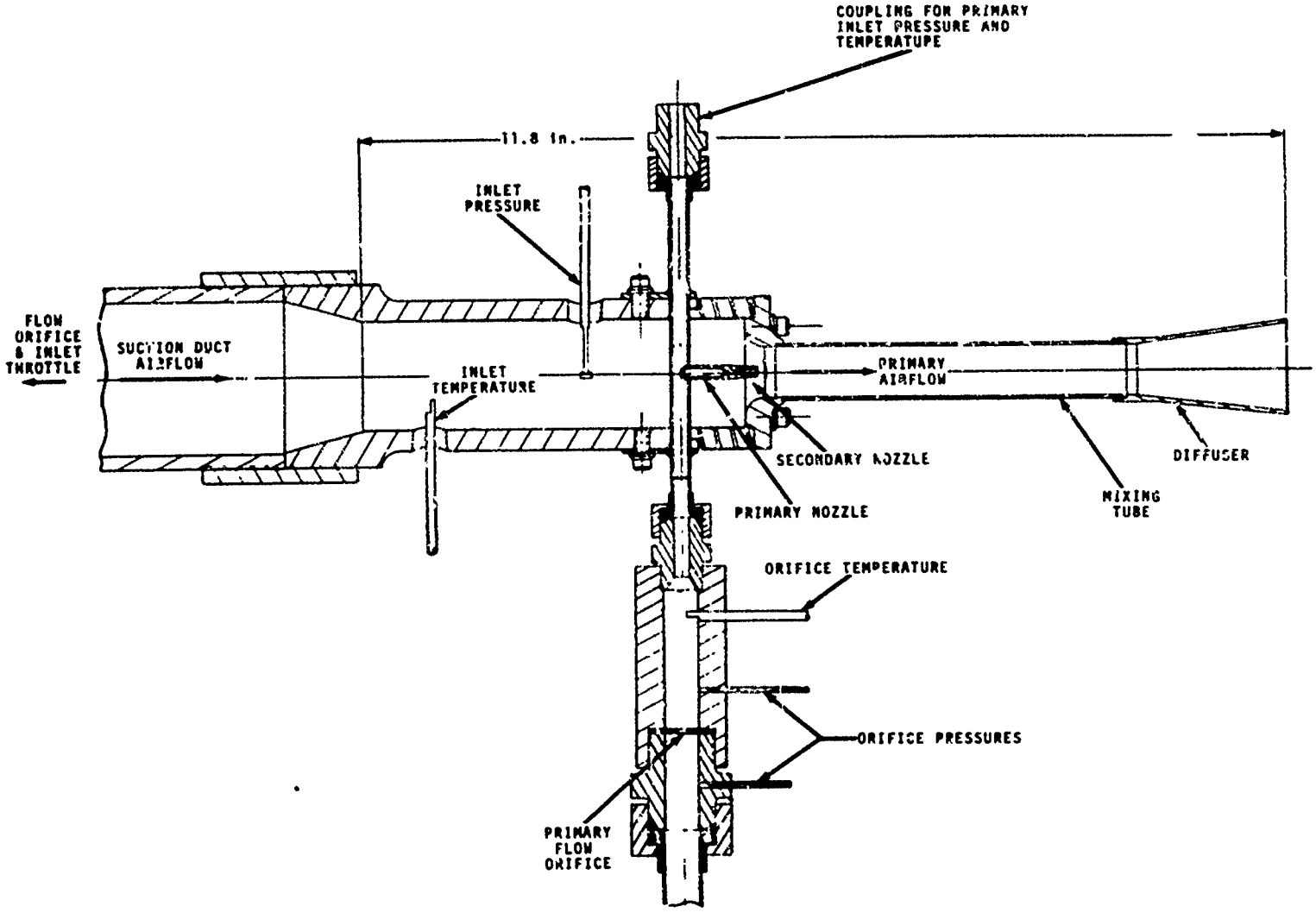

Figure 81. Alternate System Test Rig.

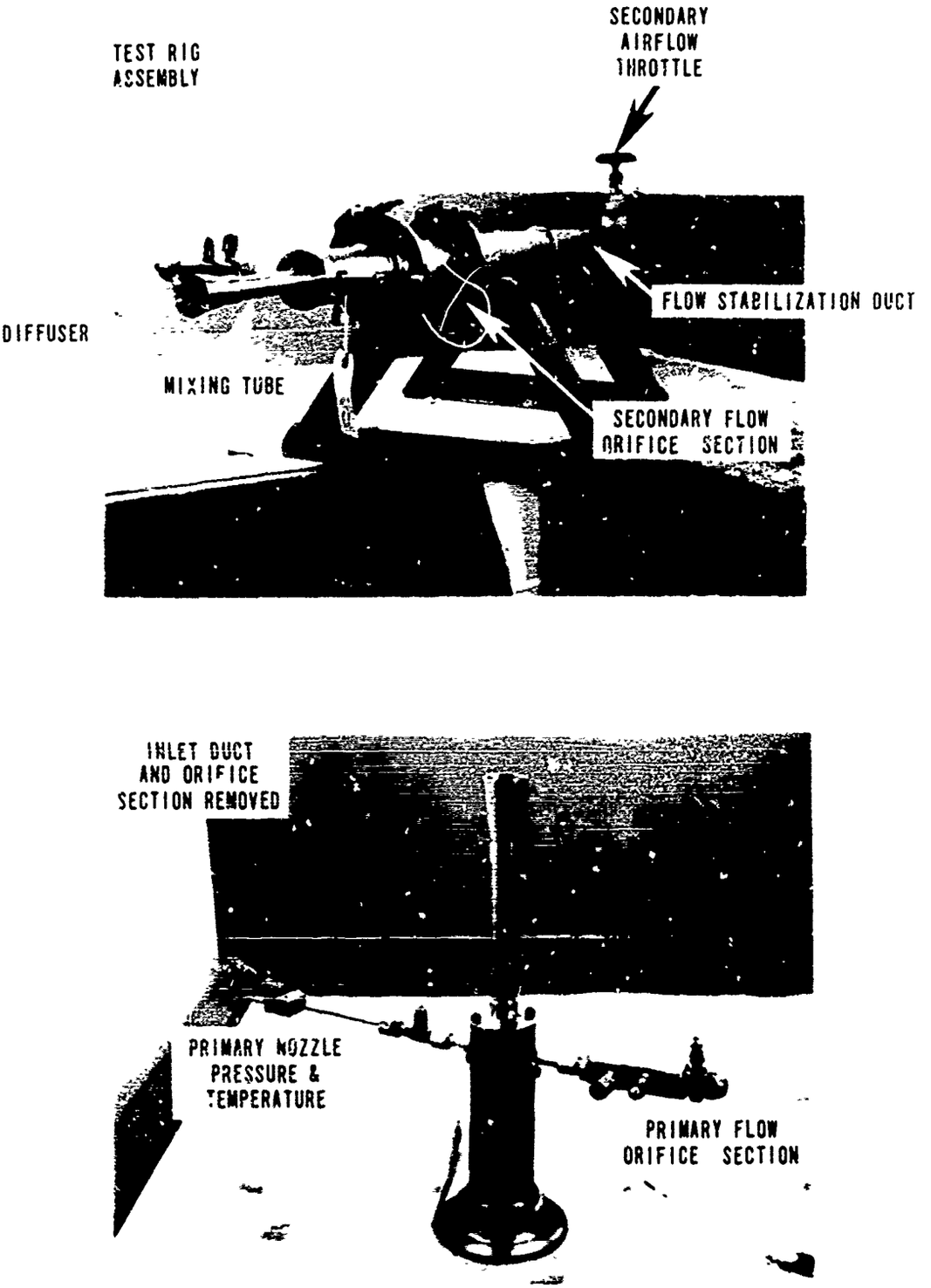

Figure 82. Alternate System Test Rig Components

MECHANICAL DESIGN - SYSTEM S1

A multiple-tube ejector assembly is shown in Figure 83. In this configuration, a rectangular 5 x 3 array is used, and most components may be fabricated from sheet metal.

The advantage of the multiple-tube design is that compact arrangements of the elements may be made to suit a given engine installation. Examples of other configurations have been shown in the feasibility study (Figure 19).

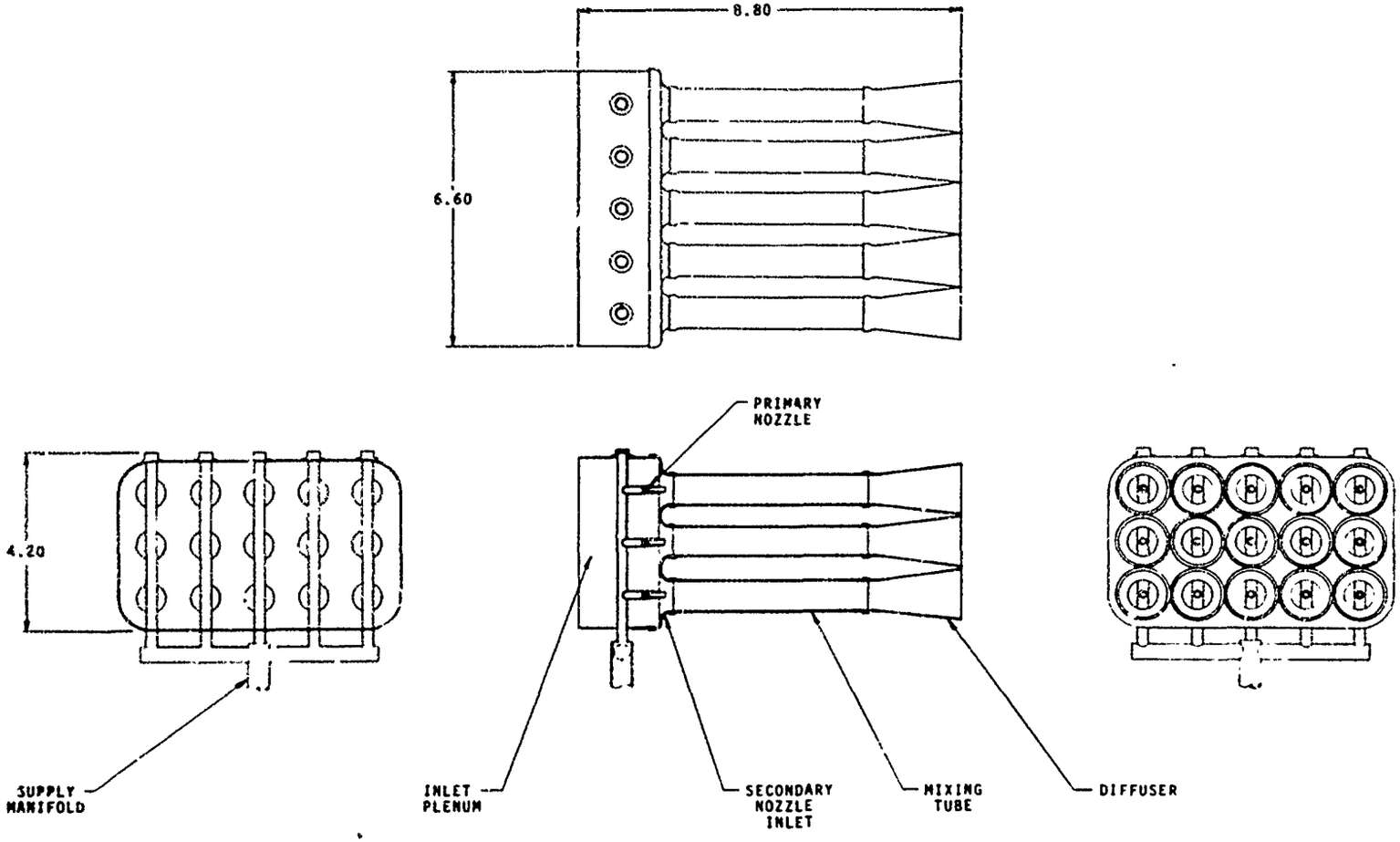

Figure 83. Multiple-Tube Ejector Assembly.

TEST PLAN OUTLINE

The test series conducted on the critical element of a multiple-tube ejector assembly (System S1) was similar in content to the evaluation program for the primary system and is oulined below:

Test A1 - System Efficiency/Power Input

Evaluate the pumping capacity and power input requirements of the ejector over a range of conditions corresponding to engine operation from idle to maximum power.

Test A2 - Ice Accumulation Test

Determine the effect of ice buildup, as a result of supercooled water carry-over from the engine separator, upon the scavenge pump performance.

Test A3 - Water Ingestion

Measure the shift in design point steady state pumping capacity, under conditions where water is introduced into the secondary flow duct.

Test A4 - Durability

Evaluate the effect of sustained operation in a erosive environment, equivalent to a military 50-hour sand ingestion test, upon the mechanical and aerodynamic performance of the ejector.

Test A5 - FOD Test

Qualitatively assess the ability of the system to ingest typical aircraft hardware in sizes appropriate to the particular scavenge system design, and measure the susceptibility of this system to damage from solid ice ingestion.

EXPERIMENTAL EVALUATION OF THE ALTERNATE SYSTEM (TASK IV)

TEST A1 - SYSTEM EFFICIENCY - POWER REQUIREMENTS

To determine the ejector power requirements, the first test conducted was a clean inlet baseline performance evaluation over a wide range of primary and secondary condtions.

These conditions were as follow:

Primary Nozzle Pressure (psia)	Primary Nozzle Temperature (^{o}R)
60	840
100	990
140	1105
188	1250

For each condition above, the test procedure was to measure the resulting secondary flow rate, beginning with the minimum inlet system depression. The suction duct pressure was then decreased in increments until the limits of the jet pump capacity were determined (i. e., the value of secondary pressure at which the flow rate approaches zero).

The results that were obtained are shown in Figure 84.

Secondary airflow is corrected to standard day test cell ambient conditions. For reference to the design point, the flow rate $(W_S\sqrt{\theta}/\delta)_{amb}$ is 0.06 lb/sec for standard day ambient conditions for an ejector suction duct pressure P_{oS} equal to -20 in. H_2O.*

The test results on Figure 84 are self-explantory. Of main interest is the data for maximum primary supply pressure, i.e., 188 psia, which shows that the required scavenge airflow is pumped when the secondary total pressure is approximately -19 in. H_2O. These results are very close to design goals:

	Design	Test
Airflow, $(W_S\sqrt{\theta}/\delta)_{amb}$	.06 lb/sec	.06 lb/sec
Inlet Pressure, $P_{o_{IN}}$	-20 in. H_2O	-19 in. H_2O

* The plane which is selected for airflow correction is a matter of choice. If, for example, the secondary nozzle inlet is chosen, then at design point $(W_S\sqrt{\theta}/\delta)_{IN}$ = .063 lb/sec at P_{oIN} -20 in. H_2O. All test data would then be scaled up by the ratio of $P_{amb}/P_{o_{IN}}$.

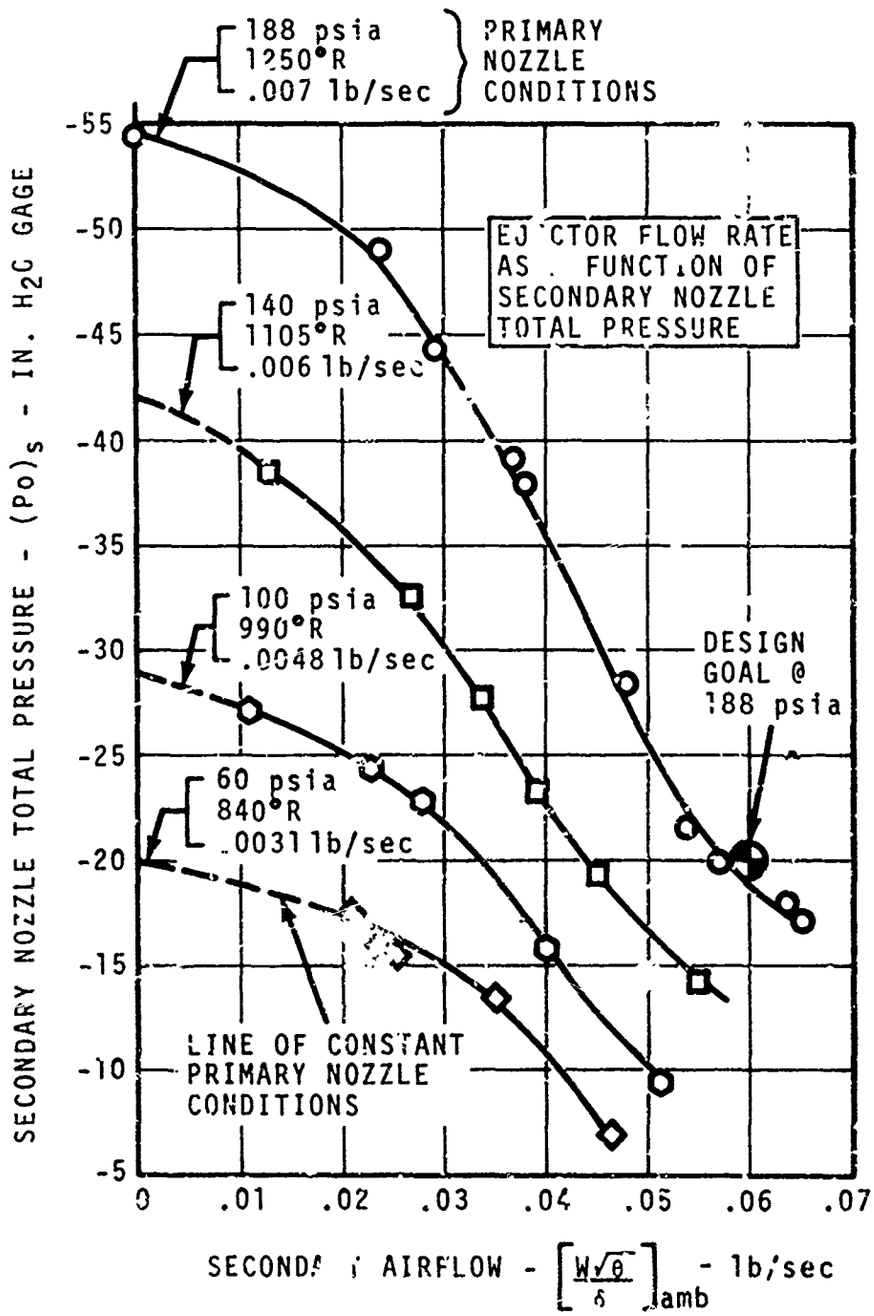

Figure 84. Alternate System Baseline Performance Test Results - Test A1.

The power input requirement to the ejector is a function of the rate of bleed extracted from the engine. Figure 85 shows the measured primary airflow (actual) as a function of supply pressure. At design conditions, the primary airflow is .0071 lb/sec, and on the basis of a 15-tube assembly:

Total Bleed Flow	=	15 (.0071 lb/sec)	=	.1065 lb/sec
Percent Bleed	=	.1065/5.0	=	2.1%
Power Penalty	=	3.2 (2.1%)*	=	6.8%

From the data presented up to this point, the performance goals of the scavenge ejector have been essentially attained, from the viewpoint of the supply conditions required, the power penalty, and the system pumping characteristics.

TEST A2 - ICE ACCUMULATION

To determine the effects of ice accumulation upon the operation of the scavenge pump, for circumstances where supercooled water is drawn from the particle separator, the ejector rig was mounted so that the inlet pumped cold air from an icing tunnel into which an atomized water spray was introduced.

Conditions established for the test were as follow:

Primary Air	-	188 psia at 900°R
Inlet Temperature	-	+21°F
Water Flow Rate	-	1.0 lb/hr
Liquid Water Content	-	≃2.3 gm/m^3

Total flow through the system was computed as a function of running time, using a combination kiel/temperature probe positioned at the diffuser discharge plane. The resulting rate pumping capacity loss is shown in Figure 86.

After 20 minutes of operation, approximately 12-percent loss in flow had resulted. The initial ice buildup occurred near the secondary nozzle; accumulation apparently never reached appreciable amounts since shedding occurred periodically, evidently due to sufficient heat conduction from the primary supply manifold.

*Reference Figure 16 for bleed/power influence coefficient.

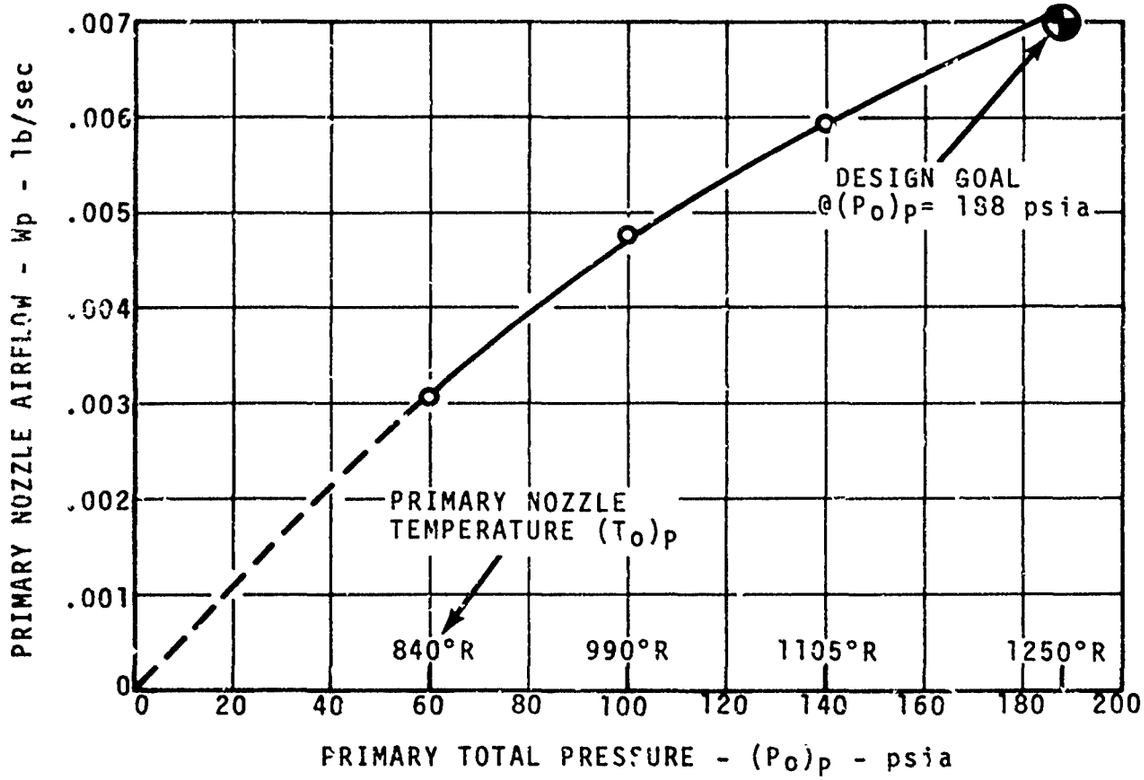

Figure 85. Primary Nozzle Flow Characteristics - Test A1.

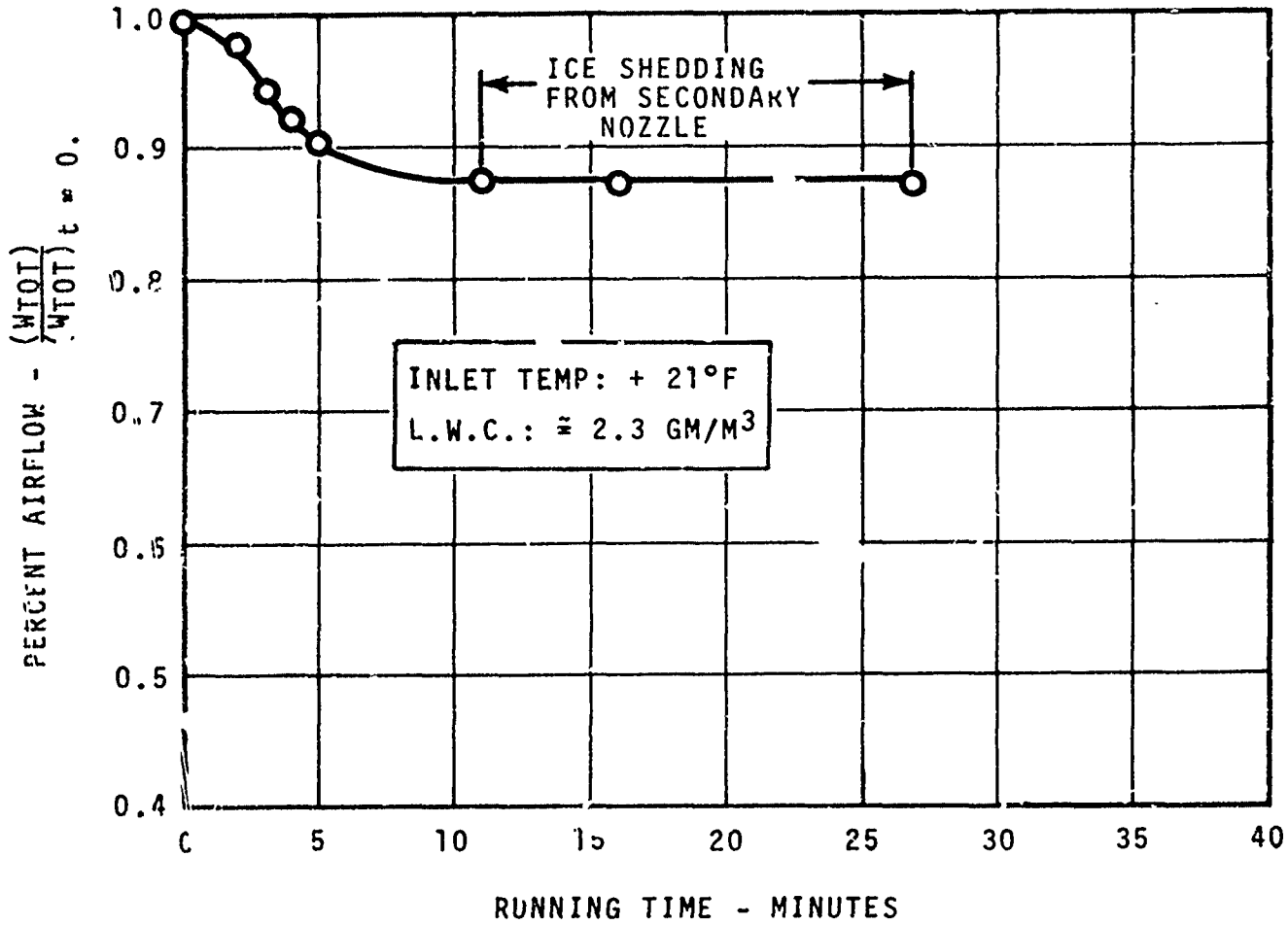

Figure 86. Effect of Ice Accumulation Ejector Pumping Capacity - Test A2.

TEST A3 - WATER INGESTION

The water ingestion test simulated operation of the scavenging system under conditions where the separator ingests water in an amount equal to 5%, by weight, that of the engine flow rate, all of which is assumed to be carried into the scavenge pump. For one ejector element, the maximum steady-state quantity is approximately 8cc/sec.

A residual "slug" of water in the suction duct presented no problem. The water was immediately (and vigorously) expelled from the system, at the moment the primary air was introduced.

Two steady-state conditions were tested and the results were as follows:

	Water Flow	Primary Conditions	Secondary Airflow	Airflow Loss
(1)	0.	188 psia @	.057 lb/sec	-
	8.8cc/sec	1250°R	.046 lb/sec	19%
(2)	0.	140 psia @	.048 lb/sec	-
	8.8cc/sec	1120°R	.040 lb/sec	17%

No adverse mechanical effects were noted from the water impingement on the primary nozzle.

TEST A4 - DURABILITY

The quantity of sand (MIL-E-5007C) delivered to the scavenging system from a 5.0-lb/sec engine separator was determined in the blower test program to be 400 gm/hr with a total test duration of 50 hours. At the rate of 400 gm/hr, assuming an equal distribution to all ejector elements, only 26.7 gm/hr would be seen by one ejector.

In view of this very low sand feed rate, the test was accelerated so as to deliver the equivalent 50-hour quantity within an 8-hour period. Therefore, the required accelerated rate of ingestion for one tube was:

$$\dot{X} = 26.7 \text{ gm/hr} \left(\frac{50}{8}\right) \cong 166 \text{ gm/hr}$$

The actual feed rate used was 170 gm/hr,* for an 8-hour period.

* $\left[170 \text{ gm/hr} / \text{Ejector}\right]$ x 15 ejectors x 8 hr = 44.9 lb sand (total).

For this test, the rig was modified to facilitate introduction of sand into the suction duct along the ejector centerline. The inlet throttle and flow orifice were removed; and to establish the required inlet depression, a stationary throttle plate was installed just upstream of the secondary nozzle. A calibrated feed hopper and ejector were used to introduce the sand directly into the suction duct.

At the conclusion of the 8-hour test, the original setup was restored in order to recheck performance, using the secondary flow orifice.

In view of the mechanical design of the ejector, the only components expected to show wear of any significance would be the upstream face of the primary nozzle manifold, and the converging secondary nozzle. These components are shown before and after the test in Figures 87 and 88.

Since the air velocities are quite low in the suction duct, the erosion was very minimal, and amounted to a "frosting" of the surfaces.

Performance of the ejector was unchanged when checked at the conclusion of the test.

TEST A5 - ICE INGESTION/FOD

The concluding test in the alternate system evaluation program was to determine the susceptibility of this design to damage resulting from the ingestion of common aircraft hardware in sizes appropriate to the configuration.

With the ejector operating at design point, the following objects were introducted:

1. Four pieces of ice, nominally 1/4 inch on a side up to 3/4 inch on a side.
2. Safety wire, 1/32-inch diameter, in lengths up to 1/2-inch.
3. No. 6-40 bolt x 3/8 inch length
   No. 6-40 nut
4. No. 10-32 bolt x 5/8 inch length
   No. 10-32 nut

Objects sufficiently small were easily expelled by the ejector, without any noticeable effect.

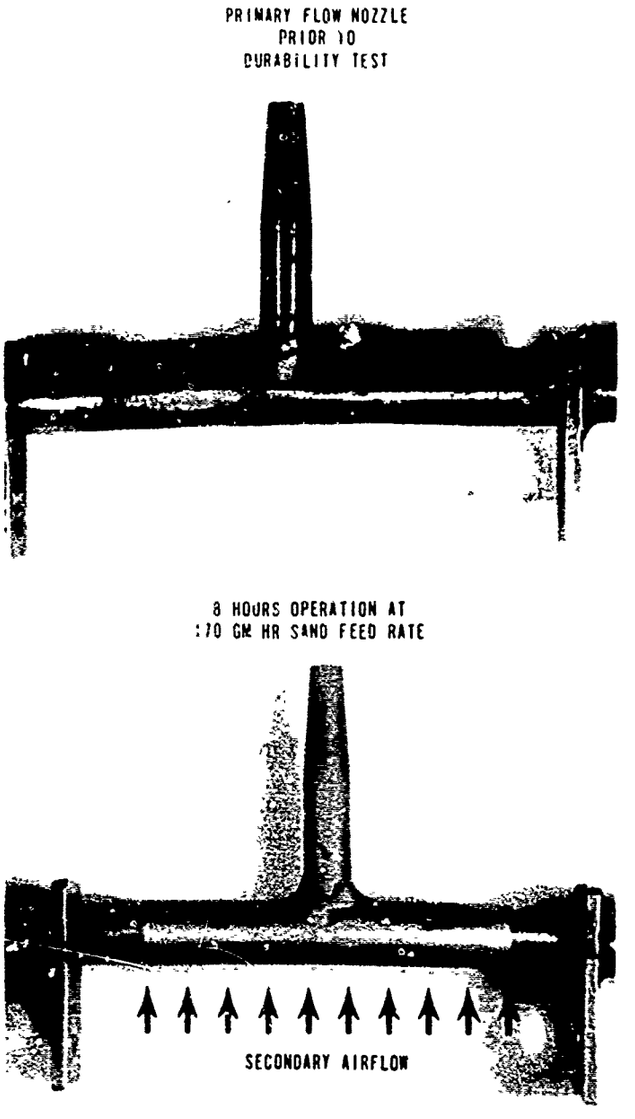

Figure 87. Effect of Sand Ingestion Upon Primary Nozzle - Test A4.

SECONDARY FLOW NOZZLE
PRIOR TO
DURABILITY TEST

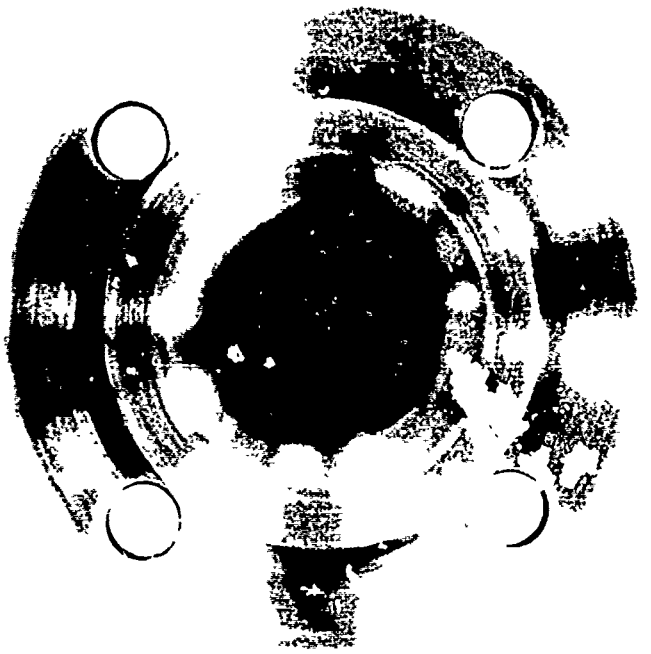

8 HOURS OPERATION AT
170 GM/HR SAND FEED RATE

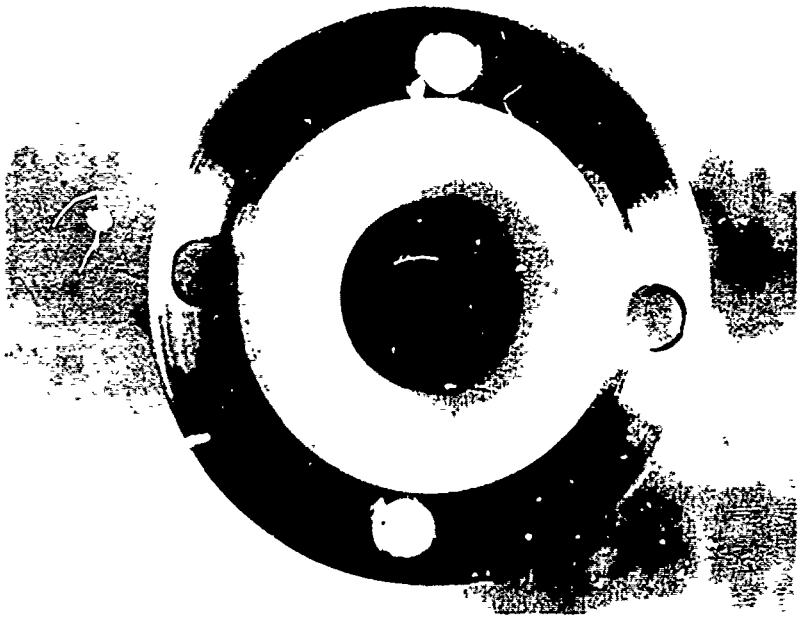

Figure 88. Effect of Sand Ingestion Upon Ejector Secondary Flow Nozzle - Test A4.

The larger objects (No. 6, No. 10 bolts) became lodged at the minimum area point, just upstream of the primary nozzle exit.

Upon teardown inspection, there was no evidence of damage to any component.

CONCLUSIONS

PRIMARY SYSTEM

The innovative concept that was introduced in this program is a practical means of achieving a durable configuration for a particle separator scavenge pump. The design concept is sufficiently flexible to permit a wide range of operational lifetimes.

Since the blower does incorporate an ejector, it will inherently draw more power than a conventional design with the same flow and headrise specifications. This power increase is solely a function of the degree of durability that is required for given applications.

In subsequent applications of the blower design described in this report, the following considerations are recommended:

1. The test data indicated some deficit in bypass airflow that was likely due to residual swirl at the mixing plane. The swirl can be eliminated by suitable modification to the turning vane assembly, such as an increase in solidity or by the selection of an alternate camberline shape. By elimination of swirl, power input is reduced for the same amount of bypass flow that is pumped.

2. For a 50-hour objective, the amount of margin built into the present design can be reduced. The labled "Design Point" (Figure 71) can be moved closer to the minimum goal point. This could be accomplished by simultaneously reducing the rotor airflow ($\cong$ 4%), the rotor pressure ratio ($\cong$ 4%), and the bypass ratio ($\beta_{NEW} \cong .15$). With these changes, power input could be reduced from 15.6 horsepower (present design) to 10.0 horsepower, at a 60 percent stage efficiency level.

3. One general development change that can be incorporated into this blower design is to use an available protective coating which is applied by a diffusion pack process in thicknesses of 0.7 to 1.5 mils to a stainless steel base material. Since both rotor and stators reached operational limits simultaneously, the coating, if used, would have to be applied to both components.

With respect to erosion resistance the referenced coating erodes at 3 percent of the rate of stainless steel, under comparable conditions.

The protective coating could be used in various ways; for example, if the coating was applied to the present design, an order of magnitude increase in lifetime would result. However, this is impractical if viewed with resepect to the basic lifetime of the gas turbine under a comparable environment.

Instead, a "hybrid" approach could be taken where, if given a required design life, some of the protection that would be provided by the inlet separator/bypass air is traded for improved erosion resistance on the critical elements. In short, the combination of the "bypassing blower" with a coated rotor results in a lower power input for a given operational life.

ALTERNATE DESIGN

Application of the jet pump concept as a means of scavenging the gas turbine engine particle separator offers significant advantages in terms of extreme simplicity, low cost, and durability and on/off capability. Available methods for analytical design have been demonstrated in this program to be very accurate, and virtually the only changes in design procedure would involve assuming less aerodynamic blockage at the primary nozzle exit.

REFERENCES

1. Fasal, J., FORCED DECISIONS FOR VALUE, Product Engineering, 12 April 1965.

2. MECHANISM OF SAND AND DUST EROSION IN GAS TURBINE ENGINES, Solar Div., International Harvester Co., USAAVLABS Technical Report 70-36, Eustis Directorate, U. S. Army Air Mobility Research and Development Laboratory, Fort Eustis, Virginia, August 1970, AD 876584.

3. Sovran, G., FLUID MECHANICS OF INTERNAL FLOW, 1967, pp. 270-319.

4. Schlicting, H., BOUNDARY LAYER THEORY, 1968, pp. 590-592.

5. Duffy, R. J., and Shattuck, B. F., INTEGRAL ENGINE INLET PARTICLE SEPARATOR, Vol. II, DESIGN GUIDE, General Electric Co., USAAMRDL TR-75-31B, Eustis Directorate, U. S. Army Air Mobility Research and Development Laboratory, Fort Eustis, Virginia, August 1975, AD AO15064.

6. Hickman, K., ANALYSIS AND TESTING OF HIGH ENTRAINMENT SINGLE NOZZLE JET PUMPS WITH VARIABLE AREA MIXING TUBES, NASA CR-2067, June 1972.

APPENDIX A

COMPUTATIONAL PROCEDURE FOR BLOWER PERFORMANCE ANALYSIS

This Appendix presents a sample computational procedure for blower performance analysis. The data values used in the sample calculation correspond to the starting conditions for the durability test (Test P4).

BLOWER PERFORMANCE CALCULATIONS

	PARAMETER	SYMBOL	SOURCE	SAMPLE VALUE
1.	Inlet Pressure	$P_{o\,in.} = P_{Baro.}$	Cell Ambient	14.642 PSIA
2.	Inlet Temperature	$T_{o\,in.}$	Cell Ambient	537.7°R
3.	Orifice Pressure Drop	$\Delta P_{Or.}$	5" Orifice/8" Pipe (2)	0.241
4.	Orifice Upstream Pressure	$P_{Or.}$	5" Orifice/8" Pipe (2)	14.825 PSIA
5.	Orifice Temperature	$T_{Or.}$	5" Orifice/8" Pipe (2)	117°F
6.	Total Flowrate	$W_{Tot.}$	ASME Standard Orifice Equation	1.109 LB/SEC
7.	Mechanical Speed	N	Speed Pickup/Counter	50800 RPM
8.	Temperature Referral	$\sqrt{\theta}$	$\sqrt{\theta} = \sqrt{T_{o\,in.}/518.7}$	1.018
9.	Pressure Referral	δ	$\delta = P_{o\,in.}/14.696$	0.996
10.	Referred Total Flow	$(W_{Tot.}\sqrt{\theta}/\delta)_{in.}$	---	1.133 LB/SEC
11.	Referred Speed	$N/\sqrt{\theta}$	---	49902 RPM
12.	Percent Speed	$\%\ N/\sqrt{\theta}$	$\%\ N/\sqrt{\theta} = (N/\sqrt{\theta})/50000$	99.8%
13.	Mean Exit Pressure	$P_{o\,Ex.}$	Exit Plane Probes (6)	15.528 PSIA
14.	Mean Exit Temperature	$T_{o\,Ex.}$	Exit Plane Probes (6)	577.7°R
15.	Overall Pressure Ratio	$Pr_{Ov.}$	$Pr_{Ov.} = P_{o\,Ex.}/P_{o\,in.}$	1.060
16.	Overall Pressure Rise	$\Delta P_{o\,Ov.}$	$\Delta P_o = (P_{o\,Ex.} - P_{o\,in.})(27.74)$	24.6"H_2O
17.	Bypass Channel Mean Total Pressure	$(P_o)_{Byp.}$	Bypass Channel Pressure Probes (4)	14.574 PSIA
18.	Bypass Channel Static Pressure	$(P)_{Byp.}$	Bypass Channel Wall Statics (4)	14.514 PSIA
19.	Bypass Channel Pressure Loss	$(\Delta P_o)_{Byp.}$	$(\Delta P_o) = (P_{o\,in.} - P_{o\,Byp.})(27.74)$	1.85"H_2O
20.	Pressure Ratio – Total to Static	$(P_o/P)_{Byp.}$	---	1.0041

	PARAMETER	SYMBOL	SOURCE	SAMPLE VALUE
21.	Flow Parameter	$(W\sqrt{T_o}/P_o)_{Byp.}$	Airflow Calibration (Figure 55)	0.300
22.	Bypass Referred Flow	$(W_{Byp.}\sqrt{\theta}/\delta)_{in.}$	$\left[\frac{W\sqrt{T_o}}{P_o}\right]_{Byp.} \times \frac{P_{o\ Byp.}}{P_{o\ in.}} \times 14.696 \times \frac{1}{\sqrt{518.7}}$	0.193 LB/SEC
23.	Rotor Referred Flow	$(W_{Rot.}\sqrt{\theta}/\delta)_{in.}$	$(W_{Tot.}\sqrt{\theta}/\delta)_{in.} - (W_{Byp.}\sqrt{\theta}/\delta)_{in.}$	0.938 LB/SEC
24.	Bypass Actual Flow	$W_{Byp.}$	$(W_{Byp.}\sqrt{\theta}/\delta)_{in.} \times \delta/\sqrt{\theta}$	.1892 LB/SEC
25.	Rotor Actual Flow	$W_{Rot.}$	$(W_{Rot.}\sqrt{\theta}/\delta)_{in.} \times \delta/\sqrt{\theta}$	.9198 LB/SEC
26.	Bypass Ratio	β_2	$W_{Byp.}/W_{Rot.}$	21%
27.	Primary Nozzle Temperature	T_{o_p}	Equation (1) Below	585.9°R
28.	Power Input	$HP_{Rot.}$	$HP_{Rot.} = W_{Rot.} C_p J(T_{o_p} - T_{o_{in.}})/550$	15.06 HP
29.	Standard Day Power	$HP_{Rot.}/\delta\sqrt{\theta}$	---	14.85 HP
30.	Secondary Nozzle Flow Area	A_s	Design Geometry and Aerodynamic Blockage Factor	1.95 in.^{2}
31.	Secondary Nozzle Flow Parameter	$\left[\frac{W_{Byp.}\sqrt{T_o}}{A P_o}\right]_s$	By Assumption that $T_{o_s} = T_{o_{in.}}$ and $P_{o_s} = P_{o_{Byp.}}$	.1542
32.	Pressure Ratio – Total to Static	$(P_o/P)_s$	Equation (II) Below → $(P)_s$	1.0206
33.	Primary Nozzle Static Pressure	P_p	$P_p = P_s$ @ Mixing Plane	14.280 PSIA
34.	Primary Nozzle Flow Area	A_p	Design Geometry and Aerodynamic Blockage Factor	2.93 in.^{2}
35.	Primary Nozzle Flow Parameter	$\left[\frac{W_{Rot.}\sqrt{T_o}}{AP}\right]_p$	---	.5242
36.	Pressure Ratio – Total to Static	$(P_o/P)_p$	Equation (III) Below → $(P_o)_p$	17.587 PSIA
37.	Stage Pressure Ratio	$P_{o_p}/P_{o_{in.}}$	---	1.201

	PARAMETER	SYMBOL	SOURCE	SAMPLE VALUE
38.	Rotor Temperature Ratio	$T_{o_p}/T_{o_{in.}}$	—	1.0898
39.	Stage Efficiency	$(\eta_{AD})_{Stg.}$	Equation (IV) Below	0.599
40.	Primary Nozzle Mach Number	M_p	Equation (V) Below	0.55
41.	Primary Nozzle Velocity	V_p	Equation (VI) Below	638 FPS.

EQUATIONS USED:

(I.) $$T_{o_p} = \left[W_{Tot.}\, T_{o_{Ex.}} - W_{Byp.}\, T_{o_{in.}}\right] \Big/ W_{Rot.}$$ (Energy Balance – Adiabatic Mixing)

(II.) $$\left[\frac{W\sqrt{T_o}}{A P_o}\right]_s = \sqrt{\frac{2\gamma g}{(\gamma-1)R}} \sqrt{\left(\frac{P}{P_o}\right)_s^{2/\gamma} - \left(\frac{P}{P_o}\right)_s^{\frac{\gamma+1}{\gamma}}}$$ (Standard Compressible Flow Tables)

(III.) $$\left[\frac{W\sqrt{T_o}}{AP}\right]_p = \sqrt{\frac{2\gamma g}{(\gamma-1)R}} \sqrt{\left(\frac{P}{P_o}\right)_p^{\frac{1-\gamma}{\gamma}} \left[\left(\frac{P}{P_o}\right)_p^{\frac{1-\gamma}{\gamma}} - 1\right]}$$ (Standard Compressible Flow Tables)

(IV.) $$\eta_{AD} = \left[\left(P_{o_p}/P_{o_{in.}}\right)^{\frac{\gamma-1}{\gamma}} - 1\right] \Big/ \left(T_{o_p}/T_{o_{in.}} - 1\right)$$ (Adiabatic Efficiency Definition)

(V.) $$(P_o/P)_p = \left[1 + \frac{\gamma-1}{2} M_p^2\right]^{\frac{\gamma}{\gamma-1}}$$ (Standard Compressor Flow Tables)

(VI.) $$(V/\sqrt{T_o})_p = M_p \sqrt{\gamma g R} \left(1 + \frac{\gamma-1}{2} M_p^2\right)^{-.5}$$ (Standard Compressor Flow Tables)

CONSTANTS USED: $C_p = 0.248/LB_m\,°R$ $\quad J = 778\ \frac{Ft\text{-}Lb_f}{B}$ $\quad R = 53.3504\ \frac{Ft\text{-}Lb_f}{Lb_m\,°R}$

$g = 32.1741\ \frac{Lb_m\,Ft}{Lb_f\,Sec^2}$ $\quad \gamma = 1.400$

LIST OF SYMBOLS

A_s ; A_{SEC} - secondary nozzle area, $in.^2$

A_p ; A_{PRIM} - primary nozzle area, $in.^2$

A_M ; A_{MIX} - mixing tube area, $in.^2$

AR - diffuser area ratio, $in.^2$

A_{EFF} - effective flow area, $in.^2$ (general)

A_{GEO} - geometric flow area, $in.^2$ (general)

(CP_a) - actual static pressure recovery = $\Delta P/(P_o-P)$

(CP_i) - ideal static pressure recovery - $(1 - \frac{1}{AR^2})$

C_p - specific heat = 0.24 $Btu/lb_m\ ^oR$

C_1 - sand-to-air concentration at the engine compressor inlet

C_0 - sand-to-air concentration at the i.p.s. inlet = 4.29E-05 $\frac{lb_{sand}}{lb_{air}}$

C_2 - sand-to-air concentration at the scavenge blower inlet

D_H - hydraulic diameter (general), in.

D_M - hydraulic diameter of the mixing tube, in.

F_1 - relative wear factor as a function of particle velocity

F_2 - relative wear factor as a function of material type

f - Fanning friction factor = 0.003

g - constant = 32.1741 $\frac{lb_m\ ft}{lb_f\ sec^2}$

$\Delta h_o'$ - ideal headrise = $C_pJT_o\ (P_r^{\frac{\gamma-1}{\gamma}} - 1)$, $ft\text{-}lb_f/lb_m$

Δh_o - actual headrise = $C_pJ\ (\Delta To)$, $ft\text{-}lb_f/lb_m$

$\Delta h_o/\bar{U}^2$ - headrise coefficient = $C_p\ gJ\ \Delta T_o/\bar{U}^2$

HP - horsepower

J	-	constant = 778 ft-lb_f/Btu
L	-	length, in. (general)
L_M	-	mixing tube length, in.
L.W.C.	-	liquid water content, gm/m^3
M	-	Mach number $=\sqrt{\gamma gRT}$
N	-	rotational speed, rpm
N_s	-	special speed parameter
Pr	-	pressure ratio(total to total)
P_o	-	total pressure, psia
P	-	static pressure, psia
P_{STD}	-	constant = 14.696 psia
ΔP_o	-	total pressure rise, in. H_2O
ΔP	-	static pressure rise, in. H_2O
q	-	dynamic head = $(P_o - P)$, psi
Q	-	volume flowrate, cu ft/sec
R-	-	constant = 53.3504 ft-lb_f/lb_m ^oR
r, R	-	radius coordinate, in.
Δr	-	channel height
R_N	-	Reynold's number = x $\bar{v}/$
SHP	-	shaft horsepower
T_o	-	total temperature, ^oR
T	-	static temperature, ^oR
Tr	-	temperature ratio (total to total)

t	-	time ; thickness, in.
T_{STD}	-	constant = 59°F = 518.7 °R
U	-	blade speed, fps
$\bar{U}$	-	mean blade speed, fps
u	-	particle relative velocity , fps
$V;V_o$	-	velocity, fps (general)
$\bar{V}$	-	mean velocity, fps
V_z	-	Axial velocity, fps
V_m	-	meridional velocity, fps
V_w	-	relative velocity, fps
$V_z/\bar{U}$	-	flow coefficient
W	-	airflow, lb/sec (general)
W_{TOT}	-	total airflow to scavenge pump, lb/sec
W_{ROT}	-	rotor channel airflow, lb/sec
W_{BYB}	-	bypass channel airflow, lb/sec
X	-	sand ingested by rotor, lb_m
$\dot{X}$	-	sand feed rate to scavenge pump, gm/hr
X	-	axial distance, in. (blading sections)
Y	-	radial distance, in. (blading sections)
z, Z	-	axial coordinate, in.
β	-	flow ratio; blade angle, relative air angle
α	-	area ratio, absolute air angle
β_1	-	engine separator scavenge rate

β_2 - blower bypass ratio

δ - pressure referral parameter = P_o/P_{std}

ϵ - coefficient of restitution

γ - specific heat ratio = 1.400

η_{SEP} - separation efficiency by weight (general) = $\frac{W_t.\ \text{bypassed}}{W_t.\ \text{into pump}}$

η_1 - separation efficiency of the engine separator

η_2 - separation efficiency of the blower inlet

η_{DIFF} - diffuser efficiency = $(CP_a)/(CP_i)$

ν - kinematic viscosity, ft^2/sec

ρ - density, lb_m/ft^3

$\eta_p; \eta_{poly}$ - polytropic efficiency = $\frac{\gamma - 1}{\gamma} \frac{\ln Pr}{\ln Tr}$

η_{AD} - adiabatic efficiency = $\frac{Pr^{\frac{\gamma-1}{\gamma}} - 1}{Tr - 1}$

ϑ - vane camber angle; blade meanline polar coordinate

θ - temperature referral parameter = T_o/T_{STD}

τ - blockage factor = A_{EFF}/A_{GEO} (general)

τ^* - ejector nozzle throat blockage factor

μ - absolute viscosity, $lb_f;sec/ft^2$

μ - micron, 10^{-6} meter

SUBSCRIPTS

amb - cell ambient

BYP - bypass measurement plane

D;DIFF - diffuser inlet

EX - blower exit plane

i	- rotor inlet plane
IN	- blower inlet plane
M;MIX	- mixing tube inlet
P;PRIM	- primary nozzle
S;SEC	- secondary nozzle
STG	- stage
W	- relative